UNIVERSITY OF BIRMINGHAM

THE CONTRIBUTION OF SIGNALS 1,2 & 3 ON THE METABOLIC PHENOTYPE OF CD4+ T CELLS

By
Kalvin Singh Sahota

A thesis submitted to the University of Birmingham for the degree of DOCTOR OF PHILOSOPHY

Supervisors
Dr. Stephen Young
Dr. Jane Falconer

School of Inflammation and Ageing
College of Medical and Dental Sciences
University of Birmingham
March 2020

Abstract

T cell metabolism is differentially regulated in order to support their activation, replication and effector functions. For example, T cells preferentially upregulate glycolysis following activation and this is a crucial determining factor at the Th_{17}/T_{reg} axis. Productive T cell activation requires several signals namely 1) antigen, 2) co-stimulation, and 3) cytokines but if, and how, these influence the metabolic changes associated T cell activation is largely unknown.

To investigate this we assessed the metabolic phenotypes of CD4+ T cells following activation with; 1) variable strengths of stimulation through antigen-T cell receptor (TCR) engagement, 2) incubation with CHO cells transfected with individual costimulatory molecules CD80 or CD86, 3) exposure to the inflammatory cytokine IL-6. Metabolism was assessed using NMR spectroscopy-based metabolomics and metabolic flux analysis to assess the balance between the major pathways of glycolysis and oxidative phosphorylation.

We optimised the techniques for determining human CD4+ T cell metabolic phenotype and have observed quantitative and qualitative differences associated with variations in the activating signals 1 to 3. In particular, we found that exposure to IL-6 prior to TCR stimulation leads to an increase in glycolysis, a response which might prepare T cells for the metabolic burden following activation. Subsequent flow cytometry analysis demonstrates that IL-6 exposed cells have an increased proliferative phenotype, greater mitochondrial mass and markedly upregulate GLUT1, however, these changes were only observed in naïve cells and not memory.

Abnormal T cell responses and systemically measurable dysregulated metabolism are hallmarks of autoimmune and inflammatory diseases such as rheumatoid arthritis. An improved understanding of T cell metabolism has implications for the treatment of these diseases and the mechanisms of action of biological therapies such as abatacept and tocilizumab which target T cell differentiation and function.

Acknowledgements

Firstly, I would like to thank my supervisor Dr Stephen Young. Thank you for sharing your infinite knowledge of practical techniques, providing constant support, challenging me and giving me enough free reign to get things wrong. I would be blessed if I have half as many interesting facts to share as you do in my life time. I am also eternally grateful to my second supervisor Dr Jane Falconer. There are a 101 things I would like to thank you for, from reminding me that ‘upstairs is for thinking’ or introducing me to the Postal Service at 7am in the morning while isolating T cells. You always had the uncanny ability to make people smile, even when you were scolding me, and I hope you never lose that superpower.

I would love to give my thanks to everyone in the RRG. Over the last few years everyone has supported me in one way or another, whether it be making me a cup of tea or helping with an experiment in the lab. I would like to give special thanks to Chelsea Regan for helping with my experiments and for keeping me company during the most mundane lab tasks. I could not have stayed sane for this long if it wasn’t for my housemates James, Kam and Joe. Thank you for every bad idea, poorly planned scheme and questionable amount of fried chicken. I truly believe this combination was the secret to getting through our PhDs together. I would also like to thank my family. Even though none of you never really understood what I was researching or why I was researching it, you provided your support regardless.

I would also like to acknowledge RACE for funding this project which has proven to be interesting and rewarding and bringing together the three arthritis research institutes to share ideas and further research.

Finally, I would like to thank Dr. Michelle James. You are my best friend and my rock. You somehow put up with my pessimistic attitude and are always the ying to my yang. Thank you always and forever.

Table of Contents

Abbreviations

1,3-BPG	1,3-Biphosphoglycerate
2DG	2-Deoxy-D-Glucose
3-PG	3-Phosphoglycerate
ACC1	Acetyl-CoA-Carboxylase 1
ADP	Adenine Diphosphate
AIA	Adjuvant-Induced Arthritis
AIRE	Autoimmune Regulator
AKT	Protein Kinase B
AMP	Adenosine Monophosphate
ANOVA	Analysis of Variance
Anti-CCP	Anti-Citrullinated
AP-1	Activator Protein 1
APC	Antigen Presenting Cells
AS	Ankylosing Spondylitis
ASS1	Arginosuccinate 1
ATF3	Activating Transcription Factor 3
ATP	Adenosine Triphosphate
ATP5A	ATP synthase F1 subunit alpha
BAZ1B	Bromodomain Adjacent to Zinc Finger Domain 1B
BCATc	Branched Chain Aminotransferase
BCL	B Cell Lymphoma
BMI	Body Mass Index
C	Carbon
C/EBP	CCAAT/enhancer-binding protein beta
CD	Crohn's Disease

CD	Cluster of Differentiation
CHO	Chinese Hamster Ovaries
CIA	Collagen-Induced Arthritis
c-MYC	Cellular Myelocytomatosis Oncogene
CoA	Coenzyme A
CTLA4	Cytotoxic T Lymphocyte Associated Protein 4
CVD	Cardiovascular Disease
CXCR5	C-X-C Motif Chemokine Receptor 5
DAP	Dihydroxyacetone Phosphate
DFTMP	Diflouro(trimethylsilyl)methylphosphonic acid
dH2O	Dionised Water
DSS	Sodium trimethylsilylpropanesulphonate
ECAR	Extracellular Acidification Rate
eIF4E	Eukaryotic Translation Initiation Factor 4E
ERK	Extracellular Signal-Regulated Kinase
ETC	Electron Transport Chain
F-1,6-P	Fructose-6-Phosphate
F6P	Fructose-6-Phosphate
FA	Fatty Acid
FAD	Flavin Adenine Dinucleotide
FADH2	Reduced Flavin Adenine Dinucleotide
FAO	Fatty Acid Oxidation
FasL	Fas Ligand
FCCP	carbonyl cyanide 4-(trifluoromethoxy) phenylhydrazone
FITC	Fluorescein Isothiocyanate
FOXP3	Forkhead Box P3

FSC	Forward Scatter
FSC-A	Forward Scatter Area
FSC-H	Forward Scatter Height
g	gravity
G0	Gap 0 Phase
G1	Gap 1 Phase
G6P	Glucose-6-Phosphate
GAP	Glyceraldehyde Phosphate
GAPDH	Glyceraldehyde Phosphate Dehydrogenase
GC-MS	Gas Chromatography-Mass Spectrometry
GITR	Glucocorticoid-induced Tumour Necrosis Factor Receptor
GLUT1	Glucose Transporter 1
Got1	Glutamate Oxaloacetate Transaminase 1
gp	glycoprotein
Grb2	Growth Factor Receptor Bound Protein 2
GWAS	Genome-wide association Studies
H+	Hydrogen / Proton
HDL	High Density Lipoprotein
HI-HS	Heat Inactivated Human Serum
HK	Hexokinase
HLA	Human Leukocyte Antigen
HRP	Horseradish Peroxidase
ICOS	Inducible Co-Stimulator
Ifng	IFNγ gene
IFNGR	Interferon Gamma Receptor
IFNγ	Interferon gamma

IL	Interleukin
IL-6R	Interleukin-6 Receptor
IMIDs	Immune-mediated Inflammatory Disease
IMM	Inner Mitochondrial Membrane
IRAK	Interleukin-1 Receptor-Associated Kinase
IRF4	Interferon Regulatory Factor 4
iT_{reg}	Inducible T regulatory
IκB	Inhibitor of kappaB
JAK	Janus Kinase
JNK	c-Jun-N-terminal Kinase
KIC	α-ketoisocaproic acid
LAT	Linked for Activation of T cells
LC-MS	Liquid Chromatography-Mass Spectrometry
LDH	Lactate Dehydrogenase
LDHA	Lactate Dehydrogenase A
LPS	Lipopolysaccharide
LYP	Lymphoid Tyrosine Phosphatase
MAPR	Mitochondrial ATP Production Rate
MAZ	Myc-associated Zince Finger Protein
MCT	Monocarboxylate Transporter
mDIVI-1	Mitochondrial Division Inhibitor 1
MetS	Metabolic Syndrome
MHC	Major Histocompatability Complex
MHz	Mega Hertz
ml	millilitre
mM	milliMolar

MTCO1	Cytochrome c Oxidase Subunit 1
mTOR	Mechanistic Target of Rapamycin
mTORC	Mechanistic Target of Rapamycin Complex
NAD+	Nicotinamide Adenine Dinucleotide
NADH	Reduced Nicotinamide Adenine Dinucleotide
NADPH	Nicotinamide Adenine Dinucleotide Phosphate
NALA	*N*-acetyl-leucine amide
NDUFB8	NADH : Ubiquinone Oxidoreductase Subunit B8
NFAT	Nuclear Factor of Activated T cells
NFKBIZ	Nuclear Factor KappaB Inhibitor Zeta
NF-κB	Nuclear Factor KappaB
ng	nanogram
nM	nanoMolar
NMR	Nuclear Magnetic Resonance
OCR	Oxygen Consumption Rate
OPLSD-A	Orthagonal Partial Least Squares Discriminant Analysis
OXPHOS	Oxidative Phosphorylation
P	Probability
PBS	Phosphate-Buffered Solution
PD-1	Programmed Cell Death Protein 1
PDGF	Platelet-Derived Growth Factor
PDK1	Phosphoinositide-dependent Kinase 1
PE	Phycoerythrin
P_i	Intracellular Phosphate
PI3K	Phosphatidylinositol-3-Kinase
PL	Phospholipase

PLSD-A	Partial Least Squares Discriminant Analysis
pMHC	peptide-Major Histocompatability Complex (MHC) Binding
PPM	Parts per million
PPP	Pentose Phosphate Pathway
PQN	Probabilistic Quotient Normalisation
PsA	Psoriatic Arthritis
PSIP1	PS4 and SFRS1 Interacting Protein
PTPN22	Protein Tyrosine Phosphatase, Non-Receptor Type 22
PVDF	Polyvinylidene Fluoride
RA	Rheumatoid Arthritis
RORγT	Retinoic Acid Receptor-Related Orphan gamma T
RPMI	Roswell Park Memorial Institute
S6K	Ribosomal S6 Kinase
SD	Standard Deviation
SDHB	Succinate Dehydrogenase Complex Iron Sulfur Subunit B
SE	Shared Epitope
sIL-6R	Soluble IL-6 Receptor
SLE	Systemic Lupus Erythematosus
SLP-76	Lymphocyte Cytosolic Protein 2
SNP	Single Nucleotide Polymorphisms
SOCS	Suppressor of Cytokine Signalling
SOP	Standard Operating Procedure
SOS	Son of Sevenless
SSC	Side Scatter
SSC-A	Side Scatter Area
SSC-H	Side Scatter Height

STAT	Signal Transducer and Activator of Transcription
Sucnr1	Succinate Receptor 1
TBS	Tris-Buffered Saline
TBST	Tris-Buffered Saline + Tween
TCA	Tricarboxylic Acid
TCR	T Cell Receptor
T_{fh}	T follicular
TG	Triglycerides
TGFβ	Transforming Growth Factor Beta
Th	T helper
T_{mem}	Memory T Cell
T_{nai}	Naïve T cell
TNFAIP3	TNFα-induced Protein 3
TNFRSF	Tumour Necrosis Factor Receptor Superfamily
TNFα	Tumour Necrosis Factor Alpha
TRAF	TNF-Receptor Associated Factors
T_{reg}	T regulatory
TSN	Transforming Growth Factor Beta
UC	Ulcerative Colitis
UCP	Uncoupling Proteins
UGCG	UDP-Glucose Ceramide Glucosyltransferase
UQCRC	Ubiquinol-cytochrome c oxidoreductase
UTR	Untranslated Region
VAV1	Vav Guanine Nucleotide Exchange Factor 1
WT	Wild Type
XF	Extracellular Flux

Zap-70	Zeta-chain-Associated Protein kinase 70
µg	microgram
µl	microlitre
µM	microMolar

List of Figures

List of Tables

Chapter 1 | Introduction

1.1 Immune Mediated Inflammatory Diseases (IMIDs)

Autoimmune or immune-mediated inflammatory disease (IMIDs) represents a significant burden on both patient and healthcare resources, affecting around 1% of the population within Western societies (El-Gabalawy et al., 2010). Disorders include, but are not limited to: rheumatoid arthritis (RA), systemic lupus erythematosus (SLE), Crohn's disease (CD), psoriatic arthritis (PsA), ulcerative colitis (UC) and ankylosing spondylitis (AS), collectively described under the "IMID" term due to dysregulation within common inflammatory pathways (Rahman et al., 2010). These similarities between these diseases and their inflammatory pathways are additionally emphasised through the use of single biologics on multiple IMIDs. An example is the use of tocilizumab in both rheumatoid and giant cell arthritis, or infliximab administration in patients suffering from CD, RA and PsA (reviewed Scott et al., 2017; Melsheimer et al., 2019).

Despite a common inflammatory imbalance, clinical manifestations of IMIDs vary - with some conditions limited to certain tissues, whilst others are systemic in nature. IMIDs, however, are believed to undergo sequential phases of failed regulation of inflammatory mechanisms associated with (1) initiation and (2) propagation phases, and (3) resolution of IMID-associated inflammatory imbalance (figure 1.1) (Rosenblum et al., 2015). The aetiology of such inflammation is unclear, yet are hypothesised to occur by two main mechanisms: (1) exertion of chronic inflammation due to perturbed control between the innate and adaptive immune responses; and (2) persistent inflammation arising from reactivation of adaptive memory immune cells and/or loss of lymphocyte tolerance. Such hypotheses are not mutually exclusive, however, with dysregulation of both adaptive and innate arms observed. Dysregulated changes contribute towards the imbalance of inflammatory processes, which are central to IMID

pathogenesis: these include the altered dialogue between the antigens presented *via* MHC, resultant changes in cell and cytokine signalling, and the persistence of leukocytes within the site of inflammation, including T cells (Rahman et al., 2010). Taken together, highlighting the role of the immune response in IMID development.

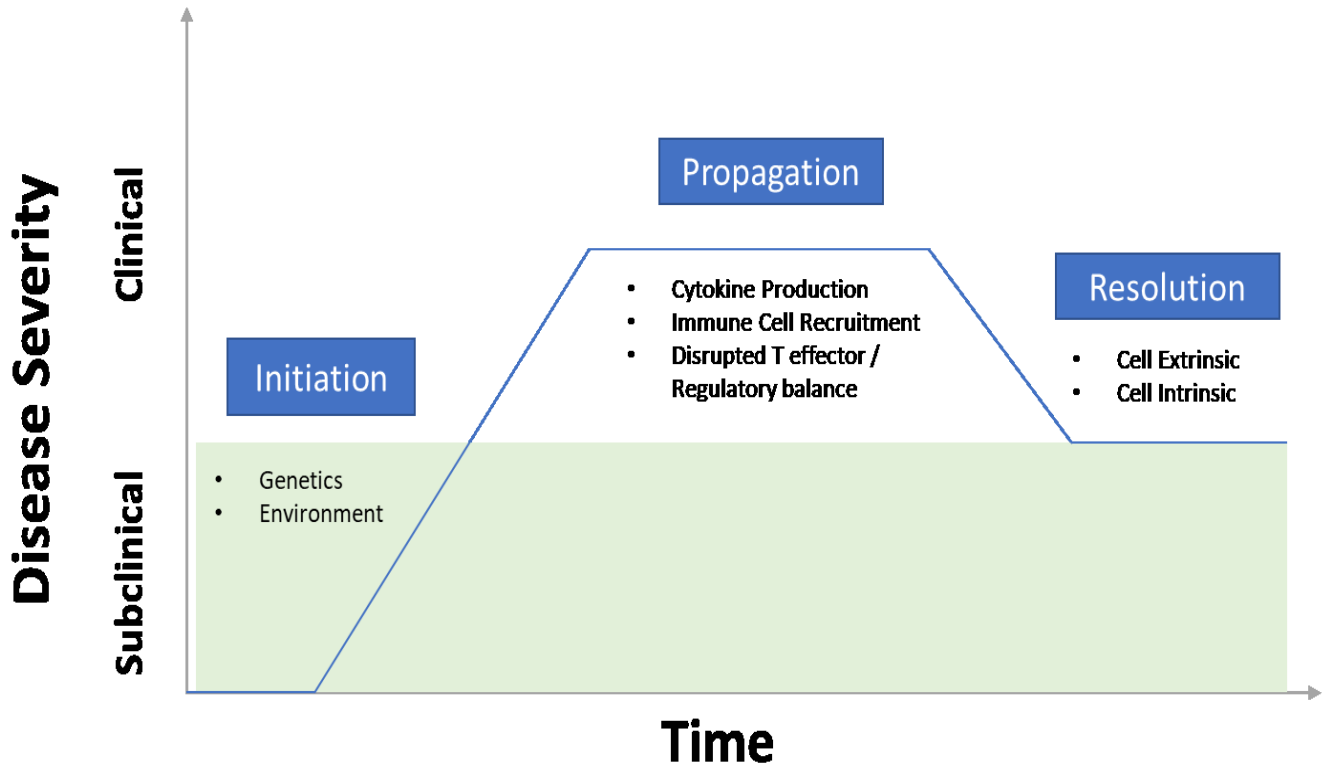

Figure 1.1 – Overview of autoimmune disease phases. Immune-mediated inflammatory disease can be broadly split into (1) initiation; (2) propagation and (3) resolution phases, in pathogenesis is initiated by a combination of genetic predisposition and environmental factors; patients are typically unaware of disease (subclinical) until manifestation of clinical symptoms, propagated by the onset of self-perpetuating inflammation and tissue damage due to cytokine production and immune cell recruitment, epitope spreading and T cell imbalance. Autoimmune reactions resolve with the activation of inhibitory (cell-intrinsic) and regulatory T cell functions; however, fails to resolve to baseline levels. Patients may also suffer from relapse and recurring disease propagation phases. Adapted from Rosenblum *et al.,* (2015).

1.1.1 Rheumatoid Arthritis

Affecting 0.5-1% of the world population, RA is a chronic immune-mediated disease primarily of the joints that results in the progressive decline of mobility and independence of the individual affected (Rudan et al., 2015). The formation of the inflammatory foci at the peripheral joints attributed to the persistence of a mixed inflammatory cell infiltrate and synovial hyperplasia, which ultimately results in erosive bone and cartilage destruction. Additional systemic involvement of other physiological systems may also be observed, such as cardiovascular and respiratory systems – intricately linked to the increased morbidity and mortality rate amongst RA patients (Crowson et al., 2013, Shaw et al., 2015).

As with the majority of IMIDs, the aetiology of RA has not been clearly elucidated; however, it is thought that both genetic and environmental risk factors play an important contributory factor in the onset and pathogenesis of RA (Yarwood et al., 2016). Those with a family history of the disease are shown to have an increased risk of RA development, with genetic risk factors accounting for 60% RA susceptibility as shown by previously conducted twin studies (MacGregor et al., 2000, Silman et al., 1993). However, these studies highlight the additional contribution of environmental factors in disease development: for example, smoking and excess BMI are thought to be factors associated with the development of future RA (de Hair et al., 2013, Arnson et al., 2010). Such correlations can appear conflicting, with no significant relationship found between smoking and RA, whilst increasing BMI is shown to be protective in certain circumstances (van de Stadt et al., 2013, Turesson, 2016, Ljung and Rantapaa-Dahlqvist, 2016).

Genome-wide association studies (GWAS) have additionally characterised hundreds of single nucleotide polymorphisms (SNP) associated with RA. The strongest genetic association with RA is on chromosome 6p21 of the human leukocyte antigen (HLA) region, previously described by Gregersen et al. (1986) to house a conserved sequence strongly related to HLA-DRB1 that encodes the β-chain of MHCII. Alleles of this gene differ between ethnic groups; however, given its role in antigen presentation during disease and infection, suggests a likely role in the dysregulated presentation of non-infectious self-peptides to the immune system (Yang et al., 2013b, Mourad and Monem, 2013, Newton et al., 2004, Bridges et al., 2008). For example, it is well understood that the development of autoimmune disease is highly dependent on T cell response to inappropriately presented self-antigens - largely ascribed to the defective removal of autoreactive T cells during thymic negative selection processes. Sakaguchi and colleagues describe point mutations within the Zap-70 gene in which thresholds of T cells to thymic selection is altered, resulting in the positive selection of autoimmune T cells, whilst mice with the induced mutation also developed autoimmune arthritis similar to that of human RA, due to their high autoreactive T cell repertoire (Sakaguchi et al., 2003). Other alternative signalling molecules have also been highlighted in GWAS, including PTPN22 – encoding lymphoid tyrosine phosphatase (LYP), a key negative regulator of T cell response (Suzuki et al., 2011).

1.2 T Cell Subtypes

T cells dramatically alter their characteristics to fulfil required functionality, involving cellular differentiation from their quiescent, prior non-activated naïve state to a more specialised subset. The differentiation of naïve T cells dependent on the external stimulus suitable to the immunological requirement: for example, early immune response is associated with T helper (Th)1 (Th_1) cell activity, whilst later immune

responses is associated with Th_2 cells (Kaiko et al., 2008). The differentiation of cells primarily mediated by the upregulation of lineage-specific inducing cytokine signalling pathways, and the attenuation of alternative lineage skewing cytokine responses by suppressor of cytokine signalling (SOCS) family of proteins (Palmer and Restifo, 2009).

Unsurprisingly, cytokines are considered well established key modulators of T cell differentiation and activity, with production proposed to underlie lineage differentiation of CD4+ T cells into one of the seven subpopulations. Extrinsic IL-12, as well as, IFNγ signalling for example, induces Th_1 development downstream of Signal Transducer and Activator of Transcription (STAT)1 and the subsequent upregulation of Th_1 transcription factor T-bet (Afkarian et al., 2002). This results in the expression of a proinflammatory cytokine profile incorporating cytokines such as further IFNγ, tumour necrosis factor alpha (TNFα) and TNFβ production (Murphy and Reiner, 2002). These proinflammatory properties mean Th_1 cells are suited for upregulation of the innate immunity, such as modulation of macrophage and CD8+ activity; pathogen clearance and anti-tumour immunity. In turn, IFNγ/STAT1-mediated differentiation appears to be negatively regulated by IL-6 induced expression of SOCS1, by which genetic ablation augments Th_1 generation (Palmer and Restifo, 2009, Alexander et al., 1999, Eyles et al., 2002).

Defined by their predominantly ‘anti-inflammatory’ expression of IL-4, IL-5, IL-10 and IL-13 cytokines, Th_2 responses are imperative in the neutralising extracellular pathogens through mediation of the humoral response (Alexander et al., 1999). Differentiation indispensably relies on the upregulation of Th_2 master regulator GATA3 in response to IL-2 and IL-4 signalling, although some evidence suggests the existence

of alternate IL-4-independent GATA3 activation pathways (Ouyang et al., 1998, Seki et al., 2004). GATA3 is shown to downregulate STAT4 and prevent Th_1 skewing through inhibition of T-bet binding at Th_1 genes: *in vivo* ablation in mice meanwhile is shown to divert naïve T cell differentiation towards Th_1 lineage, whilst reduction in GATA3 interrupts Th_2 lineage development (Kanhere et al., 2012, Pai et al., 2004, Zhu et al., 2004, Usui et al., 2003).

Shared characteristics and plasticity observed between Th_1 and Th_2 lineage has led to the identification of several additional T cell subtypes, including: T regulatory (T_{reg}), Th_9, Th_{17}, Th_{22}, and T follicular (T_{fh}) cells. For example, clarification of Th_{17} came from investigations into T_{reg} differentiation, in which naïve T cell stimulation with TGFβ upregulates forkhead box P3 (FOXP3) expression and promotes inducible T_{reg} (iT_{reg}) differentiation (Chen et al., 2003, Fantini et al., 2004). iT_{reg} and T_{reg} are understood to share similarities to effectively maintain T cell tolerance, yet when TGFβ is signalled alongside IL-6 or IL-21, cells are polarised towards producing a Th_{17} phenotype (Bettelli et al., 2006, Mangan et al., 2006). This results in the upregulation of transcription factor RORyt (retinoic-acid receptor related orphan (ROR) gamma T) and simultaneous degradation of FOXP3, producing a number of additional proinflammatory cytokines, including IL-17, IL-6, TNFα, IL-21 and IL-22 (Dienz and Rincon, 2009, Gao et al., 2012, Damsker et al., 2010). Interestingly, in naïve T cells both FOXP3 and RORyT are expressed following stimulation; however, IL-6/IL-21 induces FOXP3-mediated inhibition (Zhou et al., 2008). As such, the cytokine milieu influences effector differentiation.

Th_9 and Th_{22} are two more recently discovered T cell lineages, of which the former is derived from TGFβ signalling in the presence of immunomodulatory cytokine IL-4

(Veldhoen et al., 2006, Dardalhon et al., 2008). Specifically, Th_9 are the only source of IL-9 cytokine production - expressed under the control of transcription factors PU.1 and interferon regulatory factor (IRF)-4. These cells play a subsequent mediatory role in inflammatory processes, including in autoimmune disease: IL-9, for example, is correlated with the incidence of UC, with both IRF4 and IL-9 deficiency of in murine oxazolone-induced colitis shown to reduce disease scoring (Mudter et al., 2008, Gerlach et al., 2014). By contrast TGFβ is shown to inhibit Th_{22} generation, a subset characterised by IL-22 production in response to IL-1β, IL-6 and TNFα signalling (Duhen et al., 2009). Th_{22} were first identified in patients with dermal inflammatory skin disease, with a growing evidence base for roles in other autoimmune conditions (Kagami et al., 2010, Zhang et al., 2011, Mirshafiey et al., 2015, Sugita et al., 2013). For example, recent studies show that Th_{22} contribute to RA joint destruction through IL-22 mediated promotion of osteoclast differentiation (Miyazaki et al., 2018). Interestingly, IL-22 also forms part of the Th_{17} repertoire; yet, due to the inhibitory role of TGFβ on IL-22 signalling, Th_{17} polarisation is not favourable for the production of IL-22 (Ghoreschi et al., 2010).

Finally, T_{fh} differentiation is mediated through transcription factor B cell lymphoma (BCL)-6 and is noted to mediate B cell responses through maturation and the initiation of germinal centre formation (Crotty, 2014). Activation of these cells results in the migration to B cell follicles, this follows the upregulated expression of the homing chemokine receptor CXCR5 (C-X-C Motif Chemokine Receptor 5) (Breitfeld et al., 2000). Once migrated, T_{fh} employ a number of cell surface receptors and cytokine release to mediate B cell activity, including expression of co-stimulatory molecules inducible co-stimulator (ICOS), CD40 ligand (CD40L), IL-4 and IL-21 (Crotty, 2014).

1.3 Role of T cells in Autoimmunity

The immunological inertness to self-antigens is a defining feature of 'tolerance', in which the immune system is prevented from targeting self-molecules, cells and tissues by means of a selection processes. The concept of tolerance, first postulated in 1948, was proposed as a characteristic acquired during organismal development, as opposed to an innate feature: supported by studies by Peter Medawar demonstrating the ability to induce immune tolerance to foreign grafts in embryonic mice (Medawar, 1948). The subsequent induction of thyroiditis by autoantibodies was indeed shown to be prototypic for autoimmunity, denoting the integral role of tolerance in tissue homeostasis (Rose and Witebsky, 1956). As such, selection appears to be key in defining an individual's immune cell repertoire. For T cells specifically, tolerance primarily occurs within the thymus.

Prior to this, T cells undergo development from haematopoietic progenitors within the bone marrow ahead of thymic migration. Here T cell precursors undergo further maturation, during which they acquire a functional T cell receptor (TCR) and undergo delineation into CD4+ or CD8+ co-receptor positive mature populations, as well as additional selection processes within the thymic cortex (Wang and Bosselut, 2009, Vrisekoop et al., 2014). T cells that are autoreactive are primarily selected against within the medulla and removed before circulation following engagement with tissue specific antigens on thymic epithelial cells, expressed under the control of transcription factor autoimmune regulator (AIRE) (Anderson and Su, 2011). Those that demonstrate high affinity for self-antigens undergo removal by apoptosis, whilst autoreactive mature T cells are rendered anergic through further peripheral selection processes; autoreactive T cells may also be subjected to differentiation into regulatory T cells (T_{reg}) by means of clonal diversion (Xing and Hogquist, 2012). The resulting 'non-self' mature

CD4+ and CD8+ T cell populations can be broadly defined by their different functionalities: CD4+ T cells interact with phagocytosed exogenous peptides presented on MHCII expressed by antigen presenting cells (APCs), whilst CD8+ T cells engage with cognate receptor MHCI which presents peptides derived from transcription - a key function for cytotoxic T cell detection and removal of intracellular pathogens (Blum et al., 2013, Zhang and Bevan, 2011).

1.3.1 The Role of T cells in RA Development

Despite central and peripheral selection, self-reactive cells maintain the ability to inhabit the normal immune cell repertoire, suggesting processes within the thymus and bone marrow may not be completely sufficient. In T cell transgenic models, as many as 25-40% of autoreactive T cells are shown to escape clonal deletion despite absence of the deleting ligand (Bouneaud et al., 2000). Selection processes seemingly interdependent on B cell activity, in which B cell deficiency in autoimmune prone models removes populations of activated T cells (Yan and Mamula, 2002). Thymic output also appears to increase on encounter with self-antigen in a number of studies, following secondary rearrangement of the T cell receptor (TCR) (Buch et al., 2002).

Autoreactive T cells are therefore widely recognised to contribute towards IMID pathogenesis – albeit with a lack of mechanistic clarity. As previously mentioned, evidence suggests that CD4+ T cells primarily contribute to autoimmunity through association with MHCII alleles, including HLA-DR1 and HLA-DR4. Genes encoding a common amino acid sequence, also termed shared epitope (SE), within the MHCII third hypervariable antigen-binding region, and are indicated in a number of studies to be associated with autoimmune disease development and severity, including RA (Boki et al., 1993, Fugger and Svejgaard, 2000, Viatte et al., 2015). HLA-DRB1 alleles are

associated with the increased production of anti-citrullinated peptide autoantibodies (anti-CCP) – a post-translational modification thought to induce autobody production through generation of citrullinated neo-epitopes (Snir et al., 2009, de Brito Rocha et al., 2019, Pedersen et al., 2007). It is shown that such modifications render peptide binding to MHC (pMHC) antigenic regions more readily within SE allele seropositivity; increased citrullinated-pMHC resulting in increased CD4+ T cell activation within SE-positively expressing mice (Hill et al., 2003). The findings together propose a possible mechanism for autoimmune development in response to citrullinated peptides within SE positive patients, supported by positive correlations between the presence of both SEs and anti-CCP autoantibodies (Lundberg et al., 2005, van Gaalen et al., 2004). Interestingly, T cells specific for post-translational modifications such as citrullination are shown more recently to avoid thymic selection, resulting in the possible escape of autoreactive T cells from central tolerance (Raposo et al., 2018).

1.3.2. The Role of T cells in Established RA

T cells play a key role in disease pathogenesis of affected RA joints, assisting in the coordination of the inflammatory milieu following infiltration of the synovial membrane (figure 1.2). Within this environment, antigen-presenting cells (APCs) mediate the inflammatory recruitment of T cells to the site, enabling T cells to interact with other cells and propagate disease pathogenesis. This includes the T cell-stimulated release of proinflammatory cytokines from resident stomal and myeloid cells, including synovial fibroblasts, tissue resident macrophages and recruited monocytes, as observed during *in vitro* co-culture experiments (McInnes et al., 1997, Tran et al., 2007, van Hamburg et al., 2011, Sebbag et al., 1997). T cells are also shown to interact with B cells – forming tertiary lymphoid amalgamates to facilitate B cell differentiation and self-autoantibody production (Pitzalis et al., 2013).

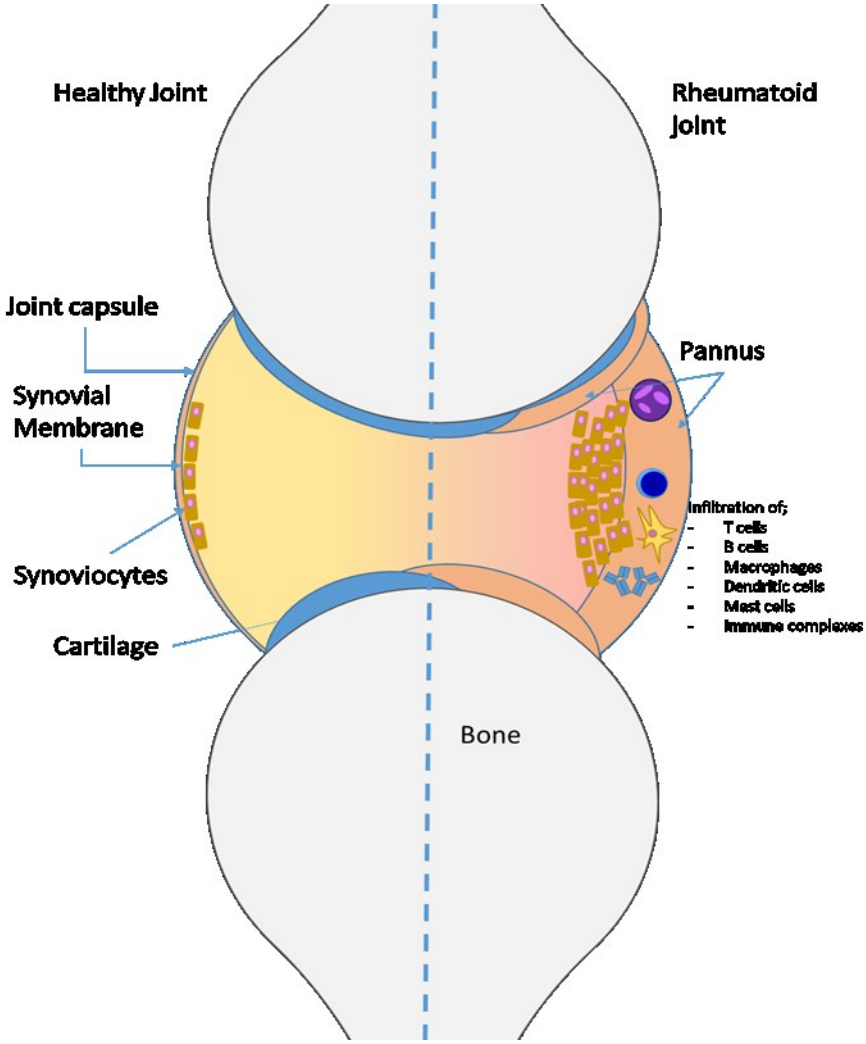

Figure 1.2 – Overview of Disease Pathogenesis within the Rheumatoid Arthritis (RA) Joint. The synovial membrane lines the healthy joint (left), which during RA (right) becomes hyperplastic and infiltrated by chronic inflammatory cells such as T cells, B cells, macrophages, dendritic cells and mast cells. This leads to the formation of the 'pannus' which migrates onto and into the underlying bone and articular cartilage that leads to joint and cartilage destruction. Pannus formation is driven by various immune modulators (cytokines and effector cells) involved in RA pathogenesis. This begins with presentation of RA-associated antigens such as rheumatoid factors and citrullinated proteins by dendritic cells, macrophages and activated B cells to T cells. Concurrently, binding of RA-associated antigens to mast cells result in their degranulation and release of vasoactive mediators which promote immune cell infiltration including T cells; RA related peptide binding to T cells results in their clonal expansion in the joint as well as secretion of proinflammatory cytokines such as IL-2 and IFNγ into the synovial membrane, leading to a feedback loop for additional T cell, macrophage and B cell interactions. Macrophages differentiate and contribute to osteoclastogenesis, whilst the additional recruitment of synoviocytes results in destruction of cartilage and bone by direct invasion into the tissue.

T cells are also additionally noted to play a prominent role in perturbating the chronic inflammatory environment within the RA joint through cellular plasticity, in which differentiation of naïve and activated T cells, along the Th_1-T_{reg}-Th_{17} axis, is observed. Indeed, increased Th_{17} levels positively correlate with disease activity in early and established RA, with subsequent knockout of characteristic IL-17 or depletion of Th_{17} pools to unsurprisingly ameliorate RA development (Nakae et al., 2003). The secretion of IL-17, for example, is widely recognised to contribute to disease pathogenesis, including the establishment of osteoclastogenesis within the RA joint, even in the absence of osteoblasts (Kotake et al., 1999, Yago et al., 2009). However, prior studies additionally note that the Th_{17} phenotype appears somewhat instable, leading to the readiness of Th_{17} cells to shift towards other T cell subtypes. In sera of untreated and early RA patients, increased ratios of Th_{17}-derived Th_1 cells versus CD161+ Th_{17} cells were indeed observed in parallel with the inverse correlation between anti-CCP autoantibodies and IFNγ levels, meanwhile in juvenile RA patients, Th_{17} and Th_1 cells demonstrate dual expression of Th_{17}/Th_1 transcription factors, T-bet and receptor-related orphan receptor C2 (Kotake et al., 1999, Nistala et al., 2010). Although Th_{17} cells within the synovial membrane additionally also show ability to differentiate into $T_{regs,}$ during RA, these cells take up a suppressive role within the inflammatory environment, rather increasing their movement towards a Th_{17} phentoype (Gao et al., 2015, Nie et al., 2013, Wang et al., 2015).

Although failure to resolve the proinflammatory environment is key in RA, studies suggest that the contribution made by T cells may be heterogenous in nature. Accordingly, early RA is characterised by a distinct increase in proinflammatory cytokine expression profile, comprising IL-2 IL-4, IL-13, IL-17, as well as fibroblast and epidermal growth factor, after which 3 months post-symptom onset was no longer

present in established disease (Raza et al., 2005). Rather early studies propose a role in established disease, whereby synovial T cells demonstrate anergy in the absence of IL-2 production (Firestein et al., 1988, Allen et al., 1995). The analysis of RA patient sera additionally revealing resistance of T cells to undergo apoptosis – ascribed to the possible pro-survival interactions made between the T cell population and other synovial cells, such as fibroblasts (Salmon et al., 1997). Secretion of IL-2, IL-4 and IL-15 may also be attributed to apoptotic resistance due to their downstream anti-apoptotic effects (Raza et al., 2005). As such, these studies may suggest a role for T cells in which activation and differentiation play an integral role in initiating an autoimmune inflammatory response; however, once established play a passive role through interactions with other cells within the synovium.

1.4 T Cell Activation

The activation of T cells involves a complex milieu of signalling factors summarised by a two-step model involving engagement of the TCR and a co-stimulatory molecule, typically CD28 (Bretscher and Cohn, 1970, Lafferty et al., 1978). Naïve T cells when activated undergo clonal expansion and differentiation into different effector subtypes. A small fraction becoming long-lived memory T cells which remain poised to subsequent re-encounters with a given antigen; the majority of other activated T cells, meanwhile undergo apoptotic clearance following stimulating-antigen removal (Omilusik and Goldrath, 2017, Zhan et al., 2017).

1.4.1 Signal 1: T Cell Receptor

TCR engagement alone does not provide enough stimuli to overcome the activation threshold required to illicit a T cell response; however, engagement is crucial for

both naïve T cell survival and the initiation of signalling pathways for cellular differentiation. Tightly controlled, TCR signalling is mediated by the effects of protein tyrosine kinases (PTK) and protein tyrosine phosphatases, phosphorylating and dephosphorylating tyrosine residues respectively on the intracellular domains of the TCR gamma chains to induce downstream effects. The strength of signalling is considered to be correlated to the affinity of pMHC, in which low affinity binding is significantly less potent than high affinity ones, as demonstrated in CD8+ T cells (Tian et al., 2007). Yet, due to the number of self- versus foreign antigens with small differences in pMHC affinity, more TCRs are likely to engage with the former (Jansson, 2011). As such, it is proposed that TCRs engage with pMHC by means of kinetic proofreading and potentially explains the observed low levels of TCR stimulation despite an excess of self-antigens (McKeithan, 1995). Longer ligand binding half-life to a few receptors encourages improved signalling compared with short-lived ligand binding to many receptors due to a quick reset of downstream signalling following dissociation of a long half-life antigen ligand. In combination with the degenerate nature of TCR, this prevents successive short-antigen binding from mimicking a long binding event and overcoming the TCR activation threshold (Daniels et al., 2006, Crites and Varma, 2010, Jansson, 2011).

The TCR appears to play a central role in effector phenotype differentiation. As mentioned, the degenerate nature of TCR leads to varying signal strengths. Weak signals that sufficiently activate CD4+ T cells promote Th_2 differentiation, while strong signals typically result in the development in Th_1 phenotypes. In a study by Siggs et al. (2007) $ZAP70^{mrd/mrd}$ mice exhibit lower TCR signalling: resulting in seemingly lower Ca2+ mobilisation and elevated immunoglobulin (Ig) G1 and IgE, indicative of a Th_2 response. Moreover, transgenic depletion of high affinity T cells for p-MHCII within a

polyclonal population to leave low affinity T cells only, leads to IL-4 production – a cytokine characteristic of Th_2 phenotypes (Milner et al., 2010). This phenotype, however, was not seen in the original polyclonal population, suggesting cells with high affinity outcompete lower affinity cells, preventing them overcoming the activation threshold and differentiating.

1.4.2 Signal 2: TCR Co-stimulation

Signal 2 is a co-stimulatory signal which synergises with signal 1 to overcome the activation threshold. As mentioned, the *'two signal model'* of activation originally described by Bretscher and Cohn (1970) states that both TCR stimulation and a co-stimulatory signal is required for T cell activation. A finding further clarified by Lafferty et al. (1978) reinforced by findings showing MHC preloaded with peptide failed to activate T cells through TCR stimulation in the absence of additional co-signals. The addition of a co-stimulator is thought to amplify TCR signals due to overlap between the signalling pathways.

1.4.2.1 CD28

CD28 is a founding 44-kDa glycoprotein member of a costimulatory receptor subfamily which binds CD80 (B7-1) and CD86 (B7-2) on APCs during states of inflammation. Other members include ICOS (inducible T cell costimulatory), CTLA4 (cytotoxic T lymphocyte associated protein 4) as well as programmed cell death protein (PD-1), in which ligation of the TCR or CD28 results in target binding via intracellular SH domains in a phosphotyrosine-dependent manner, as facilitated by Lck and Fyn kinase activity (Raab et al., 1995, King et al., 1997, Boomer and Green, 2010b). In turn, phosphatidylinositol-3 kinase (PI3K) and growth factor receptor bound protein 2 (Grb2) mediate downstream receptor signalling: the membrane-proximal YXXM motif, for

example, is a shared consensus site for p85 of the lipase kinase phosphohatidylinositol-3-kinase (PI3K) by CD28, CTLA4 and ICOS - in which activation induces phosphoinositide-dependent kinase (PDK1) and protein kinase B/Akt activity to mediate CD28 functions, including IL-2 transcription (August and Dupont, 1994, Pagès et al., 1994, Prasad et al., 1994, Boomer and Green, 2010b, Esensten et al., 2016). Meanwhile ICOS and CTLA4 lacks the ability to bind adaptor protein Grb2; instead binding son of sevenless (SOS) and guanine nucleotide exchange factor VAV1 that promote AP-1 transcription via c-Jun N-terminal kinase (JNK) and extracellular signal-regulated kinase (ERK) signalling (Kim et al., 1998). CD28-Grb2 binding is also reported to activate transcription factor nuclear factor of activated T cells (NFAT), whilst in combination with GAD mediates formation of upstream NF-κB activating complex CARMA1-Bcl-10-Matl1 (Chow et al., 1999, Dienz et al., 2007, Takeda et al., 2008, Watanabe et al., 2006). Elsewhere, VAV is shown to bind to SLP-76 (lymphocyte cytosolic protein 2) / LAT (linked for activation of T cells) complex, activating phospholipase PLCγ1 that leads to increased intracellular calcium.

The stimulation of CD28 subsequently leads to IL-2 expression, from which mutagenesis studies have shown the RE/AP (CD28-response elements) site to be central for signal integration at the IL-2 gene promotor region (Shapiro et al., 1998, Shapiro et al., 1997, Butscher et al., 1998, McGuire and Iacobelli, 1997). Within this, the IL-2 promoter region has binding elements for transcription factors AP-1, NFAT and NF-κB (Shapiro et al., 1997, McGuire and Iacobelli, 1997). Once synthesised, IL-2 mediates a number of effector functions – namely T_{reg} functionality. Indeed, deficiency in IL-2 and IL-2R is shown to have impaired development and function

of T_{reg} cells: during which cell numbers decline (Malek et al., 2002, Fontenot et al., 2005, Barron et al., 2010). Conversely, low levels of IL-2 promote Th_{17} production.

1.4.2.2 TNFRSF: Tumour Necrosis Factor Receptor Superfamily

Similar to CD28, receptors of the TNF receptor superfamily (TNFRSF) synergise with TCR signalling. These additional signals help promote T cell survival, cytokine production, as well as facilitate progression through the cell cycle. The cognate binding of APC ligands to TNFRSFs result in the recruitment of intracellular TNF-receptor associated factors (TRAF) (Chen and Flies, 2013); different members of the TNFRSF activate signalling through various TRAFs. For example, anti-apoptotic TNFRSF members, CD134, CD137 and CD27 bind TRAF1/2/3, TRAF2/3/5 and Traf2/3/5/Siva1, respectively (Croft et al., 2012). This leads to the upregulation of PI3K and promotes the expression of anti-apoptotic proteins BCL-2 and BCL-XL (So and Croft, 2013). Interestingly, the binding of Siva1 by CD27 should lead to apoptosis, due to its ability to modulate BCL-2 and ability to elicit caspase activation *via* death domain homology; however, acts as a survival signal following co-stimulation (Croft et al., 2012, Py et al., 2004). Moreover, association with similar TRAFs leads to upregulation of similar genes. TRAF2 is shown to be involved in JNK and NF-κB activation, yet recruitment of respective TRAFs leads to Th_1 cytokine profile expression on TNFRSF14 (HVEM) binding, whilst binding of CD30 has pleiotropic effects on T cell activation and survival - predominantly through NF-κB upregulation and ERK-associated pathways (Steinberg et al., 2011, Croft et al., 2012, Chen and Flies, 2013). It is clear that the effects of TNFRSF molecules cannot be defined by their associated TRAFs, suggesting additional molecules may further elucidate their function downstream.

1.4.3 Signal 3: Cytokines

Lafferty's two signal model has been crucial in understanding immune response (1978). However, understanding how effector function develops has been less clear. Although the absence of signal 3 does not prevent T cells from activating, it is crucial for development of effector function. Early studies describe increased CD4+ and CD8+ T cell proliferation in response to cytokines IL-1 and IL-12 respectively, yet in their absence diminishes effector expansion and downstream function (Magram et al., 1996, Kieper et al., 2001, Ben-Sasson et al., 2009, Curtsinger et al., 1999). The modes of action by which cytokines elicit their effects are also time dependent: for example, timing of IFNγ-mediated post-infection is shown to determine T cell fate towards apoptosis or cellular activation (Crouse et al., 2015).

1.4.3.1 Interferon gamma

Expressed by Th_1, IFNγ is required for MHCI and MHCII expression for the subsequent activation of macrophages and pathogenic removal. It binds to IFNGR1 and IFNGR2 subunit that are expressed on a wide variety of cell surfaces (Ramana et al., 2002). Dimerization of these subunits leads to phosphorylation of Janus Kinase (JAK)1, JAK2 and phosphorylation of STAT1 homodimer, subsequently leading to the upregulation of master transcription factor T-bet (Ramana et al., 2002, Afkarian et al., 2002). T-bet upregulates the expression of IL-12, leading to the activation of STAT4 and further expression of IFNγ and upregulated IL-18 production - a cytokine involved in the mature Th_1 response (Afkarian et al., 2002). Additionally, the effects of IL-12 alone can upregulate IFNγ production in mature Th_1 independently of TCR signalling. IFNγ produced by mature Th_1 cells acts as an autocrine signal that reinforces STAT1 activation yet can signal in a paracrine manner to activate naïve T cells (Szabo et al., 2000, Afkarian et al., 2002). This leads to the development of additional Th_1. Moreover, IFNγ is also linked to the modulation of autoimmunity, in which IFNγ-

deficient mice with collagen-induced arthritis showed increased inflammatory lesions versus wild type (Vermeire et al., 1997). Certainly following administration of anti-CD3, deficient mice demonstrated significantly higher IL-2 and lower IL-4 levels, suggesting IFNγ upregulates the latter to prevent arthritic development. Taken together suggesting that the dysregulation of IFNγ production is therefore likely to involved in the promotion of autoimmunity.

1.4.3.2 IL-1

IL-1 is a family of 11 cytokines, of which IL-1α and IL-1β are of particular interest (Akdis et al., 2011). Although there is little shared homology with between members of the IL-1 family, both IL-1α and IL-1β share biological properties. Ben-Sasson and colleagues (2009) demonstrated the effects on IL-1β on CD4+ T cells, in which exposure to the cytokine led to increased expansion of both naive and memory T cell (T_{mem}) populations, independent of other inflammatory cytokines (Ben-Sasson et al., 2009). In addition, when cells were exposed to an IL-1 receptor antagonist, antigen response diminished. The importance of IL-1 is also highlighted within the deficiency of IRAK-4 within humans, a signalling molecule required for correct signal transduction from the IL-1 receptor. Patients with this deficiency suffer from recurrent bacterial infections and lack of Th_{17} functionality (Heiseke et al., 2015, Picard et al., 2010). Similar findings have been echoed in IRAK4-deficient mice, who demonstrated impaired responses to viral and bacterial infections (Suzuki et al., 2002).

1.4.3.3 IL-6

Produced by APCs in response to IL-1, TNFα, lipopolysaccharide (LPS) and platelet-derived growth factor (PDGF), IL-6 expression is well established in propagating cell proliferative responses and the development of the Th_2 phenotype (Akdis et al., 2011).

Response follows binding to the cognate receptor IL-6R-glycoprotein (gp) 130, eliciting downstream effector signalling including *via* the JAK/STAT pathway. Interestingly, though gp130 is ubiquitously expressed on most cells, IL-6R expression is limited to leukocytes and hepatocytes: the immunomodulatory and proliferative effects of IL-6 therefore appearing to be limited to these cells (Wolf et al., 2014). Where IL-6R is lacking, however, there is a requisite for signalling in gp130 positive cells to elicit IL-6 mediated effects. Trans-signalling is a process that facilitates this, in which soluble IL-6R (sIL-6R) produced through proteolytic shedding or alternative splicing mediates the pleiotropic effects IL-6 through IL-6/sIL-6R complex binding to gp130 (Wolf et al., 2014, Müllberg et al., 1993). Downstream of activation JAK activity upregulates Ras, leading to the phosphorylation of STAT3 and C/EBP (CCAAT/enhancer-binding protein beta) respectively (Dienz and Rincon, 2009). Though it is not fully elucidated, it is hypothesised that both STAT3 and C/EBP downstream of IL-6 cognate binding are able to move into the nucleus and upregulate the expression of c-maf and NFATc2 - leading to the upregulation of IL-4 (Dienz and Rincon, 2009). IL-4 autocrine signalling, combined with the expression of SOCS1, suppresses IFNγ production, which in turn is shown to stimulate T cell Th_2 phenotype development whilst suppressing Th_1 development (Diehl et al., 2000).

Excess levels of IL-6 are observed within IMIDs, including RA, yet its suppressive function on Th_1 development appears at odds with the Th_1 phenotype typically associated with RA pathogenesis. Discrepancies may be attributed to other T cell subsets, T_{reg} and Th_{17} cells, in which the latter is previously mentioned to differentiate in parallel with induced TGFβ signalling. Indeed, whilst TGFβ levels are shown previously to increase in RA patients, the development of Th_{17} cells may occur in its absence (Mieliauskaite et al., 2009, Ichiyama et al., 2011, Veldhoen et al., 2006,

Mangan et al., 2006). Interestingly, the presence of IL-6 is important for lineage decision-making at the Th_{17}:T_{reg} axis. TGFβ is known for its immunosuppressive effect on IL-6 signalling and as previously mentioned, the induction of T_{reg} differentiation from naive CD4+ cells (Fu et al., 2004). Meanwhile in the presence of IL-6, cells differentiate into Th_{17}; the blockade of subsequent IL-6 pathways by therapeutic targeting, such as tocilizumab, shown to increase the number of T_{regs} in RA patients (Pesce et al., 2013). Both IL-6 and TGFβ signalling upregulate RORyt, whilst degrading master T cell transcription factor FOXP3 – the downstream effect resulting in Th_{17} differentiation and product IL-17 cytokine expression (Dienz and Rincon, 2009, Gao et al., 2012).

1.4.3.4 IL-17

IL-17 is a family of six cytokines (IL-17A-F), expressed in numerous cell types across the body, with IL-17A and IL-17F being important to T cell function (Akdis et al., 2011). Both cytokine members are thought to be involved in the recruitment of neutrophils through Th_{17}-mediated IL-17 production during an immune response - indicating its role in the clearance of pathogens. As previously mentioned, IL-6 and TGFβ are requisite for Th_{17} differentiation, with the addition of IL-1 and IL-12 to promote IL-17 production in both memory and effector CD4+ T cells. In models of collagen-induced arthritis (CIA), knockout of IL-17 appeared to notably suppress disease severity compared to wild type (WT) mice, whilst IL-12 deficiency is shown to increase disease severity (Murphy et al., 2003, McIntyre et al., 1996, Nakae et al., 2003).

1.5 Overview of Cellular Metabolism

Cell metabolism can be broadly summed as the energetic status of the cell, defined by the complex array of biochemical reactions that occur within. All cells undergo similar metabolic processes, utilising macromolecules such as lipids, amino acids, nucleotides and carbohydrates as building blocks for largely catabolic, anabolic and maintenance reactions, as mediated by specific metabolic enzymes and their corresponding co-factors. As a result, metabolic reactions facilitate the ability for the cell to function: including the ability to grow, proliferate, migrate and elicit functional effects within the body. Energy metabolism, that is the production of high energy adenosine triphosphate (ATP) molecules, consists of four main processes: glycolysis, the tricarboxylic acid (TCA) cycle, oxidative phosphorylation (OXPHOS) and fatty acid oxidation - of which the latter three take place within the mitochondria (figure 1.3).

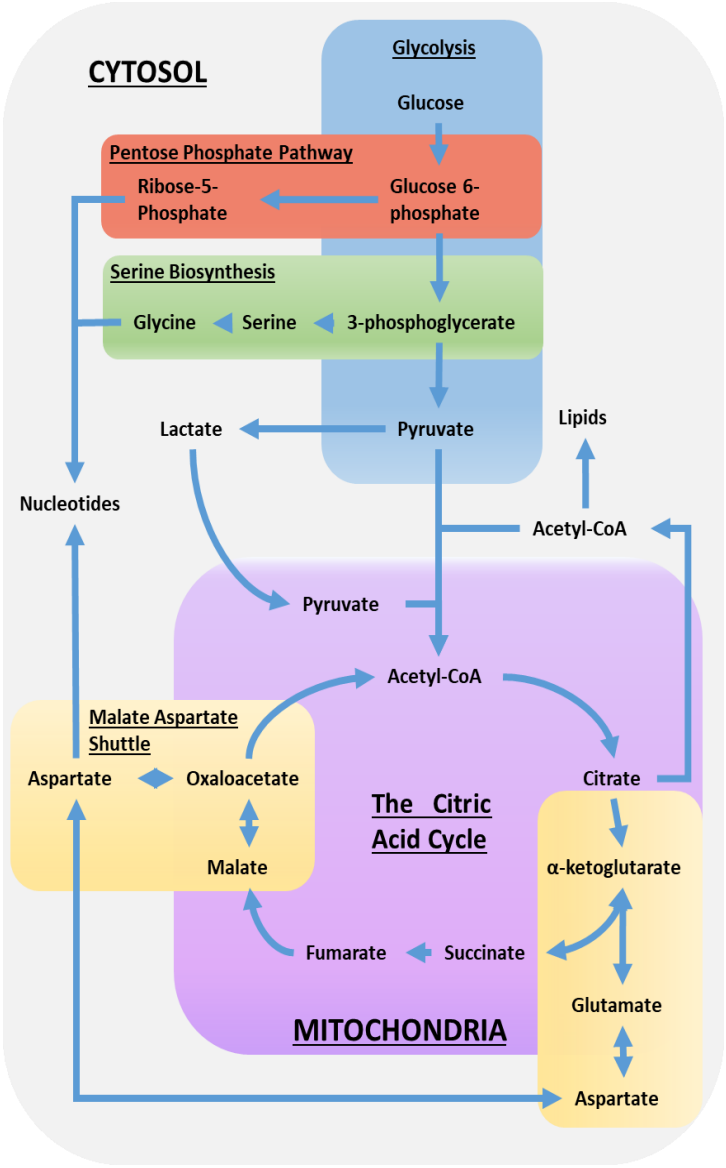

Figure 1.3 – Overview of cellular metabolism. Metabolic intermediates can be diverted from metabolic pathways macromolecules. Glucose-6-phosphate and 3-phosphoglycerate are formed during glycolysis (blue) can be used in the pentose phosphate pathway (red) or serine biosynthesis pathway (green), respectively, for nucleotide synthesis. Pyruvate enters the mitochondria and is converted to Acetyl-CoA. Similarly, lactate produced from increased aerobic glycolysis can also enter the mitochondria and be converted into pyruvate, prior to entering the tricarboxylic acid/citric acid cycle. Citrate produced can be converted to α-ketoglutarate or leave the mitochondria and be metabolised into acetyl-CoA prior to being converted into lipids for macromolecules for growth and proliferation. The malate-aspartate shuttle (yellow) involves the conversion of oxaloacetate to aspartate for use in nucleotide synthesis. Additionally, aspartate can be shuttled across the mitochondrial membrane via a glutamate-aspartate antiporter. Glutamate can be converted into α-ketoglutarate and re-enter the citric acid cycle. Similarly, aspartate can be converted back to oxaloacetate and into malate. This process allows the production of NAD+ and NADH for other metabolic processes.

1.5.1 Glycolysis

Glycolysis is the breakdown of glucose into either (1) pyruvate, under aerobic conditions or (2) lactate, under anaerobic conditions, which leads to the generation of ATP molecules. Production of these two metabolites begins within the cellular cytoplasm with the uptake of glucose, a carbon rich metabolite, from the extracellular environment *via* the transmembrane glucose transporter 1 (GLUT1) into the cell. Transportation of glucose can occur bi-directionally; however, rapid phosphorylation of glucose, utilising ATP as a phosphate source, traps glucose within the cell as glucose-6-phosphate (G6P). This phosphorylation is mediated by hexokinase (HK) enzymes HKI, HKII, HKIII and HKIV – of which HKI and HKII are most abundant, particularly in highly glycolytic dependent and insulin-sensitive tissues respectively (Wilson, 2003, Lowry and Passonneau, 1966, Purich and Fromm, 1971).

The kinetic parameters by which each isoenzyme are outlined to function are therefore markedly different: glucokinase HKIV is demonstrated to have 100 times greater affinity for glucose, yet alongside HKIII which has a high glucose affinity versus HKI and II, lacks the N-terminal domains that facilitate mitochondrial binding and subcellular localisation (Kogure et al., 1996, Houghton et al., 1996, Kumar et al., 2012). Thus, HKIII and HKIV are suggested to be likely associated with other metabolic glucose pathways outside the mitochondria, such as glycogenosis. Indeed, HKIV is not inhibited in the same manner as isozymes I-III – appearing seemingly more well adapted for glycogenic biochemistry that occur within the liver and pancreas, and by which HKIV is highly expressed (Houghton et al., 1996, Massa et al., 2011, Baldini et al., 2016). HKI by contrast is shown to have a strong binding affinity for mitochondria, which is not easily displaced by HKII: proposing a prominent role for this isozyme in catabolising glucose into G6P by glycolysis (John et al., 2011). In the same study,

HKII subcellular translocation is shown to be dynamically regulated by the presence of G6P and AKT, in which cytoplasmic location of HKII instead channels G6P into anabolic glycogen and pentose phosphate pathways rather than glycolysis. Such mitochondrial binding appears to reduce HK sensitivity to G6P, in which metabolite production is well understood in the literature to negatively regulate enzyme activity *via* allosteric inhibition (Azoulay-Zohar et al., 2004, de Cerqueira Cesar and Wilson, 2002). HKIII by contrast is most sensitive – perhaps attributed to the lack of N-terminal binding (Kumar et al., 2012).

Previous studies also show that physiological levels of intracellular phosphate (P_i) additionally appears to mediate cellular status, with reciprocal levels shown to mediate G6P regulation of HK activity (Purich and Fromm, 1971, Ellison et al., 1975, Fang et al., 1998). Increased levels are shown to antagonise G6P inhibition of HKI, yet P_i may further alter isozyme inhibition - alluding to its involvement in anabolic functions alongside HKIII and HKIV (Wilson, 2003).

Following HK-mediated conversion from glucose, G6P undergoes rearrangement by phosphoglucose isomerase into D-fructose-6-phosphate (F6P) *via* cis-enediol intermediate formation. The process by which involves acid-base catalysis that converts carbon 1 (C1) aldose of G6P into a ketose group on C2 of F6P in a reversible manner - dependent on the reciprocal levels of G6P and F6P (Berg et al., 2002). As such, conversion from G6P and F6P is therefore driven by low concentrations of F6P (Berg et al., 2002, Cordeiro et al., 2003). The resulting F6P is then phosphorylated, catalysed by enzyme phosphofructokinase coupled with ATP hydrolysis, into fructose 1,6-bisphosphate (F-1,6-P). It is this step in the pathway considered to be the rate-

limiting element of glycolysis, in which high ATP levels are shown to allosterically inhibit phosphofructokinase – lowering its binding affinity for F6P (Berg et al., 2002).

F-1,6-P is subsequently split into two three-carbon fragments products: (1) glyceraldehyde phosphate (GAP) and (2) dihydroxyacetone phosphate (DAP), catalysed by fructose biphosphate aldolase. The latter of which is readily interconverted to GAP by triose phosphate isomerase, in which ketonic DAP is isomerized to aldolic GAP through two successive proton transfers (Rozovsky and McDermott, 2007, Berg et al., 2002). Such a reaction is reversible; however, the reaction generally proceeds in DAP to GAP direction, due to the removal and use of GAP in subsequent glycolytic reactions (Berg et al., 2002). However, at equilibrium 96% of triose phosphate produced is DAP. The conversion of triphosphate molecules from glucose are summarised in the following equation:

$$Glucose + 2ATP + H^{+} \rightarrow 2GAP + ADP$$

Each GAP molecule undergoes the same reaction, in which oxidoreductase enzyme glyceraldehyde phosphate dehydrogenase (GAPDH) reduces NAD+ in parallel with GAP phosphorylation. The resulting reaction leads to the production of NADH + hydrogen (H^{+}) and 1, 3-bisphosphoglycerate (1,3-BPG), which in turn is converted to 3-phosphoglycerate (3-PG) by phosphoglycerate kinase (Berg et al., 2002). This reaction results in the release of P_i which also provides additional substrate for ADP to ATP formation. 3-PG then subsequently undergoes a three-step process before arriving at the formation of the terminal glycolytic product pyruvate: firstly involving the subsequent rearrangement by phosphoglycerate mutase to form 2-PG, by means of phosphoryl group transfer to C2 and (2) conversion of 2-PG to phosphoenolpyruvate

and water by enolase (Berg et al., 2002). Finally catalysed by pyruvate kinase, transfer of phosphoryl from phosphoenolpyruvate to ADP to form ATP results in the formation of pyruvate. As such, the reaction of glycolysis results in the net production of two ATP molecules plus two NADH and two H+:

$$Glucose + 2Pi + 2ADP + 2NAD^{+} \rightarrow 2Pyruvate + 2ATP + 2NADH + 2H_2O + 2H^{+}$$

If carried on indefinitely, glycolysis would result in the consumption of all bioavailable cellular NAD+ and eventually cease. As such, NADH oxidation is required: under aerobic conditions, mitochondrial oxidative metabolism oxidizes resulting NADH (section 1.5.3); whilst under anerobic conditions, pyruvate is converted to lactate by lactate dehydrogenase (LDH), oxidising NADH to NAD+ and H^{+} (Berg et al., 2002).

$$Pyruvate + NADH \rightarrow Lactate + H^{+} + NAD^{+}$$

Lactate may be utilised as a metabolic substrate for other cellular pathways and function, transported out of the cell for use *via* monocarboxylate transporter (MCT) SL16 solute carrier (Bosshart et al., 2019). An example of this is increased lactate production during anaerobic exercise within skeletal muscle, in which energy metabolism is maintained for function to some degree from the transport out and cycling of lactate back into pyruvate and glucose within the liver (Roef et al., 2003, Benjamin et al., 2018). A process by which is known as the Cori Cycle. Alternatively, if aerobic conditions are restored, lactate in the cytosol can be converted to pyruvate.

Further glycolytic metabolism takes place in the mitochondria matrix, during which pyruvate is decarboxylated and oxidized before being bound to Coenzyme A (CoA).

Carboxylation results in the production of carbon dioxide (CO_2) and metabolic substrate Acetyl CoA (CoA) in parallel with the NADH reduction (Berg et al., 2002).

$$Pyruvate + NAD^+ + CoA \rightarrow Acetyl\ CoA + H^+ + NADH + CO_2$$

1.5.2 The Tricarboxylic Acid Cycle

CoA is a key substrate for the tricarboxylic acid cycle (TCA) cycle, also known as the Krebs or citric acid cycle, that occurs within the mitochondrial matrix, during which CoA is oxidised to CO_2. During this, coenzymes NAD+ and flavin adenine dinucleotide ($FADH_2$) are reduced as a result of the cyclical breakdown of citrate, into electron carrier molecules NADH and $FADH_2$ (Berg et al., 2002, Martínez-Reyes and Chandel, 2020). Carriers molecules which are fed into the electron transport chain (ETC) for OXPHOS (section 1.5.3) to drive further ATP generation. Although no oxygen is consumed within the cycle, reactions only occurs in aerobic conditions due to OXPHOS-mediated transference of electrons from NADH and $FADH_2$.

The cycle is summarised in figure 1.4, in which the eight step cycle is a series of reduction and oxidation reactions that results in production of 1 NADH and 2 $FADH_2$ molecules. The cycle is a loop, with the final metabolite, oxaloacetate, reforming into starting metabolite acetyl CoA (Martínez-Reyes and Chandel, 2020, Berg et al., 2002). In brief, oxalacetete (4 carbon) binds with acetyl of acetyl CoA, producing the a six-carbon metabolite citrate, which in turn is decarboxylated to form five-carbon α-ketoglutarate. α-ketoglutarate is then further decarboxylated and bound to CoA, forming four-carbon succinyl CoA. The CoA is then bound to a phosphate group, forming a high energy intermediate, and is used for substrate level phosphorylation to produce succinate. Succinate is then oxidized to form four-carbon malate, which in turn is converted to fumarate by enzyme fumarase. The cycle is then completed by malate

dehydrogenase-mediated oxidation of fumarate into oxaloacetate, through the addition of H_2O of water. During this cycle NAD+ and FAD+ are reduced, resulting in the net formation of 1 NADH and 2 $FADH_2$, as well as two CO_2 molecules.

Interestingly, whilst the TCA cycle appears to be a closed loop, many of the intermediates can be utilised by other metabolic pathways (Martínez-Reyes and Chandel, 2020). As such, intermediary metabolites may act as metabolic precursors: including use in cellular growth, nucleotide synthesis, fatty acid synthesis and storage pathways, as well as elicit other effector functions. Recent studies, for example, have outlined an emerging role for fumarate in mediating innate inflammatory signalling, whereby treatment with monomethyl fumarate is noted to augment TNF and IL-6 secretion in LPS-stimulated macrophages (Arts et al., 2016, Ryan et al., 2019).

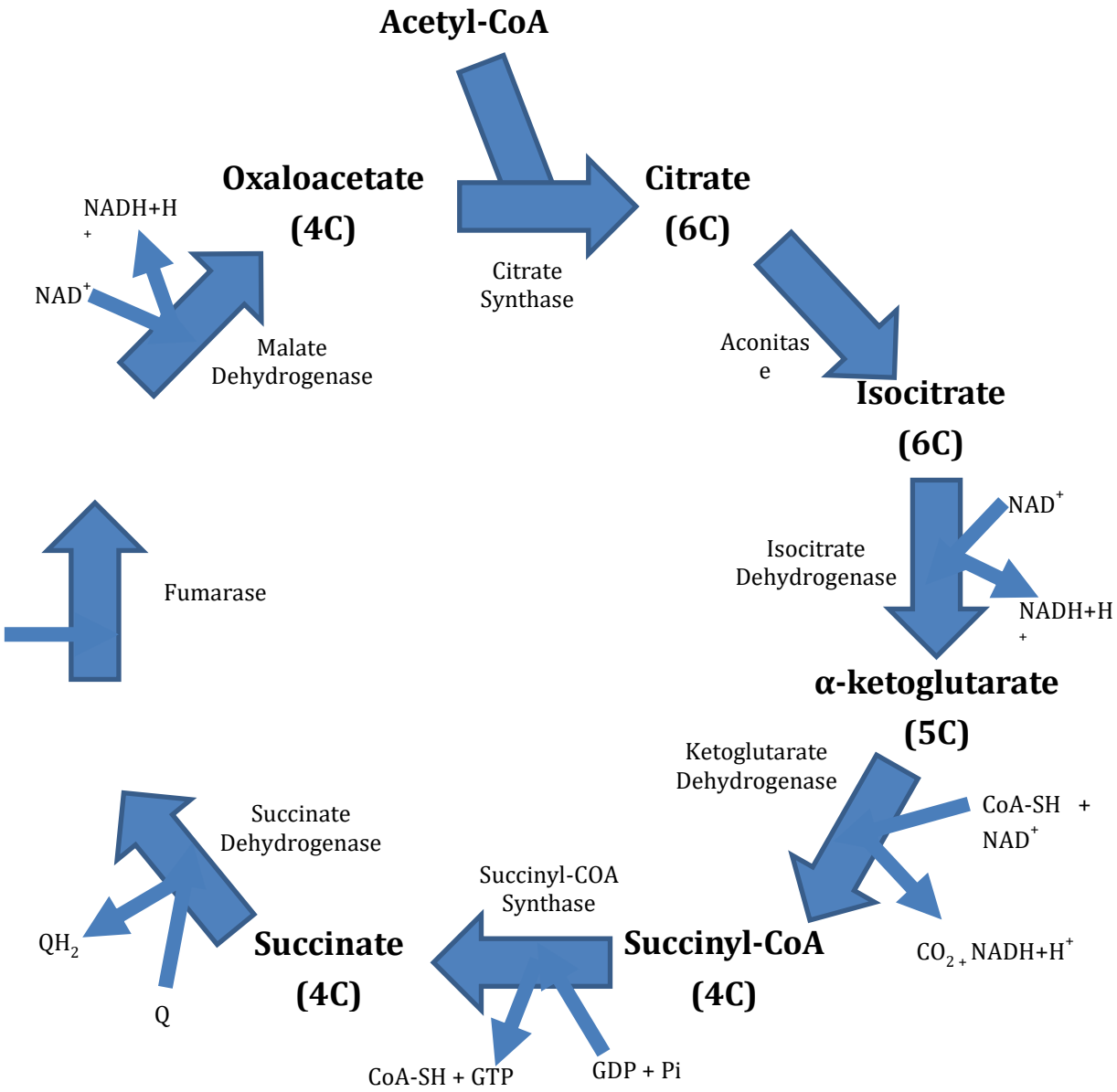

Figure 1.4 – The TCA Cycle. Acetyl-CoA feeds into the TCA, linking cytosolic metabolism to mitochondrial metabolism. Citrate subsequently undergoes cyclical breakdown to oxaloacetate mediated by various metabolic enzymes at each stage, the process resulting in the reduction of electron carrier molecules NAD+ and FAD+ to produce NADH and $FADH_2$. NADH and $FADH_2$ subsequently feed into the mitochondrial electron transport chain for oxidative (phosphorylative) metabolism.

1.5.3 Oxidative phosphorylation

As previously mentioned, the process of OXPHOS catalyses ATP production *via* the ETC, a five protein complex system (complexes I-V) located on the mitochondria's inner membrane (IMM). OXPHOS requires the presence of oxygen, to which electrons are terminally accepted to produce H_2O: this follows the coupling of electron transfer from NADH and $FADH_2$ to proton (H^+) translocation to generate a ~150-180mV proton gradient membrane potential. In turn, this encourages proton flux *via* the hydrophilic passage of complex V, ATP synthase that catalyses ATP generation – though this is dependent on the bioavailability of ADP (Alberts et al., 2002, Chance and Williams, 1956, Chance et al., 1955). Briefly, the sequence of reduction reactions are described as follows, beginning with the transfer of electrons to complex I (NADH:ubiquinone reductase) to complex III and cytochrome c – following oxidation of succinate to fumarate by succinate dehydrogenase and in turn reducing ubiquinone. Finally electrons pass to complex complex IV (Cytochrome c Oxidase) at which O_2 is reduced.

1.6 Metabolic Alterations During IMIDs

The increased prevalence of IMIDs are shown to be paralleled with alterations to systemic metabolism and the onset of metabolic syndromes (MetS). The latter of which represents a cluster of cardiovascular disease (CVD) risk factors linked by increased insulin resistance and visceral adiposity, and is identified through presence of three of the five following conditions; hypertension, high serum triglycerides (TGs), hyperglycaemia, visceral/central obesity and low serum high density lipoprotein (HDL) (Eckel et al., 2010, Medina et al., 2018). In RA patients specifically, disease appears associated with MetS and increased CVD risk, with MetS frequency ranging from 14 to 56% in various patient cohorts (Zhang et al., 2013, Medina et al., 2018). Studies show that within early RA patients, a lower incidence of MetS is observed, which

seemingly increased with high weight (body mass index (BMI) ≥30kg/m^2) and disease DAS28 scoring (Parra-Salcedo et al., 2015). Interestingly whilst obesity is a major contributing factor, MetS risk may also occur independently in RA patients without overweightness. This includes cachexic changes to body composition (i.e. increase in visceral fat mass with loss of lean mass), as well as hypercholesterolaemia, high TGs and low HDL observed only, characteristic of pre-clinical and early to developed RA (Kerekes et al., 2014). Other factors mentioned for MetS development during RA may include lack of physical inactivity and high caloric intake that in turn, contribute to alterations in patient adiposity.

The increased frequency of MetS during IMIDs may be attributed to dysregulation of inflammatory stasis through the release of cytokines and adipokines mediators from visceral adipose tissue. Cytokines such as tumour necrosis factor alpha (TNFα), interleukin (IL)-1, IL-6, IL-17 and IL-27 secreted from adipocytes are well established in their pathogenic role, for example, in RA joint destruction, whilst proinflammatory adipokine levels such as leptin are positively correlated with RA disease activity (Alam et al., 2017, Cao et al., 2016). Of interest, the release of leptin is shown to have modulatory effects on immune cell differentiation, including the promotion of effector Th_1 and Th_{17} effector cell function on cognate Ob-Rb receptor binding (Reis et al., 2015). Clarity around the role of leptin within RA pathogenesis, however, remains unclear: proposed on one hand to mediate disease in a proinflammatory capacity through TNF-α, IL-6 and IL-12 upregulation and CRP production, whilst joint damage appears to be negatively correlated with increased levels (Loffreda et al., 1998, Muraoka et al., 2013, Yoshino et al., 2011, Kerekes et al., 2014). It is thought that adipokines such as resistin and adiponectin may play an alternate pathogenic role, in which higher circulatory levels observed in RA patients have been observed: these

include adiponectin in synovitis and joint destruction, as well as resistin-induced expression of TNFα, IL-1β and IL-6 downstream of nuclear factor kappa-B (NF-κB) signalling (Silswal et al., 2005, Bokarewa et al., 2005). Indeed, these changes appear to be associated with alterations to RA body adiposity, in which cytokines and adipokines are strongly correlated with fat mass, as well as MetS (Hotamisligil et al., 1993, Elkan et al., 2009). Previous studies additionally note that Anti-CCP autoantibodies are also seropositively detected in cachexic RA patients; yet, increased detection was not observed in obese individuals – the majority of which were anti-CCP seronegative (Kerekes et al., 2014, Wesley et al., 2013).

1.6.1 Cellular Metabolism During IMIDs

Lymphocytic activation initiates a variety of downstream immunomodulatory effects, dependent upon cellular metabolic changes. Initial research can be stemmed by studies by Frauwirth and colleagues (2002) and Doughty et al. (2006) in which glycolytic activity is demonstrated to increase following PI3K signalling activation on T cell CD28 and B cell antigen-receptor binding. This initial body of work providing a platform for a growing evidence base in recent years elucidating the link between cell energy metabolism and nutrient utilisation, and immune cell activation. Indeed metabolic dysfunction has been rapidly recognised in autoimmune disease, most notably within RA and SLE. High levels of glycolytic and oxidative energy metabolism, for example, is shown to occur during CD4+ T cell activation within the SLE prone B6.Sle1Sle2.Sle3 mice - with disease state subsequently demonstrated to undergo reversal following metabolic inhibition with metformin and 2-deoxy-D-glucose (2DG) (Yin et al., 2016, Yin et al., 2015). The abrogation of glucose metabolism with 2DG is also shown to reduce clonal expansion of highly glycolytic autoreactive T_{fh} cells,

resulting in the reduction of disease severity in both murine models of SLE and RA (K/BXN) (Choi et al., 2018, Abboud et al., 2018).

Meanwhile, a number of studies demonstrate alterations in oxidative metabolism to correlate with the presence of autoimmune disease. Notably succinate, a key metabolite during TCA cycle and OXPHOS ubiquinone reduction, is shown to correlate with disease activity of adjuvant-induced arthritis (AIA) model (Saraiva et al., 2018, Littlewood-Evans et al., 2016). The subsequent ablation of its cognate receptor Sucnr1 (succinate receptor 1) shown to attenuate arthritis through reduction of dendritic cell chemotaxis and proinflammatory Th_{17} expansion (Saraiva et al., 2018). Indeed, Suncr1 is shown elsewhere to be an active component of immunity, in which abundant succinate is able to signal via the Sucnr1/GPR9-1 complex and exacerbate RA through increased macrophagic and dendritic cell activity (Littlewood-Evans et al., 2016, Rubic et al., 2008, Kim et al., 2014). However, OXPHOS metabolism is also noted to be reduced in autoimmune T cell activity, in particular ascribed to the under-utilisation of succinate in this context (Saraiva et al., 2018). Accordingly, recent studies identify a $CD4^{+}CXCR3^{+}$-$CXCR5^{-}PD\text{-}1^{hi}$ T ell subset from SLE patient sera, in which increased oxidative stress is observed in response to reverse succinate-regulated ETC – in turn providing stimulus for B cells downstream of IL-10 signalling (Caielli et al., 2019).

Finally, metabolite alterations in IMIDs is not solely limited to succinate. Itaconate, for example, is a dicarboxylic acid known to inhibit the oxidative activity of succinate dehydrogenase and is produced in anti-inflammatory manner by LPS-activated macrophages. In particular, derivatives are demonstrated to reduce macrophagic cytokine production and limit IFN response: leading to the possible role for itaconate-derived metabolites as therapeutic compounds that could alleviate IFN-driven

autoimmune disease, including SLE (Mills et al., 2018, Nonnenmacher and Hiller, 2018) Meanwhile, itaconate may also regulate Th_{17} activity, in which one study demonstrates itaconate to regulate IL-17 transcription through regulation of inhibitor of NF-κB zeta (IκB)-ATF3 (activating transcription factor 3) inflammatory axis (Bambouskova et al., 2018). Taken together highlighting the role of cellular metabolism in regulating the immune response repertoire both in health and disease.

1.6.2 T Cell Metabolism and Autoimmunity

Metabolism is understood to underpin T lymphocyte function, with cell signalling observed to induce activation of metabolic cascades which in turn, to the production of cellular products and macromolecules required for cellular function. As such, research into T cell related disease, cell function and interactions have understandably become increasingly focussed on cellular metabolism. The metabolic dysfunction T cells, for example, has been described in several IMIDs; in RA, activated CD4+ T cells found the joint show reduced glucose metabolism and diminished ATP production, while CD4+ T cells SLE show increased glycolysis and oxidative phosphorylation (Wahl et al., 2010, Yin et al., 2015).

Although a simplistic view of cellular metabolism, alterations in cellular metabolism can be thought to adhere to a *'two-pronged model'*. That is (1) changes to metabolic function, caused by random mutations or infection (e.g. human papilloma virus or human immunodeficiency virus), typically leading to cellular dysfunction or uncontrolled pathway regulation; and (2) metabolic changes induced by extracellular signalling pathways, such as cell receptors, autocrine and paracrine signals like pMHC or interleukins, leading to proliferation and differentiation – of which the latter will be of focus, in particular within CD4+ T cells.

Indeed within a healthy patient, the controlled and self-limiting inflammatory reactions which occur during infection and trauma resolve upon repair of damaged tissue and/or elimination of the pathogen by the immune system. The effector immune system mediated, as a result, by the activation and differentiation of naïve T cells into specific T cell subtypes - of which cells rely on different metabolic pathways for ATP synthesis. T cells in response to stimulus therefore dramatically alter their energy metabolism, consequently balancing the suitable rate of ATP production with cellular efficiency.

Naïve T cells are either circulating or within the lymph node and as previously mentioned, quiescent in nature. Possessing a low metabolic burden, naïve cells rely predominantly on the uptake of fatty acids and amino acids to meet their energy requirements prior to TCR-pMHC and co-stimulatory molecule engagement, such as CD28 (Salmond, 2018). In turn activation incites naïve T cells to proliferate, migrate and produce cytokines. As previously mentioned, glycolysis is proposed to be essential for T cell proliferation, with glucose deficiency in the extracellular environment shown to reduce T cell division; the marked upregulation of glycolysis observed in response to T cell stimulation as shown by prior studies (MacDonald, 1977, Greiner et al., 1994, Frauwirth et al., 2002). In turn, mitochondrial metabolism is shown to be reduced, in a characteristic shift known as the ‘Warburg effect’.

1.6.3 Warburg Metabolism within T cells

The Warburg effect is a metabolic pathway originally described by Otto Warburg and colleagues in the 1920s and describes a phenomenon originally observed in cancer cells, in which cells favour aerobic metabolism to support growth (Warburg et al., 1927). They observed cancer cell uptake of large amounts of glucose in comparison

with surrounding healthy tissue, yet respired anaerobically in the presence of oxygen to produce ATP and lactate by-products.

The function of Warburg metabolism in activated T cells is unclear given its inefficiency at supporting high bioenergetic demand. As previously shown, per unit of glucose, glycolysis net produces 2 ATP molecules - considerably less than the ~36 ATP molecules produced during OXPHOS. However, despite reduced ATP production the commitment to Warburg metabolism has been shown to be critical in supporting the function of activated T cells. The simple inhibition of glycolysis by competitive HK inhibition by 2-DG, for example, shown to impair IFNγ and IL-17 and in turn, supress Th_{17} cell differentiation (Kalim et al., 2018). Although investigations by Tan et al. (2017) conversely shows that during early T cell activation, glycolytic rate-limited enzyme HK2 may not be wholly required.

Nonetheless, support for Warburg T cell metabolism can be seen from a number of studies. Upon knockout of lactate dehydrogenase A (LDHA), Peng and colleagues (2016) demonstrate reduction in IFNγ production within CD4+ Th_1 cells, mechanistically ascribed to the reduction in histone acetylation at H3K9Ac and H3K27Ac within the promoter region of the IFNγ gene (*Ifng*). An effect independent of the gene's 3'-untranslated region (UTR), in which prior studies show glycolytic enzyme glyceraldehyde-3-phosphophate (GAPDH) to post-transcriptionally regulate IFNγ translation through 3'-UTR-*Ifng* binding (Chang et al., 2013b). It is therefore proposed that by employing glycolytic pathways, GAPDH in prohibited from *Ifng* regulation and as such, permits T cells to elicit their inflammatory functions. T cells therefore upregulate and down regulate genes in response to metabolite production, alongside extrinsic factors, such as activation signals and cytokines.

Review of the literature also proposes Warburg T cell metabolism to facilitate the flexibility needed to balance energy metabolism with biosynthetic pathways (Vander Heiden et al., 2009). A key function of glycolysis may therefore lie in its role in the shunt of glucose-6-phosphate down the pentose phosphate pathway (PPP), as well as serine biosynthesis. Accordingly, carbon tracing experiments have shown that a remaining 15% of glucose is not excreted as lactate but rather likely used to fuel biosynthesis (Fox et al., 2005). The enzyme nicotinamide adenine dinucleotide phosphate (NAPDH) produced from PPP is a rate-limiting enzyme involved in various biosynthetic pathways including the production of amino acids, fatty acids and nucleic acids (Vander Heiden et al., 2009). Therefore, Warburg metabolism is likely favoured by T cells upon activation due to its ability to support the metabolic requirements and resultant functional phenotype, due to faster flux through glycolysis as opposed to OXPHOS metabolism (Vander Heiden et al., 2009).

1.6.4 Regulation of T cell metabolism and activation by mTOR-cMYC pathways

Cellular myelocytomatosis oncogene (c-MYC) is a transcription factor of the MYC family, associated in the current literature through its oncogenic function in a broad range of cellular pathways. These include cell cycle, growth, apoptosis and of particular note, cellular metabolism – in which c-MYC is notably involved in regulating Warburg metabolism (Miller et al., 2012).

Like cancer cells, T cell activation relies on the hierarchical stimulation of signalling cascades upstream of c-MYC to mediate metabolic switching in response to nutrients. Amongst which the mechanistic target of rapamycin (mTOR) pathway is demonstrated to coordinate the various environmental, nutrient and immunological cues inputted into

the cell to elicit cell growth, proliferation and fate decisions. Briefly, mTOR complexes I (mTOR1) and II (mTORC2) are activated downstream of PI3K-Akt signalling and is demonstrated to promote T cell activation through MYC, following mTOR mediated phosphorylation of ribosomal S6 kinase (S6K) and eukaryotic translation initiation factor 4E (eIF4E) binding protein (4E-BPs) (Thoreen et al., 2012, Zeng and Chi, 2014). The subsequent inhibition of MYC by rapamycin treatment or deletion of Raptor failing to activate T cells and glycolytic metabolic reprogramming in a mTORC1-MYC dependent manner (Wang et al., 2011, Yang et al., 2013a). Inhibition of mTORC2 activity, however, is shown to block CD4+ subset differentiation (Lee et al., 2010, Delgoffe et al., 2011). In glioblastoma cells, mTORC2 activation results in the acetylation of transcription factor FOXO and release of microRNA-32c-bound cMYC; whether a similar mechanism occurs in T cells, however, is unknown (Masui et al., 2013).

1.6.5 Amino Acid Metabolism in T cells

Supporting cell growth and proliferation requires increased uptake of amino acids, where they are metabolised for the biosynthesis of cellular proteins - in addition to other functions ranging from nucleotide, polyamine and glutathione synthesis to TCA cycle anaplerosis (reviewed in Teng *et al.,* 2019). The upregulation of amino acid transporters and subsequent amino acid uptake is therefore considered to be equally critical as the mediation of glucose transport by GLUT1 following T cell activation, largely ascribed to the role of amino acids in cellular signalling. The depletion of amino acid supply, for example, results in the dephosphorylation of nutrient sensor mTOR1 and the inhibition of its downstream functions that include protein synthesis and cell proliferation pathways (Nofal et al., 2017). Meanwhile other amino acids such as

arginine, leucine and glutamine are noted to play a role in cell survival and differentiation, in particular within T cells.

1.6.5.1 Glutamine metabolism in activated T cells

Glutamine catabolism is dramatically increased following T cell activation and is shown to play an underlying role in T cell biology. Transported intracellularly by ASCT2/SLC1A5, glutamine metabolism is considered important for energy metabolism *via* TCA cycle following pyruvate depletion (Nakaya et al., 2014, Teng et al., 2019). This follows transaminase or glutamate dehydrogenase-mediated conversion to α-ketoglutaric acid, *via* intermediate formation of glutamate by glutaminase, which is then transported into the TCA cycle to aid cellular metabolism – including the production of NADH through NAD+ reduction.

Although glutamine is a non-essential amino acid, availability of the metabolite has been shown to be indispensable for T cell activation and effector function. The prohibited transport of glutamine *via* ASCT2 knockout or depletion of glutamine bioavailability in culture, for example, shown to impact naive CD4+ T cell differentiation independent of IL-2 signalling and Th_1 polarisation into Th_{17} cells respectively (Nakaya et al., 2014, Klysz et al., 2015). In specific the inhibition of glutamate conversion from glutamine shown to preferentially supress Th_{17} differentiation, whilst the enzyme glutamate oxaloacetate transaminase 1 (Got1) responsible for interconversion of glumatine-derived aspartate and oxaloacetate was shown to alter the T_{reg}-Th_{17} cell differentiation axis, in favour of the latter (Kono et al., 2018, Xu et al., 2017). Taken together, these results support the notion that glutamine metabolism is integral in activated T cell differentiation. Indeed, as previously mentioned, increased Th_{17} cell populations are observed in RA pathogenesis. Yet in SKG murine models of RA,

inhibition of glutaminase resulted in no significant alterations in Th_{17} cell numbers although a decrease in T_{reg} cells was observed (Takahashi et al., 2017). Conversely, CD8+ T cells, are shown to perform better upon glutaminase inhibition, in which blockade is shown to induce other metabolic pathways that aid in the removal tumour cells (Leone et al., 2019).

As intracellular glutamine level increase, it is also thought that this may lead to the uptake with other amino acids through antiport transporters, such as leucine *via* Slc7a5. Slc7a5, also known as LAT1, whilst exporting glutamine (Nicklin et al., 2009, Sinclair et al., 2013, Nakaya et al., 2014). CD4+ ASCT2-deficient cells treated with leucine, for example, prevents the associated polarisation effects of glutamine, suggesting leucine is also involved in T cell fate decision (Nakaya et al., 2014).

1.6.5.2 Leucine metabolism in T cells

The current literature landscape suggests that leucine metabolism may contribute to autoimmune disease through its critical role in mediating mTOR signalling. Correspondingly, leucine bioavailability is shown in earlier work to be indispensable during the activation and proliferation of primary and Jurkat T cells, in which leucine antagonist *N*-acetyl-leucine amide (NALA) induces restrictions on T cell cycle progression, cytokine production and downstream targets of mTORC1 (Zheng et al., 2009, Hidayat et al., 2003, Ananieva et al., 2016). This type of activity in is regulated: for example, cytosolic branched chain aminotransferase (BCATc) degrades intracellular leucine through transamination and in turn reduces mTORC1 activity (Ananieva et al., 2014). The degradation process encompassing the transference of nitrogen to α-ketoglutarate to convert to glutamate, and then α-ketoisocaproic acid (KIC). KIC is then converted to isovaleryl-CoA which is

subsequently oxidised to 3-methylcrontonyl-CoA. Finally, 3-methylcrontoynl-CoA is split into acetoacetate and acetyl-CoA, both of which can fed into the TCA cycle and be utilised for energy production and cellular growth.

Certainly, BCATc expression is additionally correlated with glycolysis, mediated in turn by upstream activity of the nutrient sensing protein mTORC1 in activated T cells (Ananieva et al., 2016, Ananieva et al., 2014). The impairment of BCATc expression therefore unsurprisingly enhances glycolytic activity as a result of increased mTORC1 expression; a comparison to the impairment of metabolic function that follows increased BCATc expression as observed within anergic T cells. It is noted that depleted leucine-mediated inhibition of mTOR shares similarity to that of rapamycin, with the latter shown to render T cells anergic even in the presence of stimuli from signal 1 and 2 (Zheng et al., 2009). Moreover, T_{regs} have been shown to induce expression of amino-acid consuming enzymes, including BCATc, that result in leucine depletion (Cobbold et al., 2009). This in turn promotes anergy, as well as the production of more T_{reg} cells – suggesting a role for leucine in not only T_{reg} regulation but the switch towards anergy from a glycolytically activated status (Cobbold et al., 2009).

1.6.5.3 Arginine metabolism

Arginine metabolism has been shown to play a role in macrophage polarisation, yet evidence to support a similar role within T cells remains unclear (Rath et al., 2014). Seminal work examining the metabolome and proteomic phenotype of T cells by Geiger et al. (2016) suggests arginine is linked with T cell survival in anti-tumour responses, with transcription factors BAZ1B (Bromodomain adjacent to zinc finger domain 1B), PSIP1 (PS4 and SFRS1 interacting protein) and Translin all noted

to elicit such an effect in response to high intracellular arginine levels (Geiger et al., 2016). In response to intracellular levels of arginine, activated T cells switch from a glycolytic phenotype towards OXPHOS, to promote memory-like anti-tumour activity and cell survival *via* proposed anti-apoptotic mitochondrial mechanisms (Geiger et al., 2016). Meanwhile the deprivation of the metabolite results in the abolition of G_0-G_1 phase cell cycle progression and thus T cell proliferation, as well as observed alterations to cytokine production, namely IFNγ (Rodriguez et al., 2007). Certainly in the absence of arginine, T cells are able to convert citrulline to arginine by action of arginosuccinate 1 (ASS1), yet ASS1 deletion despite the presence of sufficient arginine levels is shown to impair Th_{17} and Th_1 expression (Tarasenko et al., 2015). As such the literature suggests that arginine is critical to cell survival but not development of effector function.

1.6.6 Lipid Metabolism in T cell Function

Lipid metabolism represents a major energy source over typical Warburg-like glycolysis for some T cell populations, specifically T_{regs} – as highlighted by the seminal study by Michalek and colleagues (2011). Here, iT_{reg} cells demonstrate a distinct metabolic programme from other CD4+ effector T cells (Th_1, Th_2 and Th_{17}), in which the bioavailability of fatty acids (FAs) and their oxidation (FAO) appear highly important in T_{reg} differentiation and function, downstream of activated AMPK. The subsequent introduction of FA palmitate appears to seemingly elicit negative apoptosis-induced selection against CD4+ effector cells, due to their metabolic disadvantage within a lipid environment (Michalek et al., 2011). Indeed, the characteristic upregulation of FOXP3 during iT_{reg} differentiation is shown to be sufficient for metabolic transcriptional reprogramming in favour of protective measures, in particular against both lipotoxic and anti-proliferative low-glucose/high lactate rich environments (Angelin et al., 2017,

Howie et al., 2018). The subsequent inhibition of NAD regeneration within the low-glucose/high lactate environment, shown to ameliorate the T_{reg} proliferative phenotype (Angelin et al., 2017).

Fatty acid metabolism is also noted to seemingly mediate T cell differentiation, in particular *de novo* FA synthesis which appears to determine the fate between Th_{17} and T_{reg} subpopulations (Berod et al., 2014). In this study, ablation of acetyl-CoA-carboxylase 1 (ACC1)-mediated malonyl-CoA fatty acid production in both human and murine T cells, appears to skew T cell differentiation in favour of Th_{17} cells (Berod et al., 2014).This follows ACC1-mediated catabolism of acetyl-CoA carboxylation to malonyl-CoA essential for Th_{17} cell surface phospholipid synthesis, as opposed to the preferential use of exogenous FA and FAO in T_{reg}, as previously mentioned.

1.6.7 Metabolism in Rheumatoid Arthritis

The complex interplay between metabolism, inflammation and autoimmunity within RA is highlighted within a number of studies. Including notably, the seminal identification of distinct metabolic signatures within sera of established, disease-modifying antirheumatic drug (DMARD)-naïve RA patients by NMR spectroscopy (Young et al., 2013). The metabolomic analysis of this patient group and healthy control samples revealed distinct profiles that correlate with serum disease activity marker CRP, including increases in glucose, lactate and lipid metabolites during active RA. Such discriminatory metabolic patterns were similarly found in gas chromatography-mass spectrometry studies; however, decreases in levels of glucose, alongside decreased amino acid and increased fatty acid metabolites such as palmitate, oleate and cholesterol were observed in RA patient sera versus health controls (Zhou et al., 2016). These data suggest that metabolic changes are likely to be closely associated with RA

inflammatory activity and potential indicators for disease severity. Indeed, in studies by Lauridsen and colleagues (2010) involving patients with active RA synovitis and those in remission, discriminant analysis outlined distinct changes in the metabolic signature (lactate, acetylated glycoprotein, lipid and cholesterol) of RA patients from healthy controls. Interestingly, the metabolomes between the RA subgroups were again different between those with active disease and those in remission; however, on treating active symptomatic RA patients with an optimised therapy, including conventional DMARDs, anti-TNFα inhibitors, or a combination of both, metabolic signatures did not significantly differ from those in remission (Lauridsen et al., 2010). These results with the above therefore appearing to highlight RA metabolism as a potential direct therapeutic target, since Lauriden's findings show conventional therapeutic interventions unable to fully reverse RA and changes in metabolic signatures, despite remission, to those of healthy controls.

More specifically, chronic proinflammatory stimulation is acknowledged to alter T cell metabolism during RA disease activity, yet details in their contribution is not well known. The activation of T cells with respect to cellular metabolism itself, however, is well detailed: indeed, quiescent naïve T cells are shown in earlier studies to generate 96% of ATP *via* OXPHOS with only 4% by glycolysis, with ensuing stimulation with CD3/CD28 shown to induce a programme of rapid proliferation - upregulating protein synthesis and inducing glycolytic flux, through PI3K and Akt signalling, to meet the energetic demands required for cellular activation and subsequent cytokine production (GUPPY et al., 1993, Frauwirth et al., 2002). Increases in energy demands for activating T cells is accompanied by increased GLUT1 expression to allow for more oxygen consumption *via* predominantly aerobic glycolysis (Warburg effect) (Frauwirth et al., 2002, Jacobs et al., 2008, Finlay, 2012). Meanwhile, Th_1 cells are shown to

utilise OXPHOS for energy generation for cellular proliferation and survival (Chang et al., 2013a, Kolev et al., 2015, Okano et al., 2018).

Unsurprisingly, more recent studies have uncovered unique changes to the metabolic signatures of T cells. In RA peripheral naive CD4+ T cells, for example, cells exhibit impaired expression of the rate-limiting enzyme 6-phosphofructo-2-kinase/fructose-2,6-biphosphate (PFKFB3), which leads to delayed glycolysis whilst increasing flux to the PPP through upregulated G6PD (Yang et al., 2013c). Consequently, generation of NADPH is observed, which in turn can increase intracellular ROS consumption and contribute to immune cell differentiation towards proinflammatory subsets (Th_1 and Th_{17} (Yang et al., 2013c, Yang et al., 2016). ROS deficiency is also reported to bypass checks by cell cycle protein ataxia telangiectasia mutated leading to T cell hyperproliferation and the promotion of a chronic proinflammatory environment within the RA synovium, which is subsequently restored on replenishment of intracellular ROS (Yang et al., 2013c, Yang et al., 2016, Weyand et al., 2018). Similarly, in synovial patient biopsies treated with conventional DMARDs or biologics, recent RNA sequencing data appeared to confirm the impaired expression of glycolytic genes, coupled with increased TCA cycle gene expression and PPP shunting (Pucino et al., 2019). The same study also reported modulation of lactate metabolism which allows for CD4+ T cell survival within the disease joint.

Indeed, increased lactate within the RA synovium is reported to modulate T cell metabolism: the exposure of activated CD4+ T cells shown experimentally to decrease glucose uptake as a result of reduced levels of glycolytic enzymes HK1, HK2, PFK, enolase1α and PKM1/2 (Pucino et al., 2019). Such an observation is impeded by cellular incubation with anti-lactate transporter SLC5A12 antibody with the exception

of HK2 and PKM1/2 – indicating that only specific parts of lactate-mediated glycolysis increases NADH production (Pucino et al., 2019). Interestingly, lactate stimulation was additionally reported to mediate the mitochondrial translocation of cytosolic HK2 within 4 hours of treatment, in which subsequent voltage-depend anion channel (VDAC)-mediated binding of HK2 to the outer mitochondrial member promotes anti-apoptotic T cell survival. This data subsequently providing an important link between metabolism and the persistence of proinflammatory T cells observed within the RA synovium due to apoptotic resistance.

1.7 Aims and Objectives

Alterations in T cell metabolism are increasingly shown to support the cellular activation, proliferation and effector function of T cells. As abovementioned, effector CD4+ T cell preferentially upregulate glycolysis following activation and is crucial in determining the differentiation axis of given subsets. Activation requires several signals namely: (1) TCR engagement, (2) co-stimulation and (3) cytokines; however, the influence of each individual signal upon T cell metabolism is largely unknown. The principle aim of the project was to therefore investigate the metabolic phenotypes induced within CD4+ T cells in response to each signal (1,2 & 3).

Aim 1: To characterise the alterations to the metabolic phenotype during CD4+ T cell activation by required TCR stimulation, with and without CD28 co-stimulation, and signal 3 by utilising variable strengths of stimulation through the TCR, co-incubation with cell surface expressed co-stimulatory CD28 ligands and IL-6 pre-stimulation.

Aim 2: To assess the relative contribution of signals 1, 2 & 3 to the metabolic phenotype on CD4+ T cell activation, correlating increase gene activity identified in previous RA patient microarray data to the expression of metabolic proteins.

Aim 4: To determine the mechanisms associated with alterations in cellular metabolism in response to TCR, CD28 co-stimulation and IL-6 pre-stimulation signals.

Chapter 2 | Materials and Methods

2.1 CD4+ T cell isolation and culture conditions

CD4+ T cells were obtained from leukapheresis cones, derived from healthy anonymous donors, provided by the NHS blood and transplant services. Whole blood populations from cones were incubated for 20 minutes with Stem Cell Technologies Rosettesep© CD4+ cocktail (Stem Cell Technologies, Cambridge UK) (75ul/ml of blood) and diluted 1/3 in PBS with 1% heat inactivated human serum (HI-HS) (Sigma Aldrich, Dorset UK). Subsequently, CD4+ T cells were isolated by density gradient centrifugation (900g, 30 minutes, no brake/acceleration) using Ficoll Plaque (GE healthcare, Buckinghamshire UK). CD4+ T cells were collected and washed by centrifugation twice in PBS (600g, 10 minutes; 400g, 6 minutes) before being suspended in RPMI 1640 (Sigma Aldrich, Dorset UK) supplemented with HI-HS and 2 mM glutamine, 10U/ml penicillin, 100µg/ml streptomycin (subsequently referred to as RF10). Naïve and memory CD4+ populations were isolated using MACS CD45RO (Militenyi Biotech, Cologne Germany) and separated using MACS LS columns (Militenyi Biotech, Cologne Germany) according to manufacturer's instructions. Isolated naïve and memory T cells populations were washed twice in RF10 media (400g, 8 minutes) before being plated in 6 well plates at a density of $2x10^6$ cells/ml. For IL-6 stimulations, cells were stimulated with 0.02, 0.1, 0.5 ng/ml il-6 and equimolar soluble IL-6R (sIL-6R), 72 hours prior to anti-CD3/anti-CD28 stimulations. Purity of isolated cells were analysed using flow cytometry staining, using CD3, CD4, CD8 and CD45RO. Cell purity was determined to match manufacturer expectations for working with leukapheresis cones, with unstained cells consisting of red blood cells.

2.2 Anti-CD3/CD28 antibody stimulation of CD4+ T cells

All T cell stimulations were performed in 96 well flat-bottom plates in RF10 medium. Plates were prepared by placing 50 µl of anti-CD3, at required concentration,

(Immunotools, Friesoythe Germany) in sterile PBS overnight at 4°C. The following day anti-CD3 solution was removed and wells were washed twice using 200 µl PBS. Subsequently, $2x10^5$ T cells were added in 200 µl RF10 medium with 1 µg/ml anti-CD28 (Immunotools, Friesoythe Germany).

2.3 CD4+ T cell CHO cell stimulation

Chinese hamster ovaries (CHO) transfectants expressing CD80 or CD86 were used to stimulate T cells. Briefly, CHO cells were fixed with 0.025% glutaraldehyde for 5 minutes. Cells were washed twice with PBS at 300g for 6 minutes before being plated in flat bottom 96 well plates, coated with 50 µL poly-L-lysine. CHO cells were left to adhere to plate prior to the addition of CD4+ T cells. T cells were cultured at a ratio of 1:5 (T cell:CHO cells). CHO cells expressing no co-stimulatory molecule were used as a control (referred to as CHO Blank). 0.5 µg/ml anti-CD3 was added in suspension and cells were left for 72 hours, prior to analysis.

2.4 CD4+ T cell metabolite extraction for metabolomic analysis

Cells were washed by centrifugation in PBS (400g, 6 minutes) and subsequently, in 60% methanol, kept at -48°C using dry ice (400g, 6 minutes). Cells were re-suspended in 400 µl methanol, before being snap frozen with liquid nitrogen and thawed in dry ice three times. Cells were dried overnight using a speedvac evaporator set to room temperature. Dried pellets were suspended in 600µl:540µl methanol: dH_2O and transferred into glass vials with 600 µl chloroform. Vials were vortexed and incubated on ice for 10 minutes. Samples were centrifuged (1500g, 10 minutes, 4°C) and left at room temperature for 5 minutes. The upper polar layer was removed and dried overnight. Samples were stored at -80°C prior to NMR analysis.

2.5 NMR Spectroscopy

Phosphate NMR buffer was prepared using $NaH_2PO_4.2H_2O$, NaN_3, Diflouro(trimethylsilyl)methylphosphonic acid (DFTMP), organics N16545, NaN_3, DSS-D6, 2-(Trimethylsilyl)-1-propanesulfonic acid-d_6 sodium salt (DSS-D6), D_2O and dH_2O. The buffer was prepared at 4x concentration (400 mM phosphate, 1.6 mM DFTMP, 40% D_2O, 0.4% azide, 2 mM DSS-D6) and the pH was adjusted to 7.00 with hydrochloride (HCl). The resulting solution was filtered using a 0.2 µm filter and stored at 4°C until use.

A 1D Nuclear Overhauser Effect Spectroscopy (NOSEY) NMR Spectroscopic preset was utilised in Bruker Topspin to identify nuclear spins that underwent cross-relaxation. Solvent suppression was used to suppress the water signal on the NMR spectra. As discussed by Mckay and colleagues (2011) biological samples can be considerably dilute and have a high water signal: 1D NOSEY methods are suitable for minimising this signal (McKay, 2011). As such, a control sample of water only was used to identify the correct peak for calibrating the suppression. The identified signal was locked for all samples. To ensure relative stability of the magnet and data acquisition, shimming and lock optimisations were performed. Shimming was used to account for changes in sample effects and optimised using 0.5 mM DSS and focusing on peak symmetry. Addionally, automated lock acquisition processes were utilised to compensate for both internal and external magnetic deviations using D_2O set at 0 parts per million (PPM).

Samples were reconstituted using 15 µl NMR buffer and 45 µl H_2O. Solutions were transferred to glass champagne vials for automated loading by robot into 1.7 mm NMR tubes for acquisition. 1D spectra were acquired on 600 MHz B600 Bruker Avance III

spectrometer with TCI 1.7 mm z-PFG cryogenic probe. Data was acquired using NMR Bruker Topspin 3.2 software (Bruker, MA USA).

2.6 Metabolite processing and identification

1D spectra were aligned to DSS and scaled by probabilistic quotient normalisation (PQN) to account for dilution or variability, using Chenomx processor (Chenomx, Edmonton Canada). Post-identification analysis of metabolites was performed using Chenomx profiler (Chenomx, Edmonton Canada), by manual matching of representative spectra against the Chenomx database of known spectral signatures. Manual peak fitting was used for quantification of metabolites and peak clusters were adjusted to account for variation in pH. To provide further clarity, handling and identification of metabolites with the data, water peaks were removed using Chenomx automated deletion tool.

2.7 Seahorse metabolic flux analysis

Alterations and optimisations were carried out using previously published protocols (van der Windt et al., 2016). Briefly, oxygen consumption rates (OCR) and extracellular acidification rates (ECAR) were measured in XF assay media. Measurements were taken using the XF96 Extracellular Flux analyser (Seahorse Bioscience, MA USA). Briefly, 50 µL of poly-L-lysine (Sigma Aldrich, Dorset UK) was added to each well and incubated at room temperature for 5 minutes. Wells were washed twice using 200 µl of sterile dH_20 and air dried for 2 hours prior to use. Cells were washed by centrifugation in PBS (400g, 6 minutes) before being suspended in XF media. For mitochondrial stress tests, XF media was supplemented with 10 mM of glucose. To ensure adhesion, cells were plated in volumes of 50 µl or less, centrifuged (200g, 2 minutes, no brake) and subsequently topped up to 180 µl with XF assay media. Cells

were rested for 1 hour at 37°C 0% CO_2 before the assay. For OCR measurements 1 µM oligomycin, 1 µM carbonyl cyanide 4-(trifluoromethoxy) phenylhydrazone (FCCP), 0.5 µM rotenone and 1 µM Antimycin A were added sequentially and measurements taken prior and throughout. For ECAR measurements, 1 mM Glucose, 5 mM 2-deoxyglucose (2-DG) and 1 µM oligomycin were added. Data was collected using Wave Desktop 2.3 (Seahorse Bioscience, MA USA). Metabolic parameters were calculated as shown in figure 2.2 and used for comparison between each test condition. Subsequent analysis was carried out using PRISM 8.2 (Graphpad, CA USA) and Microsft Excel 2013 (Microsoft, WA USA).

2.8 Identification of protein expression

CD4+ T Cells were stimulated with 0, 0.02, 0.1 or 0.5 ng/ml IL-6/IL-6R for 72 hours and further stimulated with 0.5 µg/ml anti-CD3 and 1 µg/ml CD28 for 72 hours. Subsequently, cells were lysed using RIPA buffer (Sigma Aldrich, Dorset UK) and 1% phosphatase inhibitor. Cellular lysates were separated by polyacrylamide gel electrophoresis using 10% poly-acrylamide gels and proteins were transferred onto PVDF membranes (Bio-Rad Laboratories Ltd, Watford UK). Membranes were blocked for 1 hour with a buffer consisting of 5% milk in TBST (TBS +0.1% tween) before antibodies diluted is TBST supplemented with 5% BSA, used at the manufacturers recommended concentrations, were added and incubated overnight at 4°C. Membranes were washed three times for 5 minutes with TBST before being the addition of HRP-anti-rabbit antibodies. Membranes were incubated for 1 hour and protein bands were visualised using ECL detection reagent (GE Healthcare, Buckinghamshire UK). Membranes were photographed with Chemidoc XRS+ imaging system (Bio-Rad Laboratories Ltd. Watford UK) and Image Lab 6.0.1 (Bio-Rad Laboratories Ltd. Watford UK). TIFF images were transferred to ImageJ 1.53a (USA)

for densitometry analysis. Briefly, images were processed as 8-bit images, bands were identified manually and densitometry quantified and normalised to background.

2.9 Flow cytometry

Antibodies used for immunofluorescence labelling are shown in table 2.1. For analysis of cell surface proteins, cells were recovered following isolation and/or stimulation and washed twice using PBS at 300g for 6 minutes. Cells were incubated with relevant antibodies in 50 µL PBS solution with 1% HI-HS (Sigma Aldrich, Dorset UK) for 30mins at 4°C, away from light sources. Cells were washed an additional two times at 300g for 6 minutes and kept at 4°C until acquisition.

For intracellular staining using proliferation dye CellTrace Violet, $1x10^7$ /ml T cells were incubated with 5 µM CellTrace Violet in PBS for 15 minutes before being washed twice in PBS at 300g for 6 minutes. Cells underwent appropriate stimulation for experimental conditions and recovered as required. All data was acquired using BD Fortessa Flow Cytometer and BD DIVA flow cytometry software. Further analysis was carried out using FLowJo™ software v8 (TreeStar, Ashland, OR USA).

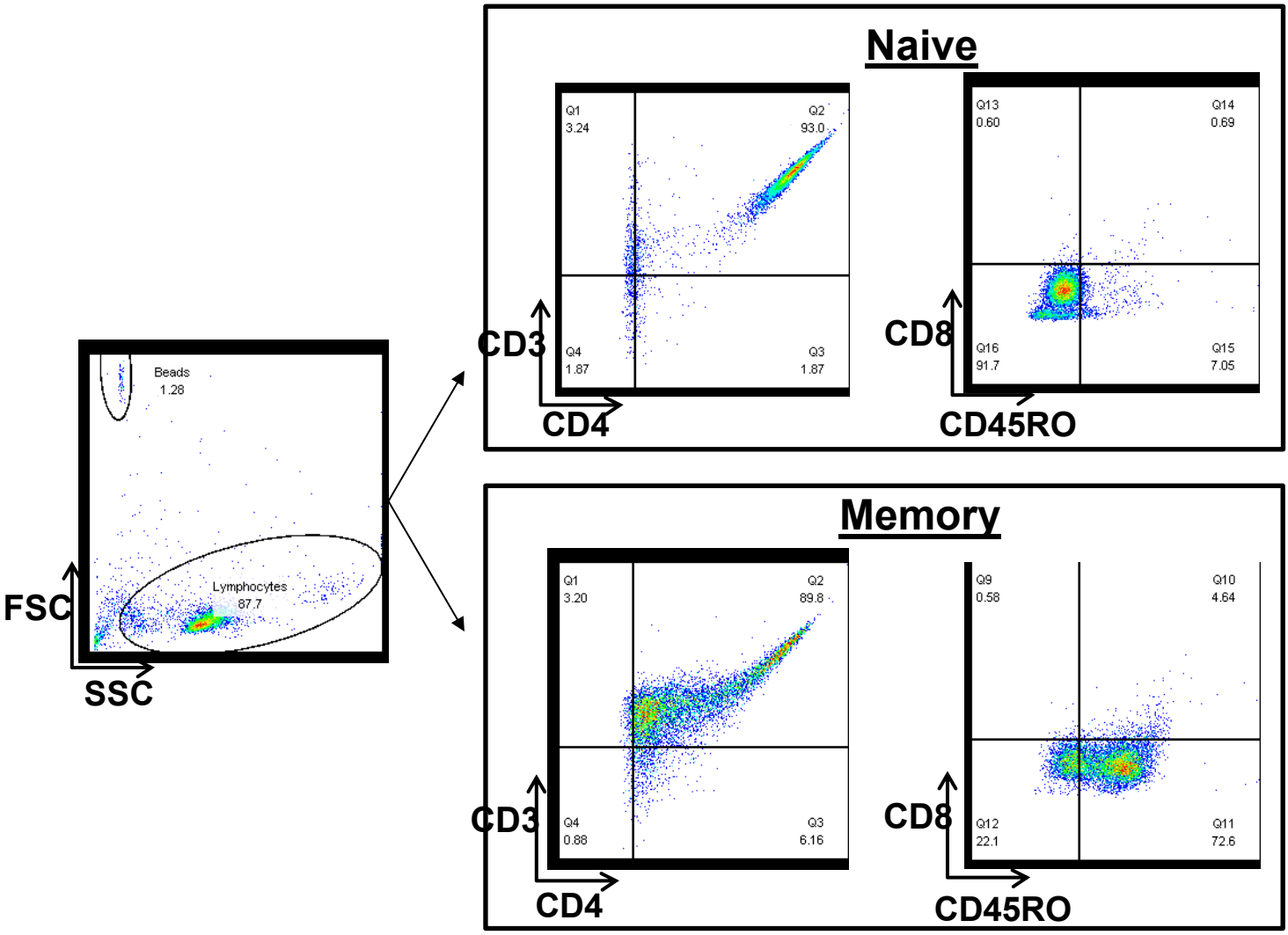

Figure 2.1 - Flow analysis of isolated naïve and memory CD4+ T cells. Cells were analysed following isolation with Rosettep and MACs magnetic isolation. Cells were isolated and purity was tested using flow cytometry. Cells were stained with markers for CD3, CD4, CD8 and CD45RO. Compensation beads were added to sample and were isolated as shown. Cell purity was determined to be a match with manufacturers expectations for working with leukapheresis cones.

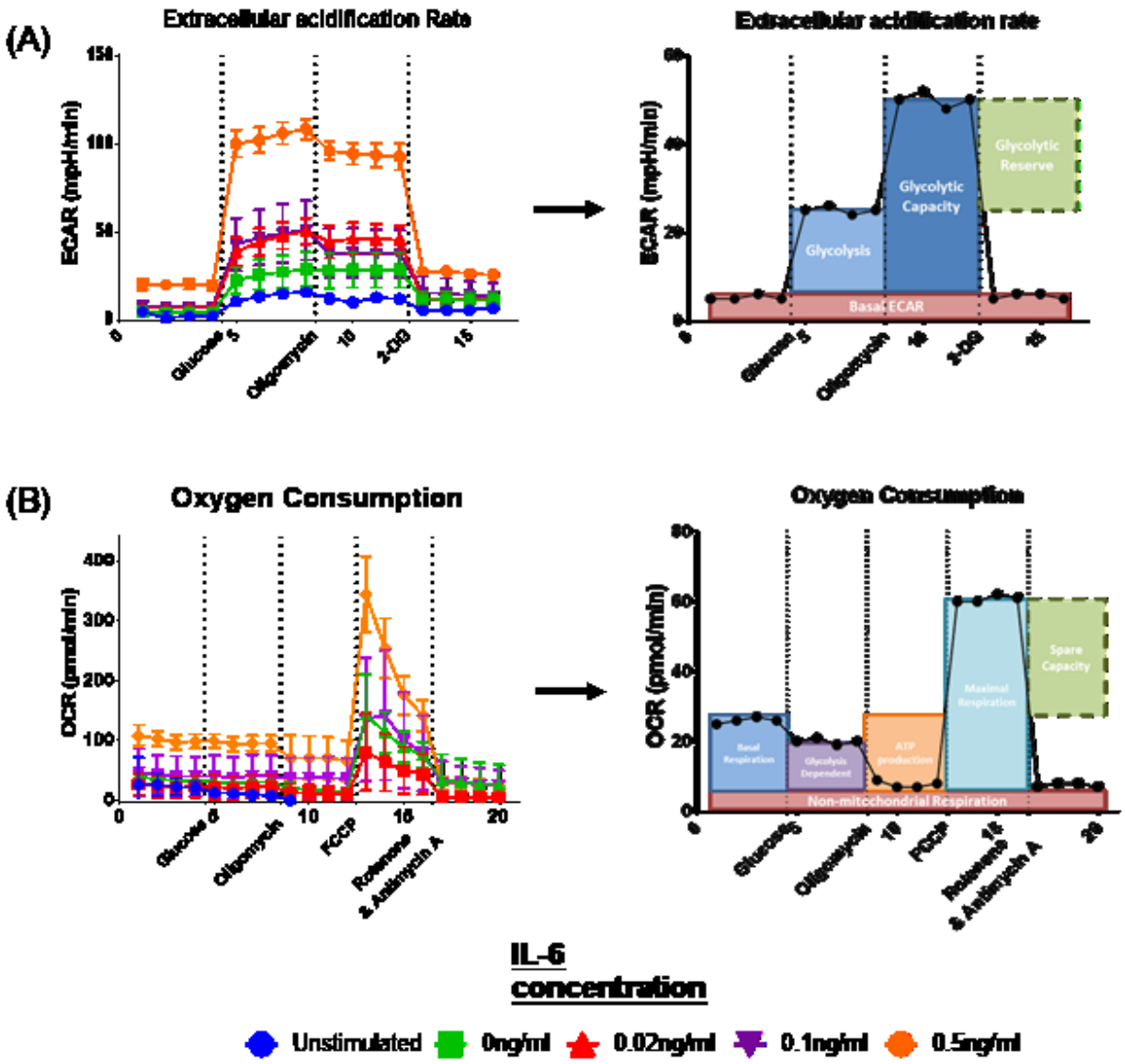

Figure 2.2 - Calculation of seahorse parameters from raw data. Metabolite injections are shown on graphs and occurred every 4 measurement cycles. (A) shows calculation of glycolytic parameters using extracellular acidification rate. (B) shows calculation of mitochondrial associated parameters using oxygen consumption rate. Example data shown is from CD4+ T cells stimulated with varying levels of IL-6 prior to CD3/CD28 stimulation.

2.10 Microarray analysis

Microarray data was acquired from Newcastle University. Datasets were analysed using EnrichR online GUI. Enrichment analysis utilised KEGG2019 database for identification of pathways. Statically significant pathways were calculated using Fischer exact test and visualised using clustergrammer tool.

2.11 Statistical analysis

Statistical analyses were performed using Prism 8.2 software (GraphPad Software, La Jolla, Ca, USA). Statistical tests were determined per experiment and normality was determined using Shapiro-Wilks normality testing. Where applicable, outlier data was removed if shown to be greater than 2 standard deviations of the mean. Component analysis was used for identifying patterns and significance in metabolite datasets using Metaboanalyst 4.0 (Montreal, Canada). Probabilistic quotient normalisation (PQN) was carried out prior to component analysis.

Metaboanalyst (Montreal, Canada) pattern hunter was used to identify linear and periodic trends with datasets (Figure 2.3). Strong correlations within the dataset are defined as >0.5 and <-0.5 correlations between metabolite levels with a pre-described pattern: the set ‘pattern’ described and inputted into the algorithm, with each number, corresponding to the expected expression pattern of the corresponding group Metaboanalyst pattern hunting attempted to identify. For example, pattern 1-2-3-4 would search for patterns that have increased linearly (figure 2.3A) between the 4 groups, while pattern 4-3-2-1 would search for patterns that have decreased linearly between 4 groups (figure 2.3D). The order of the groups is described when data is input. Alternative patterns can be used, such as 1-3-3-2. This pre-defined pattern suggests a plateau between features within samples in the middle of our series and a

decrease in the final concentration (figure 2.3C). The calculated correlations coefficients show how closely metabolites correlate with a pre-defined pattern across samples. Correlations were calculated using Spearman's Rank correlation in Metaboanalyst 4.0. Further information and package repository can be found at Rdrr.io (Rrrr.io, 2019).

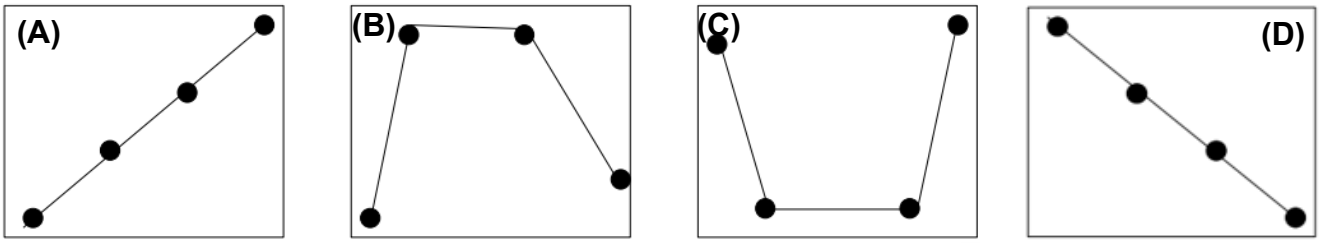

Figure 2.3 – Diagrammatic representations of example linear and periodic pre-patterns. (A) represents a linear increasing pattern, pre-defined as 1-2-3-4, (B) represents a periodic pattern, pre-defined as 1-3-3-2, (C) shows a periodic pattern, pre-defined as 2-1-1-3, and (D) shows a linear decreasing pattern, pre-defined as 4-3-2-1. Correlation coefficients show how close metabolites correlate with our predefined pattern. Positive correlations follow the pattern and negative correlations do the inverse.

2.12 Materials

Table 2.1: List of reagents

Item	Supplier	Cat #
Seahorse XFe96 FluxPak (18 cartidges, 20 plates, 500ml calibrant)	Agilent	102416-100
Seahorse XF DMEM medium, w/HEPES, w/o phenol red, pH 7.4	Agilent	103575-100
Oligomycin A	Cayman Chemical Company	11342
FCCP	Cayman Chemical Company	15218
Rotenone	Cayman Chemical Company	83-79-4
Ficoll Plaque	GE Healthcare	17144002
rh IL-6	Immunotools	11340066
Rh sIL-6R	Immunotools	11346064
Anti-CD3	Immunotools	21850034
Anti-CD28	Immunotools	21270281
Difluoro(trimethylsilyl)methylphosphonic acid	Manchester Organics	913263-04-4
CD45RO MicroBeads, human	Miltenyi Biotec	130-046-001
LS Columns`	Miltenyi Biotec	130-042-401
Protogel (30%)	National Diagnostics	50-899-90118
Bovine Serum Albumin Fraction V heat shock, fatty acid free (Roche)	Sigma Aldrich	3117057001
D-Glucose	Sigma Aldrich	G7021-1KG
2-Deoxy-D-Glucose >= 98% (GC) Crystalline	Sigma Aldrich	D8375-5G
Antimycin A	Sigma Aldrich	A8674
Human Serum	Sigma Aldrich	H6914
Trizma hydrochloride	Sigma Aldrich	T3253
SDS	Sigma Aldrich	L3771

RPMI	Sigma Aldrich	R5886
Dulbecco's Modified Eagle's Medium - high glucose	Sigma Aldrich	D5671
Sodium Azide	Sigma Aldrich	S2002-25G
Deterium Oxide	Sigma Aldrich	151882
3-(Trimethylsilyl)-1-propanesulfonic acid-d6 sodium salt (DSS-D6)	Sigma Aldrich	613150
Sodium phosphate monobasic dihydrate	Sigma Aldrich	71505
Poly-L-lysine solution	Sigma Aldrich	P4707
RosetteSep™ Human CD4+ T Cell Enrichment Cocktail	Stemcell	15062
PBS	ThermoFischer Scientific	BR0014G
Mitotracker red	ThermoFischer Scientific	M7512
CellTrace Violet	ThermoFischer Scientific	C34571
TEMED	ThermoFischer Scientific	17919
Ammonium persulphate (APS) tablets	VWR chemicals	K833-100

Table 2.2 – List of Antibodies

Antibody	**Supplier**	**Cat #**	**Concentration**
LDHA	Cell Signalling Technology	C45B	1/1000
c-Myc	Cell Signalling Technology	9402	1/1000
Anti-Rabbit IgG, HRP linked	Cell Signalling Technology	70744	1/2000
Total OXPHOS Human WB Antibody Cocktail	Abcam	ab110411	1/1000
CD3 PErCP	BD Biosciences	345766	1/25
GLUT1 APC	BD Biosciences	202915	1/25
CD4 PE	immuotools	21850044	1/50
CD8 APC	immuotools	21620086	1/50
CD45RO FITC	immuotools	21336453	1/50

Chapter 3 | The contributions of signals 1 and 2 to the metabolic phenotype of CD4+ T cells

3.1 Introduction

Increasing T cell receptor (TCR) signal strength has been shown to correlate with differentiation and response to cytokine signals. For example, the development of Th_1 over Th_2 has been linked to greater signal strengths (Snook et al., 2018), whilst in contrast, high TCR signalling is thought to lead to CD8+ effector T cell apoptosis, due to Blimp-1 and Bcl-6 downregulation (Daniels and Teixeiro, 2015). The maintenance and survival of T cells, in the absence of inflammation, requires TCR-self peptide MHC (spMHC) interactions, known as homeostatic interactions.

As previously discussed, T cell proliferation occurs following cellular activation, requiring a co-stimulatory molecule, alongside TCR stimulation. Briefly, presentation of a foreign antigen to the TCR alongside a co-stimulatory molecule, such as CD80 or CD86, by an antigen presenting cell (APC), leads to downstream activation *via* the CD28 signalling pathway (Baxter and Hodgkin, 2002). The requirement of this co-stimulatory signal, signal 2, is considered the minimum requirement, as the co-stimulatory signalling pathway overlaps with the TCR signalling pathway, amplifying the signal and allows the T cell to overcome its activation threshold, leading to cellular activation.

Subsequent T cell activation leads to the upregulation of cellular metabolism which serves to support cellular growth and proliferation, resulting in the increase of effector T cells able to respond to a given antigen. Homeostatic proliferation, however, occurs through the TCR-spMHC interactions in the absence of a signal 2, and has been shown to stimulate T cell proliferation and promote cell survival (Surh and Sprent, 2008). These homeostatic interactions, accompanied by IL-7, aid in maintaining a steady T cell pool and diverse naïve T cell repertoire, following lymphopenia. This may occur

due to effector cell apoptosis following an inflammatory event, irradiation treatment, certain viral pathogens or cytotoxic drugs; the latter of which are widely used in treatment of IMIDs i.e. azathioprine (Gómez-Martín et al., 2011, Maile et al., 2006b, Moxham et al., 2008, Maile et al., 2006a).

3.2 Aims

In this chapter the effects of increasing anti-CD3 TCR signal strength were examined, in conjunction with different co-stimulatory stimuli, to determine the effects of these signals on T cell metabolism. We aimed to assess the alterations to the metabolic phenotype caused by TCR stimulation, with and without CD28 stimulation, as well as differences in cellular metabolite following stimulation with different CD28 ligands, CD80 and CD86.

3.2 T cell stimulation protocol

As described in chapter 2, CD4+ T cells, were isolated into naïve or memory cell subpopulations using positive selection for CD45RO. Cells were stimulated in flat bottomed 96 well plates. Wells were coated with the required concentrations of anti-CD3 overnight at 4°C. Wells were washed with PBS twice and allowed to reach room temperature prior to stimulating cells. 1 µg/ml anti-CD28 was added in suspension where required. Cells were left for 72 hours prior to analysis using Seahorse XF96 or Bruker 600mHZ NMR spectrometry.

3.4 Results

3.4.1 Stimulation with anti-CD3 only leads to increased glycolysis in memory CD4+ T cells, not naïve CD4+ T cells

The metabolic profile of memory and naive CD4+ T cells was examined on addition of a CD3 stimulatory signal. Examination of isolated T cells shows that whilst no

significant changes were observed in naïve T cells (figure 3-1B), a glycolytic phenotype in response to increasing anti-CD3 concentration was observed within the memory T cell subpopulation (figure 3-1E). No other calculated glycolytic parameters appeared to significantly change as anti-CD3 concentration increased (figure 3-1); however, memory T cell glycolytic capacity (figure 3.2B) appeared to approach significance (P=0.064). The analysis of mitochondrial metabolism also showed no significant changes with increasing anti-CD3 concentrations in both naïve and memory T cells (figure 3-2). At lower concentrations of anti-CD3, CD4+ T cells show little difference between stimulated and unstimulated cells, suggesting that low anti-CD3 concentrations do not provide a high enough TCR stimulus to upregulate glycolytic metabolism.

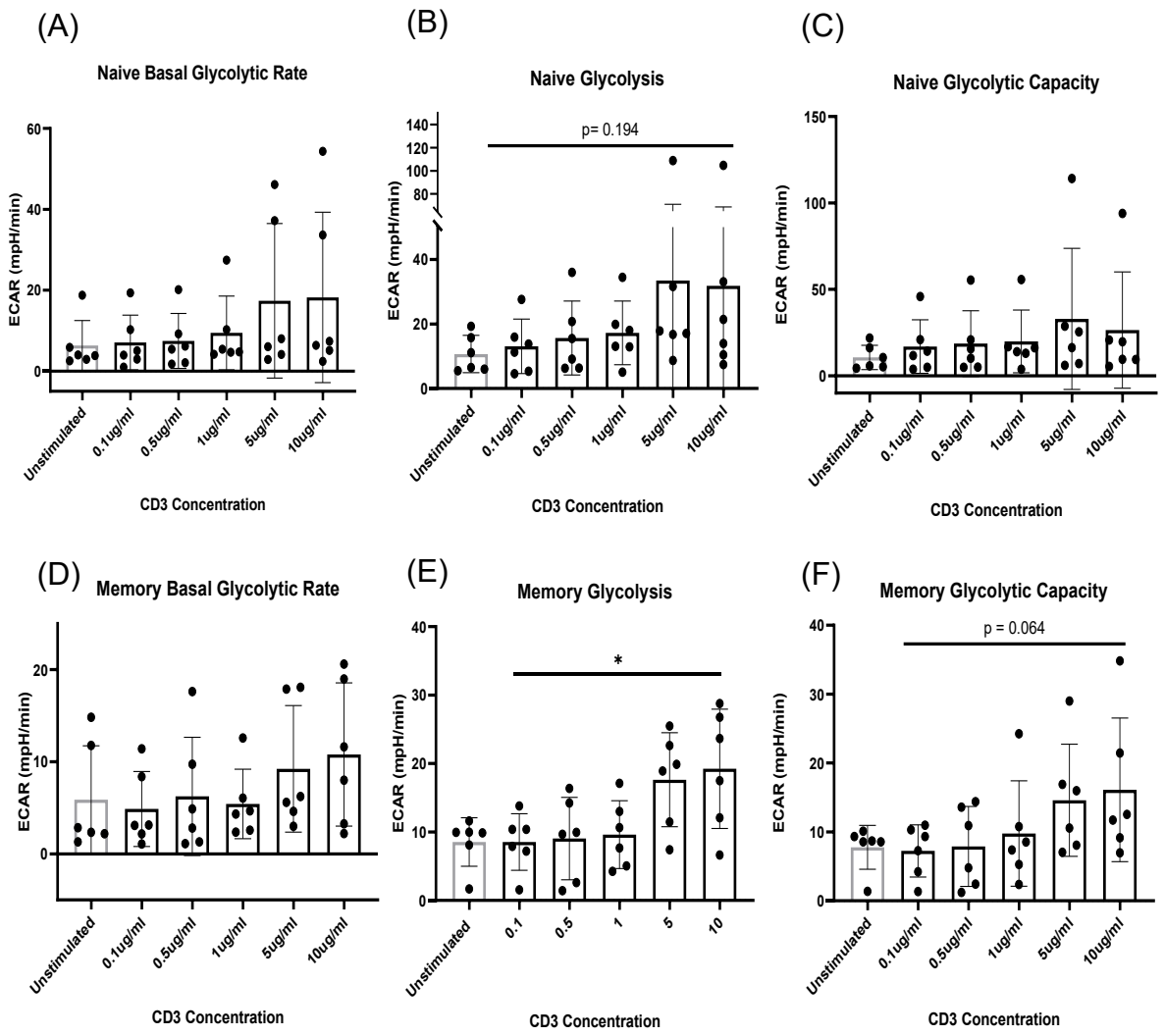

Figure 3.1 – Measurements of glycolytic parameters in naïve and memory CD4+ T cells in response to increasing anti-CD3 concentration. Cell populations were isolated and analysed using Seahorse XF96. (A), (B) & (C) show the basal glycolytic rate prior to injection of glucose, cellular glycolysis following 25mM glucose injection and the glycolytic capacity of naïve T cells, respectively. (D), (E) & (F) show the basal glycolytic rate prior to injection of glucose, cellular glycolysis following 25mM glucose injection and the glycolytic capacity of memory T cells, respectively. Data shows mean values with standard deviation. Analysis was performed using paired ANOVA with Tukey multiple comparison * = $p<0.05$. Unstimulated cell values are shown but are excluded from statistical analysis. (n=6)

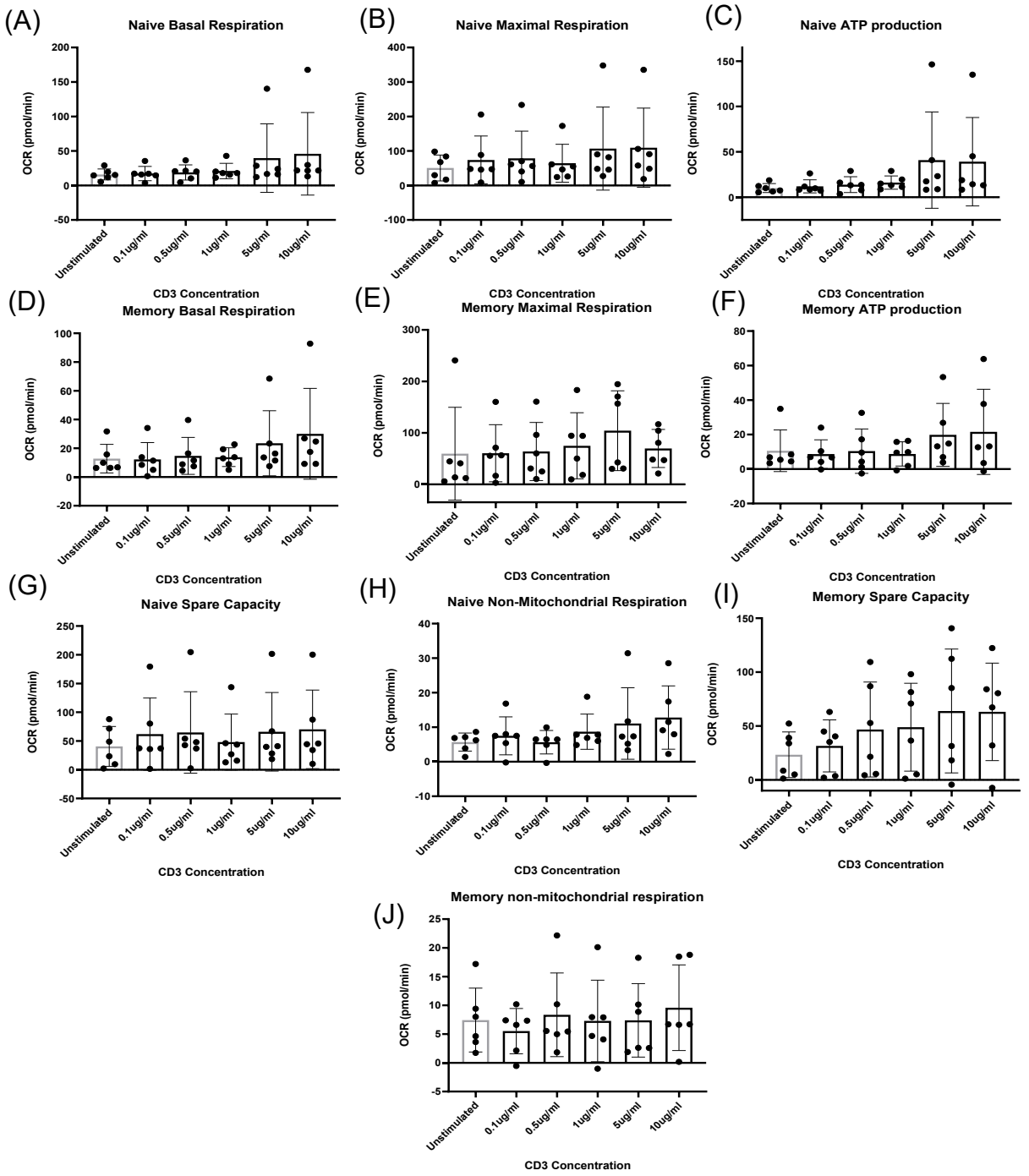

Figure 3.2 – Measurements of mitochondrial metabolism in naïve and memory CD4+ T cells on increasing anti-CD3 concentration. Cell populations were isolated and analysed using Seahorse XF96. Naive cell parameters are shown; (A) basal respiration prior to glucose injection, (B) maximal respiration following FCCP injection, (C) ATP production, (G) Spare respiratory capacity and (H) non-mitochondrial respiration following rotenone and antimycin A injections. Memory cell parameters are shown; (D) basal respiration prior to glucose injection, (E) maximal respiration following FCCP injection, (F) ATP production, (I) Spare respiratory capacity and (J) non-mitochondrial respiration following rotenone and antimycin A injections. Data shown is mean with standard deviation. Analysis was performed using paired ANOVA with Tukey multiple comparison. Unstimulated cell values are shown but are excluded from statistical analysis. (n=6)

3.4.2 Glycolysis and glycolytic capacity increase in both naïve and memory T cells as anti-CD3 concentration increases when accompanied with a co-stimulatory molecule

Previous literature indicates the requirement for additional co-stimulatory molecules alongside TCR stimulation during the activation of T cells to induce growth and cellular proliferation. Consequently, the addition of increasing amounts of anti-CD3 concentrations, alongside a fixed amount of anti-CD28 reflected this, with figure 3.3 showing significant upregulation of cellular glycolysis (figure 3.3B, E) and glycolytic capacity (3.3C,F) in both naïve and memory T cells. Accordingly, when measuring mitochondrial metabolism, figure 3.4 also showed no significant changes in response to anti-CD3/CD28 activation - indicating the ability for increased levels of anti-CD3 to upregulate glycolysis in the presence of CD28 stimulation in both cell types, but not activate mitochondrial metabolism. This is despite trends of increased ATP production (figure 3.4C, F) and maximal respiration (figure 3.4B, C) at higher anti-CD3 concentrations.

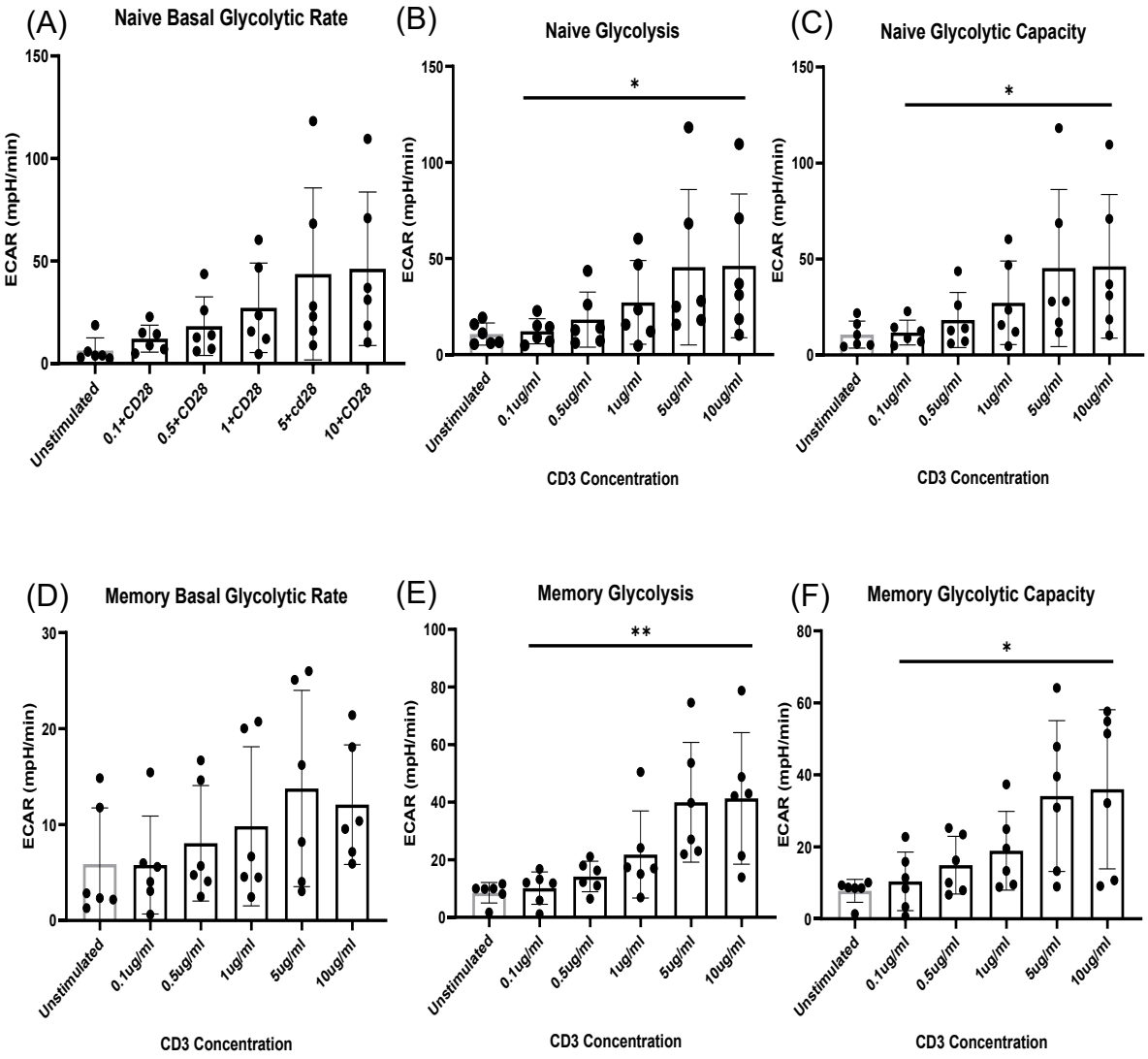

Figure 3.3 – Measurements of glycolytic parameters on increasing anti-CD3 concentration and co-stimulation with anti-CD28 in naïve and memory CD4+ T cells. (A), (B) & (C) show the basal glycolytic rate prior to injection of glucose, cellular glycolysis following 25 mM glucose injection and the glycolytic capacity of naïve T cells, respectively. (D), (E) & (F) show the basal glycolytic rate prior to injection of glucose, cellular glycolysis following 25 mM glucose injection and the glycolytic capacity of memory T cells, respectively. Data shows mean values with standard deviation. Analysis was performed using repeated measures ANOVA with Tukey multiple comparison * = $p<0.05$, **<=0.01. (n=6)

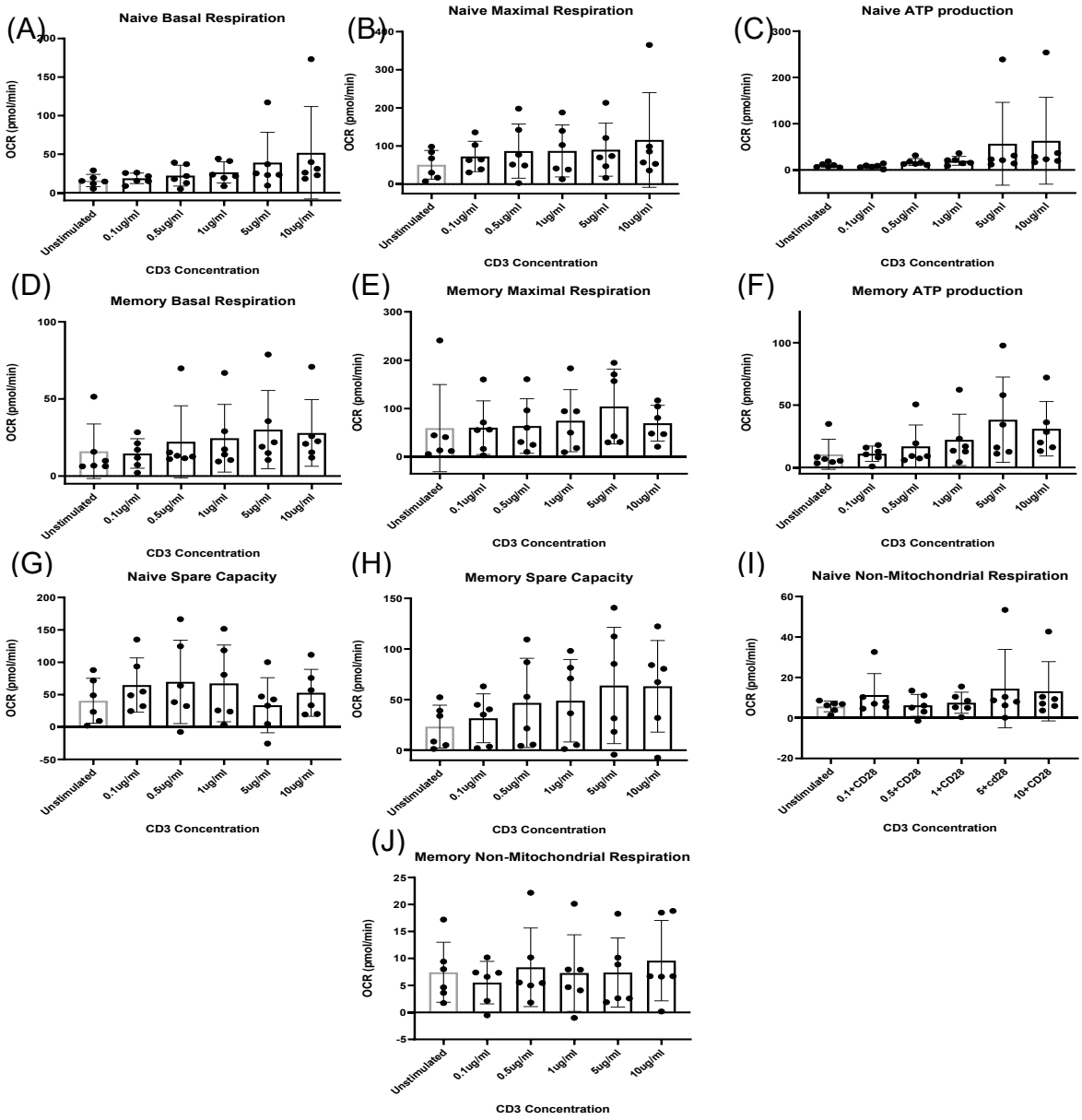

Figure 3.4 – Measurements of mitochondrial metabolism in naïve and memory CD4+ T cells following stimulation with increasing anti-CD3 concentration and co-stimulation with anti-CD28. Cell populations were isolated and analysed using Seahorse XF96. Naive cell parameters are shown; (A) basal respiration prior to glucose injection, (B) maximal respiration following FCCP injection, (C) ATP production, (G) Spare respiratory capacity and (H) non-mitochondrial respiration following rotenone and antimycin A injections. Memory cell parameters are shown; (D) basal respiration prior to glucose injection, (E) maximal respiration following FCCP injection, (F) ATP production, (I) Spare respiratory capacity and (J) non-mitochondrial respiration following rotenone and antimycin A injections. Data shown is mean with standard deviation. Analysis was performed using paired ANOVA with Tukey multiple comparison. (n=6)

3.4.3 Regardless of CD28 co-stimulation, naïve CD4+ T cells do not significantly upregulate glycolytic metabolism following stimulation anti-CD3

It has been shown that following TCR engagement, co-stimulatory molecules provide a stimulus which amplifies downstream signals: allowing the cell to overcome the activation threshold. The newly activated cell subsequently upregulates transcription and cellular metabolism to support cellular growth, proliferation, as well as the development of an effector phenotype and cytokine production. This two-signal model preventing the abhorrent activation of T cells through MHC bound with self- antigens or MHC alone. In turn the T cell pool is regulated *via* homeostatic interactions, that is between MHC self-antigens and TCR, which interact to provide small signals to T cells - preventing apoptosis and small bouts of proliferation, bolstering the T cell population during leukopenia. As such, TCR only interactions, without a co-stimulatory molecule, are thought to be able to upregulate T cell metabolism to support proliferation, but not to the same extent as a cell stimulated with a co-stimulatory molecule.

Indeed, in figure 3.5, results show that memory T cells, not naïve T cells, demonstrate significantly different rates of glycolysis (figure 3.5E) and glycolytic capacity (figure 3.5F) between anti-CD3 only stimulation and anti-CD3/anti-CD28. This significant difference only occurred at much higher concentrations of anti-CD3 (5 µg/ml), although near significance for memory glycolysis was observed at 1 µg/ml and 10 µg/ml ($p=0.06$). On further analysis of the metabolic phenotypes studied, analyses of mitochondrial metabolism, however, showed no significant difference between T cells stimulated with anti-CD3 only and those stimulated with anti-CD3/CD28 (figure 3.6).

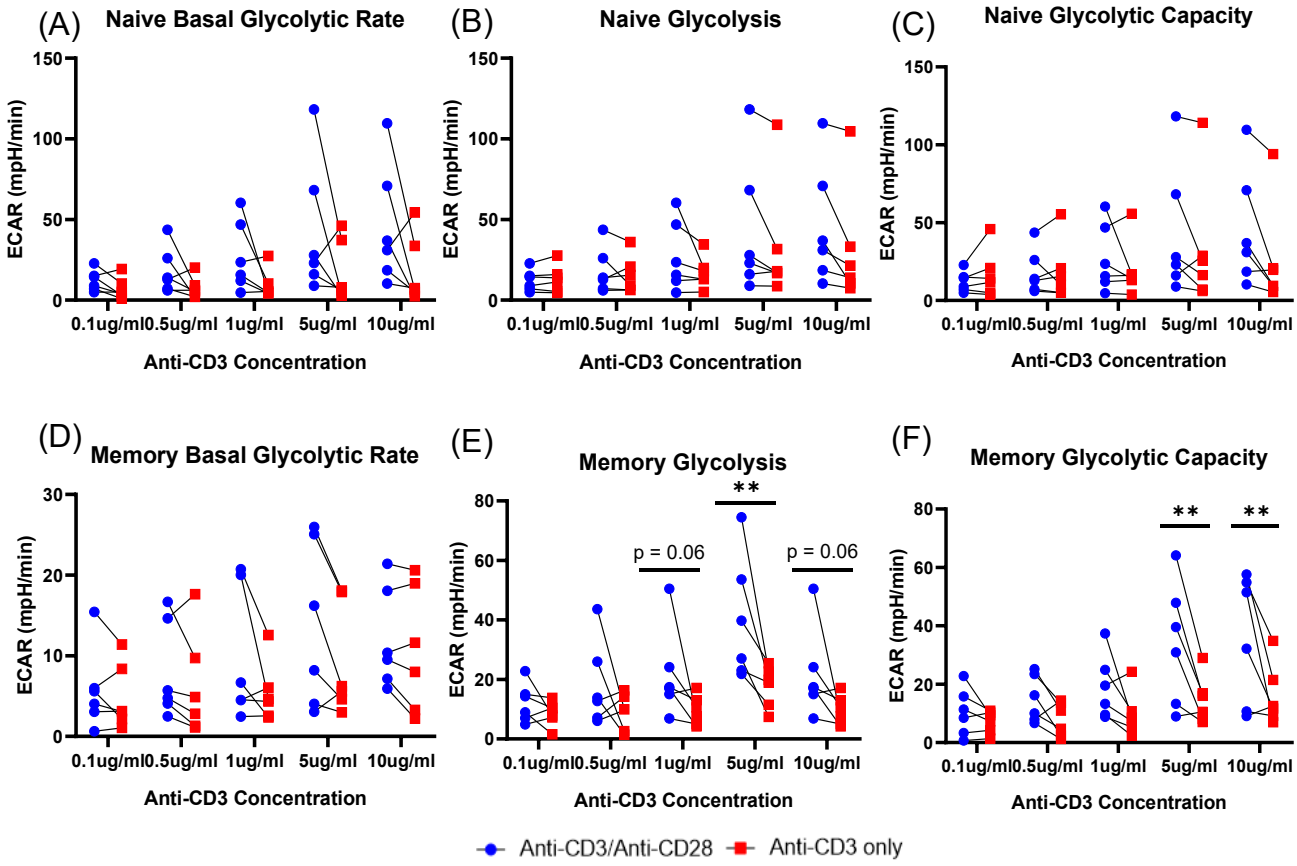

Figure 3.5 – Measurement of glycolysis and the glycolytic capacity within naïve and memory CD4+ T cells with or without CD28 co-stimulation. T cells stimulated with CD3 with CD28 (blue) or without CD28 (red) were compared using a seahorse XF96. Naïve CD4+ cells are shown in (A)-(C) and memory cells are shown in (D)-(F). Graphs (A) and (D) compare the basal glycolytic rate prior to injection of glucose, (B) and (E) compares the cellular glycolysis following 25mM glucose injection & (C) and (F) compares the glycolytic capacity following injection of oligomycin. Data shows mean values with standard deviation. Analysis was performed using Wilcoxon Paired Sign rank test * = $p<0.05$, **=$p<0.01$. (n=6)

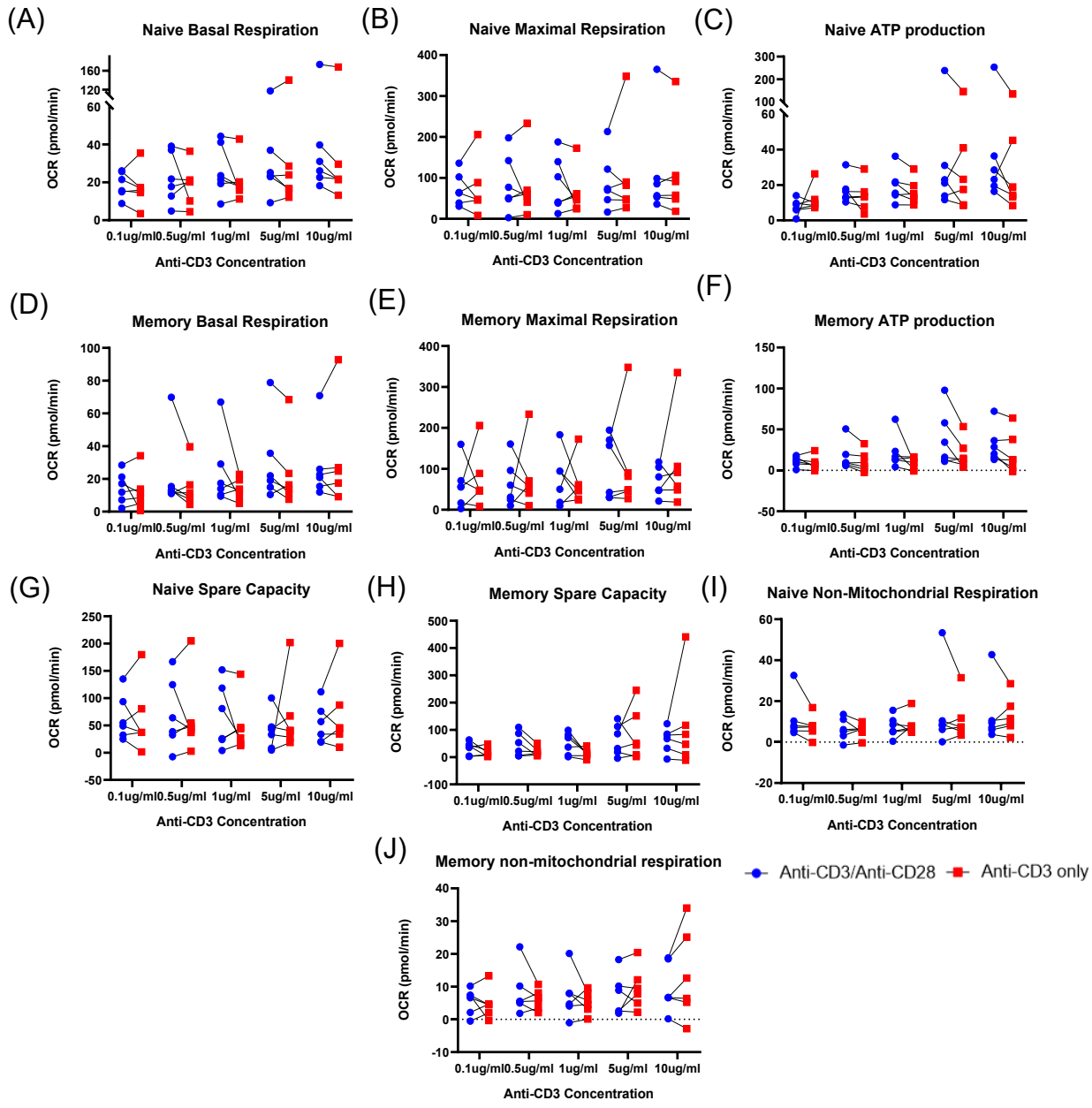

Figure 3.6 – Measurement of mitochondrial metabolism within naïve and memory CD4+ T cells with or without CD28 co-stimulation. T cells stimulated with CD3 with CD28 (blue) or without CD28 (red) were compared using a seahorse XF96. Naive CD4+ cell parameters are shown in (A)-(C), (G) and (I) and memory cells are shown in (D)-(F), (H) and (J). Graphs (A) and (D) basal respiration prior to glucose injection, (B) and (E) maximal respiration following FCCP injection, (C) and (F) show ATP production, (G) and (H) show spare respiratory capacity and (I) and (J) show non-mitochondrial respiration following rotenone and antimycin A injections. Data shown is mean with standard deviation. Data shows mean values of each experiment. Analysis was performed using Wilcoxon Paired Sign rank test. (n=6)

3.4.4 Optimisations of NMR spectroscopy protocol

Amongst the most fundamental processes for cells is the ability to access enough nutrients to support cellular activities and functions, such as the ability to undergo growth, cellular proliferation and even apoptosis through changes and adaptation of its metabolic phenotype. Indeed, T cell activation is understood to result in such shifts: quiescent naive T cells, for example, employing predominantly ATP-generating processes, whilst proliferating effector T cells access sufficient energy pools through mitochondrial metabolism. To therefore characterise the glycolytic phenotype previously observed in naïve and memory T cells, Nuclear Magnetic Resonance (NMR) spectroscopy was utilised to examine both intracellular and extracellular metabolites.

Initial NMR spectroscopy protocols outlined previously by standard operating protocols undertook examination of metabolites in adherent cells, such as monocytes, washed with -40°C methanol to remove excess salt prior to assaying. However, in the present study when employing such a technique for T cells, suspension and centrifugation in methanol resulted in no visible signal or peaks on analysis. The results indicating possible cell death and loss of intracellular metabolites within NMR sample, although no loss of extracellular metabolites was observed. As such, to therefore ensure both collection of intracellular and extracellular T cell metabolites overcome this, methanol washes were removed. This does not negatively affect NMR analysis or data collection, as NMR spectroscopy is unaffected by the presence of salt, yet hinders the ability to employ mass spectrometry techniques such as Gas Chromatography-Mass Spectrometry (GC-MS) or Liquid Chromatography-Mass Spectrometry (LC-MS) due to present salts in any given sample.

As with the above optimisations, it was also imperative to titrate the correct number of cells to use for each replicate, with both unstimulated and anti-CD3/CD28 stimulated cells tested. Unsurprisingly, unstimulated T cells did not produce a strong enough signal on spectroscopy analysis to allow us to determine any differences between unstimulated T cell populations (figure 3.7A, C and E); although stimulated T cells, shown in figure 3.7B, (D) and (F) showed an increasing signal as cell number increased. Low T cell titrations provided little signal sufficient to deduce several metabolites over background (figure 3.7B, 3.6D), when compared to spectra of higher cell titrations that show increased signal detection (figure 3.7F, 3.6G). As such, it was deduced that $20x10^6$ T cells would be used for NMR spectroscopy and for each test conditions, with cells undergoing anti-CD3 and anti-CD28 stimulation prior to assaying. To yield the required amount of cells for several test conditions, cells were not split into separate naïve and memory CD4+ populations using CD45RO; instead being conducted on a mixed naïve and memory T cell population.

3.4.5 NMR Spectra comparison between intracellular metabolites of CD80 and CD86 co-stimulation of CD4+ T cells

As previously outlined, T cell activation requires adequate adaptation of the cell's metabolic profile to ensure support of cellular function, with ligation of additional co-stimulatory receptors understood to stimulate such metabolic shifts. T cells were therefore co-cultured in the present study with Chinese hamster ovary (CHO) cells expressing co-stimulatory molecules CD80 and CD86: cellular ligands which belong to the B7 superfamily and signal *via* CD28 and CTLA-4 surface proteins. Specifically, CD80 having a higher affinity for activatory CD28, whilst CD86 a higher affinity for negative T cell regulator CTLA-4. Cells that express CD86 are associated with the

inhibition of T cell activation and proliferation. Controls in the present study comprised CHO blank cells, expressing no co-stimulatory molecules.

Metabolic profiles of T cells, stimulated prior by anti-CD3 in suspension and co-cultured at a ratio of 1:5 (T Cell:CHO Cell) with either blank, CD80 or CD86-expressing plate-adhered CHO cells, was examined by NMR spectroscopy. Our initial goal was to compare the metabolites upregulated by CD80 and CD86 co-stimulation and identify metabolites unique to one or the other stimuli. Consequently, NMR analysis of co-cultured T cell samples revealed 43 identifiable intracellular metabolites (figure 3.8). Of those identified, none were significantly different when statistically tested, despite some trends of increased metabolite concentrations when comparing blank, CD80 and CD86-stimulated cells. For example, (adenosine triphosphate) ATP is shown to be notably higher in CD86 stimulated T cells (figure 3.8A).

Indeed, it has been previously demonstrated that CD86 is an inhibitory signal. Although higher levels of ATP suggest greater levels, equal concentrations of adenosine diphosphate (ADP), adenosine monophosphate (AMP) and nicotinamide adenine dinucleotide (NAD+) were observed. This observation suggesting that ATP levels are likely to have arisen from previous energy stores, due to the absence of ADP, AMP and NAD+ in reduced forms. CD86 also showed higher glycine, glutamate and lactate, however, these differences seemed minute due to the large variation in samples as shown by the standard deviation.

Utilising the Metaboanalyst pathways and enrichment analysis tool, we attempted to further identify different pathways affected by the three experimental groups. Prior to all metabolomic analysis, samples were normalised using probabilistic quotient

normalization (PQN). This method of normalisation was chosen to remove any large variation caused by single metabolite swings and has been demonstrated as robust method for normalising NMR data (Dieterle et al., 2006). Unsurprisingly, both CD80 and CD86 stimulated cells affected the same pathways, namely pathways involving tyrosine and tryptophan biosynthesis, aspartate and glutamate metabolism, arginine and proline and D-glutamine/glutamate metabolism (figure 3.9A – 3.9B). These upregulated pathways completely differed from the analysis profiles of T cells stimulated with co-cultured CHO blank cells, suggesting that co-stimulation provides upregulation of several additional metabolic pathways over cells who only receive TCR stimulus. This is further confirmed by partial least squares – discriminant analysis (PLSD-A), which discriminates CD80 and CD86 stimulation from CHO blank T cells (figure 3.10). Further PLDS-A analysis focussed solely on CD80 and CD86, also showed discrimination between the experimental groups, although demonstrated some overlapping points (figure 3.10A). To further identify any other metabolic differences between co-stimulatory molecules, pattern hunting was used.

Metaboanalyst pattern hunting attempted to identify correlations between metabolite levels with a pre-described pattern; the set ‘pattern’ described and inputted into the algorithm, with each number corresponding to the expected expression pattern of the corresponding group. For example, pattern 1-2-3-4 would search for patterns that have increased linearly between the 4 groups, while pattern 4-3-2-1 would search for patterns that have decreased linearly between 4 groups. The order of the groups is described when data is input. In figure 3.11 the pattern stated is 1-2, with the algorithm identifying metabolites that are increased in CD86 stimulated T cells versus those co-stimulated by CD80. Each metabolite analysed is provided with a correlation coefficient: negative correlation coefficients denoting a decreased metabolite

concentration in CD86 versus CD80. As such, figure 3.11 demonstrates the majority of metabolites to have weak correlation coefficients, of which most are negative. Notably glutamate, alloisoleucine and ADP, all of which are associated with energy use and growth, are seen to have the greatest negative correlations – that is, concentration levels are lower in CD86 versus CD80-stimulated T cells, whilst the inverse is true for glycine and ATP.

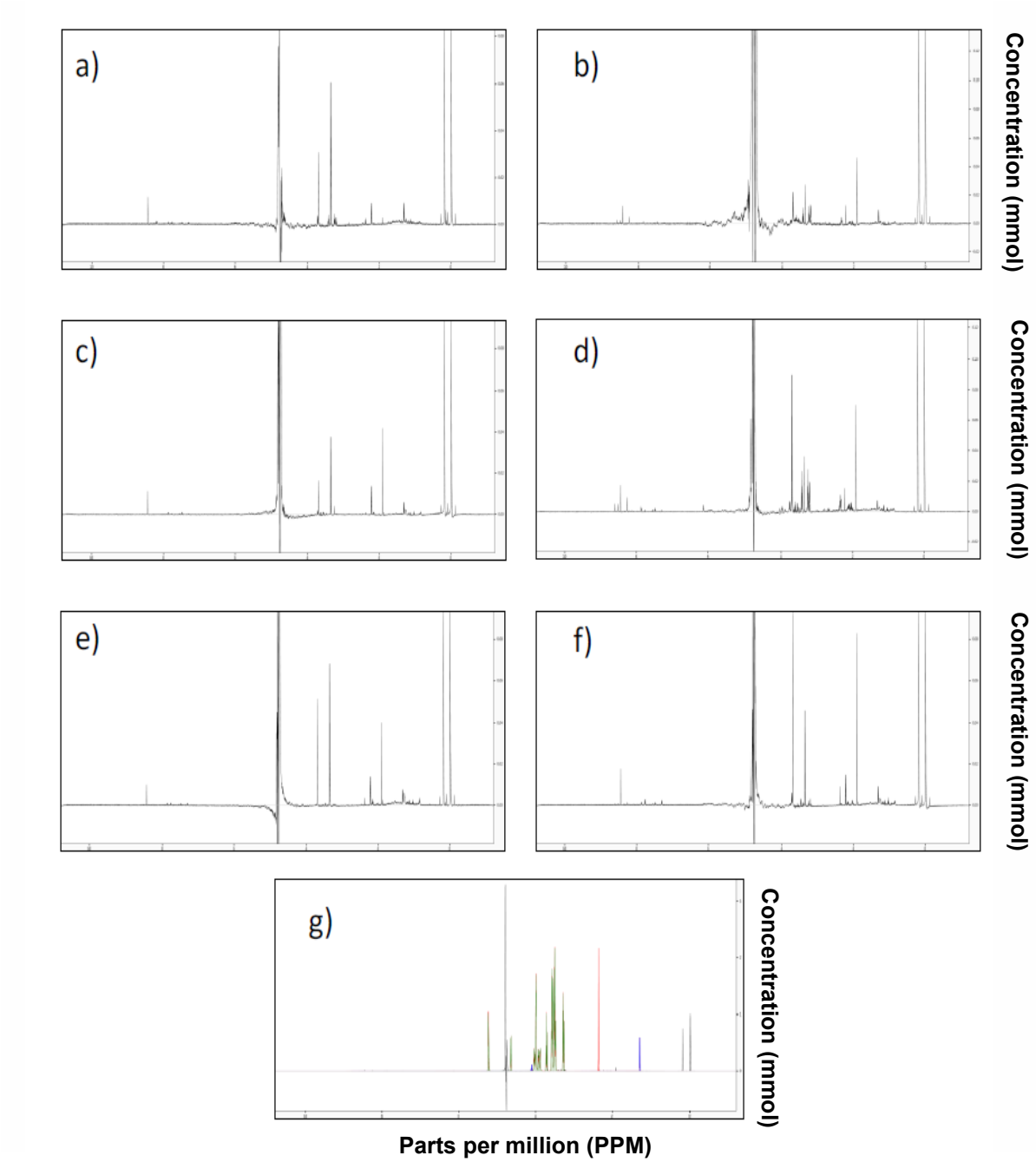

Figure 3.7 – Titration of T cell number for NMR analysis, identification of intracellular metabolites and example spectra. The spectra show metabolites detected following TCR/CD80 co-stimulation or no stimulation. Each spectra shows metabolites from one of the following conditions a) $5x10^6$ unstimulated cells, b) $5x10^6$ stimulated cells, c) $10x10^6$ unstimulated cells, d) $10x10^6$ stimulated cells, e)$20x10^6$ unstimulated cells, f) $20x10^6$ stimulated cells. Spectrum g) shows expected peaks for key metabolites glucose (green), pyruvate (blue) and lactate (red). Red boxes on figure b) show areas where metabolites are not distinct over background signal. Further in depth analysis of an NMR spectra is shown in figure 3.7H.

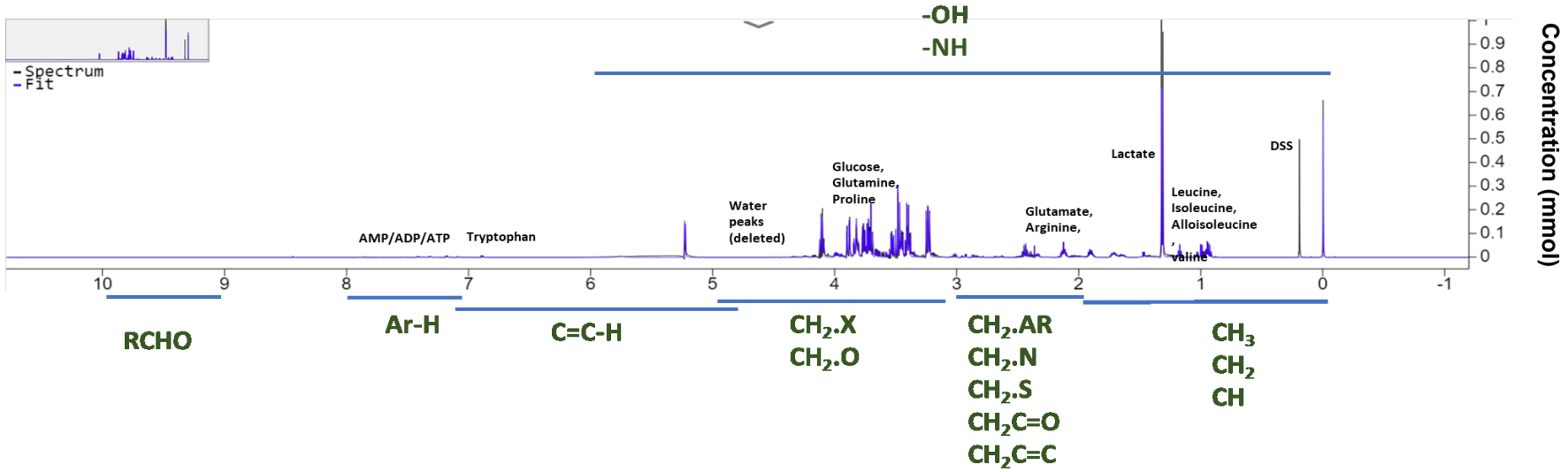

Figure 3.7 (H) – Proton NMR spectra shows locations of H^+ in chemical structures. The x axis is measurement of Parts per million (ppm) of radio waves absorbed and released by proton binding. Peaks between 10 and 9 indicate a H^+ on a RCHO group, 8-7 indicate the inclusion of an aromatic ring (as found in ATP or tryptophan). 7-5 indicate H^+ bound to C=C, 5-3 indicated CH_2.X or .O binding and are the most common bonds in metabolites with larger structures, such as glucose, while 3-2 indicate CH_2 groups bound to other structure or bonds, such as sulphide, double oxygen bonds or double carbon bond. Finally, 2-0 peaks indicate the presence of CH_2, CH_3 and CH. Additionally, -OH and -NH groups are found dispersed through the spectra between 6.5 and 0. By using a library of pre-identified metabolites, matching peaks in our spectra can identify chemicals within our samples. These can be quantified by using the internal control DSS at a concentration of 0.5 mM. For clarity and clearer identification of metabolites, solvent suppression is carried out during acquisition (as discussed in 2.5), the water peak is removed during analysis, as indicated on the spectra.

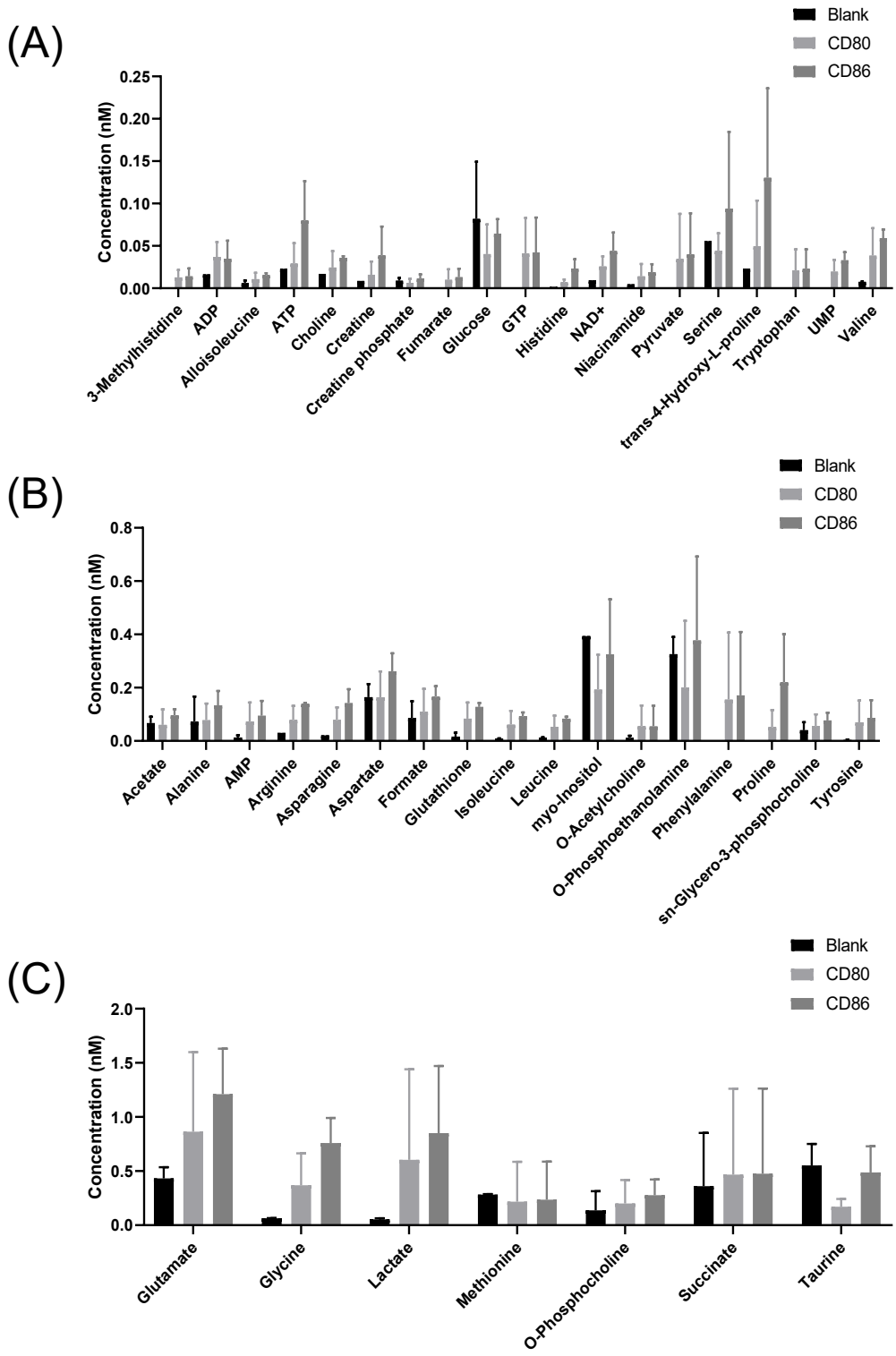

Figure 3.8 – All intracellular metabolite concentrations from CD4+ T cells cultured with CHO cells expressing co-stimulatory molecules CD80 or CD86 or no co-stimulatory molecule (blank). Statistical analysis was run using ANOVA in PRISM 8.2 statistical software. Data shown is mean with standard deviation (n=3).

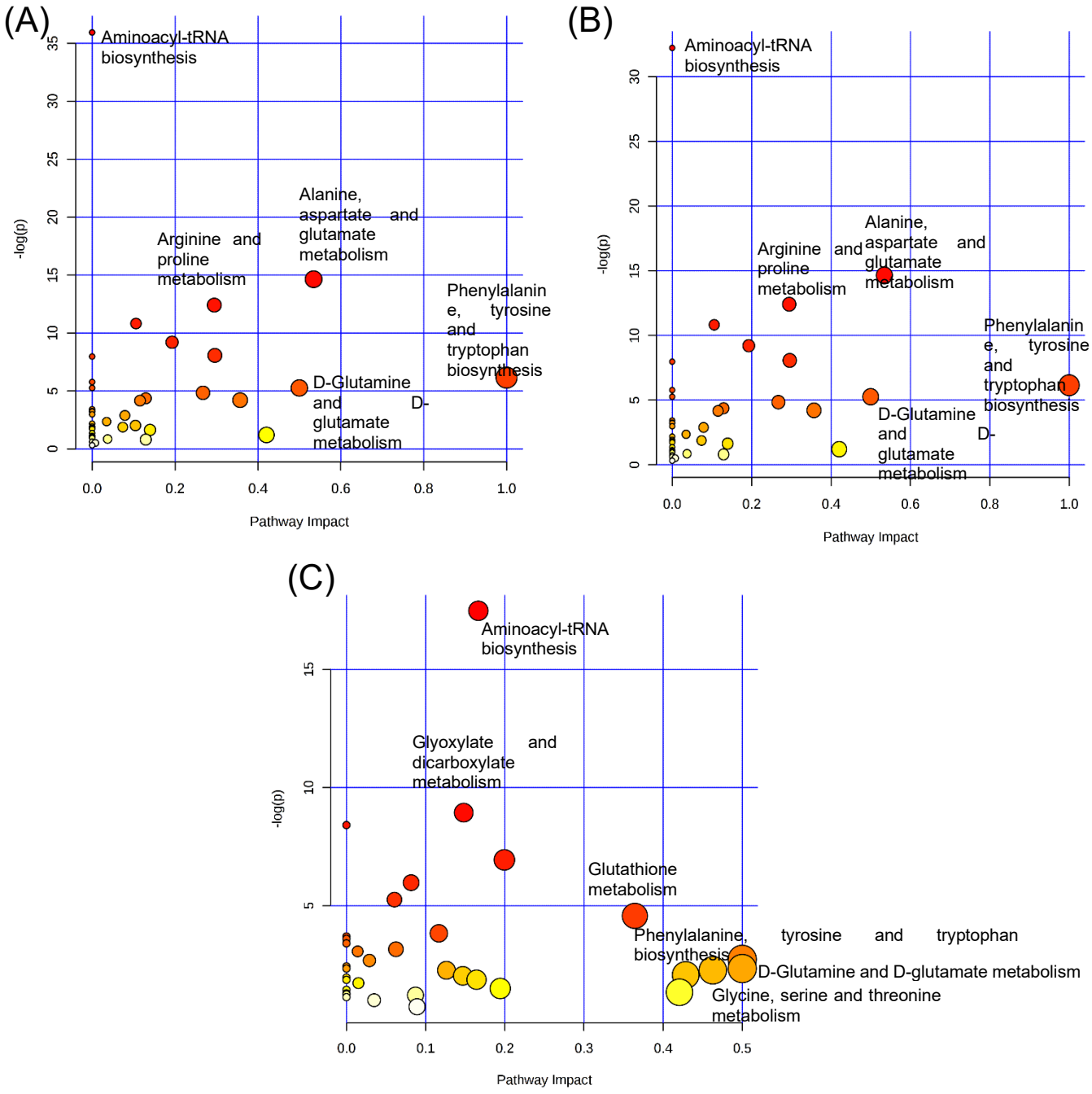

Figure 3.9 - Pathway analysis of CD4+ Cells stimulated with anti-CD3 and CHO cells expressing (A) CD80, (B) CD86 (C) or no co-stimulatory molecule. Analysis was carried out using Metaboanalyst 4.4 pathway and enrichment tool.

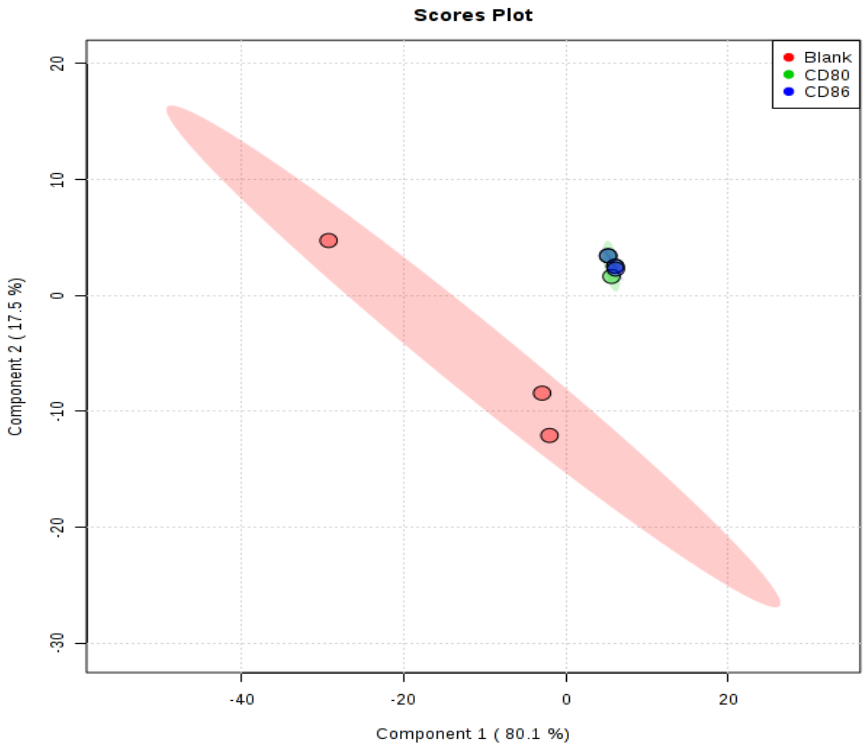

Figure 3.10 – PLSD-A of CD4+ T cells stimulated with CD80, CD86 or no co-stimulator (blank) Data was normalised using PQN prior to statistical analysis. Graph produced using Metaboanalyst 4.4 statistical analysis tools.

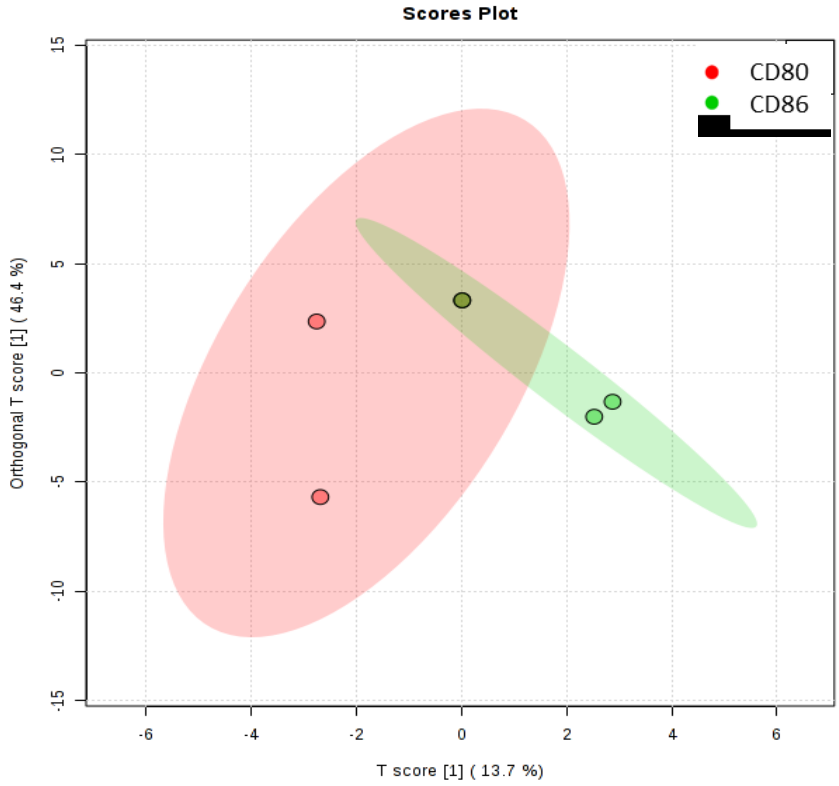

Figure 3.10A – PLSD-A of CD4+ T cells stimulated with CD80 or CD86 co-stimulatory molecules Data was normalised using PQN prior to statistical analysis. Graph produced using Metaboanalyst 4.4 statistical analysis tools.

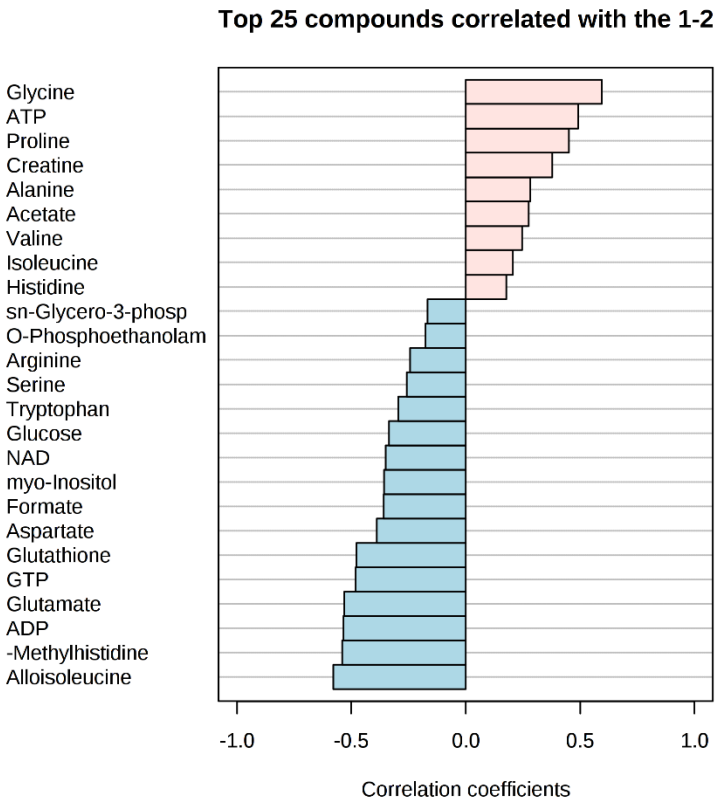

Figure 3.11 Correlations of intracellular metabolites between CD80/86 utilising Metaboanalyst pattern hunter. Pattern 1-2 was used to identify features within the dataset that increased in CD86 samples over CD80 samples. Graph produced using Metaboanalyst 4.4 pattern hunter tools.

Table 3.1: P values of intracellular metabolites of CD80/86 co-stimulated CD4+ T cells. Spearman's rank correlation test as shown in figure 3-11.

CHO (CD80/86) Intracellular	p-value
ADP	0.060331
GTP	0.21371
Glycine	0.21371
Glutamate	0.29197
ATP	0.43697
Lactate	0.43697
Methionine	0.43697
Proline	0.43697
Alloisoleucine	0.43697
Aspartate	0.43697
Glutathione	0.43697
Niacinamide	0.43697
O-Acetylcholine	0.43697
O-Phosphoethanolamine	0.43697
Tryptophan	0.43697
Tyrosine	0.43697
3-Methylhistidine	0.43697
Acetate	0.70684
Alanine	0.70684
Arginine	0.70684
Choline	0.70684
Creatine	0.70684
Formate	0.70684
Histidine	0.70684
Isoleucine	0.70684
Leucine	0.70684
myo-Inositol	0.70684
NAD	0.70684
Pyruvate	0.70684
Serine	0.70684
Succinate	0.70684
trans-4-Hydroxy-L-proline	0.70684
Creatine Phosphate	0.84501
UMP	0.84501
Valine	0.84501
AMP	1
Asparagine	1
Fumarate	1
Glucose	1
O-Phosphocholine	1
Phenylalanine	1
sn-Glycero-3-phosphocholine	1
Taurine	1

3.4.6 NMR Spectra comparison between extracellular metabolites of CD80 and CD86 co-stimulation of CD4+ T cells

Consequent NMR analysis of extracellular components collected from CHO co-cultured T cell samples revealed 26 identifiable metabolites (figure 3.12), of which no significant difference in concentration levels between experimental groups was observed when tested for significance. These included metabolites of the glycolytic pathway; glucose, pyruvate and lactate, as well as extracellular alanine: a metabolite noted in previous work to be essential in T cell activation (Ron-Harel *et al.,* 2019). As such, when employing PLSD-A analysis of extracellular metabolites, unsurprisingly no difference in clustering between CHO blank, CD80 and CD86 co-stimulated T cells was observed (figure 3.13). A change similarly reflected when focussing solely on CD80 and CD86, showing no discrimination between the two experimental groups as demonstrated by overlapping points (figure 3-14).

As with intracellular metabolites, to determine any correlation patterns between CD80 and CD86 extracellular metabolite levels, Metaboanalyst pattern hunting was utilised. Similarly employing a 1-2 pattern that compares CD86 stimulated T cells versus those co-stimulated by CHO CD80, pattern hunting revealed weak correlation coefficients between metabolites of the two experimental groups (figure 3-15). Of those metabolites identified, half in CHO CD86-stimulated T cells were negatively correlated to CD80, of which pyroglutamate and pyruvate showed the largest coefficients (not significant), whilst the remaining metabolites were positively correlated – that is higher concentration levels of CD86-positive cells. In particular, arginine ($p<0.05$) and proline.

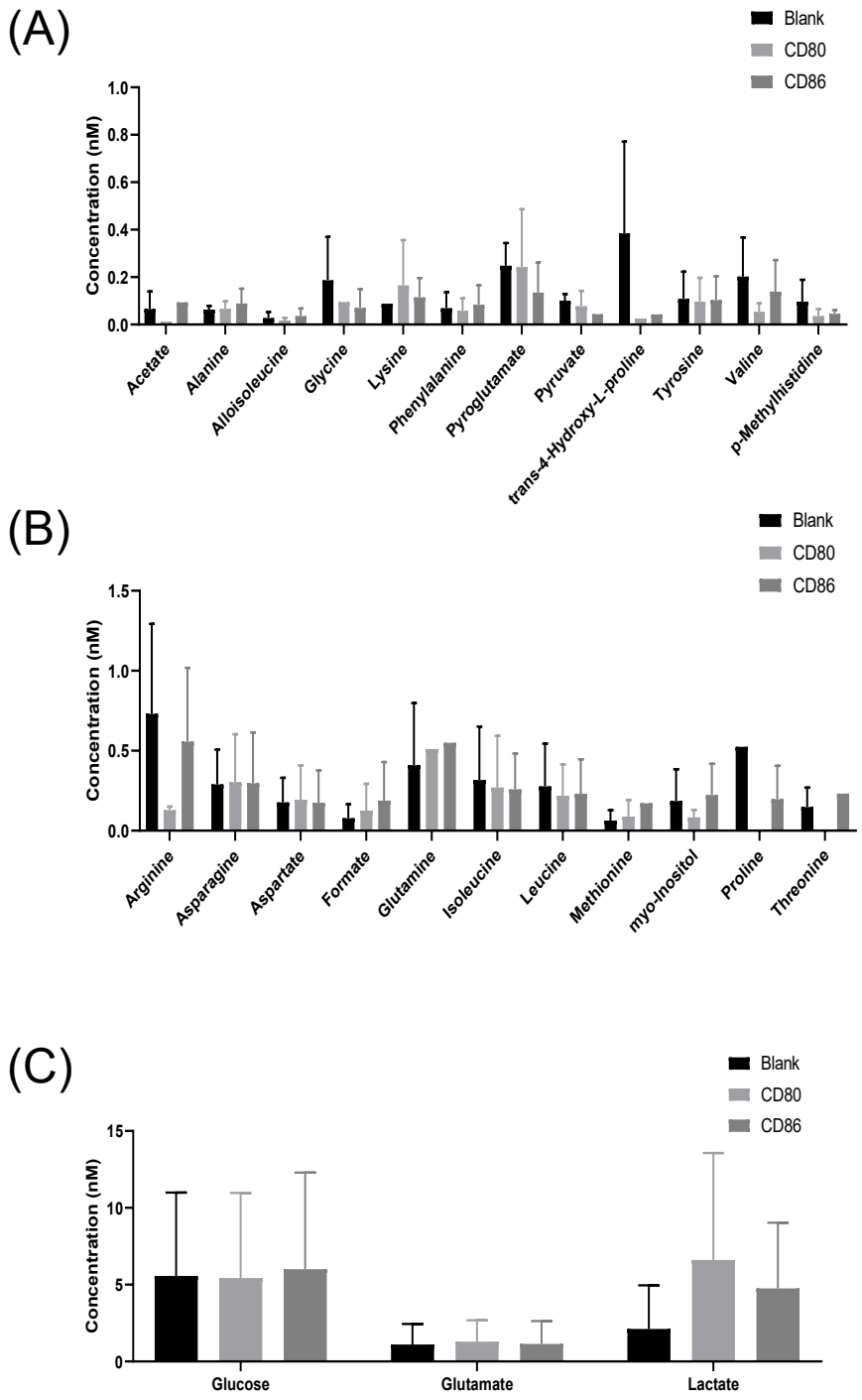

Figure 3.12 – All extracellular metabolite concentrations from CD4+ T cells cultured with CHO cells expressing co-stimulatory molecules CD80 or CD86 or no co-stimulatory molecule (blank) (n=3). Statistical analysis was run using ANOVA in PRISM statistical software. Data shown is mean with standard deviation.

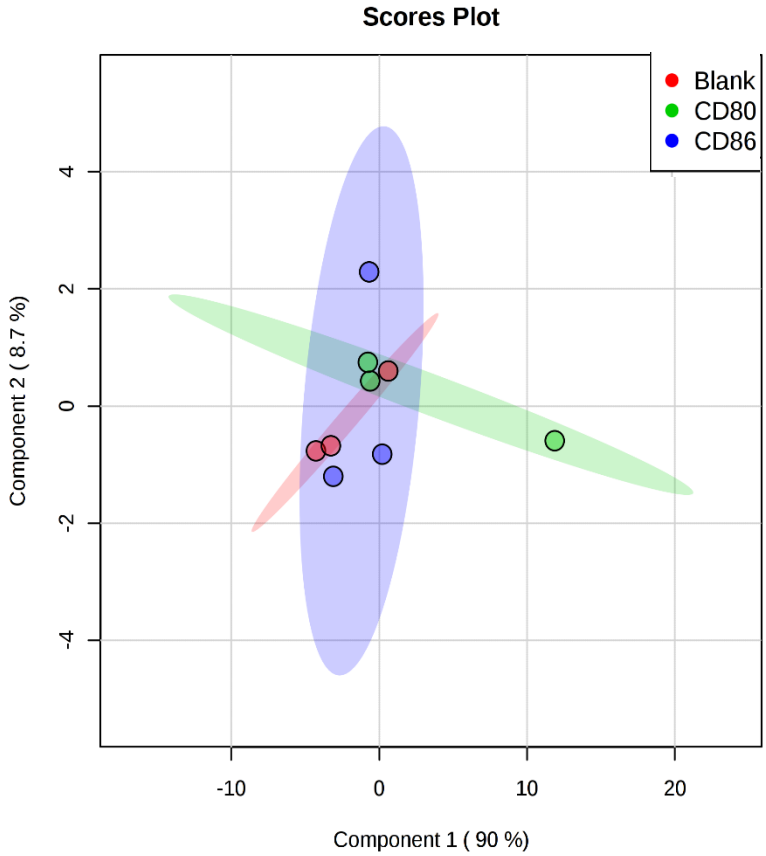

Figure 3.13 –PLSD-A of extracellular metabolites from CD4+ T cells stimulated with CD80, CD86 or no co-stimulatory molecules. Data was normalised using PQN prior to statistical analysis. Graph produced using Metaboanalyst 4.4 statistical analysis tools.

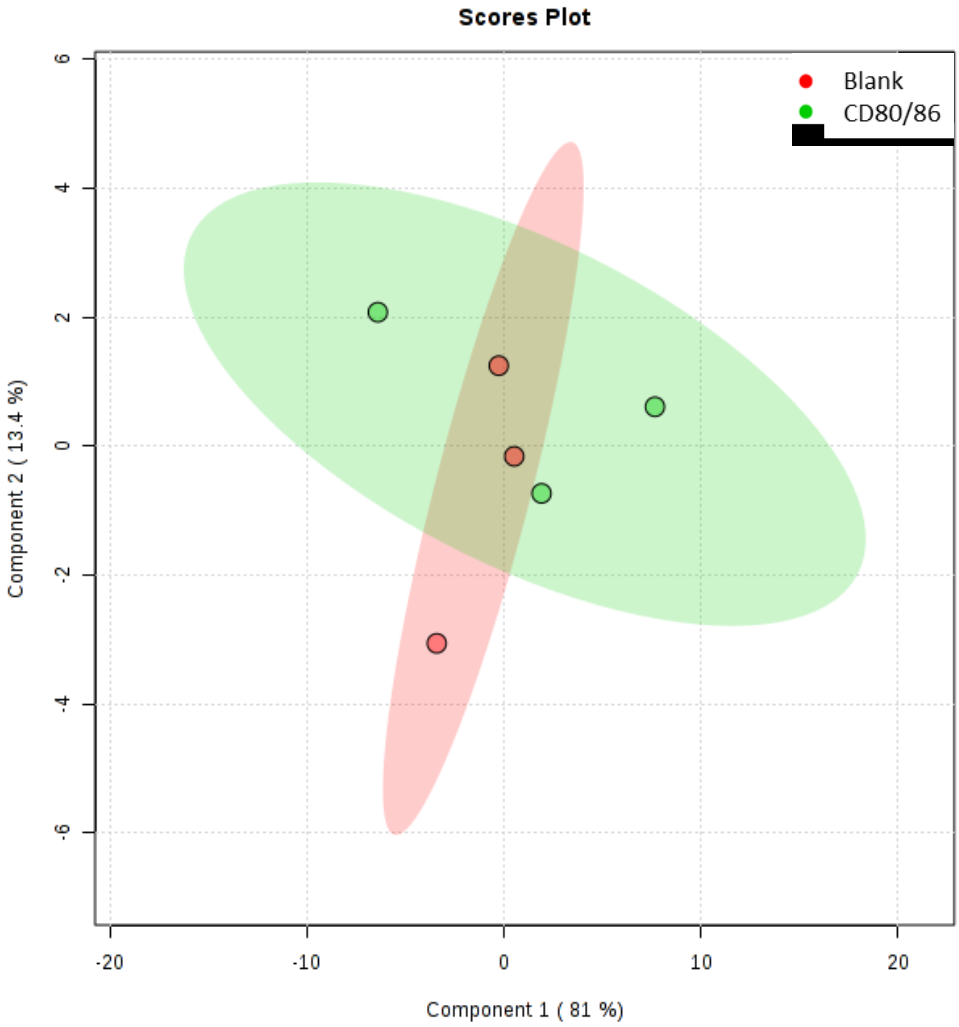

Figure 3.14 – PLSD-A of extracellular metabolites from CD4+ T cells stimulated with CD80/CD86 co-stimulatory molecules or no co-stimulatory molecule. Data was normalised using PQN prior to statistical analysis. Graph produced using Metaboanalyst 4.4 statistical analysis tools.

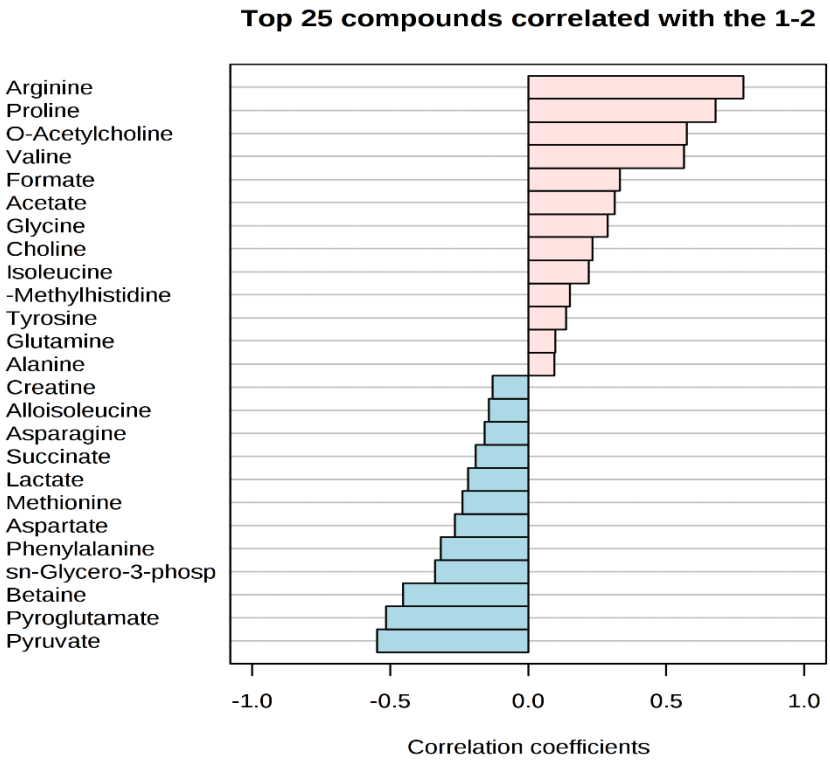

Figure 3.15 - Correlations of extracellular metabolites between CD80/86 utilising Metaboanalyst pattern hunter. Pattern 1-2 was used to identify features within the dataset that increased in CD86 samples over CD80 samples. Graph produced using Metaboanalyst 4.4 pattern hunter tools.

Table 3.2: P values of extracellular metabolites of CD80/86 co-stimulated CD4+ T cells. Spearman's rank correlation test as shown in figure 3-15.

CHO (CD80/86) Extracellular	p-value
Arginine	0.021312
Proline	0.12683
Lactate	0.32616
Pyroglutamate	0.32616
Pyruvate	0.32616
Valine	0.32616
O-Acetylcholine	0.56754
Alloisoleucine	0.57339
Aspartate	0.57339
Betaine	0.57339
Creatine	0.57339
Creatine phosphate	0.57339
Phenylalanine	0.57339
Succinate	0.57339
3-Methylhistidine	0.57339
sn-Glycero-3-phosphocholine	0.85196
trans-4-Hydroxy-L-proline	0.85196
Asparagine	0.85408
Choline	0.85408
Formate	0.85408
Glucose	0.85408
Glutamate	0.85408
Glutamine	0.85408
Leucine	0.85408
Lysine	0.85408
Methionine	0.85408
Tyrosine	0.85408
Acetate	0.85408
Alanine	0.85408
Glycine	0.85408
Isoleucine	0.85408
myo-Inositol	0.85408

3.5 Conclusion

The effects of varying TCR stimulus and their resultant cellular phenotypes is well outlined: including the examination of cellular function, differentiation, cytokine production and memory cell development. These processes underpinned by changes in T cell metabolism on cellular stimulation; for example, memory development has been linked with the cell's ability to utilise mitochondrial metabolism following infection, whilst cytokine production has been linked to glycolytic enzymes (Chang et al., 2013a, van der Windt and Pearce, 2012). TCR stimulation through small interactions with self-antigens is also well described as an anti-apoptotic mechanism in T cells, thought to promote T cell survival (Krogsgaard et al., 2007). As such, the contribution of signal 1 (anti-CD3) and signal 2 (anti-CD28) towards the T cell metabolic phenotype was investigated in the present study, with the effects of TCR only stimuli and, in turn, the increasing effects of TCR stimulus primarily examined.

Presentation of a classical two-signal T cell activation model using both anti-CD3 and anti-CD28 unsurprising resulted in a glycolytic phenotype in both naïve and memory T cells. Crucially, within these experiments, the signal 1 TCR signal was varied, whilst signal 2 was kept constant throughout. Therefore, the increasing glycolytic profile could be attributed to the increasing TCR stimulation (Figure 3.3). Although cells showed a marked increase in glycolytic metabolism, mitochondrial metabolism is unchanged, even at higher concentrations of anti-CD3. This is the hallmark of the Warburg phenotype, which has previously described in activated T cells (van der Windt and Pearce, 2012). Additionally, glycolytic metabolism plateaued at between 5 µg/ml and 10 µg/ml anti-CD3, suggesting a limit has been reached. This may be the maximal rate of glycolytic metabolism possible by only increasing CD3 stimuli and this bottleneck may be overcome if CD28 stimulation was altered.

Presentation of a CD28 co-stimulus, as per our results, is also likely to result in the cell's ability to overcome the activation threshold. Such activation arises from the stimulation of the downstream CD28 co-stimulatory pathway, that overlaps with the TCR signalling pathway, and amplifies the activatory signal (Boomer and Green, 2010a). Despite this, removal of the anti-CD28 co-stimulus in the present study (i.e. anti-CD3 TCR activation only) resulted in the significant upregulation of glycolysis solely in memory CD4+ T cells, but not naïve cells. Reasons for this remain unclear; however, may be ascribed to the subset differences between naïve and memory T cells and their associated roles: specifically, memory T cells are previously activated through TCR engagement and survey the body for repeat infections. As such they may be more prepared to upregulate their metabolism due to already having already altered their metabolic machinery as part of their phenotype and more swiftly prevent recurring infections. Furthermore, higher TCR stimuli has been association with mTOR complex 2 (mTORC2) engagement, which is associated with increased glucose uptake and glycolytic activity, alongside cell survival (Linke et al., 2017, Hawse and Cattley, 2019). Of additional interest, was the direct comparison between T cells stimulated with and without a co-stimulatory molecule, with T cell metabolism expected to be lower in cells stimulated with signal 1 alone (anti-CD3) to be less than that of T cells stimulated with both signals 1 and 2 (anti-CD3/CD28). Without signal 2, T cells are unable to undergo activation and as such, not required to upregulate their metabolic phenotype to support proliferation and cellular growth. Consequently, when assaying naïve CD4+ T cells here, metabolism appeared to be indifferent between anti-CD3 only and anti-CD3/CD28 groups (figure 3.5). The results suggest TCR stimulation alone may upregulate glycolytic metabolism in naïve cells enough to support growth and proliferation, like that of cells activated with signals 1 and 2. Indeed, homeostatic proliferation has been described previously, in which T cells repopulate the cellular

pool following events of lymphopenia (Gómez-Martín et al., 2011). It has also been suggested that lymphopenia drives the development of autoimmunity and organ-specific autoimmunity following homeostatic proliferation has been demonstrated in mice (King et al., 2004). If naïve T cells can upregulate their metabolic phenotype from solely a TCR stimulus, equal to that an activated counterpart, then homeostatic interactions are able to upregulate cellular metabolism to support an autoimmune event.

A caveat to this, however, this is the reductionist design and *in vitro* nature of the experiments employed here, with many homeostatic events having described additional cytokine signals. For example, interleukin (IL)-7 is an essential cytokine in the homeostatic maintenance of T cells, known to promote Glut1 upregulation, cell proliferation, c-Myc upregulation and cellular survival (Wofford et al., 2008, Seckinger et al., 1994). As such, in a static *in vitro* experimental model, it may be assumed that addition of IL-7 would likely exacerbate the phenotypes observed here. Secondly, our TCR signal, anti-CD3, is artificial and provides a strong TCR stimulus homogenously to each cell, as opposed to a more dynamic signal delivery expected *in vivo.* Thymic selection also removes auto-reactive T cells, that respond too strongly to self-antigen and as such, highly responding T cells may not occur naturally within the body (Klein et al., 2014). This supposed population of naïve T cells, which alter their metabolic phenotype, similar to that of activated T cells, may not exist, although naïve cells have been shown to alter their phenotypes following homeostatic interactions such as adopting a transient memory phenotype (Goldrath et al., 2000). Equally, T cell driven inflammatory diseases do occur and are increasing in prevalence within our population.

Alternatively, it could be thought that naïve T cells predominantly require TCR stimulation to alter their metabolic phenotype and signal 2 is only required for transcriptional upregulation and differentiation. As such, we can conclude that TCR stimulation (signal 1) is the main contributor to naïve cell metabolism, while co-stimulation (signal 2) plays a key role in upregulating memory cell metabolism. Within these experiments we have considered our naïve CD4+ T cell population 'activated' due to the similar metabolic phenotypes. Although the Warburg-like phenotype is characteristic of an activated T cell, activation also requires the upregulation of cell transcription, proliferation and cytokine production - parameters we have not measured here. Meanwhile it has been shown that naïve CD8+ T cells only require TCR stimulation to proliferate and differentiate and as such, would be prudent to measure these additional parameters in future investigations (Wang et al., 2000).

Finally, NMR analysis attempting to determine differences between different CD28 stimuli, CD80 and CD86 in T cells uncovered several observations. Here, our raw metabolite data appears to suggest the upregulation of several metabolites; however, due to the large amount of variation within samples, such differences were difficult to uncover between the experimental groups. Even with PLSD-A and pathway enrichment, difficulty was encountered in distinguishing CD80 and CD86 co-stimulated. Despite this, figure 3.9 did show the two test groups to be greatly different than that of the CHO blank controls, suggesting that stimulation of the T cells worked. Analysis of CHO blank controls to compare with our previous seahorse data, in particular CD3 only stimulations, would have been useful in this setting as NMR data, due to the mixed CD4+ population analysed. Conversely, for our CD80 and CD86 analysis, we were unable to analyse the effects of our CHO cells using the seahorse

due the expression of FITC from transfected cells, which would interfere with the optic fibre probes of the seahorse culture plates.

Despite this, NMR analysis required initial optimisations prior to assaying: requiring several changes to the previous standard operating procedure (SOP). Previously, experiments were carried out using a -40°C methanol wash to remove salt and allow 10% of the sample to be saved for parallel mass spectrometry analysis, either GC/MS or LC/MS. These experiments, however, had been carried out on adherent cells, which require a brief wash over the plate. Non-adherent cells, such as T cells, are suspended when washed. As such, the -40°C methanol led to cell death in the present study. In turn we decided to remove the methanol washes to allow us to carry out our NMR - though this limited our ability to utilise additional metabolomic technologies. In hindsight, development of a new protocol would have been advantageous: many previous mass spectrometry protocols have highlighted ways of utilising T cell lymphocytes, including Ulmer and colleagues (2015) demonstrating a working NMR protocol for Jurkat cell line (Ulmer et al., 2015). However, this protocol requires separate samples for both lipids and metabolites. The benefit of our current protocol is the separation of lipids from our solution, which may interfere with NMR analysis, as lipids have been shown to be indistinct and hard to identify using NMR.

A compromise to both these methods would be to use silicone oil. By placing the cell pellet onto a silicone bead and centrifuging the cells in order to trap them within the oil. This would effectively remove all salt from around them and allow the separation of lipids using chloroform, as shown in our method. Although promising, it is unclear how the cells would react once suspended in oil and whether this would adversely affect the results. Additionally, several further washes would be required to remove all the

oil, as this would interfere with both analytic techniques. However, being able to utilise both the strengths of mass spectrometry and NMR would yield very useful gains.

Chapter 4 | The effects of IL-6 pre-exposure upon the metabolic phenotype of CD4+ T cells

4.1 Introduction

Cytokines have long been known to influence the adaptive immune response, acting as a third activation signal (signal 3) to CD4+ T cells. Signal 3, unlike signal 1 and 2, is not required to initiate CD4+ T cell activation, though is well understood to amplify cell differentiation, expansion and survival. Response to such cytokine stimuli, however, varies across the CD4+ T cell population: for example, in response to interleukin (IL)-7 and IL-15, negligible response is observed in naïve CD4+ T cells when compared to effector memory CD4+ T cells, in part due to reduced cytokine receptor expression on naïve cells (Geginat *et al.,* 2001; 2003). Although in some limited studies naïve T cells have been shown to display cytokine responsiveness in the absence of TCR stimulation, resulting in upregulation and activation of downstream effector molecules (Perona-Wright *et al.,* 2010; Tough *et al.,* 1999). Despite this, the contribution of signal 3 specifically in relation to T cell metabolism has not been fully elucidated. Abnormal cellular metabolism is of particular note in immune-mediated inflammatory disease (IMIDs) and ageing, in which cytokine signalling is outlined to be exacerbated, including elevated levels of the proinflammatory cytokine IL-6. Indeed, IL-6 is noted as an important co-stimulatory molecule involved in T cell activation - able to elicit cellular proliferation independent of IL-2 gene expression (Lotz *et al.,* 1988).

First recognised as a B cell proliferation and differentiation factor, IL-6 is a pleiotropic cytokine produced by both haematopoietic and non-haematopoietic cells alike (Yoshida and Tanaka, 2014). Indeed, during inflammation following injury or infection, IL-6 is able to elicit a systemic effect following complementary binding to the cognate IL-6 receptor (IL-6R) and glycoprotein (gp)-130 complex to form heterotrimers. X-Ray crystallography shows that two heterotrimers bind to form hexameric complexes, allowing gp130 to induce an inflammatory as well as mitogenic gene expression profile

via downstream signalling pathways, including the Janus kinase (JAK)/STAT3 (Signal Transducer and Activator of Transcription 3) and P13k/AKT signalling (Baran et al., 2018). Interestingly, whilst gp130 is ubiquitously expressed on cells and is a shared component of several cytokine signalling pathways, IL-6R is predominantly expressed on leukocytes and hepatocytes. IL-6R is therefore a requisite for signalling between cells due to the lack of binding affinity between gp130 and IL-6. The release of soluble IL-6R (sIL-6R), produced through proteolytic shedding or alternatively splicing therefore facilitates IL-6/sIL-6R complex binding to gp130 to elicit such effects on non-IL-6R expressing cells – in a process known as trans-signalling (Baran et al., 2018). Trans-signalling facilitates the pleiotropic nature of IL-6 signalling in which sIL-6R is understood to predominantly induce proinflammatory activities versus the protective and anti-inflammatory profiles observed with classic membrane-bound IL-6 signalling.

As previously noted, alterations in IL-6 signalling are known to have roles both within IMIDs, as well aberrant T cell metabolism. CD4+ T cells of Crohn's and Rheumatoid Arthritis (RA) patients for example are shown to produce significantly less ATP and lactate versus healthy controls, whilst systemic lupus erythematosus (SLE) patients show increased ATP production (Yin et al., 2015, Wahl et al., 2010). This is despite elevated IL-6 and sIL-6R sera levels within all these conditions – thus allowing CD4+ T cells to be exposed to IL-6 prior to activation. Indeed, work from Newcastle University, a collaborating research centre, highlighting the importance of IL-6 on CD4+ T cell function showed increased cellular proliferation on exposure to signals 1 and 2 CD3/CD28 stimulation in to prior IL-6 given CD4+ T cells (Ridgley et al., 2017).

4.2 Aims

To follow on from these initial findings, we aimed to decipher whether pre-stimulation with IL-6 alters the metabolic phenotype of CD4+ T cells following activation by delineating transcriptional changes associated with IL-6/sIL-6R stimulation. Subsequently the proliferation of naïve and memory CD4+ T cells and assessing their metabolic phenotypes was examined.

4.3 T cell stimulation protocol

As previously described, naïve and memory populations were isolated using CD45RO microbeads, following CD4+ negative selection from leukapheresis cones. RF10 media was supplemented with equimolar IL-6/sIL-6R at 0.02, 0.1, 0.5 ng/ml. Concentrations were chosen for their physiological relevance. Cells were removed from media, washed with PBS and re-plated in well with plate bound anti-CD3 and fresh media supplemented with anti-CD28.

4.4 Results

4.4.1 Microarray analysis

Two microarray data sets were kindly provided by Newcastle University: (1) differential gene expression examined from CD4+ T cells drawn from whole blood (Pratt et al., 2012) and (2) differential gene expression in naïve *in vitro* CD4+ T cells, exposed to IL-6/sIL-6R for 72 hours, prior to stimulation with CD3/CD28 (Ridgley et al., 2019). Cells were extracted at set time points and compared against cells which had received no IL-6/sIL6R. The gene lists produced were used and analysed using EnrichR to genes which were relevant metabolically and function determines with PantherDB.

Of the initial patient microarray, differential gene expression of CD4+ T cells revealed several genes as key regulators in cellular metabolic function (figure 4.1) when stratified against the highest 4th quartile, and the lowest, 1st quartile of patient serum IL-6 expression. Genes included TNFAIP3 (TNFα-induced protein 3), NFKBIZ (NF-κB inhibitor zeta), BCL3 (B cell CLL/lymphoma 3), UGCG (UDP-glucose ceramide glucosyltransferase) and c-MYC (V-myc avlan myelocytomatosis viral oncogene homolog) – of which the latter was most distinguished by EnrichR analysis. In comparison, analysis of microarray genes differentially expressed within *in vitro* naïve CD4+ cells highlighted Myc-associated zinc finger protein (MAZ) as key (figure 4.2): described as a regulator of C-MYC as well as Glucose-6-phosphate dehydrogenase, an enzyme involved in the pentose phosphate pathway (PPP). The PPP is identified as a branch pathway from glycolytic metabolism, utilised for nucleotide synthesis and aromatic amino acid synthesis.

Symbol	Gene Name
MYC	**V-myc avlan myelocytomatosis viral oncogene homolog**
TNFAIP3	TNF alpha induced protein 3
NFKBIZ	NFKB inhibitor zeta
BCL3	B-cell CLL/lymphoma 3
UGCG	UDP-glucose ceramide glucosyltransferase
PIM1	Pim-1 proto-oncogene, serine/threonine kinase
SOCS2	Suppressor of cytokine signalling 2
SOCS3	Suppressor of cytokine signalling 3

Figure 4.1 – Gene array analysis from rheumatoid arthritis patients. CD4+ T cells were taken from patient whole blood and gene expression was analysed. Genes were stratified by patient serum IL-6 levels and differentially expressed genes were identified by comparing 1st and 4th quartiles. EnrichR was used to carry out analysis and identify gene function. Genes highlighted in orange are metabolic genes or associated with key metabolic pathways.

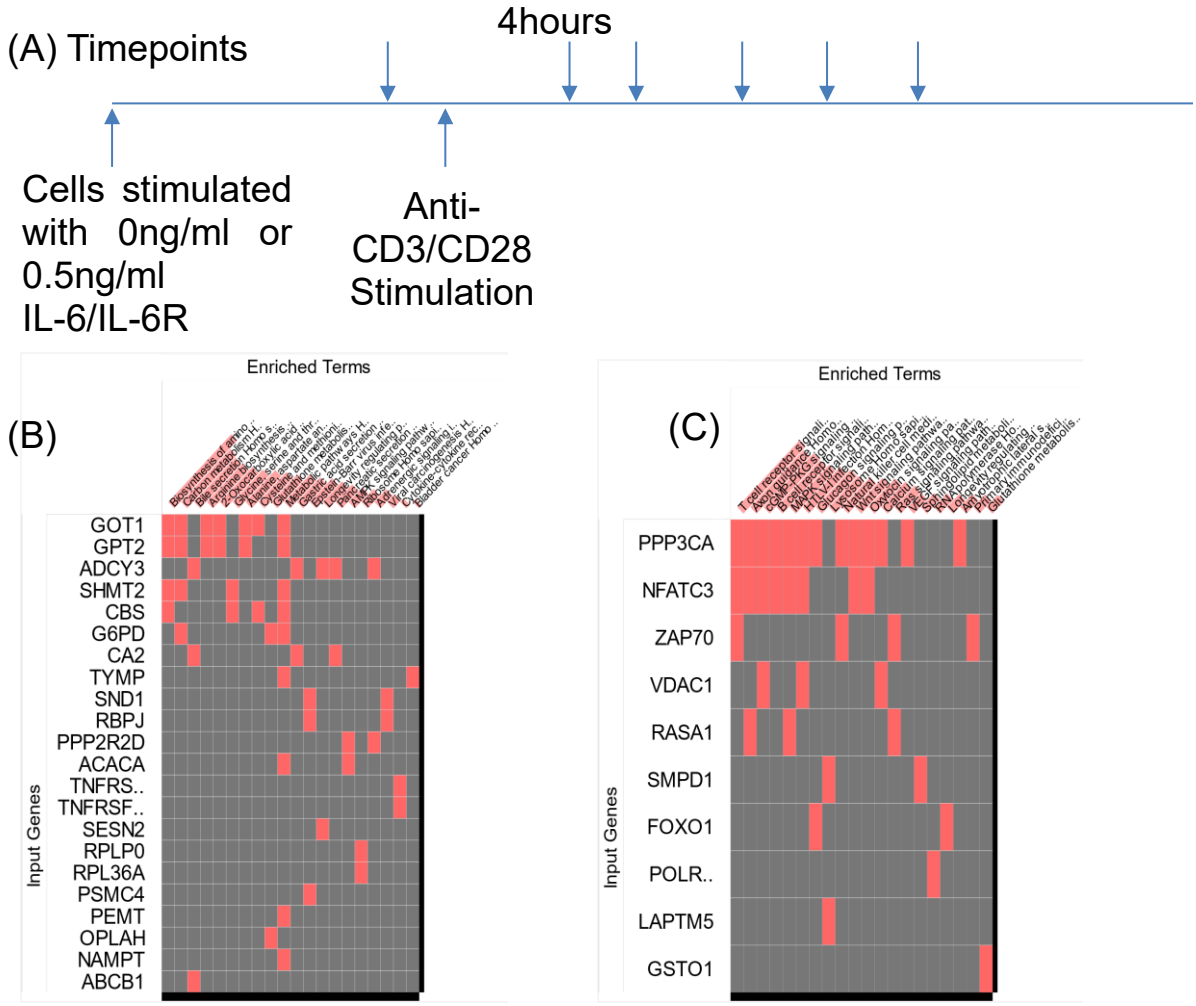

Symbol	Gene Name
GPT2	glutamic pyruvate transaminase (alanine aminotransferase) 2
OPLAH	5-oxoprolinase (ATP-hydrolysing)
GOT1	glutamic-oxaloacetic transaminase 1, soluble
SLC43A1	solute carrier family 43 (amino acid system L transporter), member 1
SHMT2	serine hydroxymethyltransferase 2 (mitochondrial)
G6PD	glucose-6-phosphate dehydrogenase
ACACA	acetyl-CoA carboxylase alpha
MAZ	MYC-associated zinc finger protein (purine-binding transcription factor)
SLC30A1	solute carrier family 30 (zinc transporter), member 1

Figure 4.2 Microarray analysis of differentially expressed genes of naïve CD4+ T cells at different time points. An enrichment map showing genes with increased expression, following IL-6/IL6-R stimulation. Timepoints from analysis are shown in (A). Analysis of data was carried out using pathway enrichment analysis, carried out using EnrichR and the KEGG 2016 database. Upregulated genes from four hours post CD3/CD28 stimulation is shown in (B) and downregulated genes are shown in (C). Enriched terms are shown across the top row, in descending order of enrichment. Genes are shown across the left-hand side of the table. Enrichment terms are ranked using the calculated combined score.

4.4.2 Cellular proliferation of CD4+ T cells are induced in response to Signal 3 IL-6R stimulation

The role of IL-6 as a co-stimulatory molecule following TCR engagement is widely noted within the literature: stimulation resulting in functional cellular changes including enhanced survival, differentiation and migration (Dienz and Rincon, 2009). Indeed, in response to stimulatory signals, CD4+ T cells are shown to expand. In the presence of IL-6, for example, the effector/memory T cell population increases as a result of downstream JAK/STAT-mediated mitogenic gene expression, as well as the downregulation of anti-apoptotic FasL that enables cellular survival (Ayroldi et al., 1998). Naive and memory T cells display differences in their ability to respond to IL-6, thought to arise as a result of cellular reprogramming that ensues following initial T cell activation (Twohig *et al.,* 2019). As expected, the genetic ablation of IL-6R appears to coincide with a reduction in T cell numbers and functionality, including within CD4+ T cell population (Nish et al., 2014).

Experiments were conducted in the present study to ascertain the role of IL-6 in CD4+ naïve and memory T cell activation. Using flow cytometry on gated CD3/CD28 co-stimulated T cells isolated from healthy controls, proliferative indexes were determined in response to increasing concentration of prior IL-6 stimuli. Exposure showed that in response to increasing IL-6, significantly greater proliferation following CD3/CD28 engagement was observed in naïve T cells when prior exposed to 0.02-0.5 ng/ml of IL-6 versus unstimulated cells (figure 4.3). Memory T cells appeared to demonstrate a no response to prior IL-6 exposure – perhaps ascribed to the cellular reprogramming thought to occur in naïve T cells when initially activated.

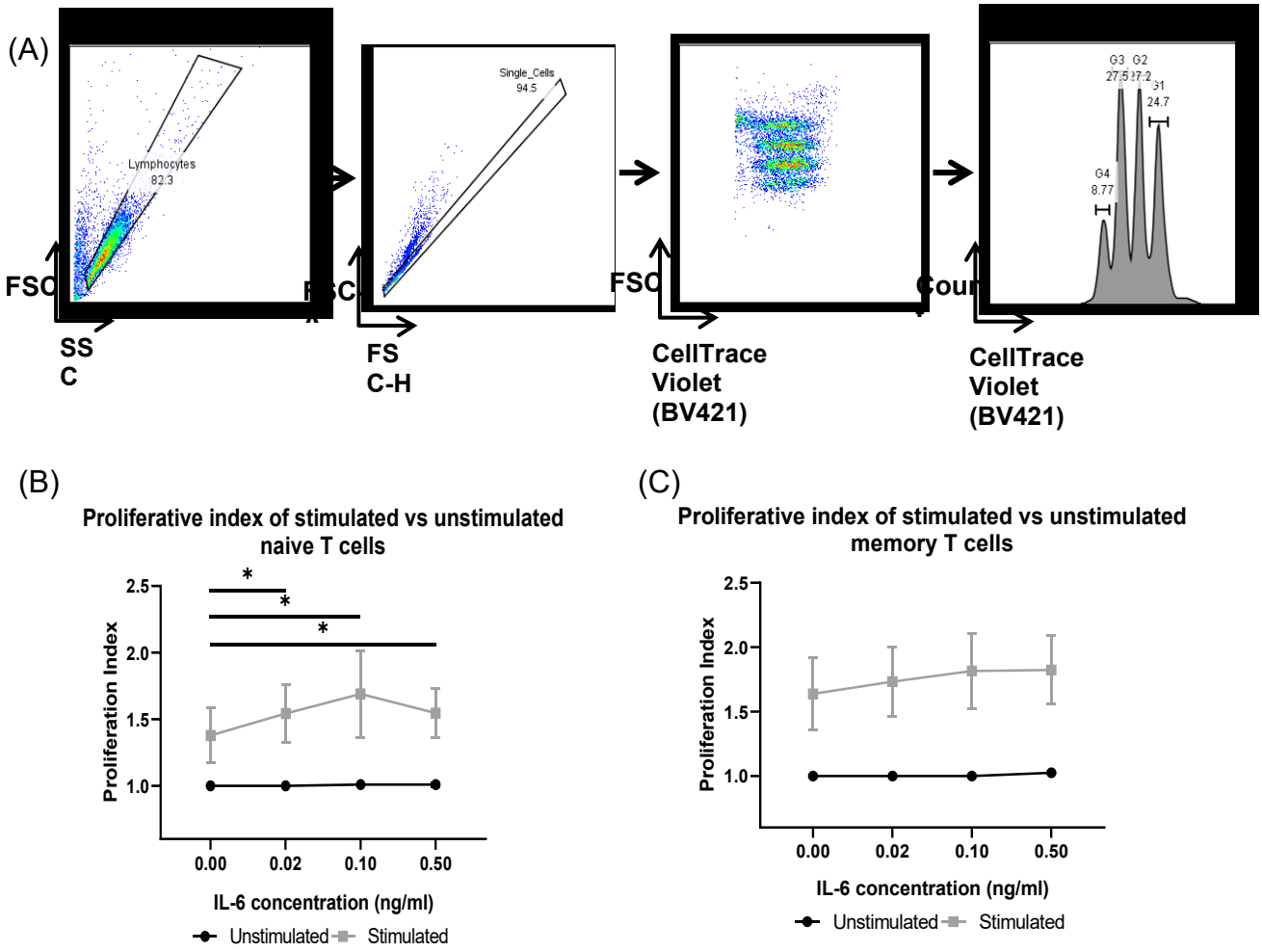

Figure 4.3 - Proliferation of CD4+ T cells after 3 days of IL-6/IL-6R treatment and subsequent activation with CD3/CD28 for 6 days (A) Gating strategy shown was used to identify lymphocytes on cell size, remove doublets and determined proliferation using cell trace violet. Cell generations were identified using FlowJo v7 proliferation tool and used to calculate the proliferation index of (B) naïve T cells and (C) memory T cells respectively. Statistical significance was calculated using multiple comparisons ANOVA in Prism v8. *p<0.05 (n=6)

4.4.3 Priming with IL-6/IL-6R leads to increased glycolysis in naïve CD4+ T cells

The genetic ablation and subsequent loss in IL-6R signalling results in the reduction of CD4+ T cell-mediated expansion and survival, highlighting the importance of IL-6 in immune cell homeostasis (Nish et al., 2014). CD4+ T cell activation and proliferation varies, however, with previous work demonstrating CD4+ memory cells have reduced effector function and blunted response in the absence of IL-6 (Strutt et al., 2016). Conversely, our results appear to show increased glycolytic ability in naïve but not memory CD4+ T cell, showing significantly increased calculated glycolysis ($p=0.01$) within the naïve T cells as IL-6 concentration increased to 0.5 ng/ml (figure 4.4B). Subsequently when assessing mitochondrial metabolism, priming with increased levels of IL-6 appeared to significantly increase oxygen consumption rate following mitochondrial ETC uncoupling within activated naïve T cells, as indicated by maximal respiration (figure 4.5B). A comparison is shown in figure 4.6. Such increases in naïve T cell mitochondrial respiration was not a result of elevated levels of oxygen consumption basally in response to IL-6, nor resulted in increased ATP production (figure 4.5A, C). Interestingly, despite previously describing increased glycolytic activity in response to CD3 and CD3/CD28 co-stimulations, no significant differences in glycolytic activity (figure 4.4C-E) nor mitochondrial metabolism (figure 4.5) was observed when primed with IL-6.

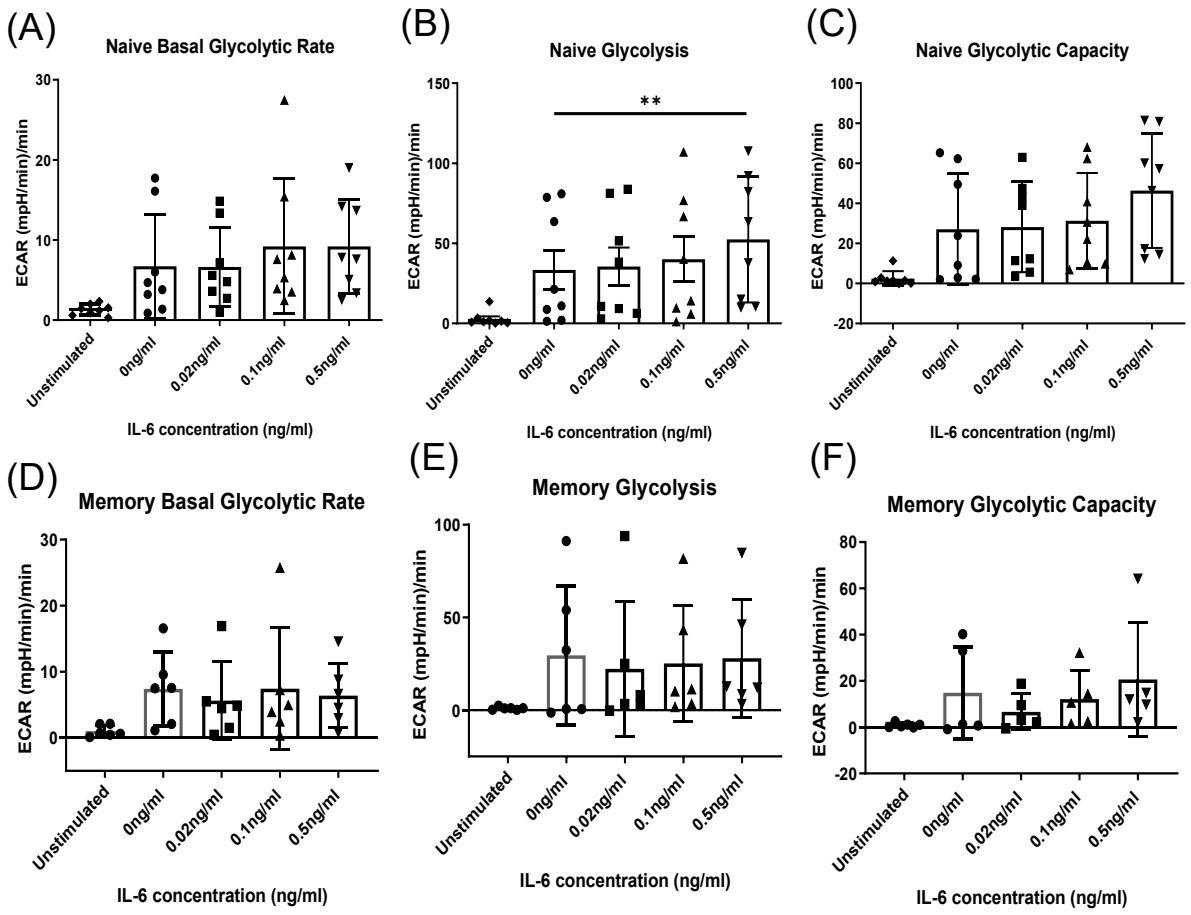

Figure 4.4 – Measurement of glycolytic parameters in naïve and memory CD4+ T cells pre-stimulated with IL-6/sIL-6R prior to CD3/CD28 activation. (A), (B) & (C) show the Basal glycolytic rate prior to injection of glucose, cellular glycolysis following 25mM glucose injection and the glycolytic capacity of Naïve T cells, respectively. (D), (E) & (F) show the basal glycolytic rate prior to injection of glucose, cellular glycolysis following 25mM glucose injection and the glycolytic capacity of memory T cells, respectively. Data shows mean values with standard deviation. Analysis was performed using repeated measures ANOVA with Tukey multiple comparison * $p<0.05$, **=0.01. (n=8)

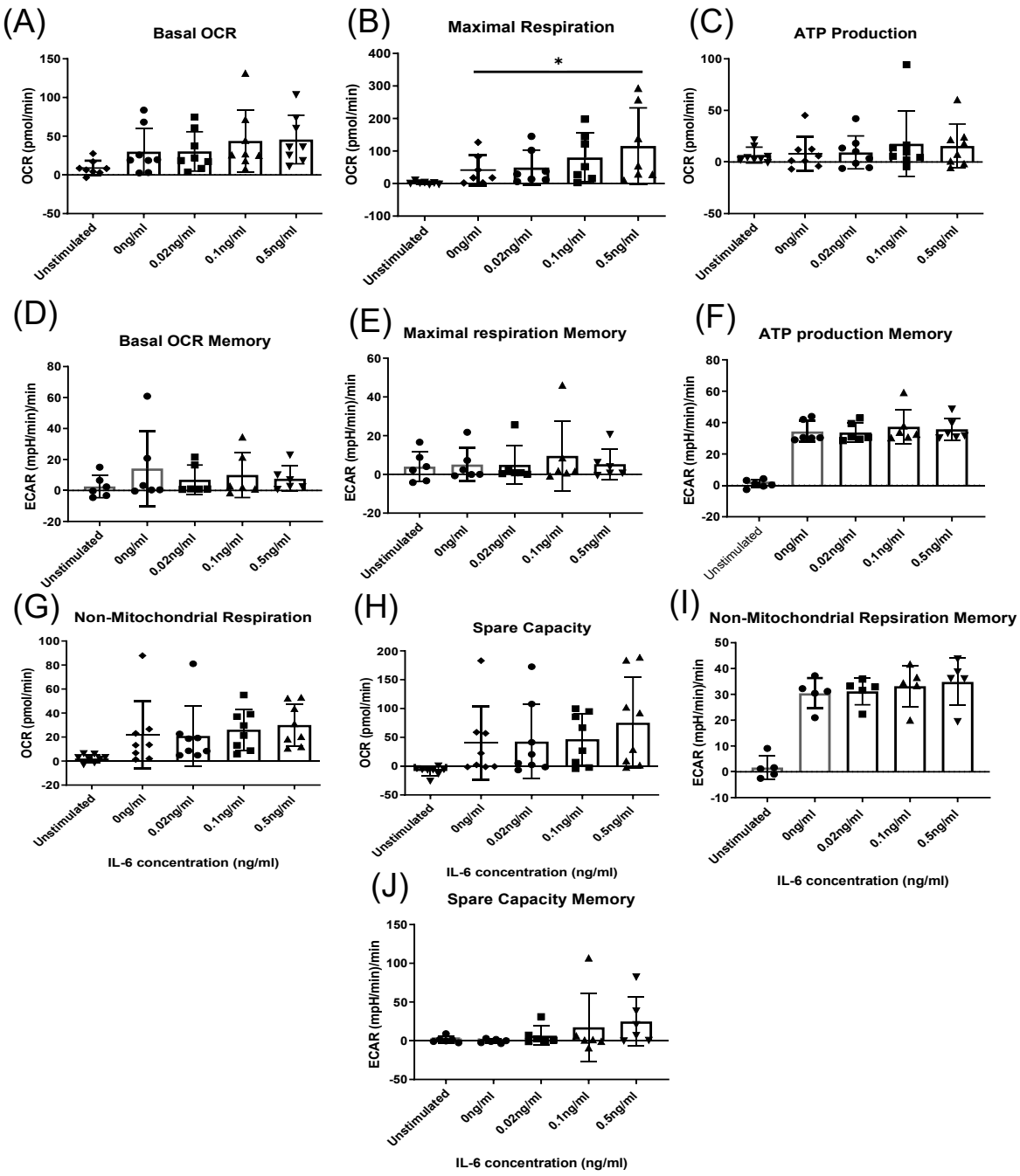

Figure 4.5 – Measurement of mitochondrial metabolism in naïve and memory CD4+ T cells pre-stimulated with IL-6/sIL-6R prior to CD3/CD28 activation. Cell populations were isolated and analysed using Seahorse XF96. Naive cell parameters are shown; (A) basal respiration prior to glucose injection, (B) maximal respiration following FCCP injection, (C) ATP production, (G) Spare respiratory capacity and (H) non-mitochondrial respiration following rotenone and antimycin A injections. Memory cell parameters are shown; (D) basal respiration prior to glucose injection, (E) maximal respiration following FCCP injection, (F) ATP production, (I) Spare respiratory capacity and (J) non-mitochondrial respiration following rotenone and antimycin A injections. Data shown is mean with standard deviation. Analysis was performed using paired ANOVA with Tukey multiple comparison. * $p<0.05$ (n=8)

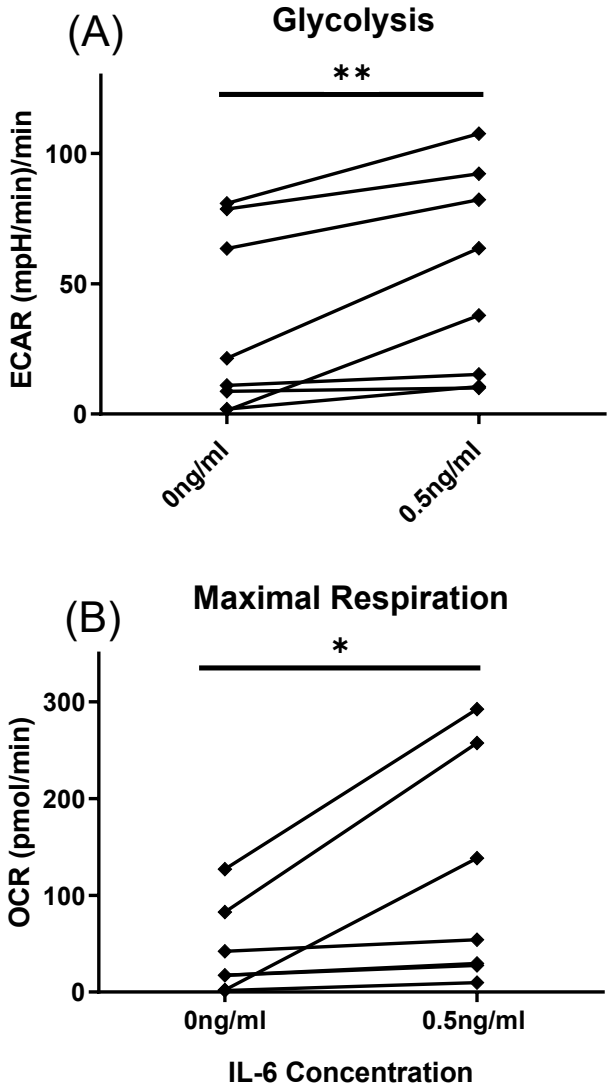

Figure 4.6 - Comparison of glycolysis and maximal capacity of naïve CD4+ T cells between 0.5ng/ml treated cells and untreated cells after 72 hours IL-6/sIL-6R stimulation prior to activation. Taken from figure 4.3B and 4.4B. * = p<0.05, ** = p<0.01. (n=8); 1 data point classified as an outlier (>mean ±1.5SD) excluded from maximal respiration.

4.4.4 NMR Spectra comparison between intracellular metabolites of CD4+ T cells treated with varying IL-6/IL-6R

To determine the metabolic profiles induced through CD3/CD28 T cell activation with the additional prior priming with cytokine IL-6, nuclear magnetic resonance (NMR) spectrometry was employed to explore any metabolic shifts within the CD4+ population. NMR analysis of T cells revealed 30 identifiable intracellular metabolites (figure 4-7). Of those identified, none were significantly different when tested, despite some trends of increased metabolite concentrations at increasing concentrations of IL-6 when compared to non-IL-6 stimulated cells. For example, concentrations of ATP (adenosine triphosphate), serine and tryptophan are shown to increase at 0.5 ng/ml concentration (figure 4.7A, B), a trend which compares to no observational changes in glucose or lactate (figure 4.7C), despite significant glycolytic activity observed in CD4+ naïve T cells.

As with chapter 3, metabolites were normalised using probabilistic quotient normalisation (PQN) prior to statistical analysis and probed for the identification of possible intracellular metabolic pathways affected by IL-6/sIL-6R stimulation. To determine metabolites discriminating between groups within the data set, partial least squares discriminant analysis (PLSD-A) was undertaken; regression revealing poor discrimination between intracellular metabolites identified in IL-6 unstimulated CD4+ T cell populations and groups primed with varying concentrations of IL-6/sIL-6R - with the majority of experimental groups showing overlapping points (figure 4.8A). Since stimulation of IL-6/sIL-6R appeared to elicit changes in glucose and OXPHOS metabolism, direct comparisons between unstimulated and 0.5 ng/ml IL-6/sIL-6R CD4+ T cell groups were additionally undertaken. In this manner, PLSD-A analysis revealed that whilst there was some considerable overlap between intracellular

metabolites between unstimulated and IL-6/sIL-6R primed T cells, there was some discrimination in n=2 samples (figure 4.8C).

Subsequent pattern hunting identifying linear correlations between metabolite levels with the pre-described pattern 1-2-3-4; that is, (1) unstimulated versus pre-stimulation with IL-6/sIL-6R at (2) 0.02 ng/ml (3) 0.1 ng/ml and (4) 0.5 ng/ml concentrations showed weak correlation coefficients across intracellular metabolites identified, of which the majority were positively correlated. Notably trans-4-hydroxl-L, taurine and O-acetylcarnitine metabolites were shown to be decreased in unstimulated CD4+ T cells when compared to IL/sIL-6 primed groups whilst the inverse is true for a number of metabolites, such as proline, fumarate and tryptophan (figure 4.8B) Pattern hunting specific to non-primed CD4+ T cells versus 0.5 ng/ml IL-6/sIL-6R revealed greater concentrations of 11 metabolites in the latter group, including alloisoleucine, pyroglutamate and citrate – all of which are associated with energy metabolism and cellular growth (figure 4.8D). Asparagine and Methylmalonate were most negatively correlated between unstimulated and 0.5 ng/ml stimulated CD4+ cells.

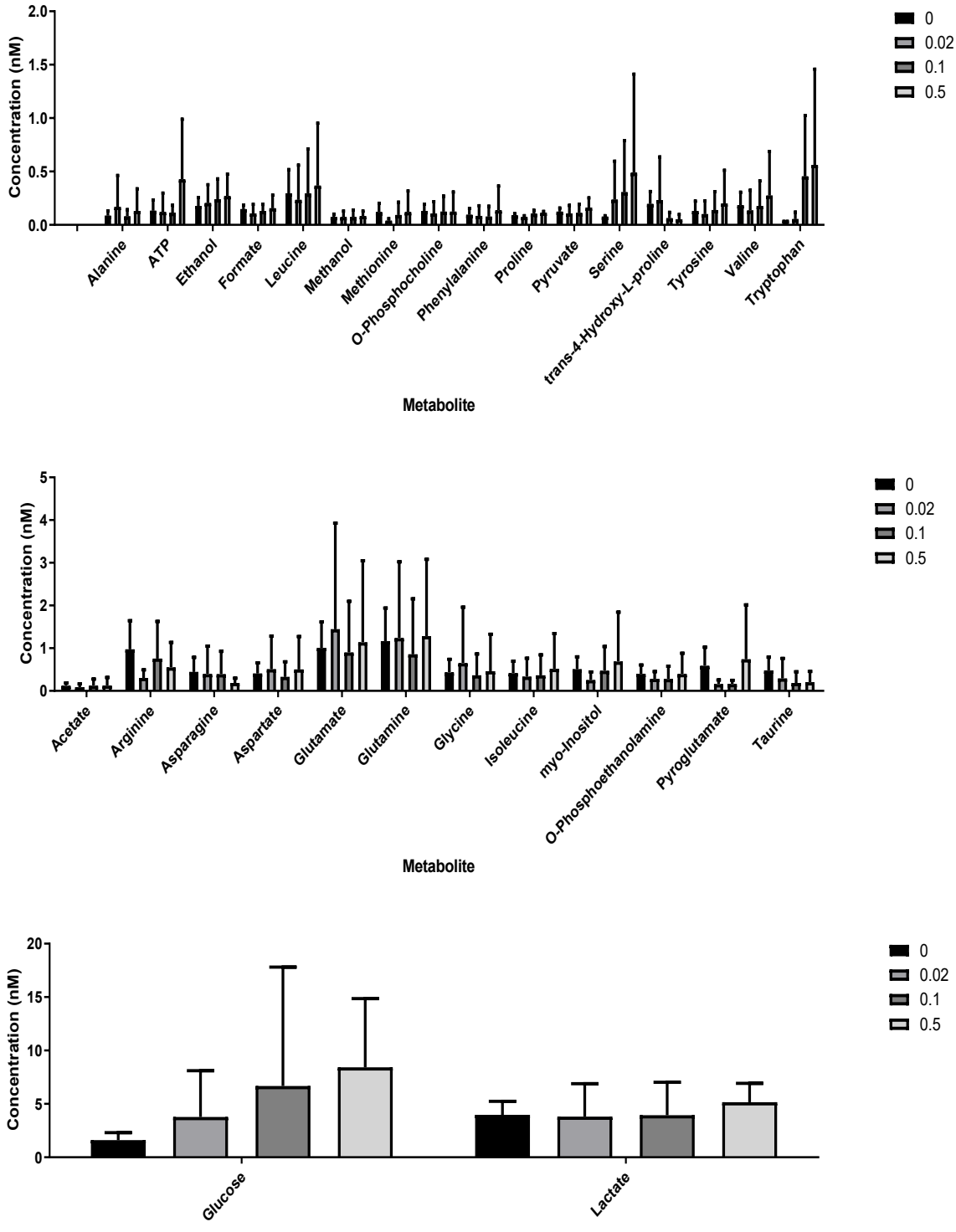

Figure 4.7 - Intracellular metabolites from CD4+ T cells treated with 0 ng/ml; 0.02 ng/ml; 0.1 ng/ml; and 0.5 ng/ml concentrations of IL-6/IL-6R for 72 hours with subsequent CD3/CD28 stimulation. Concentrations were calculated using Chenomx NMR suite and plotted using Prism v8. (n=6)

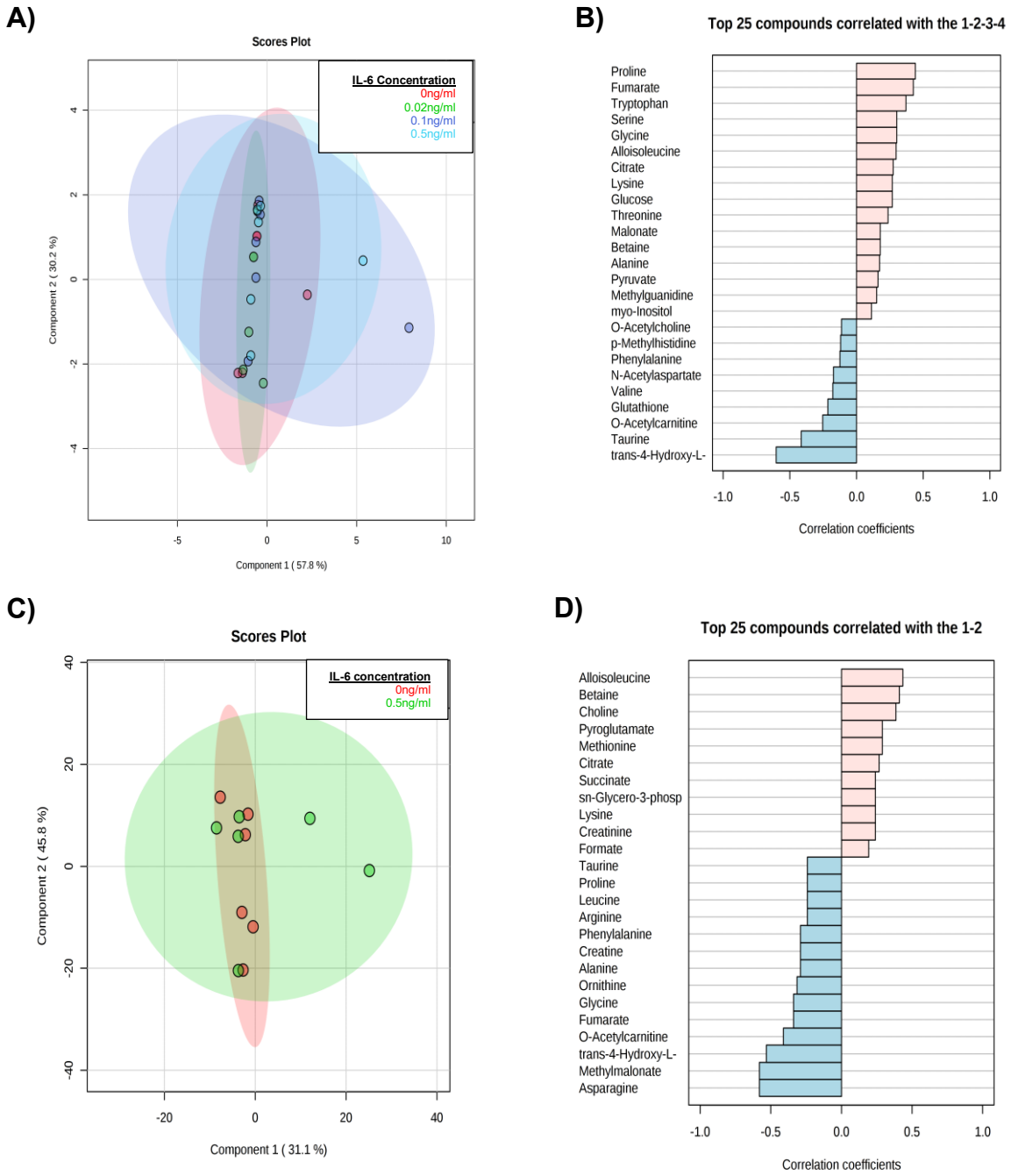

Figure 4.8 – PLS-DA and pattern hunter correlation analysis of intracellular metabolites from CD4+ T cells treated with varying concentrations of IL-6/IL-6R for 72 hours with subsequent CD3/CD28 stimulation. PLS-DA analysis of (A) intracellular metabolites between unstimulated and CD4+ T cells pre-stimulated with 0.02, 0.1 and 0.5 ng/ml IL-6/sIL-6R and (B) subsequent pattern correlation analysis. (C&D) PLS-DA analysis and pattern hunting correlation analysis of intracellular metabolites between unstimulated and 0.5 ng/ml pre-stimulated IL-6/sIL-6R CD4+ T cells. PLS-DA data was normalised using PQN prior to statistical analysis; Pattern hunting was used to identify features within the dataset that increased in unstimulated cells over IL-6/sIL-6R pre-stimulated samples. Graph produced using Metaboanalyst 4.4 statistical analysis tools.

Table 4.1: P values of intracellular metabolites of CD4+ T cells pre-treated with IL-6/sIL-6R followed by CD3/CD28 co-stimulation. Spearman's rank correlation test as shown in figure 4.8

IL-6/sIL-6R Pre-stimulated Intracellular	p-value	IL-6/sIL-6R Pre-stimulated Intracellular	p-value
trans-4-Hydroxy-L-proline	0.000845	Creatine	0.74504
Taurine	0.046994	Succinate	0.74509
Lysine	0.065082	Acetate	0.76414
Proline	0.12347	Creatine phosphate	0.76414
Tryptophan	0.18498	Glycolate	0.76414
Alloisoleucine	0.19393	NAD	0.78332
O-Acetylcarnitine	0.19393	Lactate	0.80262
Glutathione	0.20317	Niacinamide	0.82199
3-Methylhistidine	0.20317	Malonate	0.84155
ADP	0.32453	myo-Inositol	0.84155
Asparagine	0.32453	Arginine	0.84155
Sarcosine	0.35051	O-Phosphoethanolamine	0.84155
ATP	0.36395	Glycine	0.86115
Serine	0.3917	Methylmalonate	0.86115
N-Acetylaspartate	0.3917	Ethanol	0.88084
Valine	0.40602	Isoleucine	0.88084
Betaine	0.45066	Phenylalanine	0.90059
Tyrosine	0.45066	Leucine	0.92041
Alanine	0.46609	Pyroglutamate	0.92041
Threonine	0.46609	Methionine	0.94026
Choline	0.49775	Ornithine	0.96016
Citrate	0.49775	Methanol	0.96016
AMP	0.49775	O-Phosphocholine	0.98007
Fumarate	0.54717	Formate	0.98007
Glucose	0.56413	O-Acetylcholine	0.98007
Methylguanidine	0.59873	Theophylline	1
Aspartate	0.63419		
Pyruvate	0.6888		
Glutamate	0.70745		
sn-Glycero-3-phosphocholine	0.70745		
Creatinine	0.72614		
Glutamine	0.72619		

4.4.5 NMR Spectra comparison between extracellular metabolites of CD4+ T cells treated with varying IL-6/IL-6R

Consequent NMR analysis of extracellular components collected from unstimulated CD3/CD28-stimulated CD4+ T cell samples revealed 30 identifiable metabolites (figure 4.9), of which no significant difference in concentration was observed when tested for significance. As such, when employing PLSD-A of extracellular metabolites, unsurprisingly no difference was observed in clustering between IL-6 unstimulated CD4+ T cell populations and groups primed with varying concentrations of IL-6/sIL-6R (figure 4.10A) A change similarly reflected when solely focussing on 0 ng/ml and 0.5 ng/ml stimulated CD4+ T cells, in which no discrimination between the two experimental groups was shown by overlapping points (figure 4.10C).

As with intracellular metabolites, to determine any correlation patterns between IL-6/sIL-6R unstimulated and IL-6 primed, Metaboanalyst pattern hunting was utilised. Employing a 1-2-3-4 linear comparison, pattern hunting revealed predominantly negative correlations between metabolites of the four experimental groups (figure 4.10B). Interestingly, of those positively correlated were alloisoleucine, glutathione and methionine, whilst serine and threonine showed the greatest negative correlations: that is, reduced concentrations of these metabolites within unstimulated cells. Similarly, correlations made by pattern hunting between 0 ng/ml and 0.5 ng/ml IL-6 pre-stimulation groups revealed similar profiles of positively correlated metabolites – such as O-phosphocholine, methionine, tryptophan and glutathione (figure 4.10D). Thus appearing to confirm higher levels of these metabolites in pre-stimulated activated CD4+ T cells.

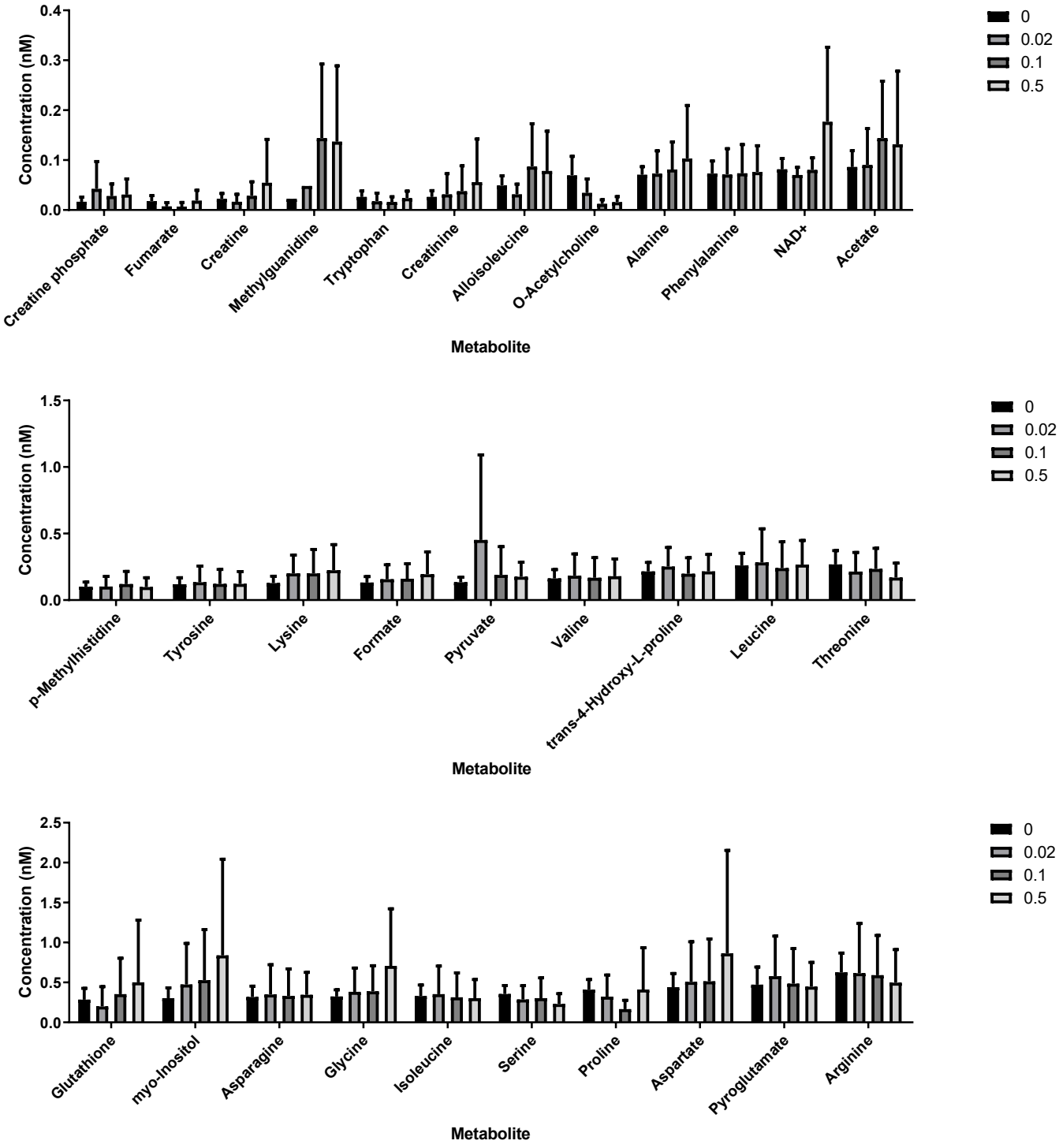

Figure 4.9 - Extracellular metabolites from CD4+ T cells treated with 0 ng/ml; 0.02 ng/ml; 0.1 ng/ml; and 0.5 ng/ml concentrations of IL-6/IL-6R for 72 hours with subsequent CD3/CD28 stimulation. Statistical analysis was run using two-way ANOVA in PRISM 8.2 statistical software. Data shown is mean with standard deviation (n=6)

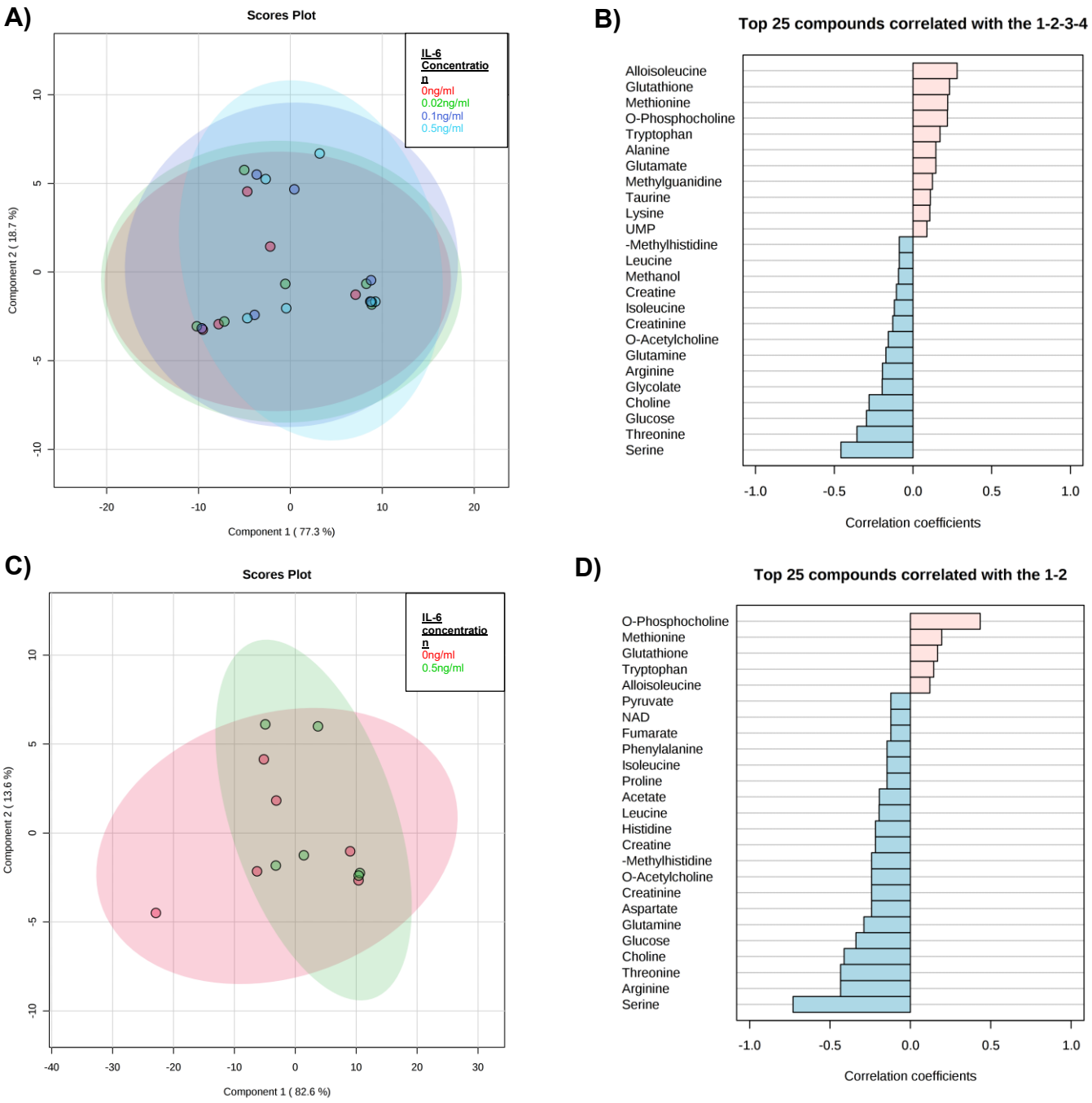

Figure 4.10 – PLS-DA and pattern hunter analysis of extracellular metabolites from CD4+ T cells treated with varying concentrations on IL-6/IL-6R for 72 hours with subsequent CD3/CD28 stimulation. PLS-DA analysis of (A) extracellular metabolites between unstimulated and CD4+ T cells pre-stimulated with 0.02, 0.1 and 0.5 ng/ml IL-6/sIL-6R and (B) subsequent pattern correlation analysis. (C&D) PLS-DA analysis and pattern hunting correlation analysis of extracellular metabolites between unstimulated and 0.5 ng/ml pre-stimulated IL-6/sIL-6R CD4+ T cells. PLS-DA data was normalised using PQN prior to statistical analysis; Pattern hunting was used to identify features within the dataset that increased in unstimulated cells over IL-6/sIL-6R pre-stimulated samples. Graph produced using Metaboanalyst 4.4 statistical analysis tools.

Table 4.2: P values of extracellular metabolites of CD4+ T cells pre-treated with IL-6/sIL-6R followed by CD3/CD28 co-stimulation. Spearman's rank correlation test as shown in figure 4.10

IL-6/sIL-6R Pre-stimulated Extracellular	p-value	IL-6/sIL-6R Pre-stimulated Extracellular	p-value
Serine	0.059332	trans-4-Hydroxy-L-proline	0.69549
Threonine	0.095041	Acetate	0.69655
Choline	0.10554	Alanine	0.69719
Methylguanidine	0.19748	Glutamate	0.71225
Tryptophan	0.20957	Creatine	0.72895
Alloisoleucine	0.21409	Proline	0.74553
Methionine	0.21846	Pyruvate	0.74871
O-Acetylcholine	0.25284	Creatine	0.72895
Histidine	0.37257	Proline	0.74553
Glucose	0.40832	Pyruvate	0.74871
N-Acetylaspartate	0.42639	Ethanol	0.77183
Formate	0.43213	UMP	0.77261
Glycolate	0.44067	Creatine phosphate	0.78213
Arginine	0.44096	3-Methylhistidine	0.78363
Glutamine	0.4551	Creatinine	0.81916
Glycine	0.4557	Tyrosine	0.83455
Taurine	0.46054	Methanol	0.83804
Glutathione	0.47588	Aspartate	0.83878
Isoleucine	0.4968	NAD	0.87569
Fumarate	0.55835	Sarcosine	0.88421
myo-Inositol	0.56455	Asparagine	0.9104
Lysine	0.58569	O-Phosphocholine	0.93723
Succinate	0.61209	Pyroglutamate	0.96491
Lactate	0.61749	Valine	0.97507
Leucine	0.65554	Phenylalanine	0.98297

4.4.6 NMR Spectra comparisons of CD4+ T cells reveals discriminations between metabolites is not attributed to CD3/CD28 co-stimulation

To fully decipher the metabolic profiles between experimental groups following IL-6/sIL-6R priming, NMR spectroscopy was conducted in the absence of CD3/CD28 stimulation of CD4+ T cells. Subsequent spectra analysis revealed the identification of 35 intracellular metabolites, of which no significant difference was observed in response to varying concentrations of priming IL-6/sIL-6R signalling (figure 4.11). The PLSD-A of four experimental groups encapsulating CD4+ T cells primed with 0, 0.02, 0.1 and 0.5 ng/ml, IL-6/sIL-6R concentrations also revealed some discrimination between the metabolic profiles of unstimulated samples and those primed with IL-6/sIL-6R – even in the absence of CD3/CD28 co-stimulation (figure 4.12A). Such findings were further highlighted in a direct comparison between IL-6/sIL-6R/CD3/CD28 unstimulated and 0.5 ng/ml IL-6/sIL-6R primed CD3/CD28 co-stimulated CD4+ T cells by PLSD-A, in which some discrimination was seen between the intracellular metabolic profiles between the two groups despite some overlapping points (figure 4.12C).

Metaboanalyst pattern hunting in a linear 1-2-3-4 manner saw the increases in 11 metabolites within IL-6/sIL-6R pre-stimulated groups, including key glycolytic metabolites pyruvate and glucose (figure 4-12B). AMP, ATP and ADP, by contrast, were shown to be amongst the 14 intracellular metabolites conversely correlated between unstimulated and IL-6/sIL-6R primed CD4+ T cells – thereby showing increased concentration levels in IL-6/sIL-6R/CD3/CD28 unstimulated CD4+ T cells. Interestingly, pyruvate and glucose were amongst those most negatively correlated when conducting pattern hunting analysis solely between 0 and 0.5 ng/ml IL-6/sIL-6R concentrations. Rather, increased levels of methylguanidine, glutathione and creatine

were present in 0.5 ng/ml primed cells when compared to unstimulated cells, reflected by positive correlations in figure 4.12C.

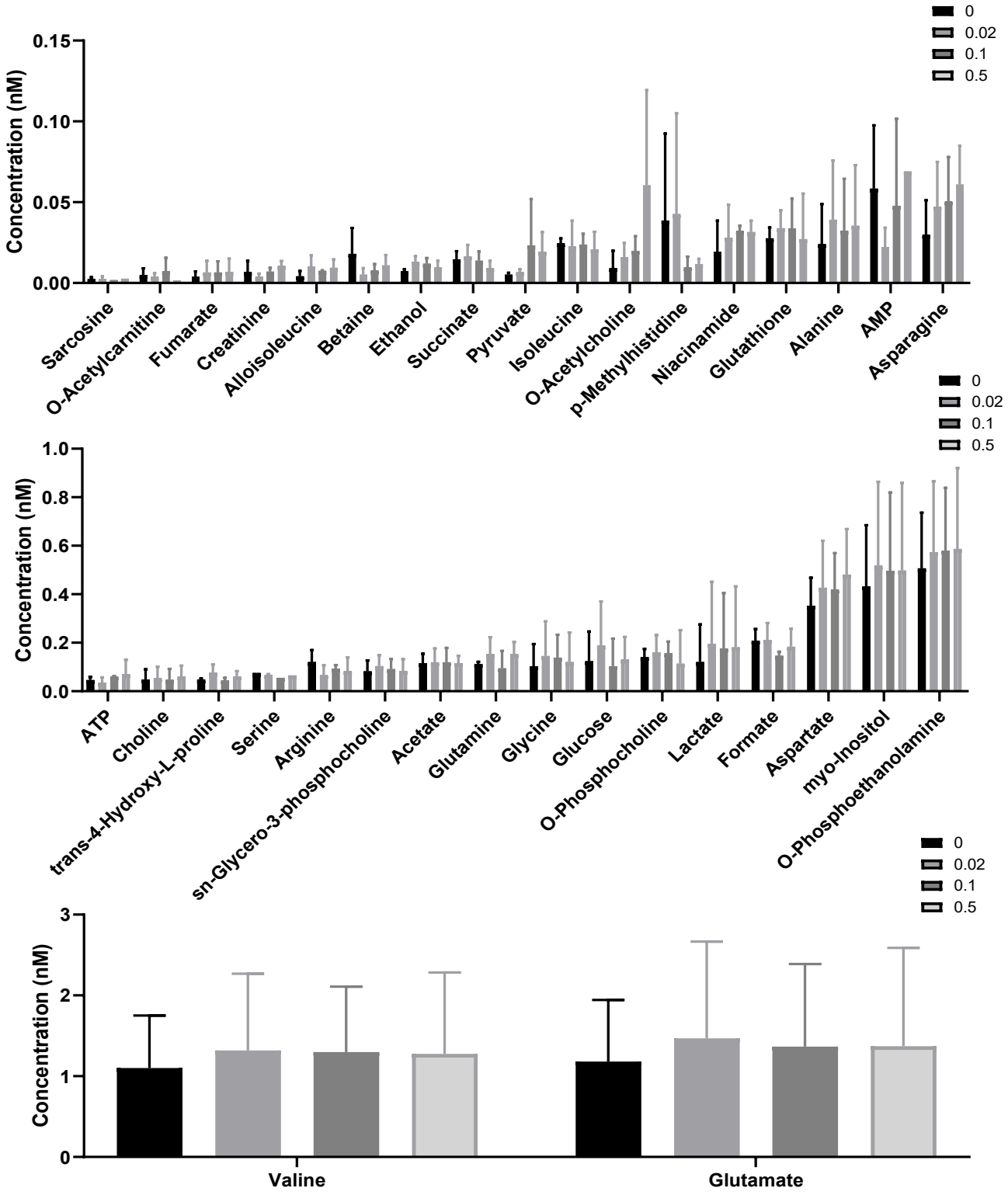

Figure 4.11 – Concentrations of intracellular metabolites from CD4+ T cells treated with 0 ng/ml; 0.02 ng/ml; 0.1 ng/ml; and 0.5 ng/ml concentrations IL-6/IL-6R for 72 hours only. Statistical analysis was run using Two-way ANOVA in PRISM 8.2 statistical software. Data shown is mean with standard deviation (n=3)

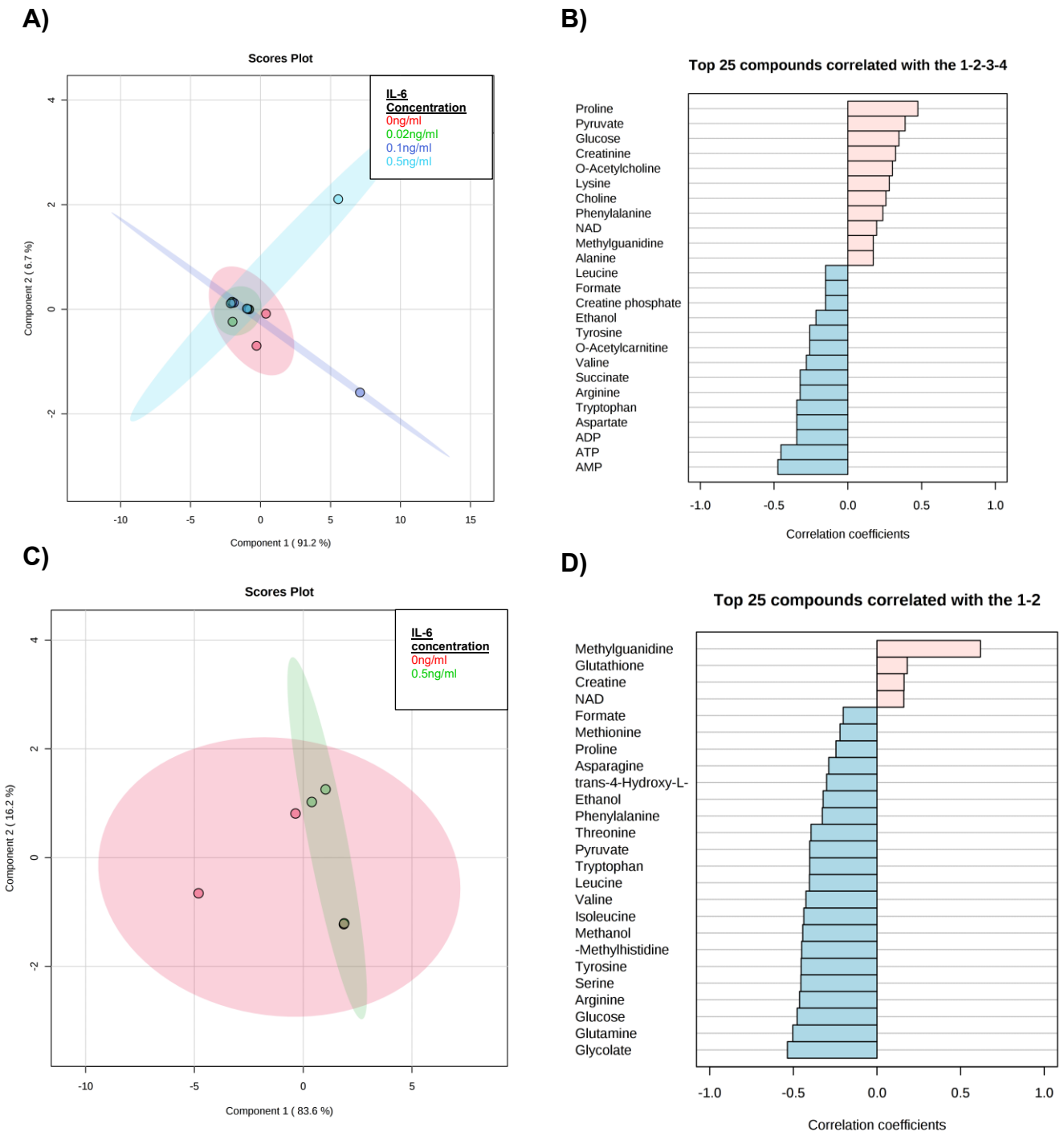

Figure 4.12 – PLS-DA and pattern hunter analysis of intracellular metabolites from CD4+ T cells treated with varying concentrations of IL-6/IL-6R. for 72 hours only. PLS-DA analysis of (A) intracellular metabolites between unstimulated and CD4+ T cells pre-stimulated with 0.02, 0.1 and 0.5 ng/ml IL-6/sIL-6R only and (B) subsequent pattern correlation analysis. (C&D) PLS-DA analysis and pattern hunting correlation analysis of intracellular metabolites between unstimulated and 0.5 ng/ml pre-stimulated IL-6/sIL-6R CD4+ T cells. PLS-DA data was normalised using PQN prior to statistical analysis; Pattern hunting was used to identify features within the dataset that increased in unstimulated cells over IL-6/sIL-6R only samples. Graph produced using Metaboanalyst 4.4 statistical analysis tools.

Table 4.3: P values of intracellular metabolites of CD4+ T cells treated with IL-6/sIL-6R for 72 hours only. Spearman's rank correlation test as shown in figure 4.12.

Unstimulated (IL-6/sIL-6R Only) Intracellular	p-value	Unstimulated (IL-6/sIL-6R Only) Intracellular	p-value
Proline	0.070065	Alloisoleucine	0.63915
Pyruvate	0.16015	O-Phosphoethanolamine	0.63915
AMP	0.21182	Creatine	0.68769
ATP	0.21182	Niacinamide	0.68769
O-Acetylcarnitine	0.21182	Creatine phosphate	0.68821
Succinate	0.21182	Fumarate	0.68821
Lysine	0.23963	Methionine	0.73796
Sarcosine	0.2705	Acetate	0.73841
ADP	0.27139	O-Phosphocholine	0.73841
Aspartate	0.27139	Alanine	0.78956
Arginine	0.30443	Glutamate	0.78956
Creatinine	0.33871	Leucine	0.78956
O-Acetylcholine	0.3396	Threonine	0.78956
Valine	0.37684	Glutamine	0.84148
Tyrosine	0.41611	Glycine	0.84148
3-Methylhistidine	0.41611	sn-Glycero-3-phosphocholine	0.84148
Phenylalanine	0.41611	Glutathione	0.84148
Formate	0.4573	Theophylline	0.89399
Glucose	0.4573	Asparagine	0.89399
Tryptophan	0.4573	Taurine	0.89399
Choline	0.50032	trans-4-Hydroxy-L-proline	0.89399
NAD	0.50032	Malonate	0.9468
Ethanol	0.54505	Serine	0.9468
Pyroglutamate	0.63855	Lactate	0.9469
Methylguanidine	0.63855	Isoleucine	0.9469
Betaine	0.63915	myo-Inositol	0.9469

Finally, 48 extracellular metabolites were identified from NMR spectroscopy of CD3/CD28 unstimulated CD4+ T cells (Figure 4.13). Spectra analysis saw no significant differences between the different concentrations of IL-6/sIL-6R; however, considerable discrimination was seen between PLSD-A plots was comparing different IL-6/sIL-6R concentrations (figure 4.14A) and directly between CD4+ T cells primed with 0 ng/ml and 0.5 ng/ml IL-6/sIL-6R in the absence of CD3/CD28 co-stimulation (figure 4.14B). Here similar metabolites appeared to be positively correlated when comparing IL-6/sIL-6R primed CD4+ T cells with IL-6/CD3/CD28 unstimulated groups: specifically, methyguanidine, glutathione, and creatine extracellular metabolites appear to be concentrated in greater levels within IL-6/sIL-6R primed cells. Meanwhile extracellular metabolites such as glucose and glycolate appeared amongst those most negatively correlated during pattern hunting analysis and therefore in greater extracellular concentration in IL-6/sIL-6R/CD3/CD28 unstimulated cells.

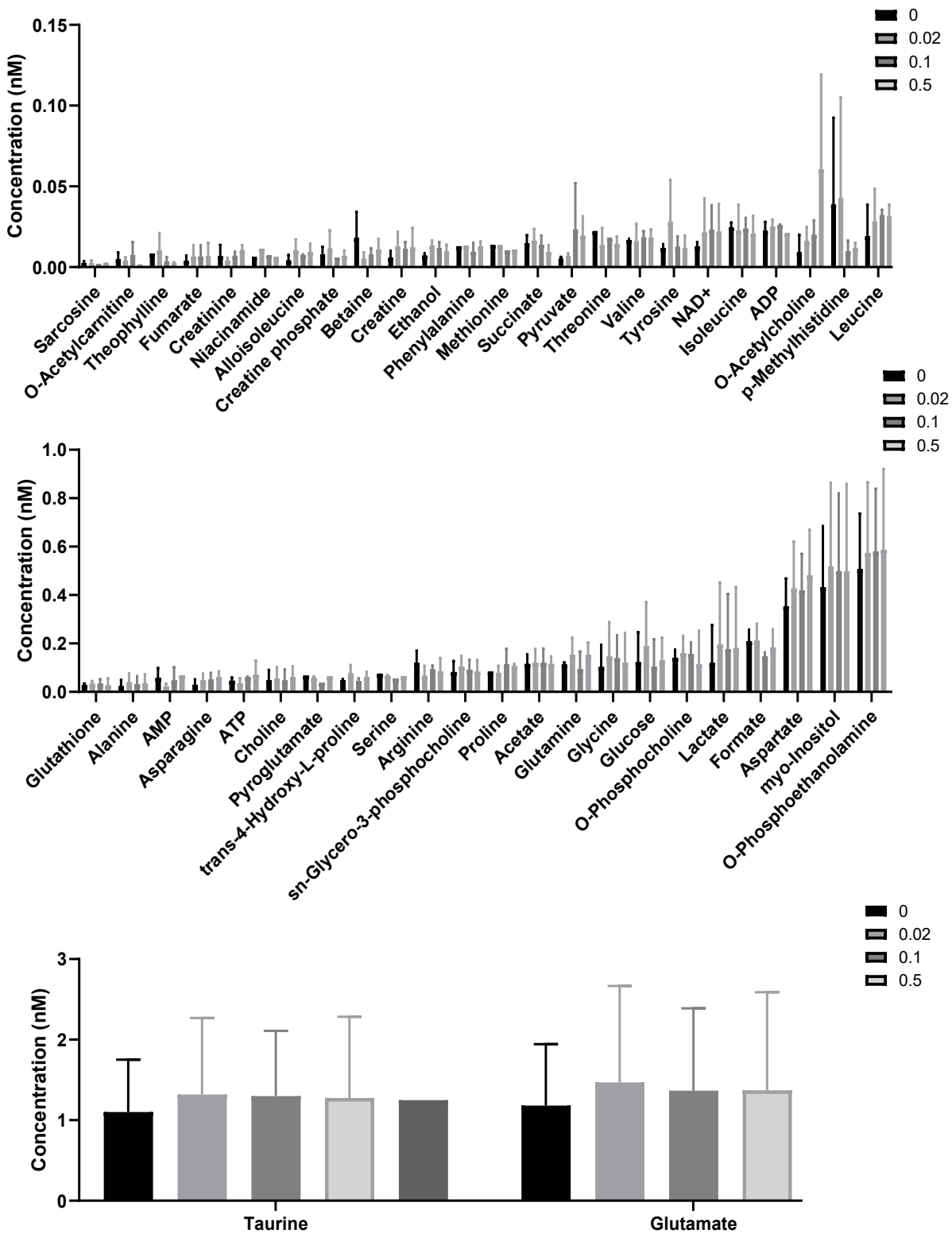

Figure 4.13 – Concentrations of extracellular metabolites from CD4+ T treated with 0 ng/ml; 0.02 ng/ml; 0.1 ng/ml; and 0.5 ng/ml concentrations IL-6/IL-6R for 72 hours. Statistical analysis was run using Two-way ANOVA in PRISM 8.2 statistical software. Data shown is mean with standard deviation (n=3)

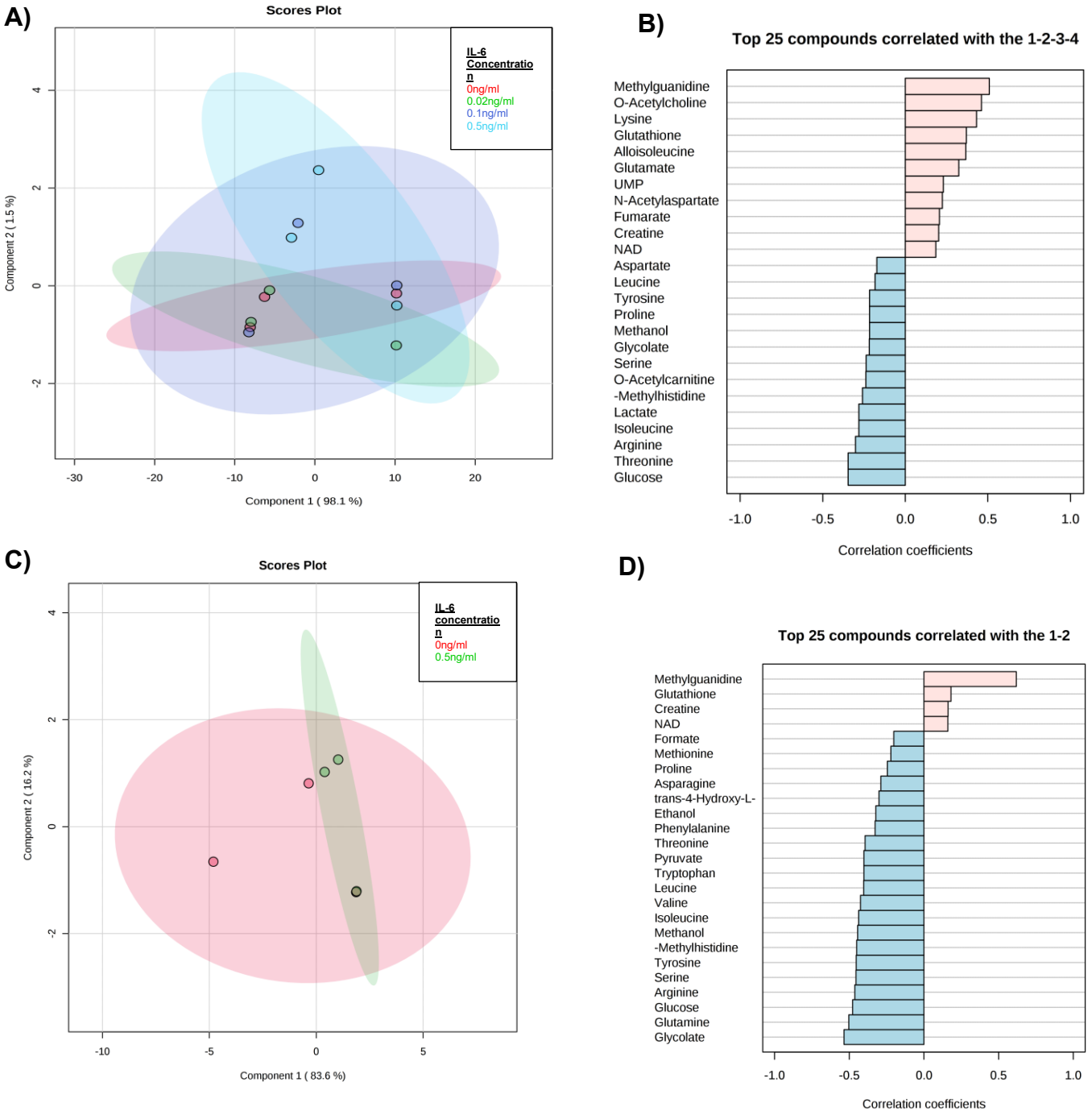

Figure 4.14 – PLS-DA and pattern hunter analysis of extracellular metabolites from CD4+ T cells treated with varying concentrations on IL-6/IL-6R for 72 hours only. PLS-DA analysis of (A) extracellular metabolites between unstimulated and CD4+ T cells pre-stimulated with 0.02, 0.1 and 0.5 ng/ml IL-6/sIL-6R only and (B) subsequent pattern correlation analysis. (C&D) PLS-DA analysis and pattern hunting correlation analysis of extracellular metabolites between unstimulated and 0.5 ng/ml pre-stimulated IL-6/sIL-6R CD4+ T cells. PLS-DA data was normalised using PQN prior to statistical analysis; Pattern hunting was used to identify features within the dataset that increased in unstimulated cells over IL-6/sIL-6R only samples. Graph produced using Metaboanalyst 4.4 statistical analysis tools.

Table 4.4: P values of extracellular metabolites from CD4+ T cells treated with IL-6/sIL-6R for 72 hours only. Spearman's rank correlation test as shown in figure 4.14.

Unstimulated (IL-6/sIL-6R Only) Extracellular	p-value
Methylguanidine	0.046651
Threonine	0.070065
Serine	0.13875
Alloisoleucine	0.16097
Lysine	0.18531
Isoleucine	0.24052
Arginine	0.27139
Glucose	0.30443
Phenylalanine	0.3396
Glutamine	0.3396
Lactate	0.37684
Glutathione	0.4573
Creatinine	0.50032
Formate	0.50032
Glutamate	0.50032
Pyroglutamate	0.54505
Aspartate	0.59138
Glycolate	0.59138
Valine	0.63915
N-Acetylaspartate	0.68821
trans-4-Hydroxy-L-proline	0.68821
Acetate	0.73841
Glycine	0.73841
Methanol	0.73841
Asparagine	0.78956
myo-Inositol	0.78956
Tryptophan	0.84148
Alanine	0.84148
Leucine	0.89399
Tyrosine	0.9469
3-Methylhistidine	0.9469
O-Phosphocholine	0.9469
Proline	0.9469
Ethanol	1

4.5 Conclusion

IL-6 as a third T cell activation signal has many implications in relation to our understanding of how our immune system changes during IMIDs. Its expression is almost ubiquitous in the body, released by a plethora of cell types in response to injury or infection. Furthermore, dysregulation of the cytokine has been implicated in several inflammatory diseases (Ishihara and Hirano, 2002), as well as the production of disease and inflammatory clinical biomarker, C-reactive protein (CRP) production, which is upregulated by IL-6 in the liver. Combined with the altered metabolic profiles of immune cells, particularly in T cells, understanding the contribution to CD4+ T cell metabolism may elucidate new treatment paradigms and molecular targets.

One the crucial design elements to these experiments was using sIL-6R to mimic shedding of the receptor in the local area. Though the current work was *in vitro*, within the context of the human body, localised shedding either at the site of injury or the chronically inflamed site (joint – RA, Illeum - Crohn's disease, Skin – PSA) does occur (Müllberg et al., 1993, Mullberg et al., 1993) (Schumacher et al., 2015). Furthermore, IL-6 overexpression associated inflammation only occurs if signalling happens *via* the IL-6R and not *via* alternatively suggested signalling pathways, such as CD5, which is linked to IL-6 associated cancers (Zhang et al., 2016, Mufazalov et al., 2019)

Our initial findings were based on microarray data from rheumatoid arthritis (RA) patients provided by Newcastle University: primarily stratified by top and bottom quartiles of patient serum IL-6 concentration to identify differentially expressed genes, and subsequently combined with *in vitro* microarray data analysing IL-6/sIL-6R pre-stimulation of CD4+ naïve T cells, both pre- and post-CD3/CD28 activation (Ridgeley et al., 2019). The metabolic exposure of CD4+ T cells to IL-6 revealed from the data

set some differential expression of genes associated with cellular proliferation and growth. These include the transcription factor c-MYC and from naïve CD4+ T cell microarray analysis, its upstream regulator MAZ - shown to have a dual role in promoting transcription initiation and termination, including through attenuation of c-MYC promoter regions ME1a1 and ME1a2 (Bossone et al., 1992). Interestingly, although differentially expressed only on CD3/CD28 post-stimulation, MAZ is also shown in previous studies to increase in responsiveness to IL-6 within transcription promoter response elements (Ray, 2000). This observation may therefore highlight the possible role for IL-6/sIL-6R priming in coordinating the CD4+ T cell proliferative and IL-6 induced proinflammatory responses; however, this was an avenue not further explored.

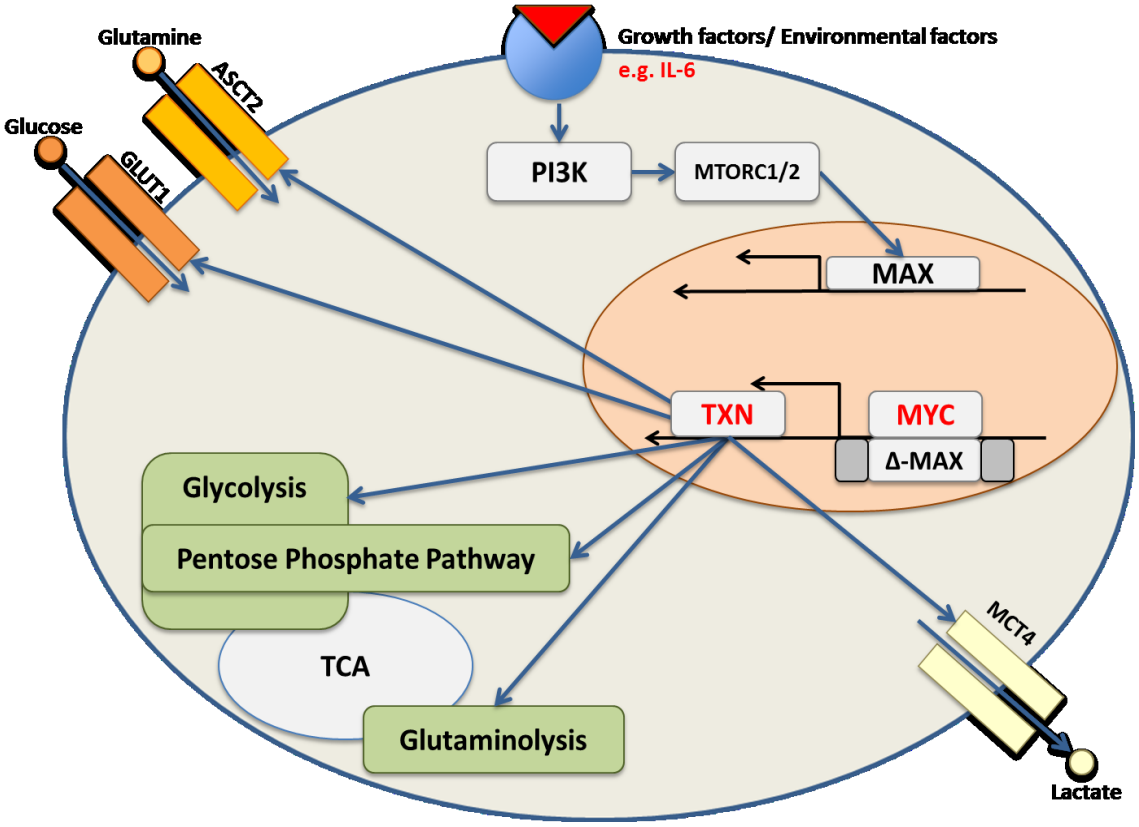

Figure 4.15 – MYC expression upregulates solute transporters and glycolytic pathways. Extrinsic signalling molecules, such as growth factors or environmental factors, upregulate PI3K and subsequently the MTORC1/2 pathways. This promotes MYC dimerization with MAC and formation of heterodimer which associate with high affinity E-box sequences. c-MYC protein binds to the promotor region of several glycolytically associated genes, such as LDHA or PFK, and several solute transporters, such as MCT4, ASCT2 and GLUT1.

Previously validated targets of c-MYC shows the transcription factor to be heavily involved in regulating metabolic processes and solute channels within the cells, as well as cellular pathways of proliferation and growth. Specifically, the targeting of glycolytic-associated genes such as lactose dehydrogenase A (LDHA), phosphofructokinase, glyceraldehyde-3-dehydrogenase and glucose transporter 1 (GLUT1) (figure 4.15).

Figure 4.3 shows a greater proliferative phenotype in cells pre-stimulated with IL-6/sIL-6R. As our previous results in chapter 3 suggest the role of CD3/CD28 signalling in promoting metabolic alterations to accommodate for T cell growth and proliferation, unsurprisingly, cell proliferation was only induced following activation with CD3/CD28 post-stimulation. Significantly greater proliferation was observed in naïve T cells only, suggesting that the pre-stimulation only affected naïve T cells. Indeed, gp130 expression, the signal transducing chain of the IL-6 signalling complex, has been shown to be present on CD4+ T cells and can be downregulated on TCR engagement (Betz and Muller, 1998). These results highlighting the possibility that memory T cells do not respond the same way to IL-6 as naïve cells, with refractory proliferation ascribed to prior downregulation of IL-6 signalling.

In keeping with significantly increased cellular proliferation, Seahorse metabolic flux analysis demonstrated increased glycolytic metabolism and increased maximal respiratory capacity within CD4+ naïve T cells, following high level stimulation with IL-6/sIL-6R, versus IL-6 unstimulated and memory CD4+ T cell groups. As discussed, T cells are reliant on glycolytic metabolism following activation to support their proliferation and function(Vander Heiden et al., 2009). Therefore, the observed glycolytic rate seen here appears to underpin the proliferative phenotype. Interestingly, the significant increases in maximal respiratory capacity were unexpected since T cells

are well described in the literature to reduce mitochondrial metabolic activity following activation - switching their metabolic phenotype in favour of a glycolytic 'Warburg-like' metabolism (Vander Heiden et al., 2009). An increase in respiratory capacity would therefore suggest that naïve CD4+ T cells may have altered their mitochondria for increased respiration. Previous studies show that despite their perceived reduced contribution to energy production, mitochondria were shown to be active during CD4+ T cell activation, whilst in some haematopoietic cell populations such as CD8+ T cells, increased dependency on mitochondrial metabolism is observed following a period of increased glycolysis to allow for other effector functions like cytokine production (Akkaya et al., 2018; Jones et al., 2017). As such, it may be plausible that increased maximal respiration in naïve T cells is attributed to the shunting of metabolites to the mitochondria to support T cell activity. However, absence of other significant mitochondrial parameters measured in the present study appears to be a caveat to this notion. Indeed, the experimental design of the study artificially uses carbonyl cyanide-p-trifluoromethoxyphenylhydrazone (FCCP) to uncouple the mitochondrial membrane to upset the proton gradient. This intervention forces mitochondria to work at their maximal rate. As such, although naïve cells have this increased capacity, this may be alternatively due increased mitochondrial size or increased expression of mitochondrial uncoupling proteins (UCP), the proteins involved in cellular metabolism and respiration. Indeed in studies elsewhere, CD4+ T cells are shown to embark on a programme of mitochondrial biogenesis following a period of prolonged CD4+ T cell activation (Akkaya *et al.,* 2018).

Finally, to further examine the effects of IL-6/sIL-6R priming upon CD4+ T cells, NMR was utilised to examine and identify both intracellular and extracellular metabolites in IL-6 primed cells, pre- and post-TCR stimulation. As previously discussed, results from

cells without a CD3/CD28 stimulation yielded poor metabolite concentrations. Notably, when comparing the highest metabolites prior to CD3/CD28 stimulation with the highest metabolites post activation, the difference is 8-fold. However, this difference does further confirm that CD4+ T cells were metabolically active after being kept in vitro for 72 hours with only IL-6.

A few differences were identified between metabolites, however using two-way ANOVAs, we were unable to identify any significantly different metabolites. To further disseminate the data, we used PLSD-A analysis to identify discriminants between treatment conditions. No distinct differences were determined between intracellular and extracellular metabolites, in CD4+ post and prior activation.

In conclusion, as summarised in figure 4.16, T cells receiving IL-6 prior to CD3/CD28 activation have a greater metabolic phenotype versus cells which do not receive a third signal. The observed greater metabolic rate support the increased proliferative phenotype and may support further cellular growth and signalling pathways providing an increased metabolic response. Exposure to IL-6 prior to activation may occur in several situations and be advantageous, such as following a injury. This in turn may allow pathogens to enter and cause an infection, or be disadvantageous, such as in chronic inflammatory disease or ageing.

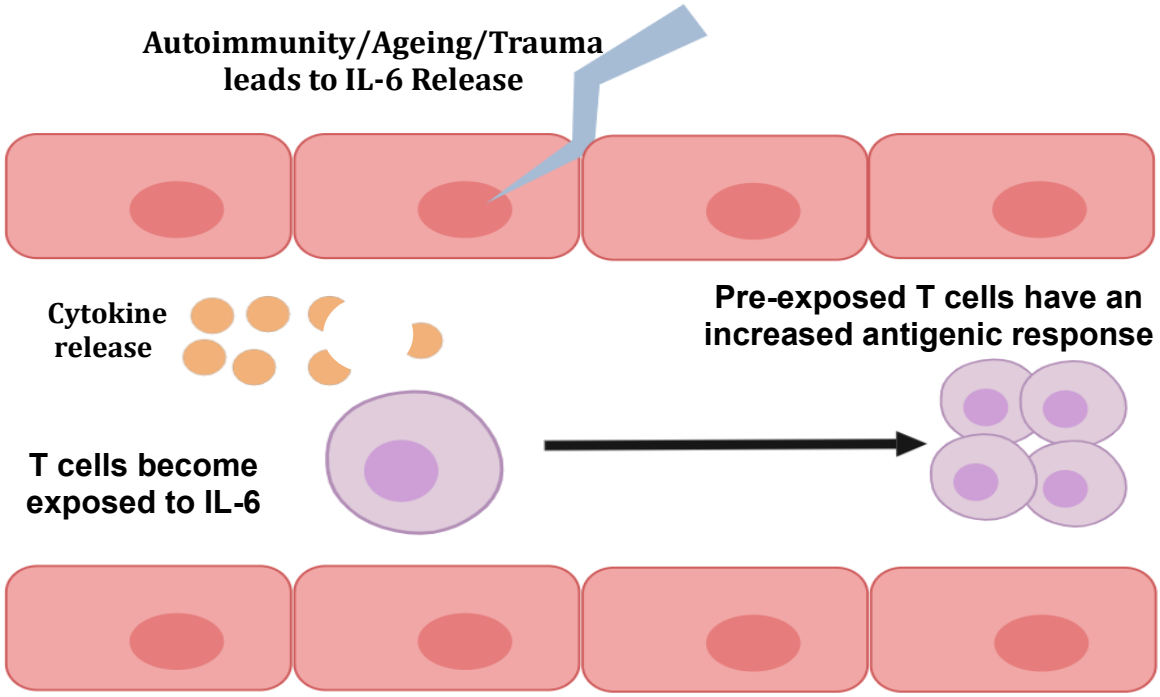

Figure 4.16 – Proposed model for IL-6 pre-stimulation. Increased IL-6 is released due to injury, inflammation due to chronic disease or infection or ageing. This prepares T cells metabolically, supporting an increased proliferative response.

Chapter 5 | Alterations of metabolic proteins of CD4+ T cells in response to IL-6/sIL-6R pre-stimulation, following CD3/CD28 stimulation

5.1 Introduction

T cell receptor (TCR) engagement is previously outlined to promote metabolic reprogramming of CD4+ naïve T cells to a glycolytic phenotype, resulting in a higher ATP generation rate thought beneficial for cellular activation and clonal expansion. However, the role of IL-6 is less well understood, despite dysregulation of the immune response during deregulation in autoimmune conditions. As shown in the previous chapter, IL-6/sIL-6R stimulation, prior to CD3/CD28 stimulation of CD4+ T cells led to alterations at both transcriptional and metabolic level. Naïve T cells primed with higher levels of IL-6/sIL-6R prior to co-stimulation showed an increased glycolytic rate, alongside increased maximal respiratory capacity. The proposed model for the present study therefore suggests that the IL-6/sIL-6R signal 3 prepares CD4+ T cells for an antigenic response, by assisting in the upregulation of their metabolic machinery.

The expression of the transcription factor protein c-MYC has been linked to the increased expression of glycolytic enzymes and glucose transporter 1 (GLUT1) channels. The inhibition of the protein is shown to prevent T cell proliferation *in vivo*: a finding reciprocated during the inhibition of glucose and glutaminolysis metabolism (Wang *et al.,* 2011). As such, given the increased glycolytic rate following the addition of glucose, key glycolytic machinery and enzymes was examined in naïve CD4+ T cells. Analysing mitochondrial mass and key mitochondrial proteins was also undertaken, to help identify the reasons for the observed changes in naïve cell maximal respiration.

5.2 Aims

The aim of the present chapter is to investigate which key metabolic components lead to the altered metabolic phenotype of CD4+ T cells following IL-6/sIL-6R pre-stimulation. We therefore aimed to:

1. Correlate increased gene activity identified in the microarray data to the expression of metabolic proteins.
2. Determine the mechanisms associated with the activation of glycolytic and mitochondrial metabolism pathways in response to IL-6/sIL-6R pre-stimulation in activated CD4+ T cells.
3. Assess mitochondrial changes following alterations to the metabolic profile of CD4+ T cells following IL-6/sIL-6R pre-stimulation.

5.3 Results

5.3.1 Naïve and memory CD4+ T cells pre-stimulated with IL-6/sIL-6R have increased expression and c-MYC protein, while LDHA expression only increases in naïve cells.

As with alterations of the metabolic phenotype of CD4+ T cells, western blotting was used to identify protein expression of metabolic associated proteins. Due to increased glycolytic activity observed within the present study's CD4+ naïve T cells (see chapter 4), protein expression of lactate dehydrogenase A (LDHA) was determined, an enzyme that catalyses the conversion of lactate and NAD+ to pyruvate and NADH during the terminal stage of anaerobic glycolysis. The examination subsequently revealing that within CD4+ naïve T cells, slight increases in LDHA protein expression are seen whilst no such observations were seen for IL-6 primed memory T cells (figure 5.1A, B; figure 5.3A, B). C-MYC expression was additionally observed to be increased in IL-6/sIL-6R

stimulated naïve T cells versus unstimulated controls; however, as with increasing IL-6 stimuli concentration, expression appeared to reduce (figure 5.1C, D). This is compared to memory CD4+ T cells, in which increasing IL-6/sIL-6R concentration appears elicit increased C-MYC expression (figure 5.3C, D). Such changes did not appear to be associated with inconsistency in protein loading as indicated by the actin loading controls.

In addition, the previous chapter appeared to reveal alterations in naïve T cell mitochondrial metabolism in response to IL-6 as indicated by maximal respiratory capacity *via* Seahorse analysis. In order to analyse mitochondrial proteins, 12% resolving gels were used and produced in house, as previously described. These findings suggest possible increased expression of mitochondrial uncoupling proteins (UCP); however, on immunoblotting of naïve T cells, no difference in mitochondrial UCP protein expression was observed (figure 5.2). Interestingly, memory CD4+ T cells treated with IL-6/sIL-6R showed a slight decrease in succinate dehydrogenase iron-sulphur subunit (SDHB), in which the protein forms a partial subunit of UCP II (figure 5.4A). However, this observation failed to reach significance during densitometry analysis (figure 5.4C).

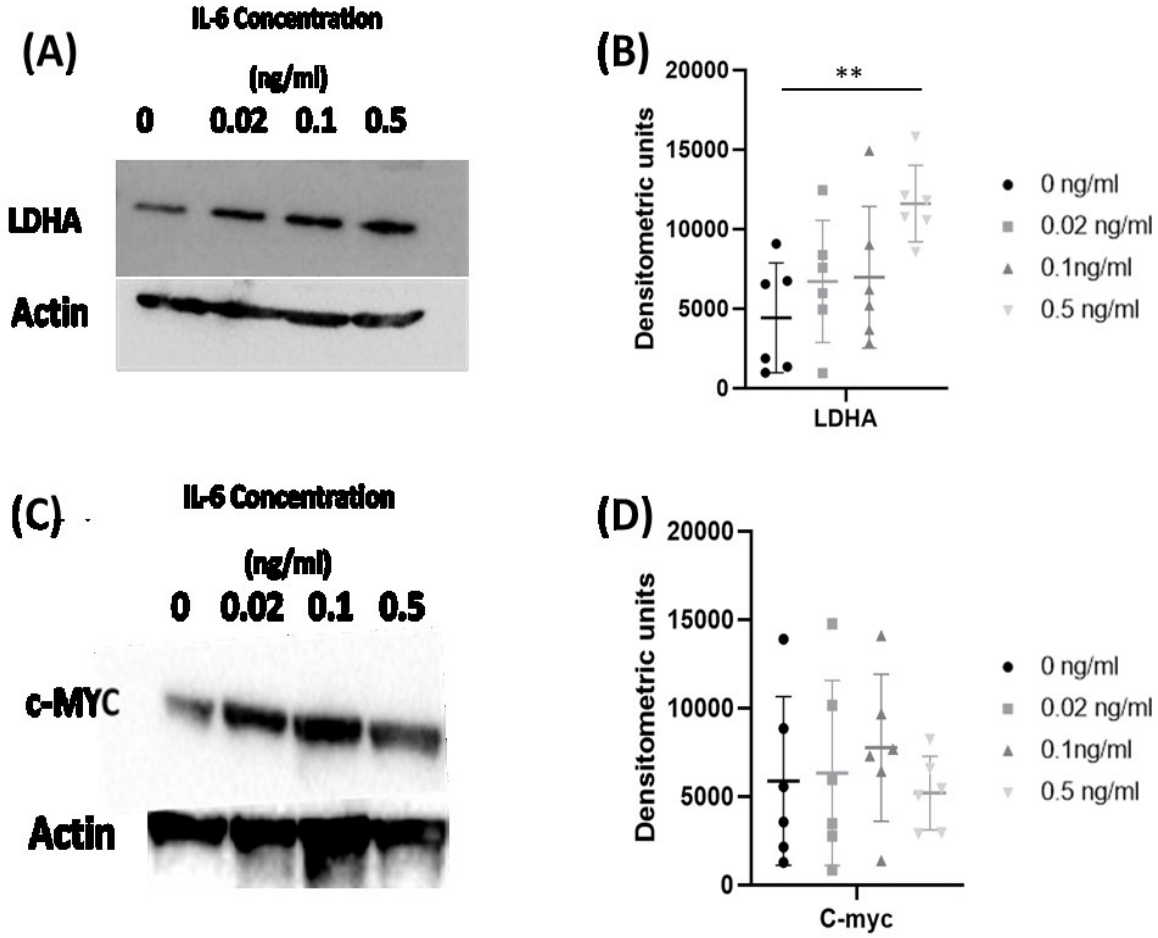

Figure 5.1 - Protein immunoblotting examining the expression of LDHA and c-MYC in naïve CD4+ T cells. (A) shows relative LDHA expression and (B) corresponding densitometry (C) shows c-MYC expression and (D) corresponding densitometry. Actin was used as a loading control in all blots. Pictures were taken using a Bio-Rad XRS Chemidoc with Bio-Rad image lab software and quantified in ImageJ 1.53a. (n=6). P values were calculated using a one-way ANOVA with Tukey comparison test. ** = $p<0.01$.

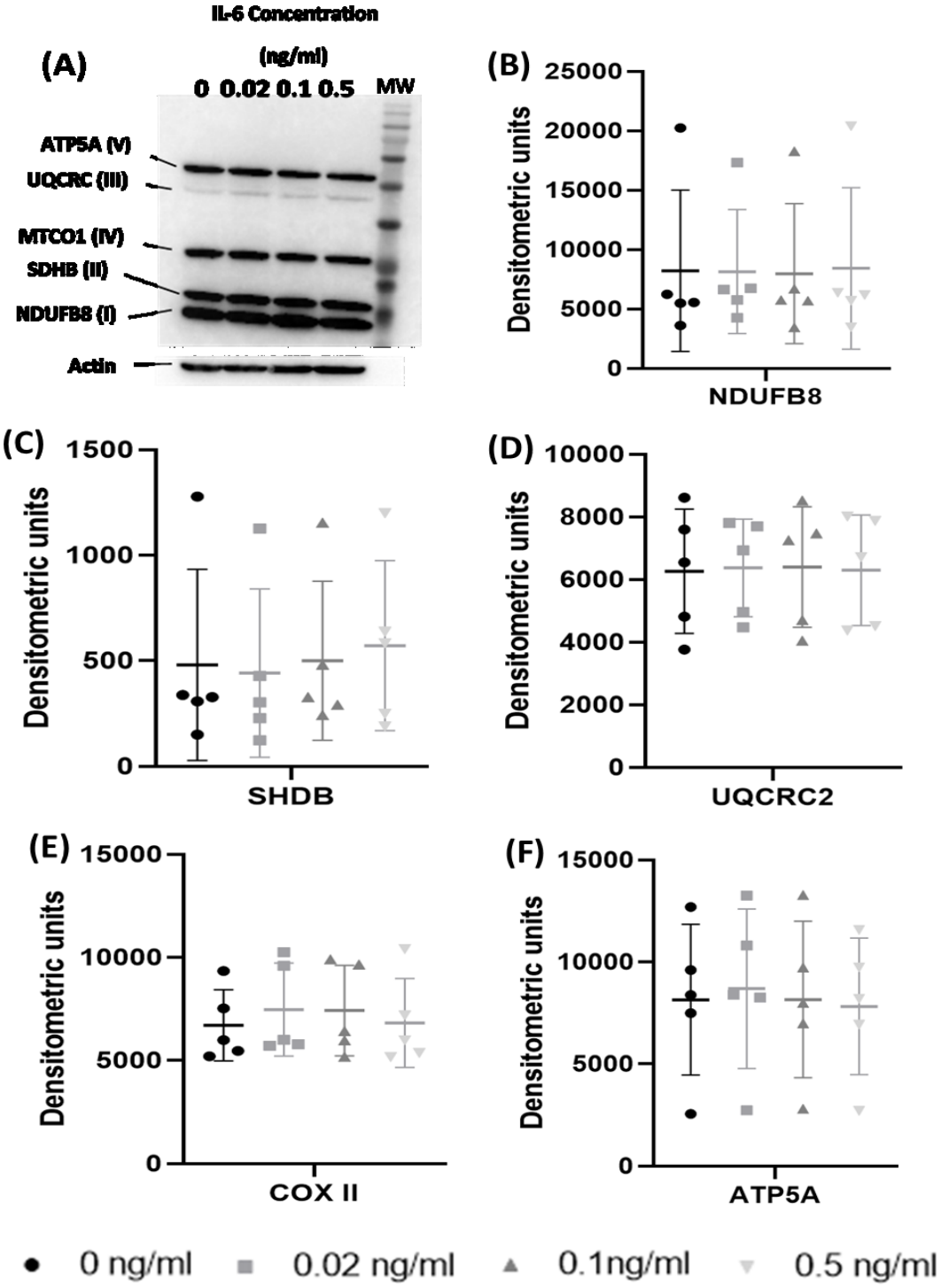

Figure 5.2 - Protein immunoblotting examining the expression of mitochondrial uncoupling proteins (UCPs) in naïve CD4+ T cells. (A) shows expression of mitochondrial UCPs and corresponding densitometry of (B) Complex I NDUFB8, (C) Complex II SHDB, (D) Complex III UQCRC2, (E) Complex IV COX II and (F) Complex V ATP5A. Pictures were taken using a Bio-Rad XRS Chemidoc with Bio-Rad image lab software and quantified in ImageJ 1.53a (n=5). Data was statistically analysed using a one-way ANOVA with Tukey multiple comparison test.

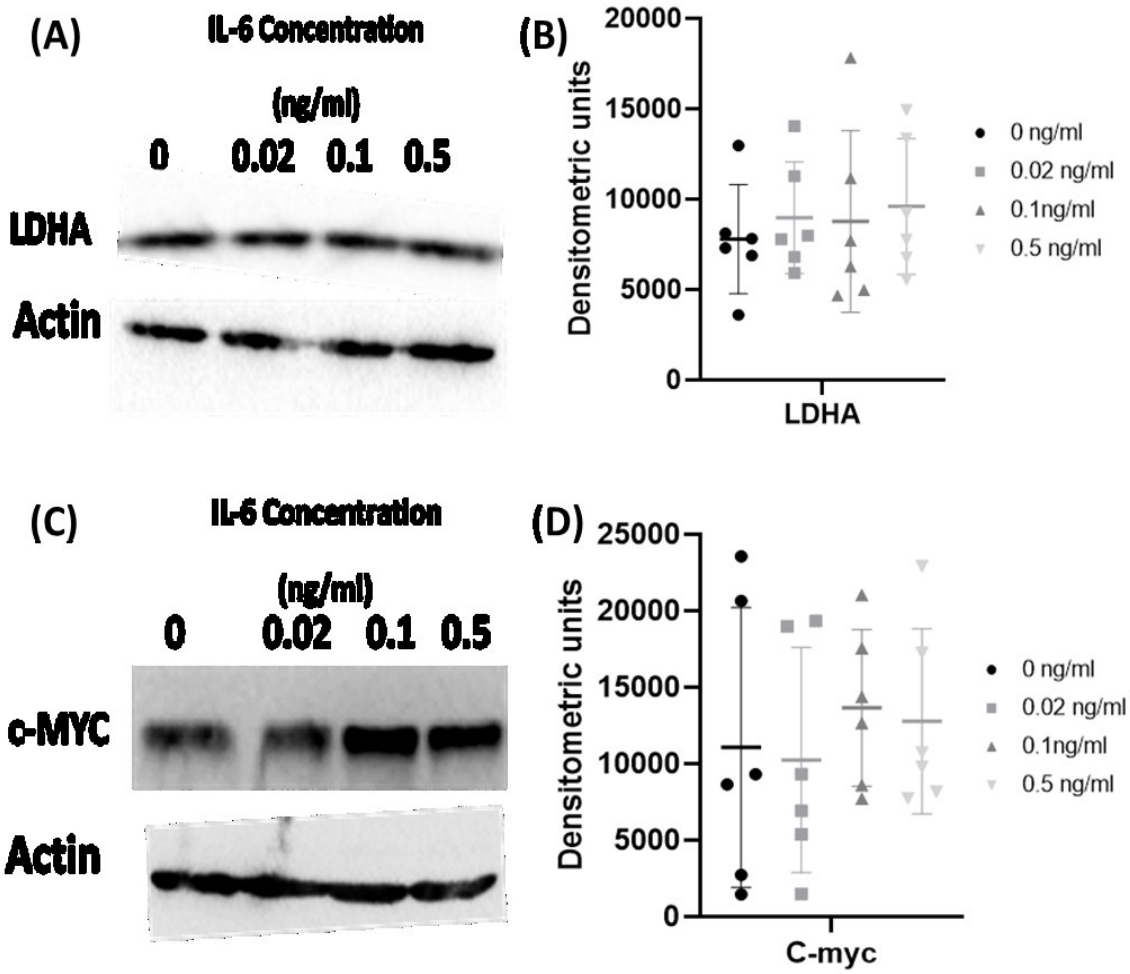

Figure 5.3 - Protein immunoblotting examining the expression of LDHA and c-MYC in memory CD4+ T cells. (A) shows relative LDHA expression and (B) corresponding densitometry, (C) shows c-MYC expression and (D) corresponding densitometry. Actin was used as a loading control in all blots. Pictures were taken using a Bio-Rad XRS Chemidoc with Bio-Rad image lab software and quantified in ImageJ 1.53a. (n=6). Data was statistically analysed using a one-way ANOVA with Tukey multiple comparison test.

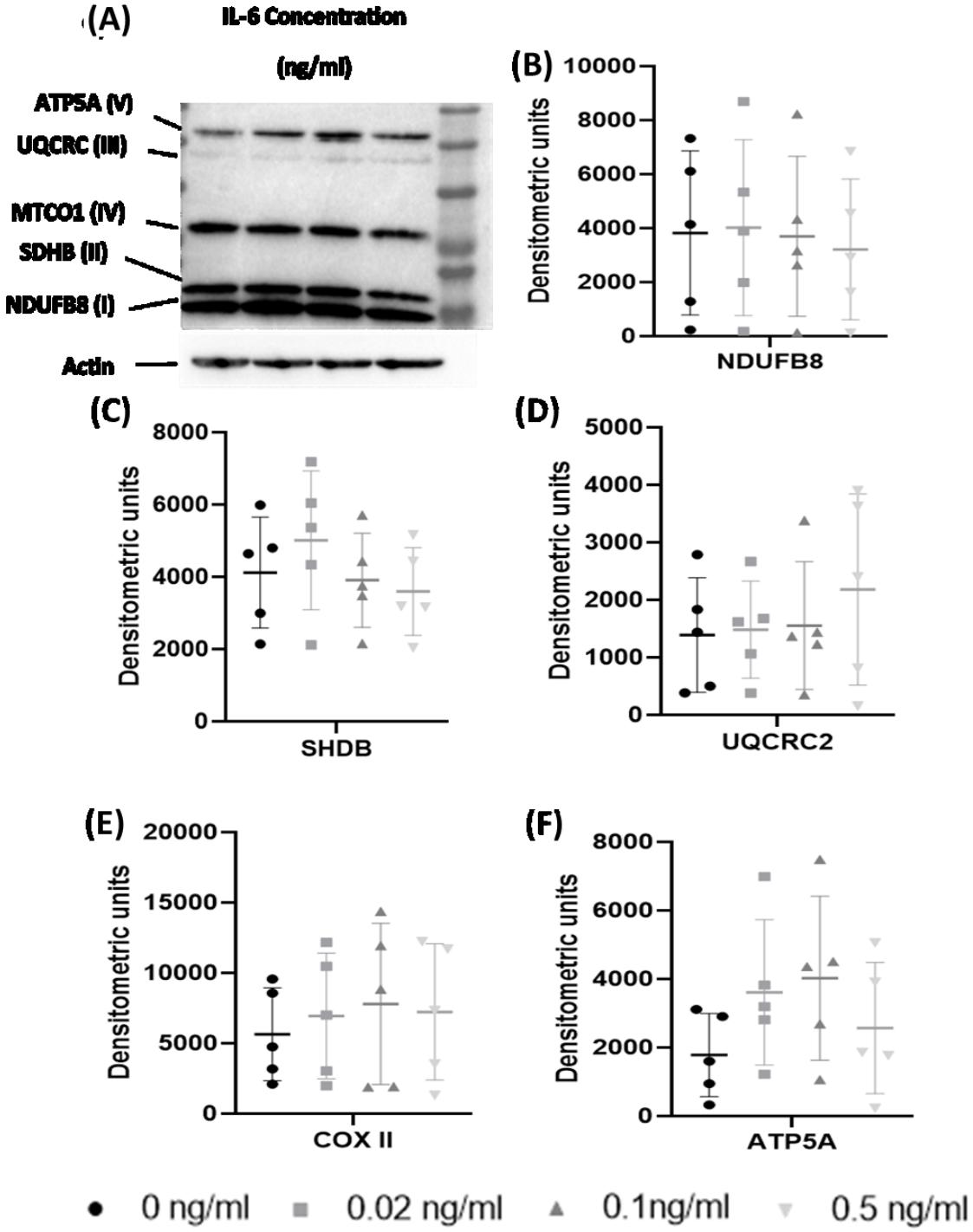

Figure 5.4 - Protein immunoblotting examining the expression of mitochondrial uncoupling proteins (UCPs) in memory CD4+ T cells. (A) shows expression of mitochondrial UCPs and corresponding densitometry of (B) Complex I NDUFB8, (C) Complex II SHDB, (D) Complex III UQCRC2, (E) Complex IV COX II and (F) Complex V ATP5A. Pictures were taken using a Bio-Rad XRS Chemidoc with Bio-Rad image lab software and quantified in imageJ 1.53a. (n=5).

5.3.2 Flow cytometry analysis shows increased MitoTracker fluorescence in naïve and memory T cells treated with IL-6/sIL-6R, 6 days after CD3/CD28 stimulation

Given the present observed changes in mitochondrial respiration in response to T cell stimuli, naïve and memory T cells were stained with MitoTracker Red to determine whether mitochondria mass had increased in cells treated with IL-6/sIL-6R. The gating strategy I is shown in figure 5.5A. Briefly, isolated cells were gated using FSC/SSC to identify the lymphocyte population. Single cells were identified using FSC-A/FSC-H and Phycoerythrin (PE) fluorescence was used to identify cell mitochondria. Cells with greater mitochondrial mass had greater fluorescence. To identify the percentage of cells with larger mitochondria in each population, high PE cells were gated and compared.

Interestingly when primed with IL-6/sIL-6R prior to TCR activation, neither naive nor memory T cells showed increased mitochondrial mass at 3 days post-stimulation (figure 5.5B, D), despite observed increases in maximal respiration within the former T cell subtype. Naïve CD4+ T cells, however, showed increased mitochondrial mass at 6 days post-stimulation, in cells all treated with IL-6/sIL-6R in comparison to IL-6 unstimulated controls (figure 5.5C). By contrast, memory CD4+ T cells treated with 0.1 ng/ml and 0.5 ng/ml concentrations of IL-6/sIL-6R showed significantly decreased PE fluorescence, suggesting decreases in mitochondrial mass (figure 5.5E).

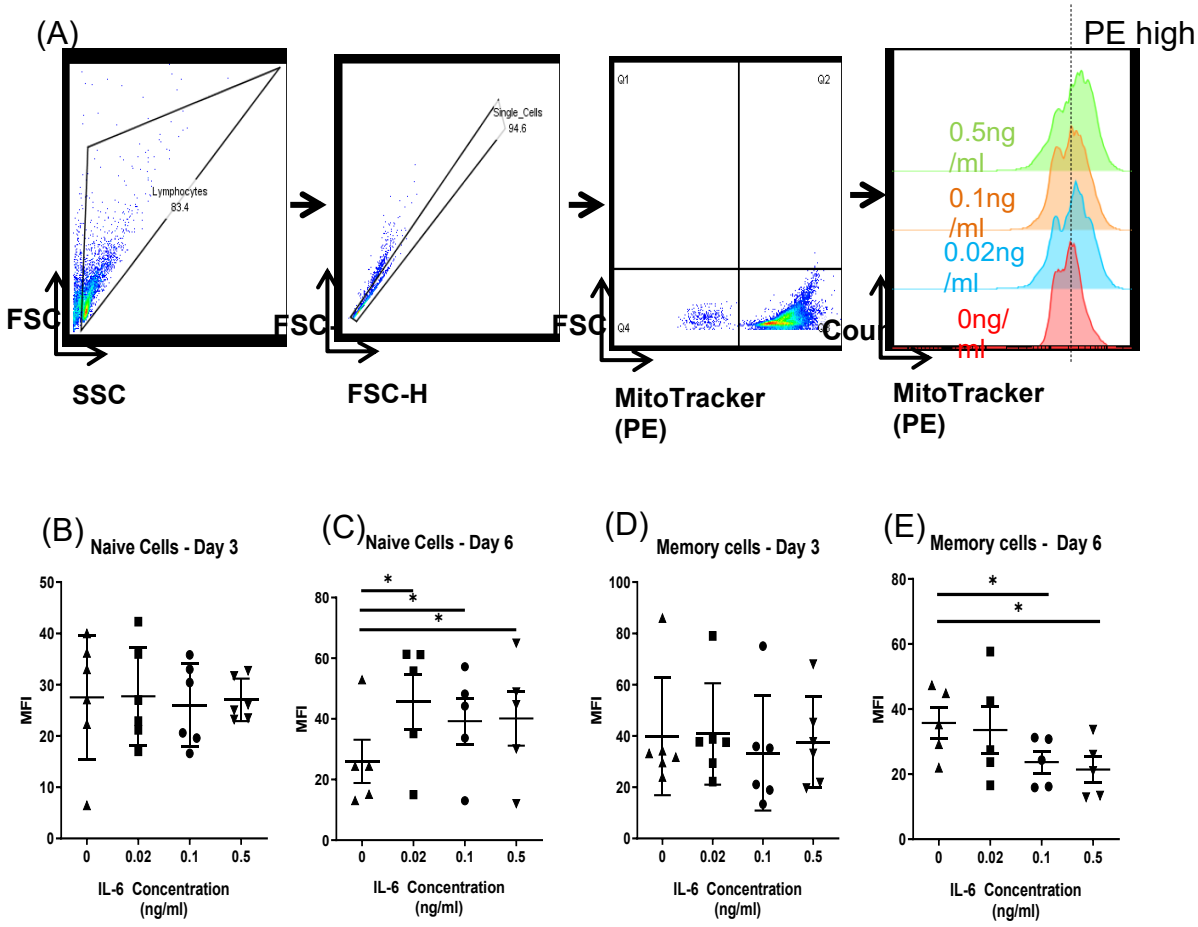

Figure 5.5 - Mitochondrial staining of CD4+ T cells after 72 hours of IL-6/IL-6R treatment and activation with CD3/CD28 for 3 days and 6 days. (A) The gating strategy shown was used to identify mitochondrial size. Briefly, Lymphocytes were gated on cell size, doublets were removed, and cells were subsequently gated using MitoTracker red fluorescence. Percentage of cells in high PE gating were compared after 3 days (B) and 6 days (C), post CD3/CD28 stimulation. Comparison of memory cells are shown after 3 days (D) and 6 days (E). Statistical significance was calculated using multiple comparison ANOVAs in Prism v8 (n=6; 1 outlier data set, determined using 2± SD, excluded from (C)). *p=<0.05. Example data used to demonstrate gating strategy shows naïve CD4+ T cells, after 6 days of CD3/CD28 stimulation (A).

5.3.3 Flow cytometry analysis of cell surface GLUT1 channels shows no upregulation in CD4+ T cells treated with IL-6/sIL-6R, 6 days after CD3/CD28 stimulation

In line with upregulated glycolytic activity in response to IL-6 primed T cell activation, naïve and memory CD3/CD28 stimulated T cells were stained for GLUT1 cell surface expression following IL-6/sIL-6R priming and analysed by flow cytometry after 6 days to decipher the role of IL-6 signalling upon glucose metabolism and its associated components. The gating strategy is shown in figure 5.6A, in which GLUT1 channels on single lymphocytic cells were identified using FSC-A/FSC-H and GLUT1 APC fluorescent staining. To identify the percentage of cells with greater GLUT1 expression in each population, high APC cells were gated and compared. Cells with greater GLUT1 expression had greater fluorescence; however, despite increased glycolysis observed in naïve T cells and changes in LDHA expression, on closer examination, the present study revealed no significant difference in GLUT1 expression at 6 days post-stimulation in both T cell subtypes (figure 5.6B).

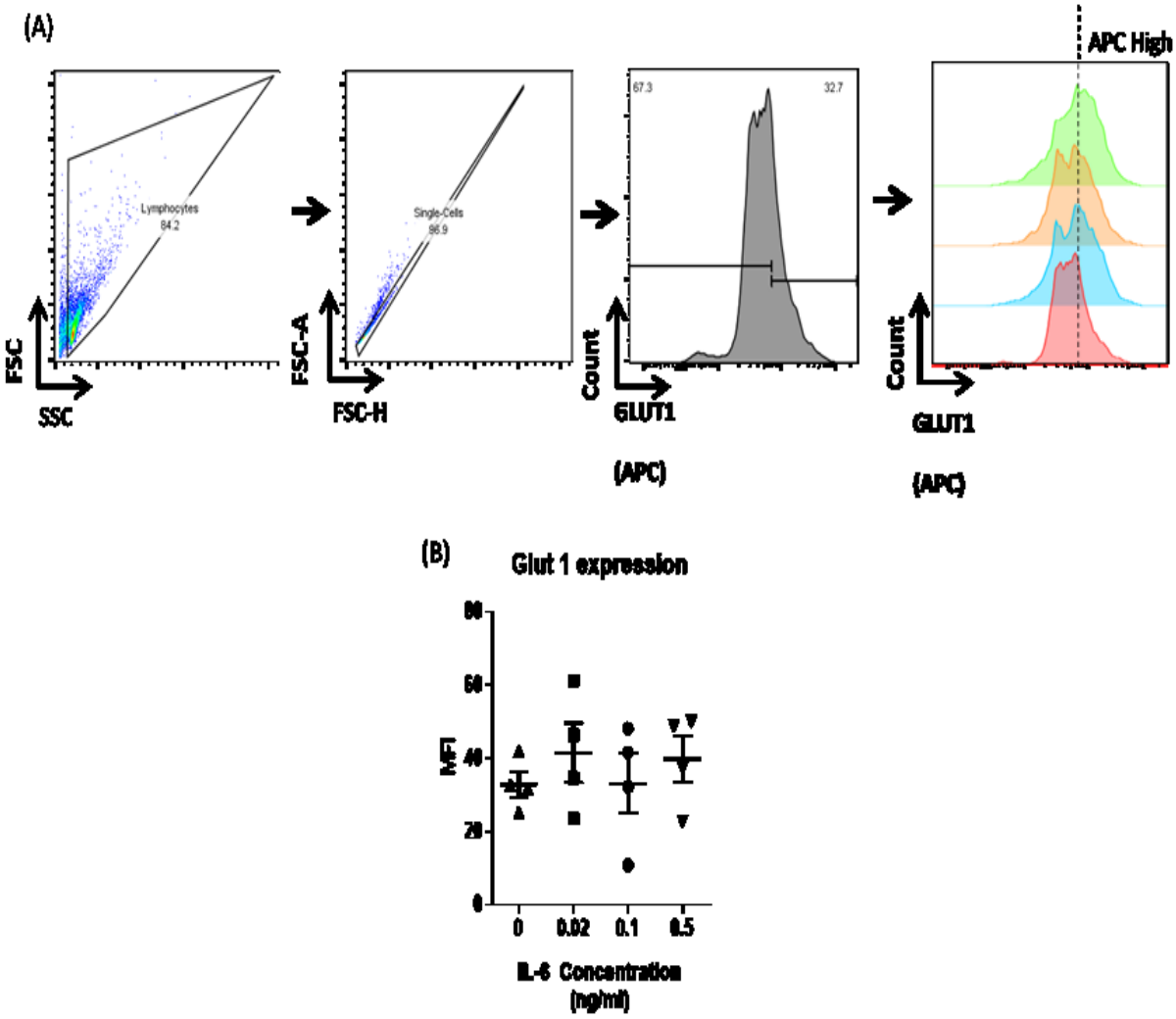

Figure 5.6 - GLUT1 expression of CD4+ T cells after 72 hours of IL-6/IL-6r treatment and subsequent activation with CD3/CD28 for 6 days. (A) The gating strategy shown was used to identify GLUT1 expression. Briefly, Lymphocytes were gated on cell size, doublets were removed, and cells were subsequently gated using GLUT1 APC expression. Percentage of cells in high APC gating were compared after 6 days (B) post CD3/CD28 stimulation. Statistical significance was calculated using multiple comparison ANOVAs in Prism v8 (n=4). Example data used to demonstrate gating strategy shows naïve CD4+ T cells, after 6 days of CD3/CD28 stimulation.

5.4 Discussion

We describe here in the present study an altered metabolic phenotype in naïve CD4+ T cells following IL-6/sIL-6R pre-stimulation. Cytokine signal 3, such as IL-6, is commonly upregulated within the body in response to injury, infection and inflammation; yet, dysregulated signalling is widely noted to play a mechanistic role in the onset and development of autoimmune conditions, including rheumatoid arthritis (Yoshida and Tanaka, 2014). Nonetheless under homeostatic conditions, the previously proposed model suggests that T cells prepare metabolically for an antigenic response, in order to respond more efficiently. In keeping with this, we examined in this chapter the expression of metabolically proteins and any mitochondrial changes in order to identify possible mechanisms that support the observed upregulated metabolic phenotype.

We previously identified from microarray data that c-MYC expression in CD4+ naïve T cells was clearly distinguishable in patients with higher levels of IL-6, in addition to the c-MYC regulatory gene, MAZ (Myc-associated zinc finger protein) following CD3/CD28 stimulation. As such, confirmatory western blot analysis was undertaken in CD4+ T cells to examine expression levels of c-Myc protein. In both naïve and memory T cells, c-Myc expression was increased with IL-6/sIL-6R pre-stimulation; however, observed increases in memory cell only did so at higher concentrations. Such findings in naïve T cells are consistent with the previously observed metabolic phenotype; increased sensitivity in CD4+ naïve T cells appeared to be in line with previous findings by Ridley and colleagues (2019), in which heightened sensitivity to IL-6 was observed in this subset. Reasons for memory T cell hypo-responsiveness was alluded to reduced gp130 expression; however, surface expression was an avenue not further explored in the present study (Ridley *et al.,* 2019). It is also possible that the threshold for IL-6 mediated varies between CD4+ T cell subtype, in which naïve T cells are readily activated due to no prior stimulation of the TCR.

Although no metabolic phenotype was observed with pre-stimulation and cells demonstrated no increased proliferation against untreated cells, memory T cells do seem to be responding. As such, although this observation is unexpected, it is in line with the patient microarray data, in which C-MYC was upregulated in patients with higher serum IL-6. The lack of any metabolic phenotype suggests that either: (1) memory T cells are inhibiting upregulation of metabolically processes downstream of c-MYC or (2) memory T cells are upregulating other metabolic processes which are not associated with glycolysis or cellular respiration. C-MYC is also known to have an effect upon cellular survival and immune cell functions, such as adhesion and mobility. As such, despite the absence of expected metabolic dysfunction from our current model, increased c-MYC protein in memory cells may prevent apoptosis after an immune response or promote adhesion within an inflammatory site. Leading to prolonged inflammation and in turn contributing to the development or progression of IMIDs.

Whilst c-MYC expression does appear to slightly reduce at the highest concentrations of IL-6/sIL-R, 0.5ng/ml within naïve T cells, it is still greater than untreated cells. Such findings may be due to a cellular plateau and subsequent downregulation of IL-6 associated metabolic changes as a protective mechanism: the 0.5 ng/ml concentration employed in the present study reflective of high IL-6 sera concentrations within patients with chronic long term immune-mediated inflammatory disease (IMIDs) and whom show abnormal immune cell metabolism. As such, whilst IL-6 is reported elsewhere to rescue T cells from cellular apoptosis, overexpression is noted to induce pathophysiological effects; the ablation of IL-6R *in vivo* in response to IL-6 overexpression, for example, is shown to protect against pathologic IL-6 triggered systemic inflammation and reasons by which our results may be ascribed (Mufazalov *et al.,*2019).

In addition, the activation of glycolysis following TCR engagement results in the upregulation of several metabolic components. Prior IL-6/sIL-1R stimulation results in increased protein expression of glycolytic-associated enzyme LDHA following CD3/CD28 stimulation as naïve T cells switch to a glycolytic phenotype. Yet, such changes surprisingly did not appear to be

supported by an increased cell surface expression of GLUT1, the predominant transporter of glucose in haematopoietic cells. Whilst precise reasons for this remain unclear, it is possible that failure to detect GLUT1 changes may be ascribed to flow cytometry detection of cell surface expressed channels, in which GLUT1 cell surface localisation has been shown previously to be tightly controlled by extrinsic IL-3 signals (Wienmann *et al.,* 2007). As such, failure to detect changes in GLUT1 expression may be ascribed to the static nature of the experiment conducted i.e. without extrinsic signalling.

The lack of effect on memory cell glycolytic metabolism is further highlighted by LDHA expression, which unlike naïve cells, does not change with IL-6/sIL-6R treatment. However, both analysis of UCP expression and mitochondrial mass indicate that as IL-6/sIL-6R treatment increased, mitochondrial function seems downregulated. c-MYc has been linked to mitochondrial biogenesis, therefore upregulated protein expression would be expected to correlate with higher mitochondrial mass and mitochondrial protein expression (figure 5.2C, figure 5.3E) (Morrish and Hockenbery, 2014). As such, our findings of seemingly downregulated mitochondrial mass and function would appear consistent with cells deficient IL-6 signalling pathways: IL-6 deficiency in cardiac metabolism, for example, is associated with reduced mitochondrial biogenesis and accumulation of acetyl-CoA, leading to inhibition of fatty acid transporters on the mitochondrial membrane (Xu *et al.,* 2018). As such, memory cells may have protective mechanisms to avoid the greater metabolic phenotype and proliferative ability, that were observed in their naïve counterparts.

It is also critical to note that neither of the observed changes in naïve or memory T cell mitochondrial mass occurred until 6 days post-activation, while the increased maximal respiratory capacity in naïve cells and the decrease in UCP expression in memory cells was observed after 3 days post activation. Moreover, significant changes to mitochondrial mass only occurred in memory cells at higher concentrations of IL-6 and all concentrations in naïve cells. This suggests that although initial metabolic phenotype in naïve cells was present after 3 days, any upregulation in mitochondrial biogenesis and mitochondrial growth are only visible

after 6 days post activation. Similarly, the decreased mitochondrial mass seen in memory cells was only visible after 6 days.

Although the data clearly shows alterations to mitochondrial mass, it unclear whether the increases observed are due to increasing mitochondrial size or mitochondrial number. Previous studies have shown altered mitochondrial structures in T cells correlate to cell survival and phenotype function. Therefore the findings in our present study would benefit from being supported with similar evidence from additional experiments. Firstly, it would be useful to determine the effects of inhibition of mitochondrial division on CD4+ T cells treated with IL-6/sIL-6R. Using an inhibitor such as mDIVI-1, a dynamin inhibitor, in cells treated with IL-6, we could see if mitochondrial mass correlates with mitochondrial number. In addition, using microscopy, we could examine mitochondrial structure and see if IL-6/sIL-6R treatment has changed these. Furthermore, analysing the proliferation and metabolic phenotype using seahorse of CD4+ T cells treated with both IL-6/sIL-6R and mDIVI-1 would identify whether the observed differences are associated with mitochondrial biogenesis.

Chapter 6 | Discussion

Understanding changes to both naïve and memory cells in response to different activation signals is imperative to developing our understanding of treatment paradigms in inflammatory disease. Alterations in cellular metabolism support aberrations in normal cellular response i.e. inhibition of glycolysis has been shown to reduce disease progression and inhibit CD4+ T cell expansion (Abboud et al., 2018).

Signal 1 (TCR engagement) and its co-stimulatory Signal 2 (CD28) are widely proposed as requisite signals that lead to full T cell activation from a naïve quiescent state (Lenschow et al,. 1996; Schwartz et al., 1990). The proposal stemming from an extensive body of work showing largely functional inactivity in the absence of one or both signals. For example, numerous studies in CD4+ T cells report absence of co-stimulatory CD28 signalling to result in T cell anergy and inactivation when stimulated with antibodies to CD3+ or pMHC on APCs *in vitro* (Harding et al., 1992; Jenkins et al., 1992; Liu and Janeway, 1992; Tan et al., 1993) and *in vivo* (Shahinian et al., 1993) – consistent with the failure to activate CD4+ cells in the absence of signal 2. Whilst the ablation of TCR is shown to result in immune dysfunction, as noted during the dysfunction of the T_{reg} subset (Levine et al., 2014). Yet, it has been shown elsewhere that in the presence of highly efficient signals that CD3/TCR signalling may overcome the absence of CD28 co-stimulation to elicit T cell activation and downstream function. Indeed, within the body, TCR is noted to be able to interact with MHC on other cells in the absence of a CD28-CD80/86 costimulatory complex signalling (Surh and Sprent, 2000). It has been shown to be both a survival signal and a mechanism in which the T cell pool can be recovered following trauma or infection (Mackall et al., 1997). As such, the present study began with investigating the effects of CD3 stimulation as examined *in vitro* from healthy donor blood.

From the results we were able to determine that CD3 only stimulation does increase cellular metabolism, as the concentration of anti-CD3 increased - yet did not significantly alter mitochondrial metabolism. In line with the previous notion that CD3/TCR signalling may overcome the activation threshold required in the absence of CD28 co-stimulation (Surh and Sprent, 2000), as well as the demonstration that activated T cells upregulate glycolysis whilst reducing mitochondrial metabolism to meet bioenergetic demands (Almeida et al., 2016). Despite this, however, anti-CD3 is considered a 'perfect' signal: reflected in observations made during T cell development within the thymus, in which TCR recombination gives rise to the wide repertoire of TCR types and provides the host immune system the tools to recognise and respond to the variation of antigens produced by pathogens. Similarly, TCR affinity for self-antigen may vary within each cell, with high affinity pMHC shown to be significantly more potent than low affinity binding antigens (6). Thus, each T cell may not receive the same strength in signal that leads to the metabolic changes observed within this study. It is therefore prudent to suggest an *in vivo* model as a suitable point for continuation of these experiments.

One suggestion may be to produce mice which cannot express CD28 and deplete their T cell pools, through the administration of immunomodulatory or immunotoxic drugs. The depletion crucially enabling us to observe through homeostatic proliferation whether there is a TCR receptor bias within the progeny towards a high affinity self-antigen, as opposed to complete removal of the T cell pool. In turn allowing us to assess whether possible bias towards a given progeny also gives rise to susceptibility to metabolic upregulation *via* TCR stimulation only, as well as examine whether repeated homeostatic proliferation increases the chance of developing immune-mediated inflammatory disease (IMID), including RA.

Indeed, the reductionist approach employed in the present study was beneficial when examining the metabolic effects of IL-6. Inflammatory conditions involve a plethora of signals acting in concert to mediate disease pathogenesis, yet the current treatment paradigm for IMIDs largely focus on blocking single inflammatory signals for treatment and maintenance of disease. A common example of this are the biologics infliximab and tocilizumab, which ameliorates disease activity through blockade of TNFα and IL-6 receptor signalling respectively; used in maintenance of several inflammatory conditions including Rheumatoid Arthritis (RA) and Crohn's disease (CD) (Maini and Feldmann, 2002, Scott, 2017, Poggioli et al., 2007). Interestingly, although metabolic deviations are observed during these inflammatory diseases, specifically within immune cells, the cause for such alterations are less well defined.

Excess IL-6 levels are typically characteristic of chronic inflammatory conditions, secreted in response to tissue injury and/or inflammatory dysfunction prior to T cell stimulation. To mimic this, T cells were exposed to IL-6 72 hours prior to CD3/CD28 activation; a 3 day timepoint chosen, in accordance with previous collaborator work by Ridley and colleagues (2019). Certainly in line with previous studies, we show that in response to IL-6/sIL-6R pre-stimulation and subsequent CD3/CD28 stimulation, that naïve T cells readily proliferate in parallel with increased glycolysis, whereas no significant differences in both glycolytic or mitochondrial metabolism of memory T cells were observed. Increases are in line with seemingly apparent cellular programming in favour of Warburg metabolism, in which greater protein expression of lactate-to-NAD+ converter enzyme LDHA is observed in response to IL-6 plus CD3/CD28, as explored in chapter 5.

Difficulty to determine a significant difference in the metabolic phenotypes between naïve and memory CD4+ T cells may potentially be ascribed to the 3-day incubation period with IL-6 prior to T cell stimulation. Although longer IL-6 pre-stimulation times were tested, including 6 and 9 day incubation (data not shown), we were unable to maintain adequate cell numbers due to cell death in culture. Interestingly, IL-6 is shown to play a pleiotropic role in cellular apoptosis versus survival pathways, in which the absence of IL-6 and downstream effector STAT3 signalling in T cell culture results in inhibited growth and spontaneous death of cells, whilst IL-6 is shown to rescue CD4+ T cells from apoptosis due to sustained expression of anti-apoptotic protein BCL-2 and downregulation of death receptor Fas ligand (FasL) (Teague et al., Regis et al., Ayladi et al., 1992). Since the presence of IL-6 stimulation appears to be implicated in a pro-survival role, it is possible T cell apoptosis during IL-6/sIL-6R pre-stimulation may be ascribed to the absence of TCR or CD28 co-stimulation, as previously described in naïve T cells (Parijs et al., 1996). Alternatively, it may have been prudent to provide an additional signal to prevent cell apoptosis, such as IL-2. However, due to the purpose of the current study in determining CD4+ metabolic phenotypes in response to signal 3 only, providing an additional pro-survival cytokine would not have allowed us to examine the effects of IL-6 alone.

As mentioned within chapter 4, the model appears to be a closer representation of a response to acute IL-6 stimulation rather than chronic IL-6 stimulation. This is because we took healthy T cells and provided them with a 72 hour IL-6 pre-stimulation. As such, even though we attempt to delineate the effect of IL-6 stimulation on T cell metabolism prior to activation, it is unclear whether a long term sustained IL-6 stimulation would exacerbate this effect and more broadly, whether this would contribute to T cell-mediated pathogenesis. Certainly, repeated IL-6 stimulation by means of

overexposure is shown *in vivo* to increase peripheral T cell numbers independent of activation, due to improved cellular survival (Hong et al., 2014). Therefore it is plausible that in the context of sustained IL-6 exposure and transcriptional reprogramming, including upregulation of key metabolic regulators like MYC (Ridley et al., 2019; figure 4.1-4.2), that long term IL-6 could contribute to autoimmune activity, including RA, through T cell persistence and bioenergetic means to support downstream effector function.

Consequently, future experiments for the examination of IL-6 on T cell activation would likely benefit from the development or use of an *in vivo* model, in which previous work predominantly centres around overexpression or ablation of IL-6 (von Felbert et al., 2005) (Woodroofe et al., 1992, Mori et al., 2016). Using these models would permit future experiments to identify and also examine T cells from lymph nodes, alongside transient cells found in the blood stream. Unfortunately, many of these previous models do not express sIL-6R at the same level.

Finally, previous evidence shows IL-6 molecules to be able to form a signalling trimer with gp130 with both sIL-6R and membrane bound IL-6R (Baran et al., 2018), however an injury model to induce IL-6/IL-6R release would allow us to repeat the experiment *in vivo* and provide us with cells local to the inflammation, draining lymph nodes and distal lymph nodes for comparison. Additional aged controls could also be utilised to examine a systemic effect on all T cells following increased chronic exposure to IL-6.

Building on the initial metabolic findings, the study aimed to determine the underlying cause for the altered metabolic phenotype. One of the most intriguing changes was an increase in mitochondrial respiratory capacity in naïve CD4+ T cells, alongside

increased glycolytic rate, as IL-6 concentration increased. To this effect, we examined the expression of key mitochondrial complex subunits *via* western blot, in which no significant differences were observed in naïve CD4+ T cells; the findings appearing to be confirmed by microarray data analysis, in which no significant log-fold changes to corresponding gene expression was observed. However, though this data demonstrates no significant alterations to mitochondrial complex protein expression, western blot data does not always directly indicate a change in OXPHOS activity, as indicated by numerous studies noting compensatory mechanisms during ETC complex dysfunction, within the mitochondria and other metabolic pathways (Ait-Aissa et al., 2019) (Vanlerberghe, 2013). This may therefore explain the slight but non-significant reductions in SDHB expression in memory CD4+ T cells with increasing IL-6 stimulation, despite no significant differences in the output readings of the mitochondrial metabolism stress tests.

Additionally, even in the absence of mitochondrial complex expression changes we observed significant increases in naïve CD4+ maximal respiratory rate - in which rates are calculated following the addition of FCCP which disrupts the mitochondrial membrane potential. This forces mitochondrial complexes to work at their maximal rate by reset of the proton gradient under artificial conditions. As such, it would have been prudent to conduct further assays to conclude individual mitochondrial complex activity, as although NMR data does provide an insight into cell metabolites, there is little to no data to indicate a significant change in metabolites is associated with complex function. Of assays suggested is the characterisation of respiratory chain function and mitochondrial ATP production rate (MAPR) by biochemical means, as conducted previously by Wimbom and colleagues (2002). Further examination of complex function and alterations due to IL-6 may also be carried out by utilising

inhibitors or siRNA knockdown of specific complexes, rather than during the seahorse assay, to determine whether inhibition of the complex function reverts the effects of the IL-6.

Although the data clearly shows alterations to mitochondrial mass, it is unclear whether the increases observed are due to increasing mitochondrial size or mitochondrial number. Previous studies have shown altered mitochondrial structures in T cells correlate to cell survival and phenotype function: more recently by Akkaya and colleages (2018), in which CD3/CD28-mediated activation of murine CD4+ T cells results in the increase of both mitochondrial content and volume and in mitochondrial biogenesis – supporting their observed commitment to glycolytic metabolism. Although, previous work has noted an absence of IL-6 led to reduced mitochondrial biogenesis in cardiac tissue (Xu et al., 2018), the adverse effects in immune cells have not been studied. As such, findings in our present study would benefit from being supported with similar evidence from additional experiments. Firstly, it would be useful to determine the inhibited effects of mitochondrial division on CD4+ T cells treated with IL-6/sIL-6R. Using an inhibitor such as mDIVI-1, a dynamin inhibitor, in cells treated with IL-6, we could see if mitochondrial mass correlates with mitochondrial number. In addition, using microscopy, we could examine mitochondrial structure and volume to examine if IL-6/sIL-6R treatment elicits an effect upon these parameters. Furthermore, analysing the proliferation and metabolic phenotype using seahorse of CD4+ T cells treated with both IL-6/sIL-6R and mDIVI-1 would identify whether the observed differences are associated with mitochondrial biogenesis.

Finally, some of the more difficult and early work carried out focused heavily on optimisation of techniques. As shown in chapter 2 and 3, both NMR required a

significant amount of optimisation. Although the NMR data did not provide any significant results, there are no published SOP for analysing T cells using NMR. As such, this current body of work does provide a suitable protocol for starting analysis with NMR.

Within the context of IMIDs, specifically RA, the infiltration of CD4+ T cells into the joint is a characteristic feature of disease activity; yet how cellular signals within the synovial milieu influence T cell metabolism and downstream function, which in turn contribute to disease pathogenesis, is largely unknown. From the current body of work we were able to identify that the requirement for signals 1, 2 and 3 to induce together alterations in T cell metabolism is not a pre-requisite and in the case of memory CD4+ T cells, able to overcome the activation threshold with a CD3-only stimulus to induce cellular glycolysis whilst naïve cells are observed presently to require CD3/CD28 to induce a similar effect. Indeed, glycolytic metabolism is previously noted to contribute RA joint inflammation and destruction, which when inhibited is shown to reduce disease severity including ensuing activation of both adaptive and innate immune cell in murine models (Thomas et al., 1992, Abboud et al., 2018). Interestingly, glycolysis-mediated inhibition by Abboud and colleagues did not correlate reduced joint inflammation with any observation of a reduction in the number of memory CD4+ T cells, although reduced frequencies of Th_{17} and T_{reg} subsets were observed. To this extent it would be useful in further studies, if allowed more time, to provide further granularity around T cell subsets and alterations to cellular metabolism including glycolysis and mitochondrial metabolism.

Indeed, the reliance of glycolytic metabolism following activation to support T cell proliferation and function is well noted in the literature; therefore, unsurprisingly the

metabolic phenotype promotes an environment of high-glucose utilisation in RA. The RA joint is characterised by a low glucose/high lactate ratio which suggests a favoured Warburg-like metabolism in activated CD4+ T cells (Goetzl et al., 1971, Treuhaft and DJ, 1971, Vander Heiden et al., 2009). Whilst lactate levels were not directly measured, we note in chapter 5 increased expression of LDHA in naïve CD4+ T cells when stimulated with signals 1, 2 & 3 – supporting the notion of increased lactate production from increased glycolysis and in turn, end-step conversion of lactate to pyruvate for feeding into the mitochondrial energy hub.

RA pathogenesis is additionally characterised by the dysfunction of cytokine signalling. In particular, there growing body of evidence suggesting IL-6/sIL-6R as a driver of RA development, with studies showing elevated levels to correlate with disease severity (Ishihara and Hirano, 2002, Houssiau et al., 1988, Madhok et al., 1993). While physiological levels of serum IL-6 is normally in the low pg/ml range, synthesis can be rapidly induced by immune cells to stimulate an acute inflammatory response against infection and tissue injury during host defence mechanisms (Maggio et al., 2006). Yet when production is persistent and uncontrolled, IL-6 may lead to the development of autoimmunity. Indeed in RA, IL-6/sIL-6R is shown to be abundantly expressed in the RA synovium and correlates with immune cell infiltration and histological symptoms of chronic synovitis (Madhok et al., 1993, Sack et al., 1993, Jones et al., 2005). Furthermore, in longitudinal studies of RA, elevated IL-6 levels were independently correlated with structural damage to the synovium in early RA (Baillet et al., 2015). Suggesting that tissue injury during early stages of RA development may propagate disease activity through IL-6/sIL-6R pre-stimulated CD4+ T cell activation.

IL-6 binding to its cognate receptor is shown to induce a programme of IL-6 driven STAT3-induced transcriptional signalling observed within CD4+ T cells during RA (Pratt et al., 2012, Anderson et al., 2019, Anderson et al., 2016, Isomäki et al., 2015, Ye et al., 2015). Highlighted within this programme is the overexpression of pro-survival genes and proinflammatory cytokines, including anti-apoptotic BCL3 identified in the present study by IL-6 stratified microarray data analysis of RA patients (Anderson et al., 2019, Anderson et al., 2016, Pratt et al., 2012). Since pSTAT3 and STAT3-inducible genes are positively correlated with IL-6 levels, these findings suggest IL-6 to control proliferation and apoptotic-resistance of CD4+ T cells – ultimately leading to their pathological persistence within the RA joint. STAT3-inducible genes were also particularly over-represented in anti-CCP negative patients, in which the mechanism of antigen-independent RA development remains unclear (Pratt et al., 2012, Anderson et al., 2016). It is therefore considered that RA disease potentiation in patients may arise from cytokine “priming” of CD4+ T cells - a notion supported in the present study by increases in glycolysis and ensuing cell proliferation observed within IL-6/sIL-6R pre-stimulated naïve CD4+ T cells vs. unstimulated cells (Ridgley et al., 2019, Anderson et al., 2019).

It is therefore tantalising to suggest that under physiological conditions, elevations in IL-6 typically associated with RA development and disease activity, may prime CD4+ T cells metabolically for subsequent activity. Present stratification of microarray data by RA IL-6 levels, for example, demonstrates differential expression of metabolic-associated genes, c-MYC and MAZ - key regulators of the PPP and branch pathway from glycolytic metabolism. Such metabolic priming may lead to an exacerbated CD4+ T cell response during RA disease development, alluding to the promotion of an anti-apoptotic, proinflammatory environment within the synovium. Moreover, in studies by

Yang and colleagues (2015), IL-6 is shown to have an additional direct effect on the metabolism of CD4+ T cells. Prolonged hyperpolarisation of the mitochondrial membrane is reported to occur in an IL-6 driven STAT3-dependent manner during cellular activation, inducing Ca^{2+} signalling and downstream cytokine expression (Yang et al., 2015). Alterations were shown to be uncoupled from mitochondrial oxidative phosphorylation: accounting for the minimal changes in OCR and ATP production within CD4+ T cells, we observe in the present study.

Taken together with the above, we therefore propose in the context of RA that IL-6/sIL-6R likely primes CD4+ naïve T cells, but not memory cells for metabolic-driven activity during T cell activation. IL-6 pre-stimulation significantly increases glycolysis in activated naïve CD4+ T cells: in turn, promoting a high lactate environment characteristic of the RA and of which interestingly is shown to metabolically reprogrammed CD4+ T cells to a proinflammatory phenotype (Pucino et al., 2019). To this extent, IL-6/sIL-6R priming therefore potentiates RA disease activity; which in the context of this study requires further examination to confirm such a hypothesis. This includes confirmation of the ability for IL-6 to directly modulate the expression of STAT3-inducible proinflammatory genes and OXPHOS-independent Ca^{2+} signalling vs non IL-6-stimulated cells, as well as anti-apoptotic genes which likely contribute to the persistence of activated proinflammatory CD4+ T cells within the RA joint.

References

ABBOUD, G., CHOI, S.-C., KANDA, N., ZEUMER-SPATARO, L., ROOPENIAN, D. C. & MOREL, L. 2018. Inhibition of Glycolysis Reduces Disease Severity in an Autoimmune Model of Rheumatoid Arthritis. *Frontiers in immunology,* 9**,** 1973-1973.

AFKARIAN, M., SEDY, J. R., YANG, J., JACOBSON, N. G., CEREB, N., YANG, S. Y., MURPHY, T. L. & MURPHY, K. M. 2002. T-bet is a STAT1-induced regulator of IL-12R expression in naïve CD4+ T cells. *Nature Immunology,* 3**,** 549-557.

AIT-AISSA, K., BLASZAK, S., BEUTNER, G., TSAIH, S.-W., MORGAN, G., SANTOS, J., FLISTER, M., JOYCE, D., CAMARA, A., GUTTERMAN, D., DONATO, A., PORTER, G. & BEYER, A. 2019. Mitochondrial Oxidative Phosphorylation defect in the Heart of Subjects with Coronary Artery Disease. *Scientific Reports,* 9**,** 7623.

AKDIS, M., BURGLER, S., CRAMERI, R., EIWEGGER, T., FUJITA, H., GOMEZ, E., KLUNKER, S., MEYER, N., O'MAHONY, L., PALOMARES, O., RHYNER, C., OUAKED, N., SCHAFFARTZIK, A., VAN DE VEEN, W., ZELLER, S., ZIMMERMANN, M. & AKDIS, C. A. 2011. Interleukins, from 1 to 37, and interferon-γ: receptors, functions, and roles in diseases. *The Journal of allergy and clinical immunology,* 127**,** 701-21.e270.

ALAM, J., JANTAN, I. & BUKHARI, S. N. A. 2017. Rheumatoid arthritis: Recent advances on its etiology, role of cytokines and pharmacotherapy. *Biomedicine & pharmacotherapy = Biomedecine & pharmacotherapie,* 92**,** 615-633.

ALBERTS, B., JOHNSON, A. & LEWIS, J. 2002. *Molecular Biology of the Cell,* New York, Garland Science.

ALEXANDER, W. S., STARR, R., FENNER, J. E., SCOTT, C. L., HANDMAN, E., SPRIGG, N. S., CORBIN, J. E., CORNISH, A. L., DARWICHE, R., OWCZAREK, C. M., KAY, T. W., NICOLA, N. A., HERTZOG, P. J., METCALF, D. & HILTON, D. J. 1999. SOCS1 is a critical inhibitor of interferon gamma signaling and prevents the potentially fatal neonatal actions of this cytokine. *Cell,* 98**,** 597-608.

ALLEN, M. E., YOUNG, S. P., MICHELL, R. H. & BACON, P. A. 1995. Altered T lymphocyte signaling in rheumatoid arthritis. *European journal of immunology,* 25**,** 1547-1554.

ALMEIDA, L., LOCHNER, M., BEROD, L. & SPARWASSER, T. 2016. Metabolic pathways in T cell activation and lineage differentiation. *Seminars in Immunology,* 28**,** 514-524.

ANANIEVA, E. A., PATEL, C. H., DRAKE, C. H., POWELL, J. D. & HUTSON, S. M. 2014. Cytosolic branched chain aminotransferase (BCATc) regulates mTORC1 signaling and glycolytic metabolism in CD4+ T cells. *The Journal of biological chemistry,* 289**,** 18793-18804.

ANANIEVA, E. A., POWELL, J. D. & HUTSON, S. M. 2016. Leucine Metabolism in T Cell Activation: mTOR Signaling and Beyond. *Advances in nutrition (Bethesda, Md.),* 7**,** 798S-805S.

ANDERSON, A. E., MANEY, N. J., NAIR, N., LENDREM, D. W., SKELTON, A. J., DIBOLL, J., BROWN, P. M., SMITH, G. R., CARMODY, R. J., BARTON, A., ISAACS, J. D. & PRATT, A. G. 2019. Expression of STAT3-regulated genes in circulating CD4+ T cells discriminates rheumatoid arthritis independently of clinical parameters in early arthritis. *Rheumatology,* 58**,** 1250-1258.

ANDERSON, A. E., PRATT, A. G., SEDHOM, M. A., DORAN, J. P., ROUTLEDGE, C., HARGREAVES, B., BROWN, P. M., KA, L. C., ISAACS, J. D. & THOMAS,

R. 2016. IL-6-driven STAT signalling in circulating CD4+ lymphocytes is a marker for early anticitrullinated peptide antibody-negative rheumatoid arthritis. *Ann Rheum Dis,* 75**,** 466-73.
ANDERSON, M. S. & SU, M. A. 2011. Aire and T cell development. *Current opinion in immunology,* 23**,** 198-206.
ANGELIN, A., GIL-DE-GÓMEZ, L., DAHIYA, S., JIAO, J., GUO, L., LEVINE, M. H., WANG, Z., QUINN, W. J., 3RD, KOPINSKI, P. K., WANG, L., AKIMOVA, T., LIU, Y., BHATTI, T. R., HAN, R., LASKIN, B. L., BAUR, J. A., BLAIR, I. A., WALLACE, D. C., HANCOCK, W. W. & BEIER, U. H. 2017. Foxp3 Reprograms T Cell Metabolism to Function in Low-Glucose, High-Lactate Environments. *Cell metabolism,* 25**,** 1282-1293.e7.
ARNSON, Y., SHOENFELD, Y. & AMITAL, H. 2010. Effects of tobacco smoke on immunity, inflammation and autoimmunity. *J Autoimmun,* 34**,** J258-65.
ARTS, R. J. W., NOVAKOVIC, B., TER HORST, R., CARVALHO, A., BEKKERING, S., LACHMANDAS, E., RODRIGUES, F., SILVESTRE, R., CHENG, S.-C., WANG, S.-Y., HABIBI, E., GONÇALVES, L. G., MESQUITA, I., CUNHA, C., VAN LAARHOVEN, A., VAN DE VEERDONK, F. L., WILLIAMS, D. L., VAN DER MEER, J. W. M., LOGIE, C., O'NEILL, L. A., DINARELLO, C. A., RIKSEN, N. P., VAN CREVEL, R., CLISH, C., NOTEBAART, R. A., JOOSTEN, L. A. B., STUNNENBERG, H. G., XAVIER, R. J. & NETEA, M. G. 2016. Glutaminolysis and Fumarate Accumulation Integrate Immunometabolic and Epigenetic Programs in Trained Immunity. *Cell metabolism,* 24**,** 807-819.
AUGUST, A. & DUPONT, B. 1994. CD28 of T lymphocytes associates with phosphatidylinositol 3-kinase. *International immunology,* 6**,** 769-774.
AYROLDI, E., ZOLLO, O., CANNARILE, L., F, D. A., GROHMANN, U., DELFINO, D. V. & RICCARDI, C. 1998. Interleukin-6 (IL-6) prevents activation-induced cell death: IL-2-independent inhibition of Fas/fasL expression and cell death. *Blood,* 92**,** 4212-9.
AZOULAY-ZOHAR, H., ISRAELSON, A., ABU-HAMAD, S. & SHOSHAN-BARMATZ, V. 2004. In self-defence: hexokinase promotes voltage-dependent anion channel closure and prevents mitochondria-mediated apoptotic cell death. *Biochem J,* 377**,** 347-55.
BAILLET, A., GOSSEC, L., PATERNOTTE, S., ETCHETO, A., COMBE, B., MEYER, O., MARIETTE, X., GOTTENBERG, J.-E. & DOUGADOS, M. 2015. Evaluation of Serum Interleukin-6 Level as a Surrogate Marker of Synovial Inflammation and as a Factor of Structural Progression in Early Rheumatoid Arthritis: Results From a French National Multicenter Cohort. *Arthritis Care & Research,* 67**,** 905-912.
BALDINI, S. F., STEENACKERS, A., OLIVIER-VAN STICHELEN, S., MIR, A.-M., MORTUAIRE, M., LEFEBVRE, T. & GUINEZ, C. 2016. Glucokinase expression is regulated by glucose through O-GlcNAc glycosylation. *Biochemical and biophysical research communications,* 478**,** 942-948.
BAMBOUSKOVA, M., GORVEL, L., LAMPROPOULOU, V., SERGUSHICHEV, A., LOGINICHEVA, E., JOHNSON, K., KORENFELD, D., MATHYER, M. E., KIM, H., HUANG, L.-H., DUNCAN, D., BREGMAN, H., KESKIN, A., SANTEFORD, A., APTE, R. S., SEHGAL, R., JOHNSON, B., AMARASINGHE, G. K., SOARES, M. P., SATOH, T., AKIRA, S., HAI, T., DE GUZMAN STRONG, C., AUCLAIR, K., RODDY, T. P., BILLER, S. A., JOVANOVIC, M., KLECHEVSKY, E., STEWART, K. M., RANDOLPH, G. J. & ARTYOMOV, M. N. 2018. Electrophilic properties of itaconate and derivatives regulate the IκBζ-ATF3 inflammatory axis. *Nature,* 556**,** 501-504.

BARAN, P., HANSEN, S., WAETZIG, G. H., AKBARZADEH, M., LAMERTZ, L., HUBER, H. J., AHMADIAN, M. R., MOLL, J. M. & SCHELLER, J. 2018. The balance of interleukin (IL)-6, IL-6·soluble IL-6 receptor (sIL-6R), and IL-6·sIL-6R·sgp130 complexes allows simultaneous classic and trans-signaling. *Journal of Biological Chemistry,* 293**,** 6762-6775.

BARRON, L., DOOMS, H., HOYER, K. K., KUSWANTO, W., HOFMANN, J., O'GORMAN, W. E. & ABBAS, A. K. 2010. Cutting edge: mechanisms of IL-2-dependent maintenance of functional regulatory T cells. *Journal of immunology (Baltimore, Md. : 1950),* 185**,** 6426-6430.

BAXTER, A. G. & HODGKIN, P. D. 2002. Activation rules: the two-signal theories of immune activation. *Nature Reviews Immunology,* 2**,** 439-446.

BEN-SASSON, S. Z., HU-LI, J., QUIEL, J., CAUCHETAUX, S., RATNER, M., SHAPIRA, I., DINARELLO, C. A. & PAUL, W. E. 2009. IL-1 acts directly on CD4 T cells to enhance their antigen-driven expansion and differentiation. *Proceedings of the National Academy of Sciences of the United States of America,* 106**,** 7119-7124.

BENJAMIN, D., ROBAY, D., HINDUPUR, S. K., POHLMANN, J., COLOMBI, M., EL-SHEMERLY, M. Y., MAIRA, S.-M., MORONI, C., LANE, H. A. & HALL, M. N. 2018. Dual Inhibition of the Lactate Transporters MCT1 and MCT4 Is Synthetic Lethal with Metformin due to NAD+ Depletion in Cancer Cells. *Cell Reports,* 25**,** 3047-3058.e4.

BERG, J. M., TYMOCZKO, J. L. & STRYER, L. 2002. *Biochemistry,* New York, W.H. Freeman.

BEROD, L., FRIEDRICH, C., NANDAN, A., FREITAG, J., HAGEMANN, S., HARMROLFS, K., SANDOUK, A., HESSE, C., CASTRO, C. N., BAHRE, H., TSCHIRNER, S. K., GORINSKI, N., GOHMERT, M., MAYER, C. T., HUEHN, J., PONIMASKIN, E., ABRAHAM, W. R., MULLER, R., LOCHNER, M. & SPARWASSER, T. 2014. De novo fatty acid synthesis controls the fate between regulatory T and T helper 17 cells. *Nat Med,* 20**,** 1327-33.

BETTELLI, E., CARRIER, Y., GAO, W., KORN, T., STROM, T. B., OUKKA, M., WEINER, H. L. & KUCHROO, V. K. 2006. Reciprocal developmental pathways for the generation of pathogenic effector TH17 and regulatory T cells. *Nature,* 441**,** 235-238.

BETZ, U. A. & MULLER, W. 1998. Regulated expression of gp130 and IL-6 receptor alpha chain in T cell maturation and activation. *Int Immunol,* 10**,** 1175-84.

BLUM, J. S., WEARSCH, P. A. & CRESSWELL, P. 2013. Pathways of antigen processing. *Annual review of immunology,* 31**,** 443-473.

BOKAREWA, M., NAGAEV, I., DAHLBERG, L., SMITH, U. & TARKOWSKI, A. 2005. Resistin, an adipokine with potent proinflammatory properties. *Journal of immunology (Baltimore, Md. : 1950),* 174**,** 5789-5795.

BOKI, K. A., DROSOS, A. A., TZIOUFAS, A. G., LANCHBURY, J. S., PANAYI, G. S. & MOUTSOPOULOS, H. M. 1993. Examination of HLA-DR4 as a severity marker for rheumatoid arthritis in Greek patients. *Annals of the rheumatic diseases,* 52**,** 517-519.

BOOMER, J. S. & GREEN, J. M. 2010a. An enigmatic tail of CD28 signaling. *Cold Spring Harbor perspectives in biology,* 2**,** a002436-a002436.

BOOMER, J. S. & GREEN, J. M. 2010b. An enigmatic tail of CD28 signaling. *Cold Spring Harb Perspect Biol,* 2**,** a002436.

BOSSHART, P. D., KALBERMATTER, D., BONETTI, S. & FOTIADIS, D. 2019. Mechanistic basis of L-lactate transport in the SLC16 solute carrier family. *Nature Communications,* 10**,** 2649.

BOSSONE, S. A., ASSELIN, C., PATEL, A. J. & MARCU, K. B. 1992. MAZ, a zinc finger protein, binds to c-MYC and C2 gene sequences regulating transcriptional initiation and termination. *Proceedings of the National Academy of Sciences of the United States of America,* 89**,** 7452-7456.
BOUNEAUD, C., KOURILSKY, P. & BOUSSO, P. 2000. Impact of Negative Selection on the T Cell Repertoire Reactive to a Self-Peptide: A Large Fraction of T Cell Clones Escapes Clonal Deletion. *Immunity,* 13**,** 829-840.
BREITFELD, D., OHL, L., KREMMER, E., ELLWART, J., SALLUSTO, F., LIPP, M. & FÖRSTER, R. 2000. Follicular B helper T cells express CXC chemokine receptor 5, localize to B cell follicles, and support immunoglobulin production. *The Journal of experimental medicine,* 192**,** 1545-1552.
BRETSCHER, P. & COHN, M. 1970. A theory of self-nonself discrimination. *Science (New York, N.Y.),* 169**,** 1042-1049.
BRIDGES, S. L., JR., KELLEY, J. M. & HUGHES, L. B. 2008. The HLA-DRB1 shared epitope in Caucasians with rheumatoid arthritis: a lesson learned from tic-tac-toe. *Arthritis and rheumatism,* 58**,** 1211-1215.
BUCH, T., RIEUX-LAUCAT, F., FÖRSTER, I. & RAJEWSKY, K. 2002. Failure of HY-Specific Thymocytes to Escape Negative Selection by Receptor Editing. *Immunity,* 16**,** 707-718.
BUTSCHER, W. G., POWERS, C., OLIVE, M., VINSON, C. & GARDNER, K. 1998. Coordinate transactivation of the interleukin-2 CD28 response element by c-Rel and ATF-1/CREB2. *J Biol Chem,* 273**,** 552-60.
CAIELLI, S., VEIGA, D. T., BALASUBRAMANIAN, P., ATHALE, S., DOMIC, B., MURAT, E., BANCHEREAU, R., XU, Z., CHANDRA, M., CHUNG, C.-H., WALTERS, L., BAISCH, J., WRIGHT, T., PUNARO, M., NASSI, L., STEWART, K., FULLER, J., UCAR, D., UENO, H., ZHOU, J., BANCHEREAU, J. & PASCUAL, V. 2019. A CD4(+) T cell population expanded in lupus blood provides B cell help through interleukin-10 and succinate. *Nature medicine,* 25**,** 75-81.
CAO, H., LIN, J., CHEN, W., XU, G. & SUN, C. 2016. Baseline adiponectin and leptin levels in predicting an increased risk of disease activity in rheumatoid arthritis: A meta-analysis and systematic review. *Autoimmunity,* 49**,** 547-553.
CHANCE, B. & WILLIAMS, G. R. 1956. Respiratory enzymes in oxidative phosphorylation. VI. The effects of adenosine diphosphate on azide-treated mitochondria. *J Biol Chem,* 221**,** 477-89.
CHANCE, B., WILLIAMS, G. R., HOLMES, W. F. & HIGGINS, J. 1955. Respiratory enzymes in oxidative phosphorylation. V. A mechanism for oxidative phosphorylation. *J Biol Chem,* 217**,** 439-51.
CHANG, C.-H., CURTIS, J., MAGGI, L., FAUBERT, B., VILLARINO, A., O'SULLIVAN, D., HUANG, S., WINDT, G., BLAGIH, J., QIU, J., WEBER, J., PEARCE, E., JONES, R. & PEARCE, E. 2013a. Posttranscriptional Control of T Cell Effector Function by Aerobic Glycolysis. *Cell,* 153**,** 1239-51.
CHANG, C.-H., CURTIS, J. D., MAGGI, L. B., JR., FAUBERT, B., VILLARINO, A. V., O'SULLIVAN, D., HUANG, S. C.-C., VAN DER WINDT, G. J. W., BLAGIH, J., QIU, J., WEBER, J. D., PEARCE, E. J., JONES, R. G. & PEARCE, E. L. 2013b. Posttranscriptional control of T cell effector function by aerobic glycolysis. *Cell,* 153**,** 1239-1251.
CHEN, L. & FLIES, D. B. 2013. Molecular mechanisms of T cell co-stimulation and co-inhibition. *Nature reviews. Immunology,* 13**,** 227-242.
CHEN, W., JIN, W., HARDEGEN, N., LEI, K.-J., LI, L., MARINOS, N., MCGRADY, G. & WAHL, S. M. 2003. Conversion of peripheral CD4+CD25- naive T cells to

CD4+CD25+ regulatory T cells by TGF-beta induction of transcription factor Foxp3. *The Journal of experimental medicine,* 198**,** 1875-1886.
CHOI, S.-C., TITOV, A. A., ABBOUD, G., SEAY, H. R., BRUSKO, T. M., ROOPENIAN, D. C., SALEK-ARDAKANI, S. & MOREL, L. 2018. Inhibition of glucose metabolism selectively targets autoreactive follicular helper T cells. *Nature communications,* 9**,** 4369-4369.
CHOW, C. W., RINCON, M. & DAVIS, R. J. 1999. Requirement for transcription factor NFAT in interleukin-2 expression. *Mol Cell Biol,* 19**,** 2300-7.
COBBOLD, S. P., ADAMS, E., FARQUHAR, C. A., NOLAN, K. F., HOWIE, D., LUI, K. O., FAIRCHILD, P. J., MELLOR, A. L., RON, D. & WALDMANN, H. 2009. Infectious tolerance via the consumption of essential amino acids and mTOR signaling. *Proceedings of the National Academy of Sciences of the United States of America,* 106**,** 12055-12060.
CORDEIRO, A. T., GODOI, P. H. C., SILVA, C. H. T. P., GARRATT, R. C., OLIVA, G. & THIEMANN, O. H. 2003. Crystal structure of human phosphoglucose isomerase and analysis of the initial catalytic steps. *Biochimica et biophysica acta,* 1645**,** 117-122.
CRITES, T. J. & VARMA, R. 2010. On the issue of peptide recognition in T cell development. *Self/nonself,* 1**,** 55-61.
CROFT, M., DUAN, W., CHOI, H., EUN, S.-Y., MADIREDDI, S. & MEHTA, A. 2012. TNF superfamily in inflammatory disease: translating basic insights. *Trends in immunology,* 33**,** 144-152.
CROTTY, S. 2014. T follicular helper cell differentiation, function, and roles in disease. *Immunity,* 41**,** 529-542.
CROUSE, J., KALINKE, U. & OXENIUS, A. 2015. Regulation of antiviral T cell responses by type I interferons. *Nat Rev Immunol,* 15**,** 231-42.
CROWSON, C. S., LIAO, K. P., DAVIS, J. M., 3RD, SOLOMON, D. H., MATTESON, E. L., KNUTSON, K. L., HLATKY, M. A. & GABRIEL, S. E. 2013. Rheumatoid arthritis and cardiovascular disease. *Am Heart J,* 166**,** 622-628 e1.
CURTSINGER, J. M., SCHMIDT, C. S., MONDINO, A., LINS, D. C., KEDL, R. M., JENKINS, M. K. & MESCHER, M. F. 1999. Inflammatory cytokines provide a third signal for activation of naive CD4+ and CD8+ T cells. *J Immunol,* 162**,** 3256-62.
DAMSKER, J. M., HANSEN, A. M. & CASPI, R. R. 2010. Th1 and Th17 cells Adversaries and collaborators. *Year in Immunology 2,* 1183**,** 211-221.
DANIELS, M. & TEIXEIRO, E. 2015. TCR signaling in T cell memory. *Frontiers in Immunology,* 6.
DANIELS, M. A., TEIXEIRO, E., GILL, J., HAUSMANN, B., ROUBATY, D., HOLMBERG, K., WERLEN, G., HOLLÄNDER, G. A., GASCOIGNE, N. R. J. & PALMER, E. 2006. Thymic selection threshold defined by compartmentalization of Ras/MAPK signalling. *Nature,* 444**,** 724-729.
DARDALHON, V., AWASTHI, A., KWON, H., GALILEOS, G., GAO, W., SOBEL, R. A., MITSDOERFFER, M., STROM, T. B., ELYAMAN, W., HO, I. C., KHOURY, S., OUKKA, M. & KUCHROO, V. K. 2008. IL-4 inhibits TGF-beta-induced Foxp3+ T cells and, together with TGF-beta, generates IL-9+ IL-10+ Foxp3(-) effector T cells. *Nature immunology,* 9**,** 1347-1355.
DE BRITO ROCHA, S., BALDO, D. C. & ANDRADE, L. E. C. 2019. Clinical and pathophysiologic relevance of autoantibodies in rheumatoid arthritis. *Advances in Rheumatology,* 59**,** 2.
DE CERQUEIRA CESAR, M. & WILSON, J. E. 2002. Functional characteristics of hexokinase bound to the type a and type B sites of bovine brain mitochondria. *Archives of biochemistry and biophysics,* 397**,** 106-112.

DE HAIR, M. J., LANDEWE, R. B., VAN DE SANDE, M. G., VAN SCHAARDENBURG, D., VAN BAARSEN, L. G., GERLAG, D. M. & TAK, P. P. 2013. Smoking and overweight determine the likelihood of developing rheumatoid arthritis. *Ann Rheum Dis,* 72**,** 1654-8.

DELGOFFE, G. M., POLLIZZI, K. N., WAICKMAN, A. T., HEIKAMP, E., MEYERS, D. J., HORTON, M. R., XIAO, B., WORLEY, P. F. & POWELL, J. D. 2011. The kinase mTOR regulates the differentiation of helper T cells through the selective activation of signaling by mTORC1 and mTORC2. *Nature immunology,* 12**,** 295-303.

DIEHL, S., ANGUITA, J., HOFFMEYER, A., ZAPTON, T., IHLE, J. N., FIKRIG, E. & RINCÓN, M. 2000. Inhibition of Th1 differentiation by IL-6 is mediated by SOCS1. *Immunity,* 13**,** 805-815.

DIENZ, O., EATON, S. M., KRAHL, T. J., DIEHL, S., CHARLAND, C., DODGE, J., SWAIN, S. L., BUDD, R. C., HAYNES, L. & RINCON, M. 2007. Accumulation of NFAT mediates IL-2 expression in memory, but not naïve, CD4⁺ T cells. *Proceedings of the National Academy of Sciences,* 104**,** 7175.

DIENZ, O. & RINCON, M. 2009. The effects of IL-6 on CD4 T cell responses. *Clinical immunology (Orlando, Fla.),* 130**,** 27-33.

DIETERLE, F., ROSS, A., SCHLOTTERBECK, G. & SENN, H. 2006. Probabilistic Quotient Normalization as Robust Method to Account for Dilution of Complex Biological Mixtures. Application in 1H NMR Metabonomics. *Analytical Chemistry,* 78**,** 4281-4290.

DOUGHTY, C. A., BLEIMAN, B. F., WAGNER, D. J., DUFORT, F. J., MATARAZA, J. M., ROBERTS, M. F. & CHILES, T. C. 2006. Antigen receptor-mediated changes in glucose metabolism in B lymphocytes: role of phosphatidylinositol 3-kinase signaling in the glycolytic control of growth. *Blood,* 107**,** 4458-4465.

DUHEN, T., GEIGER, R., JARROSSAY, D., LANZAVECCHIA, A. & SALLUSTO, F. 2009. Production of interleukin 22 but not interleukin 17 by a subset of human skin-homing memory T cells. *Nat Immunol,* 10**,** 857-63.

ECKEL, R. H., ALBERTI, K. G. M. M., GRUNDY, S. M. & ZIMMET, P. Z. 2010. The metabolic syndrome. *Lancet (London, England),* 375**,** 181-183.

EL-GABALAWY, H., GUENTHER, L. C. & BERNSTEIN, C. N. 2010. Epidemiology of Immune-Mediated Inflammatory Diseases: Incidence, Prevalence, Natural History, and Comorbidities. *The Journal of Rheumatology,* 85**,** 2.

ELKAN, A.-C., ENGVALL, I.-L., CEDERHOLM, T. & HAFSTRÖM, I. 2009. Rheumatoid cachexia, central obesity and malnutrition in patients with low-active rheumatoid arthritis: feasibility of anthropometry, Mini Nutritional Assessment and body composition techniques. *European journal of nutrition,* 48**,** 315-322.

ELLISON, W. R., LUECK, J. D. & FROMM, H. J. 1975. Studies on the mechanism of orthophosphate regulation of bovine brain hexokinase. *J Biol Chem,* 250**,** 1864-71.

ESENSTEN, J. H., HELOU, Y. A., CHOPRA, G., WEISS, A. & BLUESTONE, J. A. 2016. CD28 Costimulation: From Mechanism to Therapy. *Immunity,* 44**,** 973-88.

EYLES, J. L., METCALF, D., GRUSBY, M. J., HILTON, D. J. & STARR, R. 2002. Negative regulation of interleukin-12 signaling by suppressor of cytokine signaling-1. *J Biol Chem,* 277**,** 43735-40.

FANG, T. Y., ALECHINA, O., ALESHIN, A. E., FROMM, H. J. & HONZATKO, R. B. 1998. Identification of a phosphate regulatory site and a low affinity binding

site for glucose 6-phosphate in the N-terminal half of human brain hexokinase. *J Biol Chem,* 273**,** 19548-53.
FANTINI, M. C., BECKER, C., MONTELEONE, G., PALLONE, F., GALLE, P. R. & NEURATH, M. F. 2004. Cutting edge: TGF-beta induces a regulatory phenotype in CD4+CD25- T cells through Foxp3 induction and down-regulation of Smad7. *Journal of immunology (Baltimore, Md. : 1950),* 172**,** 5149-5153.
FINLAY, D. 2012. Regulation of glucose metabolism in T cells: new insight into the role of Phosphoinositide 3-kinases. *Frontiers in Immunology,* 3.
FIRESTEIN, G. S., XU, W. D., TOWNSEND, K., BROIDE, D., ALVARO-GRACIA, J., GLASEBROOK, A. & ZVAIFLER, N. J. 1988. Cytokines in chronic inflammatory arthritis. I. Failure to detect T cell lymphokines (interleukin 2 and interleukin 3) and presence of macrophage colony-stimulating factor (CSF-1) and a novel mast cell growth factor in rheumatoid synovitis. *The Journal of experimental medicine,* 168**,** 1573-1586.
FONTENOT, J. D., RASMUSSEN, J. P., GAVIN, M. A. & RUDENSKY, A. Y. 2005. A function for interleukin 2 in Foxp3-expressing regulatory T cells. *Nature immunology,* 6**,** 1142-1151.
FOX, C. J., HAMMERMAN, P. S. & THOMPSON, C. B. 2005. Fuel feeds function: energy metabolism and the T-cell response. *Nature reviews. Immunology,* 5**,** 844-852.
FRAUWIRTH, K. A., RILEY, J. L., HARRIS, M. H., PARRY, R. V., RATHMELL, J. C., PLAS, D. R., ELSTROM, R. L., JUNE, C. H. & THOMPSON, C. B. 2002. The CD28 Signaling Pathway Regulates Glucose Metabolism. *Immunity,* 16**,** 769-777.
FU, S., ZHANG, N., YOPP, A. C., CHEN, D., MAO, M., CHEN, D., ZHANG, H., DING, Y. & BROMBERG, J. S. 2004. TGF-beta induces Foxp3 + T-regulatory cells from CD4 + CD25 - precursors. *American journal of transplantation : official journal of the American Society of Transplantation and the American Society of Transplant Surgeons,* 4**,** 1614-1627.
FUGGER, L. & SVEJGAARD, A. 2000. Association of MHC and rheumatoid arthritis: HLA-DR4 and rheumatoid arthritis - studies in mice and men. *Arthritis Research & Therapy,* 2**,** 208.
GAO, Y., TANG, J., CHEN, W., LI, Q., NIE, J., LIN, F., WU, Q., CHEN, Z., GAO, Z., FAN, H., TSUN, A., SHEN, J., CHEN, G., LIU, Z., LOU, Z., OLSEN, N. J., ZHENG, S. G. & LI, B. 2015. Inflammation negatively regulates FOXP3 and regulatory T-cell function via DBC1. *Proceedings of the National Academy of Sciences of the United States of America,* 112**,** E3246-E3254.
GAO, Z., GAO, Y., LI, Z., CHEN, Z., LU, D., TSUN, A. & LI, B. 2012. Synergy between IL-6 and TGF-β signaling promotes FOXP3 degradation. *International journal of clinical and experimental pathology,* 5**,** 626-633.
GEIGER, R., RIECKMANN, J. C., WOLF, T., BASSO, C., FENG, Y., FUHRER, T., KOGADEEVA, M., PICOTTI, P., MEISSNER, F., MANN, M., ZAMBONI, N., SALLUSTO, F. & LANZAVECCHIA, A. 2016. L-Arginine Modulates T Cell Metabolism and Enhances Survival and Anti-tumor Activity. *Cell,* 167**,** 829-842.e13.
GERLACH, K., HWANG, Y., NIKOLAEV, A., ATREYA, R., DORNHOFF, H., STEINER, S., LEHR, H.-A., WIRTZ, S., VIETH, M., WAISMAN, A., ROSENBAUER, F., MCKENZIE, A. N. J., WEIGMANN, B. & NEURATH, M. F. 2014. TH9 cells that express the transcription factor PU.1 drive T cell-mediated colitis via IL-9 receptor signaling in intestinal epithelial cells. *Nature immunology,* 15**,** 676-686.

GHORESCHI, K., LAURENCE, A., YANG, X.-P., TATO, C. M., MCGEACHY, M. J., KONKEL, J. E., RAMOS, H. L., WEI, L., DAVIDSON, T. S., BOULADOUX, N., GRAINGER, J. R., CHEN, Q., KANNO, Y., WATFORD, W. T., SUN, H.-W., EBERL, G., SHEVACH, E. M., BELKAID, Y., CUA, D. J., CHEN, W. & O'SHEA, J. J. 2010. Generation of pathogenic T(H)17 cells in the absence of TGF-β signalling. *Nature,* 467**,** 967-971.

GOETZL, E. J., FALCHUK, K. H., ZEIGER, L. S., SULLIVAN, A. L., HEBERT, C. L., ADAMS, J. P. & DECKER, J. L. 1971. A physiological approach to the assessment of disease activity in rheumatoid arthritis. *J Clin Invest,* 50**,** 1167-80.

GOLDRATH, A. W., BOGATZKI, L. Y. & BEVAN, M. J. 2000. Naive T cells transiently acquire a memory-like phenotype during homeostasis-driven proliferation. *The Journal of experimental medicine,* 192**,** 557-564.

GÓMEZ-MARTÍN, D., DÍAZ-ZAMUDIO, M., VANOYE, G., CRISPÍN, J. C. & ALCOCER-VARELA, J. 2011. Quantitative and functional profiles of CD4+ lymphocyte subsets in systemic lupus erythematosus patients with lymphopenia. *Clinical and experimental immunology,* 164**,** 17-25.

GREGERSEN, P. K., MORIUCHI, T., KARR, R. W., OBATA, F., MORIUCHI, J., MACCARI, J., GOLDBERG, D., WINCHESTER, R. J. & SILVER, J. 1986. Polymorphism of HLA-DR beta chains in DR4, -7, and -9 haplotypes: implications for the mechanisms of allelic variation. *Proceedings of the National Academy of Sciences,* 83**,** 9149.

GREINER, E. F., GUPPY, M. & BRAND, K. 1994. Glucose is essential for proliferation and the glycolytic enzyme induction that provokes a transition to glycolytic energy production. *J Biol Chem,* 269**,** 31484-90.

GUPPY, M., GREINER, E. & BRAND, K. 1993. The role of the Crabtree effect and an endogenous fuel in the energy metabolism of resting and proliferating thymocytes. *European Journal of Biochemistry,* 212**,** 95-99.

HAWSE, W. F. & CATTLEY, R. T. 2019. T cells transduce T-cell receptor signal strength by generating different phosphatidylinositols. *J Biol Chem,* 294**,** 4793-4805.

HEISEKE, A. F., JEUK, B. H., MARKOTA, A., STRAUB, T., LEHR, H.-A., REINDL, W. & KRUG, A. B. 2015. IRAK1 Drives Intestinal Inflammation by Promoting the Generation of Effector Th Cells with Optimal Gut-Homing Capacity. *Journal of immunology (Baltimore, Md. : 1950),* 195**,** 5787-5794.

HIDAYAT, S., YOSHINO, K.-I., TOKUNAGA, C., HARA, K., MATSUO, M. & YONEZAWA, K. 2003. Inhibition of amino acid-mTOR signaling by a leucine derivative induces G1 arrest in Jurkat cells. *Biochemical and biophysical research communications,* 301**,** 417-423.

HILL, J. A., SOUTHWOOD, S., SETTE, A., JEVNIKAR, A. M., BELL, D. A. & CAIRNS, E. 2003. Cutting edge: the conversion of arginine to citrulline allows for a high-affinity peptide interaction with the rheumatoid arthritis-associated HLA-DRB1*0401 MHC class II molecule. *Journal of immunology (Baltimore, Md. : 1950),* 171**,** 538-541.

HOTAMISLIGIL, G. S., SHARGILL, N. S. & SPIEGELMAN, B. M. 1993. Adipose expression of tumor necrosis factor-alpha: direct role in obesity-linked insulin resistance. *Science (New York, N.Y.),* 259**,** 87-91.

HOUGHTON, F. D., SHETH, B., MORAN, B., LEESE, H. J. & FLEMING, T. P. 1996. Expression and activity of hexokinase in the early mouse embryo. *Molecular human reproduction,* 2**,** 793-798.

HOUSSIAU, F. A., DEVOGELAER, J. P., VAN DAMME, J., DE DEUXCHAISNES, C. N. & VAN SNICK, J. 1988. Interleukin-6 in synovial fluid and serum of patients

with rheumatoid arthritis and other inflammatory arthritides. *Arthritis Rheum,* 31**,** 784-8.
HOWIE, D., TEN BOKUM, A., NECULA, A. S., COBBOLD, S. P. & WALDMANN, H. 2018. The Role of Lipid Metabolism in T Lymphocyte Differentiation and Survival. *Frontiers in immunology,* 8**,** 1949-1949.
ICHIYAMA, K., SEKIYA, T., INOUE, N., TAMIYA, T., KASHIWAGI, I., KIMURA, A., MORITA, R., MUTO, G., SHICHITA, T., TAKAHASHI, R. & YOSHIMURA, A. 2011. Transcription factor Smad-independent T helper 17 cell induction by transforming-growth factor-beta is mediated by suppression of eomesodermin. *Immunity,* 34**,** 741-54.
ISHIHARA, K. & HIRANO, T. 2002. IL-6 in autoimmune disease and chronic inflammatory proliferative disease. *Cytokine Growth Factor Rev,* 13**,** 357-68.
ISOMÄKI, P., JUNTTILA, I., VIDQVIST, K. L., KORPELA, M. & SILVENNOINEN, O. 2015. The activity of JAK-STAT pathways in rheumatoid arthritis: constitutive activation of STAT3 correlates with interleukin 6 levels. *Rheumatology (Oxford),* 54**,** 1103-13.
JACOBS, S. R., HERMAN, C. E., MACIVER, N. J., WOFFORD, J. A., WIEMAN, H. L., HAMMEN, J. J. & RATHMELL, J. C. 2008. Glucose uptake is limiting in T cell activation and requires CD28-mediated Akt-dependent and independent pathways. *J Immunol,* 180**,** 4476-86.
JANSSON, A. 2011. Kinetic proofreading and the search for nonself-peptides. *Self/nonself,* 2**,** 1-3.
JOHN, S., WEISS, J. N. & RIBALET, B. 2011. Subcellular localization of hexokinases I and II directs the metabolic fate of glucose. *PLoS One,* 6**,** e17674.
JONES, S. A., RICHARDS, P. J., SCHELLER, J. & ROSE-JOHN, S. 2005. IL-6 transsignaling: the in vivo consequences. *J Interferon Cytokine Res,* 25**,** 241-53.
KAGAMI, S., RIZZO, H. L., LEE, J. J., KOGUCHI, Y. & BLAUVELT, A. 2010. Circulating Th17, Th22, and Th1 cells are increased in psoriasis. *The Journal of investigative dermatology,* 130**,** 1373-1383.
KAIKO, G. E., HORVAT, J. C., BEAGLEY, K. W. & HANSBRO, P. M. 2008. Immunological decision-making: how does the immune system decide to mount a helper T-cell response? *Immunology,* 123**,** 326-38.
KALIM, K. W., YANG, J.-Q., LI, Y., MENG, Y., ZHENG, Y. & GUO, F. 2018. Reciprocal Regulation of Glycolysis-Driven Th17 Pathogenicity and Regulatory T Cell Stability by Cdc42. *Journal of immunology (Baltimore, Md. : 1950),* 200**,** 2313-2326.
KANHERE, A., HERTWECK, A., BHATIA, U., GÖKMEN, M. R., PERUCHA, E., JACKSON, I., LORD, G. M. & JENNER, R. G. 2012. T-bet and GATA3 orchestrate Th1 and Th2 differentiation through lineage-specific targeting of distal regulatory elements. *Nature Communications,* 3**,** 1268.
KEREKES, G., NURMOHAMED, M. T., GONZÁLEZ-GAY, M. A., SERES, I., PARAGH, G., KARDOS, Z., BARÁTH, Z., TAMÁSI, L., SOLTÉSZ, P. & SZEKANECZ, Z. 2014. Rheumatoid arthritis and metabolic syndrome. *Nature reviews. Rheumatology,* 10**,** 691-696.
KIEPER, W. C., PRLIC, M., SCHMIDT, C. S., MESCHER, M. F. & JAMESON, S. C. 2001. IL-12 Enhances CD8 T Cell Homeostatic Expansion. *The Journal of Immunology,* 166**,** 5515.
KIM, H. H., THARAYIL, M. & RUDD, C. E. 1998. Growth factor receptor-bound protein 2 SH2/SH3 domain binding to CD28 and its role in co-signaling. *The Journal of biological chemistry,* 273**,** 296-301.

KIM, S., HWANG, J., XUAN, J., JUNG, Y. H., CHA, H.-S. & KIM, K. H. 2014. Global metabolite profiling of synovial fluid for the specific diagnosis of rheumatoid arthritis from other inflammatory arthritis. *PloS one,* 9**,** e97501-e97501.

KING, C., ILIC, A., KOELSCH, K. & SARVETNICK, N. 2004. Homeostatic Expansion of T Cells during Immune Insufficiency Generates Autoimmunity. *Cell,* 117**,** 265-277.

KING, P. D., SADRA, A., TENG, J. M., XIAO-RONG, L., HAN, A., SELVAKUMAR, A., AUGUST, A. & DUPONT, B. 1997. Analysis of CD28 cytoplasmic tail tyrosine residues as regulators and substrates for the protein tyrosine kinases, EMT and LCK. *J Immunol,* 158**,** 580-90.

KLEIN, L., KYEWSKI, B., ALLEN, P. M. & HOGQUIST, K. A. 2014. Positive and negative selection of the T cell repertoire: what thymocytes see (and don't see). *Nature reviews. Immunology,* 14**,** 377-391.

KLYSZ, D., TAI, X., ROBERT, P. A., CRAVEIRO, M., CRETENET, G., OBUROGLU, L., MONGELLAZ, C., FLOESS, S., FRITZ, V., MATIAS, M. I., YONG, C., SURH, N., MARIE, J. C., HUEHN, J., ZIMMERMANN, V., KINET, S., DARDALHON, V. & TAYLOR, N. 2015. Glutamine-dependent α-ketoglutarate production regulates the balance between T helper 1 cell and regulatory T cell generation. *Science Signaling,* 8**,** ra97.

KOGURE, K., YAMAMOTO, K., MAJIMA, E., SHINOHARA, Y., YAMASHITA, K. & TERADA, H. 1996. Alteration of enzyme function of the type II hexokinase C-terminal half on replacements of restricted regions by corresponding regions of glucokinase. *The Journal of biological chemistry,* 271**,** 15230-15236.

KOLEV, M., DIMELOE, S., LE FRIEC, G., NAVARINI, A., ARBORE, G., POVOLERI, GIOVANNI A., FISCHER, M., BELLE, R., LOELIGER, J., DEVELIOGLU, L., BANTUG, GLENN R., WATSON, J., COUZI, L., AFZALI, B., LAVENDER, P., HESS, C. & KEMPER, C. 2015. Complement Regulates Nutrient Influx and Metabolic Reprogramming during Th1 Cell Responses. *Immunity,* 42**,** 1033-1047.

KONO, M., YOSHIDA, N., MAEDA, K. & TSOKOS, G. C. 2018. Transcriptional factor ICER promotes glutaminolysis and the generation of Th17 cells. *Proceedings of the National Academy of Sciences of the United States of America,* 115**,** 2478-2483.

KOTAKE, S., UDAGAWA, N., TAKAHASHI, N., MATSUZAKI, K., ITOH, K., ISHIYAMA, S., SAITO, S., INOUE, K., KAMATANI, N., GILLESPIE, M. T., MARTIN, T. J. & SUDA, T. 1999. IL-17 in synovial fluids from patients with rheumatoid arthritis is a potent stimulator of osteoclastogenesis. *The Journal of clinical investigation,* 103**,** 1345-1352.

KROGSGAARD, M., JUANG, J. & DAVIS, M. M. A role for “self” in T-cell activation. Seminars in immunology, 2007. Elsevier, 236-244.

KUMAR, Y. N., KUMAR, P. S., SOWJENYA, G., RAO, V. K., YESWANTH, S., PRASAD, U. V., PRADEEPKIRAN, J. A., SARMA, P. & BHASKAR, M. 2012. Comparison and correlation of binding mode of ATP in the kinase domains of Hexokinase family. *Bioinformation,* 8**,** 543-7.

LAFFERTY, K. J., WARREN, H. S., WOOLNOUGH, J. A. & TALMAGE, D. W. 1978. Immunological induction of T lymphocytes: role of antigen and the lymphocyte costimulator. *Blood cells,* 4**,** 395-406.

LAURIDSEN, M. B., BLIDDAL, H., CHRISTENSEN, R., DANNESKIOLD-SAMSØE, B., BENNETT, R., KEUN, H., LINDON, J. C., NICHOLSON, J. K., DORFF, M. H., JAROSZEWSKI, J. W., HANSEN, S. H. & CORNETT, C. 2010. 1H NMR Spectroscopy-Based Interventional Metabolic Phenotyping: A Cohort Study of Rheumatoid Arthritis Patients. *Journal of Proteome Research,* 9**,** 4545-4553.

LEE, K., GUDAPATI, P., DRAGOVIC, S., SPENCER, C., JOYCE, S., KILLEEN, N., MAGNUSON, M. A. & BOOTHBY, M. 2010. Mammalian target of rapamycin protein complex 2 regulates differentiation of Th1 and Th2 cell subsets via distinct signaling pathways. *Immunity,* 32**,** 743-753.

LEONE, R. D., ZHAO, L., ENGLERT, J. M., SUN, I.-M., OH, M.-H., SUN, I.-H., ARWOOD, M. L., BETTENCOURT, I. A., PATEL, C. H., WEN, J., TAM, A., BLOSSER, R. L., PRCHALOVA, E., ALT, J., RAIS, R., SLUSHER, B. S. & POWELL, J. D. 2019. Glutamine blockade induces divergent metabolic programs to overcome tumor immune evasion. *Science,* 366**,** 1013.

LINKE, M., FRITSCH, S. D., SUKHBAATAR, N., HENGSTSCHLÄGER, M. & WEICHHART, T. 2017. mTORC1 and mTORC2 as regulators of cell metabolism in immunity. *FEBS Letters,* 591**,** 3089-3103.

LITTLEWOOD-EVANS, A., SARRET, S., APFEL, V., LOESLE, P., DAWSON, J., ZHANG, J., MULLER, A., TIGANI, B., KNEUER, R., PATEL, S., VALEAUX, S., GOMMERMANN, N., RUBIC-SCHNEIDER, T., JUNT, T. & CARBALLIDO, J. M. 2016. GPR91 senses extracellular succinate released from inflammatory macrophages and exacerbates rheumatoid arthritis. *The Journal of experimental medicine,* 213**,** 1655-1662.

LJUNG, L. & RANTAPAA-DAHLQVIST, S. 2016. Abdominal obesity, gender and the risk of rheumatoid arthritis - a nested case-control study. *Arthritis Res Ther,* 18**,** 277.

LOFFREDA, S., YANG, S. Q., LIN, H. Z., KARP, C. L., BRENGMAN, M. L., WANG, D. J., KLEIN, A. S., BULKLEY, G. B., BAO, C., NOBLE, P. W., LANE, M. D. & DIEHL, A. M. 1998. Leptin regulates proinflammatory immune responses. *FASEB J,* 12**,** 57-65.

LOWRY, O. H. & PASSONNEAU, J. V. 1966. Kinetic evidence for multiple binding sites on phosphofructokinase. *J Biol Chem,* 241**,** 2268-79.

LUNDBERG, K., NIJENHUIS, S., VOSSENAAR, E. R., PALMBLAD, K., VAN VENROOIJ, W. J., KLARESKOG, L., ZENDMAN, A. J. W. & HARRIS, H. E. 2005. Citrullinated proteins have increased immunogenicity and arthritogenicity and their presence in arthritic joints correlates with disease severity. *Arthritis research & therapy,* 7**,** R458-R467.

MACDONALD, H. R. 1977. Energy metabolism and T-cell-mediated cytolysis. II. Selective inhibition of cytolysis by 2-deoxy-D-glucose. *The Journal of experimental medicine,* 146**,** 710-719.

MACGREGOR, A. J., SNIEDER, H., RIGBY, A. S., KOSKENVUO, M., KAPRIO, J., AHO, K. & SILMAN, A. J. 2000. Characterizing the quantitative genetic contribution to rheumatoid arthritis using data from twins. *Arthritis and rheumatism,* 43**,** 30-37.

MACKALL, C. L., HAKIM, F. T. & GRESS, R. E. 1997. Restoration of T-cell homeostasis after T-cell depletion. *Semin Immunol,* 9**,** 339-46.

MADHOK, R., CRILLY, A., WATSON, J. & CAPELL, H. A. 1993. Serum interleukin 6 levels in rheumatoid arthritis: correlations with clinical and laboratory indices of disease activity. *Ann Rheum Dis,* 52**,** 232-4.

MAGGIO, M., GURALNIK, J. M., LONGO, D. L. & FERRUCCI, L. 2006. Interleukin-6 in aging and chronic disease: a magnificent pathway. *The journals of gerontology. Series A, Biological sciences and medical sciences,* 61**,** 575-584.

MAGRAM, J., CONNAUGHTON, S. E., WARRIER, R. R., CARVAJAL, D. M., WU, C. Y., FERRANTE, J., STEWART, C., SARMIENTO, U., FAHERTY, D. A. & GATELY, M. K. 1996. IL-12-deficient mice are defective in IFN gamma production and type 1 cytokine responses. *Immunity,* 4**,** 471-481.

MAILE, R., BARNES, C. M., NIELSEN, A. I., MEYER, A. A., FRELINGER, J. A. & CAIRNS, B. A. 2006a. Lymphopenia-Induced Homeostatic Proliferation of CD8⁺ T Cells Is a Mechanism for Effective Allogeneic Skin Graft Rejection following Burn Injury. *The Journal of Immunology,* 176**,** 6717.

MAILE, R., BARNES, C. M., NIELSEN, A. I., MEYER, A. A., FRELINGER, J. A. & CAIRNS, B. A. 2006b. Lymphopenia-induced homeostatic proliferation of CD8+ T cells is a mechanism for effective allogeneic skin graft rejection following burn injury. *The Journal of Immunology,* 176**,** 6717.

MAINI, R. N. & FELDMANN, M. 2002. How does infliximab work in rheumatoid arthritis? *Arthritis research,* 4 Suppl 2**,** S22-S28.

MALEK, T. R., YU, A., VINCEK, V., SCIBELLI, P. & KONG, L. 2002. CD4 regulatory T cells prevent lethal autoimmunity in IL-2Rbeta-deficient mice. Implications for the nonredundant function of IL-2. *Immunity,* 17**,** 167-178.

MANGAN, P. R., HARRINGTON, L. E., O'QUINN, D. B., HELMS, W. S., BULLARD, D. C., ELSON, C. O., HATTON, R. D., WAHL, S. M., SCHOEB, T. R. & WEAVER, C. T. 2006. Transforming growth factor-beta induces development of the T(H)17 lineage. *Nature,* 441**,** 231-234.

MARTÍNEZ-REYES, I. & CHANDEL, N. S. 2020. Mitochondrial TCA cycle metabolites control physiology and disease. *Nature Communications,* 11**,** 102.

MASSA, M. L., GAGLIARDINO, J. J. & FRANCINI, F. 2011. Liver glucokinase: An overview on the regulatory mechanisms of its activity. *IUBMB life,* 63**,** 1-6.

MASUI, K., TANAKA, K., AKHAVAN, D., BABIC, I., GINI, B., MATSUTANI, T., IWANAMI, A., LIU, F., VILLA, G. R., GU, Y., CAMPOS, C., ZHU, S., YANG, H., YONG, W. H., CLOUGHESY, T. F., MELLINGHOFF, I. K., CAVENEE, W. K., SHAW, R. J. & MISCHEL, P. S. 2013. mTOR complex 2 controls glycolytic metabolism in glioblastoma through FoxO acetylation and upregulation of c-Myc. *Cell metabolism,* 18**,** 726-739.

MCGUIRE, K. L. & IACOBELLI, M. 1997. Involvement of Rel, Fos, and Jun proteins in binding activity to the IL-2 promoter CD28 response element/AP-1 sequence in human T cells. *J Immunol,* 159**,** 1319-27.

MCINNES, I. B., LEUNG, B. P., STURROCK, R. D., FIELD, M. & LIEW, F. Y. 1997. Interleukin-15 mediates T cell-dependent regulation of tumor necrosis factor-alpha production in rheumatoid arthritis. *Nature medicine,* 3**,** 189-195.

MCINTYRE, K. W., SHUSTER, D. J., GILLOOLY, K. M., WARRIER, R. R., CONNAUGHTON, S. E., HALL, L. B., ARP, L. H., GATELY, M. K. & MAGRAM, J. 1996. Reduced incidence and severity of collagen-induced arthritis in interleukin-12-deficient mice. *European journal of immunology,* 26**,** 2933-2938.

MCKAY, R. T. 2011. How the 1D-NOESY suppresses solvent signal in metabonomics NMR spectroscopy: An examination of the pulse sequence components and evolution. *Concepts in Magnetic Resonance Part A,* 38A**,** 197-220.

MCKEITHAN, T. W. 1995. Kinetic proofreading in T-cell receptor signal transduction. *Proceedings of the National Academy of Sciences of the United States of America,* 92**,** 5042-5046.

MEDAWAR, P. B. 1948. Immunity to homologous grafted skin; the fate of skin homografts transplanted to the brain, to subcutaneous tissue, and to the anterior chamber of the eye. *British journal of experimental pathology,* 29**,** 58-69.

MEDINA, G., VERA-LASTRA, O., PERALTA-AMARO, A. L., JIMÉNEZ-ARELLANO, M. P., SAAVEDRA, M. A., CRUZ-DOMÍNGUEZ, M. P. & JARA, L. J. 2018.

Metabolic syndrome, autoimmunity and rheumatic diseases. *Pharmacological Research,* 133**,** 277-288.
MELSHEIMER, R., GELDHOF, A., APAOLAZA, I. & SCHAIBLE, T. 2019. Remicade(®) (infliximab): 20 years of contributions to science and medicine. *Biologics : targets & therapy,* 13**,** 139-178.
MICHALEK, R. D., GERRIETS, V. A., JACOBS, S. R., MACINTYRE, A. N., MACIVER, N. J., MASON, E. F., SULLIVAN, S. A., NICHOLS, A. G. & RATHMELL, J. C. 2011. Cutting edge: distinct glycolytic and lipid oxidative metabolic programs are essential for effector and regulatory CD4+ T cell subsets. *Journal of immunology (Baltimore, Md. : 1950),* 186**,** 3299-3303.
MIELIAUSKAITE, D., VENALIS, P., DUMALAKIENE, I., VENALIS, A. & DISTLER, J. 2009. Relationship between serum levels of TGF-beta1 and clinical parameters in patients with rheumatoid arthritis and Sjogren's syndrome secondary to rheumatoid arthritis. *Autoimmunity,* 42**,** 356-8.
MILLER, D. M., THOMAS, S. D., ISLAM, A., MUENCH, D. & SEDORIS, K. 2012. c-Myc and cancer metabolism. *Clinical cancer research : an official journal of the American Association for Cancer Research,* 18**,** 5546-5553.
MILLS, E. L., RYAN, D. G., PRAG, H. A., DIKOVSKAYA, D., MENON, D., ZASLONA, Z., JEDRYCHOWSKI, M. P., COSTA, A. S. H., HIGGINS, M., HAMS, E., SZPYT, J., RUNTSCH, M. C., KING, M. S., MCGOURAN, J. F., FISCHER, R., KESSLER, B. M., MCGETTRICK, A. F., HUGHES, M. M., CARROLL, R. G., BOOTY, L. M., KNATKO, E. V., MEAKIN, P. J., ASHFORD, M. L. J., MODIS, L. K., BRUNORI, G., SEVIN, D. C., FALLON, P. G., CALDWELL, S. T., KUNJI, E. R. S., CHOUCHANI, E. T., FREZZA, C., DINKOVA-KOSTOVA, A. T., HARTLEY, R. C., MURPHY, M. P. & O'NEILL, L. A. 2018. Itaconate is an anti-inflammatory metabolite that activates Nrf2 via alkylation of KEAP1. *Nature,* 556**,** 113-117.
MILNER, J. D., FAZILLEAU, N., MCHEYZER-WILLIAMS, M. & PAUL, W. 2010. Cutting edge: lack of high affinity competition for peptide in polyclonal CD4+ responses unmasks IL-4 production. *Journal of immunology (Baltimore, Md. : 1950),* 184**,** 6569-6573.
MIRSHAFIEY, A., SIMHAG, A., EL ROUBY, N. M. M. & AZIZI, G. 2015. T-helper 22 cells as a new player in chronic inflammatory skin disorders. *International journal of dermatology,* 54**,** 880-888.
MIYAZAKI, Y., NAKAYAMADA, S., KUBO, S., NAKANO, K., IWATA, S., MIYAGAWA, I., MA, X., TRIMOVA, G., SAKATA, K. & TANAKA, Y. 2018. Th22 Cells Promote Osteoclast Differentiation via Production of IL-22 in Rheumatoid Arthritis. *Frontiers in immunology,* 9**,** 2901-2901.
MORI, T., MURASAWA, Y., IKAI, R., HAYAKAWA, T., NAKAMURA, H., OGISO, N., NIIDA, S. & WATANABE, K. 2016. Generation of a transgenic mouse line for conditional expression of human IL-6. *Experimental animals,* 65**,** 455-463.
MOURAD, J. & MONEM, F. 2013. HLA-DRB1 allele association with rheumatoid arthritis susceptibility and severity in Syria. *Revista Brasileira de Reumatologia (English Edition),* 53**,** 47-56.
MOXHAM, V. F., KAREGLI, J., PHILLIPS, R. E., BROWN, K. L., TAPMEIER, T. T., HANGARTNER, R., SACKS, S. H. & WONG, W. 2008. Homeostatic Proliferation of Lymphocytes Results in Augmented Memory-Like Function and Accelerated Allograft Rejection. *The Journal of Immunology,* 180**,** 3910.
MUDTER, J., AMOUSSINA, L., SCHENK, M., YU, J., BRÜSTLE, A., WEIGMANN, B., ATREYA, R., WIRTZ, S., BECKER, C., HOFFMAN, A., ATREYA, I., BIESTERFELD, S., GALLE, P. R., LEHR, H. A., ROSE-JOHN, S., MUELLER, C., LOHOFF, M. & NEURATH, M. F. 2008. The transcription factor IFN

regulatory factor-4 controls experimental colitis in mice via T cell-derived IL-6. *The Journal of clinical investigation,* 118**,** 2415-2426.
MUFAZALOV, I., BRANDFALD, M., SCHELMBAUER, C., ANDRUSZEWSKI, D., TANG, Y., MASRI, J., KARBACH, S., EICH, C., WUNDERLICH, T., KORN, T., BLUESTONE, J. & WAISMAN, A. 2019. IL-6 overexpression triggers inflammation through its only relevant receptor IL-6R. *The Journal of Immunology,* 202**,** 181.4.
MULLBERG, J., DITTRICH, E., GRAEVE, L., GERHARTZ, C., YASUKAWA, K., TAGA, T., KISHIMOTO, T., HEINRICH, P. C. & ROSE-JOHN, S. 1993. Differential shedding of the two subunits of the interleukin-6 receptor. *FEBS Lett,* 332**,** 174-8.
MÜLLBERG, J., SCHOOLTINK, H., STOYAN, T., GÜNTHER, M., GRAEVE, L., BUSE, G., MACKIEWICZ, A., HEINRICH, P. C. & ROSE-JOHN, S. 1993. The soluble interleukin-6 receptor is generated by shedding. *European journal of immunology,* 23**,** 473-480.
MURAOKA, S., KUSUNOKI, N., TAKAHASHI, H., TSUCHIYA, K. & KAWAI, S. 2013. Leptin stimulates interleukin-6 production via janus kinase 2/signal transducer and activator of transcription 3 in rheumatoid synovial fibroblasts. *Clin Exp Rheumatol,* 31**,** 589-95.
MURPHY, C. A., LANGRISH, C. L., CHEN, Y., BLUMENSCHEIN, W., MCCLANAHAN, T., KASTELEIN, R. A., SEDGWICK, J. D. & CUA, D. J. 2003. Divergent pro- and antiinflammatory roles for IL-23 and IL-12 in joint autoimmune inflammation. *The Journal of experimental medicine,* 198**,** 1951-1957.
MURPHY, K. M. & REINER, S. L. 2002. The lineage decisions of helper T cells. *Nat Rev Immunol,* 2**,** 933-44.
NAKAE, S., SAIJO, S., HORAI, R., SUDO, K., MORI, S. & IWAKURA, Y. 2003. IL-17 production from activated T cells is required for the spontaneous development of destructive arthritis in mice deficient in IL-1 receptor antagonist. *Proc Natl Acad Sci U S A,* 100**,** 5986-90.
NAKAYA, M., XIAO, Y., ZHOU, X., CHANG, J.-H., CHANG, M., CHENG, X., BLONSKA, M., LIN, X. & SUN, S.-C. 2014. Inflammatory T cell responses rely on amino acid transporter ASCT2 facilitation of glutamine uptake and mTORC1 kinase activation. *Immunity,* 40**,** 692-705.
NEWTON, J. L., HARNEY, S. M. J., WORDSWORTH, B. P. & BROWN, M. A. 2004. A review of the MHC genetics of rheumatoid arthritis. *Genes and immunity,* 5**,** 151-157.
NICKLIN, P., BERGMAN, P., ZHANG, B., TRIANTAFELLOW, E., WANG, H., NYFELER, B., YANG, H., HILD, M., KUNG, C., WILSON, C., MYER, V. E., MACKEIGAN, J. P., PORTER, J. A., WANG, Y. K., CANTLEY, L. C., FINAN, P. M. & MURPHY, L. O. 2009. Bidirectional transport of amino acids regulates mTOR and autophagy. *Cell,* 136**,** 521-534.
NIE, H., ZHENG, Y., LI, R., GUO, T. B., HE, D., FANG, L., LIU, X., XIAO, L., CHEN, X., WAN, B., CHIN, Y. E. & ZHANG, J. Z. 2013. Phosphorylation of FOXP3 controls regulatory T cell function and is inhibited by TNF-α in rheumatoid arthritis. *Nature Medicine,* 19**,** 322-328.
NISH, S. A., SCHENTEN, D., WUNDERLICH, F. T., POPE, S. D., GAO, Y., HOSHI, N., YU, S., YAN, X., LEE, H. K., PASMAN, L., BRODSKY, I., YORDY, B., ZHAO, H., BRÜNING, J. & MEDZHITOV, R. 2014. T cell-intrinsic role of IL-6 signaling in primary and memory responses. *eLife,* 3**,** e01949-e01949.
NISTALA, K., ADAMS, S., CAMBROOK, H., URSU, S., OLIVITO, B., DE JAGER, W., EVANS, J. G., CIMAZ, R., BAJAJ-ELLIOTT, M. & WEDDERBURN, L. R.

2010. Th17 plasticity in human autoimmune arthritis is driven by the inflammatory environment. *Proceedings of the National Academy of Sciences of the United States of America,* 107**,** 14751-14756.
NOFAL, M., ZHANG, K., HAN, S. & RABINOWITZ, J. D. 2017. mTOR Inhibition Restores Amino Acid Balance in Cells Dependent on Catabolism of Extracellular Protein. *Molecular cell,* 67**,** 936-946.e5.
NONNENMACHER, Y. & HILLER, K. 2018. Biochemistry of proinflammatory macrophage activation. *Cell Mol Life Sci,* 75**,** 2093-2109.
OKANO, T., SAEGUSA, J., TAKAHASHI, S., UEDA, Y. & MORINOBU, A. 2018. Immunometabolism in rheumatoid arthritis. *Immunological Medicine,* 41**,** 89-97.
OMILUSIK, K. D. & GOLDRATH, A. W. 2017. The origins of memory T cells. *Nature,* 552**,** 337-339.
OUYANG, W., RANGANATH, S. H., WEINDEL, K., BHATTACHARYA, D., MURPHY, T. L., SHA, W. C. & MURPHY, K. M. 1998. Inhibition of Th1 development mediated by GATA-3 through an IL-4-independent mechanism. *Immunity,* 9**,** 745-755.
PAGÈS, F., RAGUENEAU, M., ROTTAPEL, R., TRUNEH, A., NUNES, J., IMBERT, J. & OLIVE, D. 1994. Binding of phosphatidylinositol-3-OH kinase to CD28 is required for T-cell signalling. *Nature,* 369**,** 327-329.
PAI, S.-Y., TRUITT, M. L. & HO, I. C. 2004. GATA-3 deficiency abrogates the development and maintenance of T helper type 2 cells. *Proceedings of the National Academy of Sciences of the United States of America,* 101**,** 1993-1998.
PALMER, D. C. & RESTIFO, N. P. 2009. Suppressors of cytokine signaling (SOCS) in T cell differentiation, maturation, and function. *Trends in immunology,* 30**,** 592-602.
PARRA-SALCEDO, F., CONTRERAS-YANEZ, I., ELIAS-LOPEZ, D., AGUILAR-SALINAS, C. A. & PASCUAL-RAMOS, V. 2015. Prevalence, incidence and characteristics of the metabolic syndrome (MetS) in a cohort of Mexican Mestizo early rheumatoid arthritis patients treated with conventional disease modifying anti-rheumatic drugs: the complex relationship between MetS and disease activity. *Arthritis Res Ther,* 17**,** 34.
PEDERSEN, M., JACOBSEN, S., GARRED, P., MADSEN, H. O., KLARLUND, M., SVEJGAARD, A., PEDERSEN, B. V., WOHLFAHRT, J. & FRISCH, M. 2007. Strong combined gene-environment effects in anti-cyclic citrullinated peptide-positive rheumatoid arthritis: a nationwide case-control study in Denmark. *Arthritis and rheumatism,* 56**,** 1446-1453.
PENG, M., YIN, N., CHHANGAWALA, S., XU, K., LESLIE, C. S. & LI, M. O. 2016. Aerobic glycolysis promotes T helper 1 cell differentiation through an epigenetic mechanism. *Science (New York, N.Y.),* 354**,** 481-484.
PESCE, B., SOTO, L., SABUGO, F., WURMANN, P., CUCHACOVICH, M., LOPEZ, M. N., SOTELO, P. H., MOLINA, M. C., AGUILLON, J. C. & CATALAN, D. 2013. Effect of interleukin-6 receptor blockade on the balance between regulatory T cells and T helper type 17 cells in rheumatoid arthritis patients. *Clin Exp Immunol,* 171**,** 237-42.
PICARD, C., VON BERNUTH, H., GHANDIL, P., CHRABIEH, M., LEVY, O., ARKWRIGHT, P. D., MCDONALD, D., GEHA, R. S., TAKADA, H., KRAUSE, J. C., CREECH, C. B., KU, C.-L., EHL, S., MARÓDI, L., AL-MUHSEN, S., AL-HAJJAR, S., AL-GHONAIUM, A., DAY-GOOD, N. K., HOLLAND, S. M., GALLIN, J. I., CHAPEL, H., SPEERT, D. P., RODRIGUEZ-GALLEGO, C., COLINO, E., GARTY, B.-Z., ROIFMAN, C., HARA, T., YOSHIKAWA, H.,

NONOYAMA, S., DOMACHOWSKE, J., ISSEKUTZ, A. C., TANG, M., SMART, J., ZITNIK, S. E., HOARAU, C., KUMARARATNE, D. S., THRASHER, A. J., DAVIES, E. G., BETHUNE, C., SIRVENT, N., DE RICAUD, D., CAMCIOGLU, Y., VASCONCELOS, J., GUEDES, M., VITOR, A. B., RODRIGO, C., ALMAZÁN, F., MÉNDEZ, M., ARÓSTEGUI, J. I., ALSINA, L., FORTUNY, C., REICHENBACH, J., VERBSKY, J. W., BOSSUYT, X., DOFFINGER, R., ABEL, L., PUEL, A. & CASANOVA, J.-L. 2010. Clinical features and outcome of patients with IRAK-4 and MyD88 deficiency. *Medicine,* 89**,** 403-425.

PITZALIS, C., KELLY, S. & HUMBY, F. 2013. New learnings on the pathophysiology of RA from synovial biopsies. *Curr Opin Rheumatol,* 25**,** 334-44.

POGGIOLI, G., LAURETI, S., CAMPIERI, M., PIERANGELI, F., GIONCHETTI, P., UGOLINI, F., GENTILINI, L., BAZZI, P., RIZZELLO, F. & COSCIA, M. 2007. Infliximab in the treatment of Crohn's disease. *Therapeutics and clinical risk management,* 3**,** 301-308.

PRASAD, K. V., CAI, Y. C., RAAB, M., DUCKWORTH, B., CANTLEY, L., SHOELSON, S. E. & RUDD, C. E. 1994. T-cell antigen CD28 interacts with the lipid kinase phosphatidylinositol 3-kinase by a cytoplasmic Tyr(P)-Met-Xaa-Met motif. *Proceedings of the National Academy of Sciences of the United States of America,* 91**,** 2834-2838.

PRATT, A. G., SWAN, D. C., RICHARDSON, S., WILSON, G., HILKENS, C. M., YOUNG, D. A. & ISAACS, J. D. 2012. A CD4 T cell gene signature for early rheumatoid arthritis implicates interleukin 6-mediated STAT3 signalling, particularly in anti-citrullinated peptide antibody-negative disease. *Ann Rheum Dis,* 71**,** 1374-81.

PUCINO, V., CERTO, M., BULUSU, V., CUCCHI, D., GOLDMANN, K., PONTARINI, E., HAAS, R., SMITH, J., HEADLAND, S. E., BLIGHE, K., RUSCICA, M., HUMBY, F., LEWIS, M. J., KAMPHORST, J. J., BOMBARDIERI, M., PITZALIS, C. & MAURO, C. 2019. Lactate Buildup at the Site of Chronic Inflammation Promotes Disease by Inducing CD4+ T Cell Metabolic Rewiring. *Cell Metabolism,* 30**,** 1055-1074.e8.

PURICH, D. L. & FROMM, H. J. 1971. The kinetics and regulation of rat brain hexokinase. *J Biol Chem,* 246**,** 3456-63.

PY, B., SLOMIANNY, C., AUBERGER, P., PETIT, P. X. & BENICHOU, S. 2004. Siva-1 and an Alternative Splice Form Lacking the Death Domain, Siva-2, Similarly Induce Apoptosis in T Lymphocytes via a Caspase-Dependent Mitochondrial Pathway. *The Journal of Immunology,* 172**,** 4008.

RAAB, M., CAI, Y. C., BUNNELL, S. C., HEYECK, S. D., BERG, L. J. & RUDD, C. E. 1995. p56Lck and p59Fyn regulate CD28 binding to phosphatidylinositol 3-kinase, growth factor receptor-bound protein GRB-2, and T cell-specific protein-tyrosine kinase ITK: implications for T-cell costimulation. *Proceedings of the National Academy of Sciences of the United States of America,* 92**,** 8891-8895.

RAHMAN, P., INMAN, R. D., EL-GABALAWY, H. & KRAUSE, D. O. 2010. Pathophysiology and pathogenesis of immune-mediated inflammatory diseases: commonalities and differences. *The Journal of rheumatology. Supplement,* 85**,** 11-26.

RAMANA, C. V., GIL, M. P., SCHREIBER, R. D. & STARK, G. R. 2002. Stat1-dependent and -independent pathways in IFN-gamma-dependent signaling. *Trends in immunology,* 23**,** 96-101.

RAPOSO, B., MERKY, P., LUNDQVIST, C., YAMADA, H., URBONAVICIUTE, V., NIAUDET, C., VILJANEN, J., KIHLBERG, J., KYEWSKI, B., EKWALL, O.,

HOLMDAHL, R. & BÄCKLUND, J. 2018. T cells specific for post-translational modifications escape intrathymic tolerance induction. *Nature communications,* 9**,** 353-353.
RATH, M., MÜLLER, I., KROPF, P., CLOSS, E. I. & MUNDER, M. 2014. Metabolism via Arginase or Nitric Oxide Synthase: Two Competing Arginine Pathways in Macrophages. *Frontiers in immunology,* 5**,** 532-532.
RAY, A. 2000. A SAF Binding Site in the Promoter Region of Human γ-Fibrinogen Gene Functions as an IL-6 Response Element. *The Journal of Immunology,* 165**,** 3411-3417.
RAZA, K., FALCIANI, F., CURNOW, S. J., ROSS, E. J., LEE, C.-Y., AKBAR, A. N., LORD, J. M., GORDON, C., BUCKLEY, C. D. & SALMON, M. 2005. Early rheumatoid arthritis is characterized by a distinct and transient synovial fluid cytokine profile of T cell and stromal cell origin. *Arthritis research & therapy,* 7**,** R784-R795.
REIS, B. S., LEE, K., FANOK, M. H., MASCARAQUE, C., AMOURY, M., COHN, L. B., ROGOZ, A., DALLNER, O. S., MORAES-VIEIRA, P. M., DOMINGOS, A. I. & MUCIDA, D. 2015. Leptin receptor signaling in T cells is required for Th17 differentiation. *Journal of immunology (Baltimore, Md. : 1950),* 194**,** 5253-5260.
RIDGLEY, L., ANDERSON, A., SKELTON, A., YOUNG, D., ISAACS, J., CARMODY, R. & PRATT, A. 2017. 08.13 Understanding aberrant il-6 mediated cd4+ t-cell signalling in early rheumatoid arthritis. *Annals of the Rheumatic Diseases,* 76**,** A80-A80.
RIDGLEY, L. A., ANDERSON, A. E., MANEY, N. J., NAAMANE, N., SKELTON, A. J., LAWSON, C. A., EMERY, P., ISAACS, J. D., CARMODY, R. J. & PRATT, A. G. 2019. IL-6 Mediated Transcriptional Programming of Naïve CD4+ T Cells in Early Rheumatoid Arthritis Drives Dysregulated Effector Function. *Frontiers in immunology,* 10**,** 1535-1535.
RODRIGUEZ, P. C., QUICENO, D. G. & OCHOA, A. C. 2007. L-arginine availability regulates T-lymphocyte cell-cycle progression. *Blood,* 109**,** 1568-1573.
ROEF, M. J., DE MEER, K., KALHAN, S. C., STRAVER, H., BERGER, R. & REIJNGOUD, D.-J. 2003. Gluconeogenesis in humans with induced hyperlactatemia during low-intensity exercise. *American journal of physiology. Endocrinology and metabolism,* 284**,** E1162-E1171.
ROSE, N. R. & WITEBSKY, E. 1956. Studies on organ specificity. V. Changes in the thyroid glands of rabbits following active immunization with rabbit thyroid extracts. *Journal of immunology (Baltimore, Md. : 1950),* 76**,** 417-427.
ROSENBLUM, M. D., REMEDIOS, K. A. & ABBAS, A. K. 2015. Mechanisms of human autoimmunity. *J Clin Invest,* 125**,** 2228-33.
ROZOVSKY, S. & MCDERMOTT, A. E. 2007. Substrate product equilibrium on a reversible enzyme, triosephosphate isomerase. *Proceedings of the National Academy of Sciences,* 104**,** 2080.
RRRR.IO. 2019. *PatternHunter: Pattern hunter*
In flajole/MApckg: R package of MetaboAnalyst functions [Online]. Available: https://rdrr.io/github/flajole/MApckg/man/PatternHunter.html [Accessed].
RUBIC, T., LAMETSCHWANDTNER, G., JOST, S., HINTEREGGER, S., KUND, J., CARBALLIDO-PERRIG, N., SCHWÄRZLER, C., JUNT, T., VOSHOL, H., MEINGASSNER, J. G., MAO, X., WERNER, G., ROT, A. & CARBALLIDO, J. M. 2008. Triggering the succinate receptor GPR91 on dendritic cells enhances immunity. *Nature immunology,* 9**,** 1261-1269.
RUDAN, I., SIDHU, S., PAPANA, A., MENG, S.-J., XIN-WEI, Y., WANG, W., CAMPBELL-PAGE, R. M., DEMAIO, A. R., NAIR, H., SRIDHAR, D.,

THEODORATOU, E., DOWMAN, B., ADELOYE, D., MAJEED, A., CAR, J., CAMPBELL, H., CHAN, K. Y. & GLOBAL HEALTH EPIDEMIOLOGY REFERENCE, G. 2015. Prevalence of rheumatoid arthritis in low- and middle-income countries: A systematic review and analysis. *Journal of global health,* 5**,** 010409-010409.

RYAN, D. G., MURPHY, M. P., FREZZA, C., PRAG, H. A., CHOUCHANI, E. T., O'NEILL, L. A. & MILLS, E. L. 2019. Coupling Krebs cycle metabolites to signalling in immunity and cancer. *Nature Metabolism,* 1**,** 16-33.

SACK, U., KINNE, R. W., MARX, T., HEPPT, P., BENDER, S. & EMMRICH, F. 1993. Interleukin-6 in synovial fluid is closely associated with chronic synovitis in rheumatoid arthritis. *Rheumatol Int,* 13**,** 45-51.

SAKAGUCHI, N., TAKAHASHI, T., HATA, H., NOMURA, T., TAGAMI, T., YAMAZAKI, S., SAKIHAMA, T., MATSUTANI, T., NEGISHI, I., NAKATSURU, S. & SAKAGUCHI, S. 2003. Altered thymic T-cell selection due to a mutation of the ZAP-70 gene causes autoimmune arthritis in mice. *Nature,* 426**,** 454-460.

SALMON, M., SCHEEL-TOELLNER, D., HUISSOON, A. P., PILLING, D., SHAMSADEEN, N., HYDE, H., D'ANGEAC, A. D., BACON, P. A., EMERY, P. & AKBAR, A. N. 1997. Inhibition of T cell apoptosis in the rheumatoid synovium. *The Journal of clinical investigation,* 99**,** 439-446.

SALMOND, R. J. 2018. mTOR Regulation of Glycolytic Metabolism in T Cells. *Frontiers in cell and developmental biology,* 6**,** 122-122.

SARAIVA, A. L., VERAS, F. P., PERES, R. S., TALBOT, J., DE LIMA, K. A., LUIZ, J. P., CARBALLIDO, J. M., CUNHA, T. M., CUNHA, F. Q., RYFFEL, B. & ALVES-FILHO, J. C. 2018. Succinate receptor deficiency attenuates arthritis by reducing dendritic cell traffic and expansion of T(h)17 cells in the lymph nodes. *FASEB journal : official publication of the Federation of American Societies for Experimental Biology***,** fj201800285-fj201800285.

SCHUMACHER, N., MEYER, D., MAUERMANN, A., VON DER HEYDE, J., WOLF, J., SCHWARZ, J., KNITTLER, K., MURPHY, G., MICHALEK, M., GARBERS, C., BARTSCH, J. W., GUO, S., SCHACHER, B., EICKHOLZ, P., CHALARIS, A., ROSE-JOHN, S. & RABE, B. 2015. Shedding of Endogenous Interleukin-6 Receptor (IL-6R) Is Governed by A Disintegrin and Metalloproteinase (ADAM) Proteases while a Full-length IL-6R Isoform Localizes to Circulating Microvesicles. *J Biol Chem,* 290**,** 26059-71.

SCOTT, L. J. 2017. Tocilizumab: A Review in Rheumatoid Arthritis. *Drugs,* 77**,** 1865-1879.

SEBBAG, M., PARRY, S. L., BRENNAN, F. M. & FELDMANN, M. 1997. Cytokine stimulation of T lymphocytes regulates their capacity to induce monocyte production of tumor necrosis factor-alpha, but not interleukin-10: possible relevance to pathophysiology of rheumatoid arthritis. *Eur J Immunol,* 27**,** 624-32.

SECKINGER, P., MILILI, M., SCHIFF, C. & FOUGEREAU, M. 1994. Interleukin-7 regulates c-myc expression in murine T cells and thymocytes: a role for tyrosine kinase(s) and calcium mobilization. *Eur J Immunol,* 24**,** 716-22.

SEKI, N., MIYAZAKI, M., SUZUKI, W., HAYASHI, K., ARIMA, K., MYBURGH, E., IZUHARA, K., BROMBACHER, F. & KUBO, M. 2004. IL-4-induced GATA-3 expression is a time-restricted instruction switch for Th2 cell differentiation. *Journal of immunology (Baltimore, Md. : 1950),* 172**,** 6158-6166.

SHAPIRO, V. S., MOLLENAUER, M. N. & WEISS, A. 1998. Cutting Edge: Nuclear Factor of Activated T Cells and AP-1 Are Insufficient for IL-2 Promoter

Activation: Requirement for CD28 Up-Regulation of RE/AP. *The Journal of Immunology,* 161**,** 6455.
SHAPIRO, V. S., TRUITT, K. E., IMBODEN, J. B. & WEISS, A. 1997. CD28 mediates transcriptional upregulation of the interleukin-2 (IL-2) promoter through a composite element containing the CD28RE and NF-IL-2B AP-1 sites. *Molecular and cellular biology,* 17**,** 4051-4058.
SHAW, M., COLLINS, B. F., HO, L. A. & RAGHU, G. 2015. Rheumatoid arthritis-associated lung disease. *Eur Respir Rev,* 24**,** 1-16.
SIGGS, O. M., MIOSGE, L. A., YATES, A. L., KUCHARSKA, E. M., SHEAHAN, D., BRDICKA, T., WEISS, A., LISTON, A. & GOODNOW, C. C. 2007. Opposing functions of the T cell receptor kinase ZAP-70 in immunity and tolerance differentially titrate in response to nucleotide substitutions. *Immunity,* 27**,** 912-926.
SILMAN, A. J., MACGREGOR, A. J., THOMSON, W., HOLLIGAN, S., CARTHY, D., FARHAN, A. & OLLIER, W. E. 1993. Twin concordance rates for rheumatoid arthritis: results from a nationwide study. *Br J Rheumatol,* 32**,** 903-7.
SILSWAL, N., SINGH, A. K., ARUNA, B., MUKHOPADHYAY, S., GHOSH, S. & EHTESHAM, N. Z. 2005. Human resistin stimulates the pro-inflammatory cytokines TNF-alpha and IL-12 in macrophages by NF-kappaB-dependent pathway. *Biochemical and biophysical research communications,* 334**,** 1092-1101.
SINCLAIR, L. V., ROLF, J., EMSLIE, E., SHI, Y.-B., TAYLOR, P. M. & CANTRELL, D. A. 2013. Control of amino-acid transport by antigen receptors coordinates the metabolic reprogramming essential for T cell differentiation. *Nature immunology,* 14**,** 500-508.
SNIR, O., WIDHE, M., VON SPEE, C., LINDBERG, J., PADYUKOV, L., LUNDBERG, K., ENGSTRÖM, A., VENABLES, P. J., LUNDEBERG, J., HOLMDAHL, R., KLARESKOG, L. & MALMSTRÖM, V. 2009. Multiple antibody reactivities to citrullinated antigens in sera from patients with rheumatoid arthritis: association with HLA-DRB1 alleles. *Annals of the rheumatic diseases,* 68**,** 736-743.
SNOOK, J. P., KIM, C. & WILLIAMS, M. A. 2018. TCR signal strength controls the differentiation of CD4(+) effector and memory T cells. *Science immunology,* 3**,** eaas9103.
SO, T. & CROFT, M. 2013. Regulation of PI-3-Kinase and Akt Signaling in T Lymphocytes and Other Cells by TNFR Family Molecules. *Frontiers in immunology,* 4**,** 139-139.
STEINBERG, M. W., CHEUNG, T. C. & WARE, C. F. 2011. The signaling networks of the herpesvirus entry mediator (TNFRSF14) in immune regulation. *Immunological reviews,* 244**,** 169-187.
STRUTT, T. M., MCKINSTRY, K. K., KUANG, Y., FINN, C. M., HWANG, J. H., DHUME, K., SELL, S. & SWAIN, S. L. 2016. Direct IL-6 Signals Maximize Protective Secondary CD4 T Cell Responses against Influenza. *The Journal of Immunology,* 197**,** 3260.
SUGITA, S., KAWAZOE, Y., IMAI, A., KAWAGUCHI, T., HORIE, S., KEINO, H., TAKAHASHI, M. & MOCHIZUKI, M. 2013. Role of IL-22- and TNF-alpha-producing Th22 cells in uveitis patients with Behcet's disease. *J Immunol,* 190**,** 5799-808.
SURH, C. D. & SPRENT, J. 2000. Homeostatic T cell proliferation: how far can T cells be activated to self-ligands? *The Journal of experimental medicine,* 192**,** F9-F14.

SURH, C. D. & SPRENT, J. 2008. Homeostasis of Naive and Memory T Cells. *Immunity,* 29**,** 848-862.
SUZUKI, A., KOCHI, Y., OKADA, Y. & YAMAMOTO, K. 2011. Insight from genome-wide association studies in rheumatoid arthritis and multiple sclerosis. *FEBS letters,* 585**,** 3627-3632.
SUZUKI, N., SUZUKI, S., DUNCAN, G. S., MILLAR, D. G., WADA, T., MIRTSOS, C., TAKADA, H., WAKEHAM, A., ITIE, A., LI, S., PENNINGER, J. M., WESCHE, H., OHASHI, P. S., MAK, T. W. & YEH, W.-C. 2002. Severe impairment of interleukin-1 and Toll-like receptor signalling in mice lacking IRAK-4. *Nature,* 416**,** 750-754.
SZABO, S. J., KIM, S. T., COSTA, G. L., ZHANG, X., FATHMAN, C. G. & GLIMCHER, L. H. 2000. A novel transcription factor, T-bet, directs Th1 lineage commitment. *Cell,* 100**,** 655-669.
TAKAHASHI, S., SAEGUSA, J., SENDO, S., OKANO, T., AKASHI, K., IRINO, Y. & MORINOBU, A. 2017. Glutaminase 1 plays a key role in the cell growth of fibroblast-like synoviocytes in rheumatoid arthritis. *Arthritis Research & Therapy,* 19**,** 76.
TAKEDA, K., HARADA, Y., WATANABE, R., INUTAKE, Y., OGAWA, S., ONUKI, K., KAGAYA, S., TANABE, K., KISHIMOTO, H. & ABE, R. 2008. CD28 stimulation triggers NF-kappaB activation through the CARMA1-PKCtheta-Grb2/Gads axis. *International immunology,* 20**,** 1507-1515.
TAN, H., YANG, K., LI, Y., SHAW, T. I., WANG, Y., BLANCO, D. B., WANG, X., CHO, J.-H., WANG, H., RANKIN, S., GUY, C., PENG, J. & CHI, H. 2017. Integrative Proteomics and Phosphoproteomics Profiling Reveals Dynamic Signaling Networks and Bioenergetics Pathways Underlying T Cell Activation. *Immunity,* 46**,** 488-503.
TARASENKO, T. N., GOMEZ-RODRIGUEZ, J. & MCGUIRE, P. J. 2015. Impaired T cell function in argininosuccinate synthetase deficiency. *Journal of leukocyte biology,* 97**,** 273-278.
TENG, X., LI, W., CORNABY, C. & MOREL, L. 2019. Immune cell metabolism in autoimmunity. *Clinical & Experimental Immunology,* 197**,** 181-192.
THOMAS, R., MCILRAITH, M., DAVIS, L. S. & LIPSKY, P. E. 1992. Rheumatoid synovium is enriched in CD45RBdim mature memory T cells that are potent helpers for B cell differentiation. *Arthritis Rheum,* 35**,** 1455-65.
THOREEN, C. C., CHANTRANUPONG, L., KEYS, H. R., WANG, T., GRAY, N. S. & SABATINI, D. M. 2012. A unifying model for mTORC1-mediated regulation of mRNA translation. *Nature,* 485**,** 109-113.
TIAN, S., MAILE, R., COLLINS, E. J. & FRELINGER, J. A. 2007. CD8+ T cell activation is governed by TCR-peptide/MHC affinity, not dissociation rate. *Journal of immunology (Baltimore, Md. : 1950),* 179**,** 2952-2960.
TRAN, C. N., LUNDY, S. K., WHITE, P. T., ENDRES, J. L., MOTYL, C. D., GUPTA, R., WILKE, C. M., SHELDEN, E. A., CHUNG, K. C., URQUHART, A. G. & FOX, D. A. 2007. Molecular interactions between T cells and fibroblast-like synoviocytes: role of membrane tumor necrosis factor-alpha on cytokine-activated T cells. *The American journal of pathology,* 171**,** 1588-1598.
TREUHAFT, P. S. & DJ, M. C. 1971. Synovial fluid pH, lactate, oxygen and carbon dioxide partial pressure in various joint diseases. *Arthritis Rheum,* 14**,** 475-84.
TURESSON, C. 2016. Comorbidity in rheumatoid arthritis. *Swiss Med Wkly,* 146**,** w14290.
ULMER, C. Z., YOST, R. A., CHEN, J., MATHEWS, C. E. & GARRETT, T. J. 2015. Liquid Chromatography-Mass Spectrometry Metabolic and Lipidomic Sample

Preparation Workflow for Suspension-Cultured Mammalian Cells using Jurkat T lymphocyte Cells. *Journal of proteomics & bioinformatics,* 8**,** 126-132.
USUI, T., NISHIKOMORI, R., KITANI, A. & STROBER, W. 2003. GATA-3 suppresses Th1 development by downregulation of Stat4 and not through effects on IL-12Rbeta2 chain or T-bet. *Immunity,* 18**,** 415-28.
VAN DE STADT, L. A., WITTE, B. I., BOS, W. H. & VAN SCHAARDENBURG, D. 2013. A prediction rule for the development of arthritis in seropositive arthralgia patients. *Ann Rheum Dis,* 72**,** 1920-6.
VAN DER WINDT, G. J. W., CHANG, C. H. & PEARCE, E. L. 2016. Measuring Bioenergetics in T Cells Using a Seahorse Extracellular Flux Analyzer. *Curr Protoc Immunol,* 113**,** 3.16b.1-3.16b.14.
VAN DER WINDT, G. J. W. & PEARCE, E. L. 2012. Metabolic switching and fuel choice during T-cell differentiation and memory development. *Immunological reviews,* 249**,** 27-42.
VAN GAALEN, F. A., VAN AKEN, J., HUIZINGA, T. W., SCHREUDER, G. M., BREEDVELD, F. C., ZANELLI, E., VAN VENROOIJ, W. J., VERWEIJ, C. L., TOES, R. E. & DE VRIES, R. R. 2004. Association between HLA class II genes and autoantibodies to cyclic citrullinated peptides (CCPs) influences the severity of rheumatoid arthritis. *Arthritis Rheum,* 50**,** 2113-21.
VAN HAMBURG, J. P., ASMAWIDJAJA, P. S., DAVELAAR, N., MUS, A. M. C., COLIN, E. M., HAZES, J. M. W., DOLHAIN, R. J. E. M. & LUBBERTS, E. 2011. Th17 cells, but not Th1 cells, from patients with early rheumatoid arthritis are potent inducers of matrix metalloproteinases and proinflammatory cytokines upon synovial fibroblast interaction, including autocrine interleukin-17A production. *Arthritis and rheumatism,* 63**,** 73-83.
VANDER HEIDEN, M. G., CANTLEY, L. C. & THOMPSON, C. B. 2009. Understanding the Warburg effect: the metabolic requirements of cell proliferation. *Science (New York, N.Y.),* 324**,** 1029-1033.
VANLERBERGHE, G. C. 2013. Alternative oxidase: a mitochondrial respiratory pathway to maintain metabolic and signaling homeostasis during abiotic and biotic stress in plants. *International journal of molecular sciences,* 14**,** 6805-6847.
VELDHOEN, M., HOCKING, R. J., ATKINS, C. J., LOCKSLEY, R. M. & STOCKINGER, B. 2006. TGFbeta in the context of an inflammatory cytokine milieu supports de novo differentiation of IL-17-producing T cells. *Immunity,* 24**,** 179-189.
VERMEIRE, K., HEREMANS, H., VANDEPUTTE, M., HUANG, S., BILLIAU, A. & MATTHYS, P. 1997. Accelerated collagen-induced arthritis in IFN-gamma receptor-deficient mice. *Journal of immunology (Baltimore, Md. : 1950),* 158**,** 5507-5513.
VIATTE, S., PLANT, D., HAN, B., FU, B., YARWOOD, A., THOMSON, W., SYMMONS, D. P. M., WORTHINGTON, J., YOUNG, A., HYRICH, K. L., MORGAN, A. W., WILSON, A. G., ISAACS, J. D., RAYCHAUDHURI, S. & BARTON, A. 2015. Association of HLA-DRB1 haplotypes with rheumatoid arthritis severity, mortality, and treatment response. *JAMA,* 313**,** 1645-1656.
VON FELBERT, V., CÓRDOBA, F., WEISSENBERGER, J., VALLAN, C., KATO, M., NAKASHIMA, I., BRAATHEN, L. R. & WEIS, J. 2005. Interleukin-6 gene ablation in a transgenic mouse model of malignant skin melanoma. *The American journal of pathology,* 166**,** 831-841.
VRISEKOOP, N., MONTEIRO, J. P., MANDL, J. N. & GERMAIN, R. N. 2014. Revisiting thymic positive selection and the mature T cell repertoire for antigen. *Immunity,* 41**,** 181-190.

WAHL, D. R., PETERSEN, B., WARNER, R., RICHARDSON, B. C., GLICK, G. D. & OPIPARI, A. W. 2010. Characterization of the metabolic phenotype of chronically activated lymphocytes. *Lupus,* 19**,** 1492-501.
WANG, B., MAILE, R., GREENWOOD, R., COLLINS, E. J. & FRELINGER, J. A. 2000. Naive CD8⁺ T Cells Do Not Require Costimulation for Proliferation and Differentiation into Cytotoxic Effector Cells. *The Journal of Immunology,* 164**,** 1216.
WANG, L. & BOSSELUT, R. 2009. CD4-CD8 lineage differentiation: Thpok-ing into the nucleus. *Journal of immunology (Baltimore, Md. : 1950),* 183**,** 2903-2910.
WANG, R., DILLON, C. P., SHI, L. Z., MILASTA, S., CARTER, R., FINKELSTEIN, D., MCCORMICK, L. L., FITZGERALD, P., CHI, H., MUNGER, J. & GREEN, D. R. 2011. The transcription factor Myc controls metabolic reprogramming upon T lymphocyte activation. *Immunity,* 35**,** 871-882.
WANG, T., SUN, X., ZHAO, J., ZHANG, J., ZHU, H., LI, C., GAO, N., JIA, Y., XU, D., HUANG, F.-P., LI, N., LU, L. & LI, Z.-G. 2015. Regulatory T cells in rheumatoid arthritis showed increased plasticity toward Th17 but retained suppressive function in peripheral blood. *Annals of the rheumatic diseases,* 74**,** 1293-1301.
WARBURG, O., WIND, F. & NEGELEIN, E. 1927. THE METABOLISM OF TUMORS IN THE BODY. *The Journal of general physiology,* 8**,** 519-530.
WATANABE, R., HARADA, Y., TAKEDA, K., TAKAHASHI, J., OHNUKI, K., OGAWA, S., OHGAI, D., KAIBARA, N., KOIWAI, O., TANABE, K., TOMA, H., SUGAMURA, K. & ABE, R. 2006. Grb2 and Gads Exhibit Different Interactions with CD28 and Play Distinct Roles in CD28-Mediated Costimulation. *The Journal of Immunology,* 177**,** 1085.
WESLEY, A., BENGTSSON, C., ELKAN, A. C., KLARESKOG, L., ALFREDSSON, L., WEDREN, S. & EPIDEMIOLOGICAL INVESTIGATION OF RHEUMATOID ARTHRITIS STUDY, G. 2013. Association between body mass index and anti-citrullinated protein antibody-positive and anti-citrullinated protein antibody-negative rheumatoid arthritis: results from a population-based case-control study. *Arthritis Care Res (Hoboken),* 65**,** 107-12.
WEYAND, C. M., SHEN, Y. & GORONZY, J. J. 2018. Redox-sensitive signaling in inflammatory T cells and in autoimmune disease. *Free Radical Biology and Medicine,* 125**,** 36-43.
WILSON, J. E. 2003. Isozymes of mammalian hexokinase: structure, subcellular localization and metabolic function. *Journal of Experimental Biology,* 206**,** 2049.
WOFFORD, J. A., WIEMAN, H. L., JACOBS, S. R., ZHAO, Y. & RATHMELL, J. C. 2008. IL-7 promotes Glut1 trafficking and glucose uptake via STAT5-mediated activation of Akt to support T-cell survival. *Blood,* 111**,** 2101-11.
WOLF, J., ROSE-JOHN, S. & GARBERS, C. 2014. Interleukin-6 and its receptors: A highly regulated and dynamic system. *Cytokine,* 70**,** 11-20.
WOODROOFE, C., MULLER, W. & RUTHER, U. 1992. Long-term consequences of interleukin-6 overexpression in transgenic mice. *DNA Cell Biol,* 11**,** 587-92.
XING, Y. & HOGQUIST, K. A. 2012. T-cell tolerance: central and peripheral. *Cold Spring Harbor perspectives in biology,* 4**,** a006957.
XU, T., STEWART, K. M., WANG, X., LIU, K., XIE, M., RYU, J. K., LI, K., MA, T., WANG, H., NI, L., ZHU, S., CAO, N., ZHU, D., ZHANG, Y., AKASSOGLOU, K., DONG, C., DRIGGERS, E. M. & DING, S. 2017. Metabolic control of T(H)17 and induced T(reg) cell balance by an epigenetic mechanism. *Nature,* 548**,** 228-233.

XU, Y., ZHANG, Y. & YE, J. 2018. IL-6: A Potential Role in Cardiac Metabolic Homeostasis. *International Journal of Molecular Sciences,* 19**,** 2474.
YAGO, T., NANKE, Y., ICHIKAWA, N., KOBASHIGAWA, T., MOGI, M., KAMATANI, N. & KOTAKE, S. 2009. IL-17 induces osteoclastogenesis from human monocytes alone in the absence of osteoblasts, which is potently inhibited by anti-TNF-alpha antibody: a novel mechanism of osteoclastogenesis by IL-17. *Journal of cellular biochemistry,* 108**,** 947-955.
YAN, J. & MAMULA, M. J. 2002. Autoreactive T cells revealed in the normal repertoire: escape from negative selection and peripheral tolerance. *Journal of immunology (Baltimore, Md. : 1950),* 168**,** 3188-3194.
YANG, K., SHRESTHA, S., ZENG, H., KARMAUS, P. W. F., NEALE, G., VOGEL, P., GUERTIN, D. A., LAMB, R. F. & CHI, H. 2013a. T cell exit from quiescence and differentiation into Th2 cells depend on Raptor-mTORC1-mediated metabolic reprogramming. *Immunity,* 39**,** 1043-1056.
YANG, M., KUANG, X., LI, J., PAN, Y., TAN, M., LU, B., CHENG, Q., WU, L. & PANG, G. 2013b. Meta-analysis of the association of HLA-DRB1 with rheumatoid arthritis in Chinese populations. *BMC musculoskeletal disorders,* 14**,** 307-307.
YANG, R., LIRUSSI, D., THORNTON, T. M., JELLEY-GIBBS, D. M., DIEHL, S. A., CASE, L. K., MADESH, M., TAATJES, D. J., TEUSCHER, C., HAYNES, L. & RINCÓN, M. 2015. Mitochondrial Ca^{2+} and membrane potential, an alternative pathway for Interleukin 6 to regulate CD4 cell effector function. *eLife,* 4**,** e06376.
YANG, Z., FUJII, H., MOHAN, S. V., GORONZY, J. J. & WEYAND, C. M. 2013c. Phosphofructokinase deficiency impairs ATP generation, autophagy, and redox balance in rheumatoid arthritis T cells. *The Journal of experimental medicine,* 210**,** 2119-2134.
YANG, Z., SHEN, Y., OISHI, H., MATTESON, E. L., TIAN, L., GORONZY, J. J. & WEYAND, C. M. 2016. Restoring oxidant signaling suppresses proarthritogenic T cell effector functions in rheumatoid arthritis. *Sci Transl Med,* 8**,** 331ra38.
YARWOOD, A., HUIZINGA, T. W. J. & WORTHINGTON, J. 2016. The genetics of rheumatoid arthritis: risk and protection in different stages of the evolution of RA. *Rheumatology (Oxford, England),* 55**,** 199-209.
YE, H., ZHANG, J., WANG, J., GAO, Y., DU, Y., LI, C., DENG, M., GUO, J. & LI, Z. 2015. CD4 T-cell transcriptome analysis reveals aberrant regulation of STAT3 and Wnt signaling pathways in rheumatoid arthritis: evidence from a case-control study. *Arthritis Res Ther,* 17**,** 76.
YIN, Y., CHOI, S.-C., XU, Z., PERRY, D. J., SEAY, H., CROKER, B. P., SOBEL, E. S., BRUSKO, T. M. & MOREL, L. 2015. Normalization of CD4+ T cell metabolism reverses lupus. *Science translational medicine,* 7**,** 274ra18-274ra18.
YIN, Y., CHOI, S. C., XU, Z., ZEUMER, L., KANDA, N., CROKER, B. P. & MOREL, L. 2016. Glucose Oxidation Is Critical for CD4+ T Cell Activation in a Mouse Model of Systemic Lupus Erythematosus. *J Immunol,* 196**,** 80-90.
YOSHIDA, Y. & TANAKA, T. 2014. Interleukin 6 and rheumatoid arthritis. *BioMed research international,* 2014**,** 698313-698313.
YOSHINO, T., KUSUNOKI, N., TANAKA, N., KANEKO, K., KUSUNOKI, Y., ENDO, H., HASUNUMA, T. & KAWAI, S. 2011. Elevated serum levels of resistin, leptin, and adiponectin are associated with C-reactive protein and also other clinical conditions in rheumatoid arthritis. *Intern Med,* 50**,** 269-75.

YOUNG, S. P., KAPOOR, S. R., VIANT, M. R., BYRNE, J. J., FILER, A., BUCKLEY, C. D., KITAS, G. D. & RAZA, K. 2013. The impact of inflammation on metabolomic profiles in patients with arthritis. *Arthritis Rheum,* 65**,** 2015-23.
ZENG, H. & CHI, H. 2014. mTOR signaling and transcriptional regulation in T lymphocytes. *Transcription,* 5**,** e28263-e28263.
ZHAN, Y., CARRINGTON, E. M., ZHANG, Y., HEINZEL, S. & LEW, A. M. 2017. Life and Death of Activated T Cells: How Are They Different from Naïve T Cells? *Frontiers in Immunology,* 8.
ZHANG, C., XIN, H., ZHANG, W., YAZAKI, P. J., ZHANG, Z., LE, K., LI, W., LEE, H., KWAK, L., FORMAN, S., JOVE, R. & YU, H. 2016. CD5 Binds to Interleukin-6 and Induces a Feed-Forward Loop with the Transcription Factor STAT3 in B Cells to Promote Cancer. *Immunity,* 44**,** 913-923.
ZHANG, J., FU, L., SHI, J., CHEN, X., LI, Y., MA, B. & ZHANG, Y. 2013. The risk of metabolic syndrome in patients with rheumatoid arthritis: a meta-analysis of observational studies. *PloS one,* 8**,** e78151-e78151.
ZHANG, L., LI, J.-M., LIU, X.-G., MA, D.-X., HU, N.-W., LI, Y.-G., LI, W., HU, Y., YU, S., QU, X., YANG, M.-X., FENG, A. L. & WANG, G.-H. 2011. Elevated Th22 cells correlated with Th17 cells in patients with rheumatoid arthritis. *Journal of clinical immunology,* 31**,** 606-614.
ZHANG, N. & BEVAN, M. J. 2011. CD8(+) T cells: foot soldiers of the immune system. *Immunity,* 35**,** 161-168.
ZHENG, Y., DELGOFFE, G. M., MEYER, C. F., CHAN, W. & POWELL, J. D. 2009. Anergic T cells are metabolically anergic. *Journal of immunology (Baltimore, Md. : 1950),* 183**,** 6095-6101.
ZHOU, J., CHEN, J., HU, C., XIE, Z., LI, H., WEI, S., WANG, D., WEN, C. & XU, G. 2016. Exploration of the serum metabolite signature in patients with rheumatoid arthritis using gas chromatography-mass spectrometry. *J Pharm Biomed Anal,* 127**,** 60-7.
ZHOU, L., LOPES, J. E., CHONG, M. M. W., IVANOV, I. I., MIN, R., VICTORA, G. D., SHEN, Y., DU, J., RUBTSOV, Y. P., RUDENSKY, A. Y., ZIEGLER, S. F. & LITTMAN, D. R. 2008. TGF-beta-induced Foxp3 inhibits T(H)17 cell differentiation by antagonizing RORgammat function. *Nature,* 453**,** 236-240.
ZHU, J., MIN, B., HU-LI, J., WATSON, C. J., GRINBERG, A., WANG, Q., KILLEEN, N., URBAN, J. F., JR., GUO, L. & PAUL, W. E. 2004. Conditional deletion of Gata3 shows its essential function in T(H)1-T(H)2 responses. *Nature immunology,* 5**,** 1157-1165.